

**BALL SURFACE REPRESENTATIONS USING PARTIAL
DIFFERENTIAL EQUATIONS**

AHMED SALEH ABDULLAH KHERD

**DOCTOR OF PHILOSOPHY
UNIVERSITI UTARA MALAYSIA
2015**



Awang Had Salleh
Graduate School
of Arts And Sciences

Universiti Utara Malaysia

PERAKUAN KERJA TESIS / DISERTASI
(Certification of thesis / dissertation)

Kami, yang bertandatangan, memperakukan bahawa
(We, the undersigned, certify that)

AHMAD SALEH ABDULLAH KHERD

93357

calon untuk Ijazah _____ PhD _____
(candidate for the degree of)

telah mengemukakan tesis / disertasi yang bertajuk:
(has presented his/her thesis / dissertation of the following title):

"BALL SURFACE REPRESENTATIONS USING PARTIAL DIFFERENTIAL EQUATIONS"

seperti yang tercatat di muka surat tajuk dan kulit tesis / disertasi.
(as it appears on the title page and front cover of the thesis / dissertation).

Bahawa tesis/disertasi tersebut boleh diterima dari segi bentuk serta kandungan dan meliputi bidang ilmu dengan memuaskan, sebagaimana yang ditunjukkan oleh calon dalam ujian lisan yang diadakan pada : **04 Jun 2015.**

That the said thesis/dissertation is acceptable in form and content and displays a satisfactory knowledge of the field of study as demonstrated by the candidate through an oral examination held on: June 04, 2015.

Pengerusi Viva:
(Chairman for VIVA)

Assoc. Prof. Dr. Sharipah Soaad Syed Yahaya

Tandatangan
(Signature)

Pemeriksa Luar:
(External Examiner)

Assoc. Prof. Dr. Abd Fatah Wahab

Tandatangan
(Signature)

Pemeriksa Dalam:
(Internal Examiner)

Dr. Teh Yuan Ying

Tandatangan
(Signature)

Nama Penyelia/Penyelia-penyelia: Dr. Azizan Saaban
(Name of Supervisor/Supervisors)

Tandatangan
(Signature)

Tarikh:
(Date) June 04, 2015

Permission to Use

In presenting this thesis in fulfilment of the requirements for a postgraduate degree from Universiti Utara Malaysia, I agree that the Universiti Library may make it freely available for inspection. I further agree that permission for the copying of this thesis in any manner, in whole or in part, for scholarly purpose may be granted by my supervisor or, in their absence, by the Dean of Awang Had Salleh Graduate School of Arts and Sciences. It is understood that any copying or publication or use of this thesis or parts thereof for financial gain shall not be allowed without my written permission. It is also understood that due recognition shall be given to me and to Universiti Utara Malaysia for any scholarly use which may be made of any material from my thesis.

Requests for permission to copy or to make other use of materials in this thesis, in whole or in part, should be addressed to:

Dean of Awang Had Salleh Graduate School of Arts and Sciences
UUM College of Arts and Sciences
Universiti Utara Malaysia
06010 UUM Sintok

Abstrak

Sejak dua dekad lalu, pemodelan geometri menggunakan pendekatan persamaan pembezaan separa (PPS) telah dikaji secara meluas dalam Rekabentuk Geometri Bantuan Komputer (RGBK). Pendekatan ini pada mulanya diperkenalkan oleh beberapa orang penyelidik berdasarkan kepada permukaan Bézier yang berkaitan dengan luas permukaan minimum ditentukan oleh lengkung sempadan yang ditetapkan. Walau bagaimanapun, perwakilan permukaan Bézier boleh diperbaiki dari segi masa pengiraan dan luas permukaan minimum dengan menggunakan perwakilan permukaan Ball. Sehubungan itu, kajian ini membangunkan satu algoritma untuk mengitlak permukaan Ball dari lengkung sempadan menggunakan PPS eliptik. Dua permukaan Ball khusus iaitu harmonik dan dwiharmonik pertamanya dibina dalam membangunkan algoritma yang dicadangkan. Permukaan terdahulu dan kemudian masing-masing memerlukan dua dan empat syarat sempadan. Bagi mengitlak permukaan Ball dalam penyelesaian polinomial untuk sebarang PPS peringkat empat, kaedah Dirichlet digunakan. Keputusan berangka diperolehi keatas contoh titik data yang diketahui umum menunjukkan algoritma permukaan Ball teritlak yang dicadangkan mempamerkan keputusan lebih baik daripada perwakilan permukaan Bézier dari segi masa pengiraan dan luas permukaan minimum. Tambahan pula, algoritma yang baharu dibina juga memenuhi sebarang permukaan dalam RGBK termasuk permukaan Bézier. Algoritma ini kemudiannya diuji dalam permasalahan pengekalan kepositifan permukaan dan pembesaran imej. Keputusan menunjukkan algoritma yang dicadangkan adalah setanding dengan kaedah yang sedia ada dari segi kejituan. Justeru, algoritma ini adalah satu alternatif berdaya maju untuk membina permukaan Ball teritlak. Dapatan daripada kajian ini menyumbang kearah bidang pengetahuan untuk pembinaan semula permukaan berdasarkan pendekatan PPS dalam bidang pemodelan geometri dan grafik komputer.

Kata kunci: Permukaan Ball, Persamaan pembezaan separa, Kaedah Dirichlet, Pengekalan kepositifan, Pembesaran imej.

Abstract

Over two decades ago, geometric modelling using partial differential equations (PDEs) approach was widely studied in Computer Aided Geometric Design (CAGD). This approach was initially introduced by some researchers to deal with Bézier surface related to the minimal surface area determined by prescribed boundary curves. However, Bézier surface representation can be improved in terms of computation time and minimal surface area by employing Ball surface representation. Thus, this research develops an algorithm to generalise Ball surfaces from boundary curves using elliptic PDEs. Two specific Ball surfaces, namely harmonic and biharmonic, are first constructed in developing the proposed algorithm. The former and later surfaces require two and four boundary conditions respectively. In order to generalise Ball surfaces in the polynomial solution of any fourth order PDEs, the Dirichlet method is then employed. The numerical results obtained on well-known example of data points show that the proposed generalised Ball surfaces algorithm performs better than Bézier surface representation in terms of computation time and minimal surface area. Moreover, the new constructed algorithm also holds for any surfaces in CAGD including the Bezier surface. This algorithm is then tested in positivity preserving of surface and image enlargement problems. The results show that the proposed algorithm is comparable with the existing methods in terms of accuracy. Hence, this new algorithm is a viable alternative for constructing generalized Ball surfaces. The findings of this study contribute towards the body of knowledge for surface reconstruction based on PDEs approach in the area of geometric modelling and computer graphics.

Keywords: Ball surface, Partial differential equation, Dirichlet method, Positivity preserving, Image enlargement.

Acknowledgements

I would like to express my sincere gratitude to my supervisor Dr. Azizan Bin Saaban who gave me a lot of guidances and advices. I thanked him not only as my supervisor, but also as my counselor.

I am grateful to the Ministry of Higher Education of Malaysia for providing me with the Fundamental Research Grant Scheme (FRGS) (S/O: 12380) to enable me to pursue this research.

I wish to thank the staff from the School of Quantitative Sciences, Universiti Utara Malaysia. This research would not have been possible without the facilities provided by the School of Quantitative Sciences, Universiti Utara Malaysia.

I would like to dedicate this thesis to my parents, my wives and Al-Ahgaff University, Yemen, for their support.

Table of Contents

Permission to Use	i
Abstrak	ii
Abstract	iii
Acknowledgements	iv
Table of Contents	v
List of Tables	xi
List of Figures	xiii
List of Symbols	xviii
CHAPTER ONE INTRODUCTION	1
1.1 Research Background	1
1.2 Problem Statement	3
1.3 Research Questions	3
1.4 Objective of the Research	4
1.5 Research Framework	5
1.6 Scope of the study	5
1.7 Significance of the Study	6
1.8 Thesis Organization	6
CHAPTER TWO LITERATURE REVIEW	8
2.1 Introduction	8
2.2 Review on Bézier Curves	9
2.2.1 Derivative and Integral of Bernstein Polynomials	11
2.2.2 Bézier Monomial Form	12
2.2.3 Degree Elevation of Bézier Curves	12
2.2.4 Bézier Rectangular Surfaces	13
2.3 Review on Ball Curves	13
2.3.1 Said-Ball Representation	14
2.3.1.1 Said-Ball Monomial Form	17
2.3.1.2 Conversion of Said-Ball Curve to Bézier Curve	17
2.3.1.3 Said-Ball Rectangular Surfaces	19

2.3.1.4	Converting Said-Ball Surface into Bézier Surface	19
2.3.2	DP-Ball Curves Representation	20
2.3.2.1	DP Monomial Form	22
2.3.2.2	Conversion of DP-Ball Curve to Bézier Curve	22
2.3.2.3	DP-Ball Rectangular Surfaces	24
2.3.2.4	Converting DP-Ball Surface into Bézier Surface	24
2.3.3	Wang-Ball Curves	26
2.3.3.1	Wang-Ball Monomial Form	28
2.3.3.2	Conversion of Wang-Ball Curve to Bézier Curve	29
2.3.3.3	Wang-Ball Rectangular Surfaces	30
2.3.3.4	Converting Wang-Ball Surface into Bézier Surface	30
2.4	Parametric Surface	31
2.5	Harmonic and Biharmonic Surface	31
2.5.1	The First Fundamental Form	32
2.5.2	Monomial Matrix Form	33
2.5.2.1	Bézier Monomial Matrix	33
2.5.2.2	Said-Ball Monomial Matrix	34
2.5.2.3	DP-Ball Monomial Matrix	34
2.5.2.4	Wang-Ball Monomial Matrix	35
2.5.2.5	Converting the Control Points of Bézier Surface into Control Points of Ball Surface using Monomial Matrix	35
2.6	Definition of Isothermal Surface	36
2.7	Estimate the Partial Derivative with respect to x and y for the Control Points at the Boundary Curves	38
CHAPTER THREE HARMONIC AND BIHARMONIC SURFACE . . .		39
3.1	Harmonic of $X(u, v)$ Surface	39
3.1.1	Biquadratic Harmonic Patches	43
3.1.1.1	Said-Ball Patch	43
3.1.2	Bicubical Harmonic Patches	45
3.1.2.1	Bicubical Harmonic Said-Ball Patches	46
3.1.2.2	Bicubical Harmonic DP-Ball Patches	47
3.1.3	Graphical Examples for Harmonic Bicubic Surface	49

3.1.3.1	Graphical Examples for Harmonic Bicubic Said/Wang-Ball Surface	50
3.1.3.2	Graphical Examples for Harmonic Bicubic DP-Ball Surface	52
3.2	Biharmonic of $X(u, v)$ Patch	58
3.2.1	Bicubic Biharmonic Patch	63
3.2.1.1	Bicubic Said/Wang-Ball Biharmonic Equation	64
3.2.1.2	DP-Ball Biharmonic Equation	64
3.2.2	Graphical Examples for Biharmonic Bicubic Patch	65
3.2.2.1	Graphical Examples for Biharmonic Bicubic Said/Wang-Ball Patch	66
3.2.2.2	Graphical Examples for Biharmonic Bicubic DP-Ball Surface	68
3.2.3	Biquartic Biharmonic Equation	74
3.2.3.1	Biquartic Said-Ball Biharmonic Equation	75
3.2.3.2	Biquartic DP-Ball Biharmonic Equation	78
3.2.3.3	Biquartic Wang-Ball Biharmonic Equation	81
3.2.4	Graphical Examples for Biharmonic Biquartic Patch	85
3.2.4.1	Graphical Examples for Biharmonic Biquartic Said-Ball Patch	85
3.2.4.2	Graphical Examples for Biharmonic Biquartic DP-Ball Patch	88
3.2.4.3	Graphical Examples for Biharmonic Biquartic Wang-Ball Patch	90
3.3	Summary	97

CHAPTER FOUR POLYNOMIAL SOLUTIONS OF FOURTH ORDER LINEAR ELLIPTIC PARTIAL DIFFERENTIAL EQUATIONS AND EXTREMAL OF THE DIRICHLET FUNCTIONAL IN TERMS OF BALL SURFACE 99

4.1	Polynomial Solutions of Fourth Order Linear Elliptic PDEs in terms of Ball Surface	99
-----	--	----

4.1.1	Said-Ball Polynomial Solutions for Fourth Order Partial Differential Equations	103
4.1.1.1	Odd Degree- n Said-Ball Boundary Curves Defined on Rectangular Grid	104
4.1.1.2	Relation Between Cubic Said-Ball Boundary Coefficients and Polynomial Coefficients Using Fourth Order PDEs	104
4.1.1.3	Relation Between Quintic Said-Ball Boundary Coefficients and Polynomial Coefficients Using Fourth Order PDEs	105
4.1.2	DP-Ball Polynomial Solutions for Fourth-Order Partial Differential Equations	108
4.1.3	Odd Degree- n DP-Ball Boundary Curves Defined on Rectangular Grid	108
4.1.3.1	Relation Between Cubic DP-Ball Boundary Coefficients and Polynomial Coefficients Using Fourth Order PDEs	108
4.1.3.2	Relation Between Quintic DP-Ball Boundary Coefficients and Polynomial Coefficients Using Fourth Order PDEs	110
4.1.4	Wang-Ball Polynomial Solutions for Fourth Order Partial Differential Equations	112
4.1.4.1	Odd Degree- n Wang-Ball Boundary Curves Defined on Rectangular Grid	112
4.1.4.2	Relation Between Cubic Wang-Ball Boundary Coefficients and Polynomial Coefficients Using Fourth Order PDEs	112
4.1.4.3	Relation Between quintic Wang-Ball Boundary Coefficients and Polynomial Coefficients Using Fourth Order PDEs	113
4.1.5	Surface Construction	115
4.1.6	Graphical Examples	116
4.1.6.1	Bicubic Said/Wang-Ball	116
4.1.6.2	Biquintic Said-Ball	118
4.1.6.3	Bicubic DP-Ball	119

4.1.6.4	Biquintic DP-Ball	119
4.1.6.5	Biquintic Wang-Ball	120
4.2	Dirichlet Functional	123
4.2.1	Biquadratic Dirichlet Surface	126
4.2.2	Bicubic Dirichlet Surface	127
4.2.2.1	Said-Ball and Wang-Ball	127
4.2.2.2	DP-Ball	128
4.2.3	Dirichlet Mask for Bicubic Pathes	129
4.2.4	Graphical Examples for Extremal of the Dirichlet Bicubic Surface	130
4.2.4.1	Graphical Examples for Extremal of the Dirichlet Bicubic Wang-Ball Surface	130
4.2.4.2	Graphical Examples for Extremal of the Dirichlet Bicubic DP-Ball Surface	132
4.3	Summary	140
CHAPTER FIVE IMPLEMENTATION AND APPLICATIONS		141
5.1	An Improved Positivity Preserving Said-Ball, DP-Ball and Wang-Ball Curves of Odd Degree- n	141
5.1.1	Sufficient Condition for Positivity Preserving Odd Degree- n Said-Ball Curves	141
5.1.2	Sufficient Condition for Positivity Preserving Odd Degree- n DP-Ball Curves	145
5.1.3	Sufficient Condition for Positivity Preserving Odd Degree- n Wang-Ball Curves	149
5.2	Sufficient Condition for Positivity Preserving Cubic Ball (Said-Ball, DP-Ball and Wang-Ball Curves)	150
5.2.1	Sufficient Condition for Positivity Preserving Cubic Said-Ball Curves	151
5.2.2	Sufficient Condition for Positivity Preserving Cubic DP-Ball Curves	152
5.2.3	Sufficient Condition for Positivity Preserving Cubic Wang-Ball Curves	152
5.3	Sufficient Condition for Positivity Preserving Quintic Ball (Said-Ball, DP-Ball and Wang-Ball Curves)	153

5.3.1	Sufficient Condition for Positivity Preserving Quintic Said-Ball Curves	154
5.3.2	Sufficient Condition for Positivity Preserving Quintic DP-Ball Curves	154
5.3.3	Sufficient Condition for Positivity Preserving Quintic Wang-Ball Curves	154
5.4	Surface Interpolation Using Positivity Preserving Boundary Curves	155
5.4.1	Graphical Examples	155
5.4.1.1	Bicubic Patches	155
5.4.1.2	Biquintic Pathes	158
5.5	Image Enlargement Using Cubic Said-Ball, Wang-Ball and DP-Ball Boundary Curves with PDEs	162
5.5.1	Introduction	162
5.5.2	Image Scaling Concept	164
5.5.3	Image Interpolation using Rectangular Patches	165
5.5.4	Experimental Result	166
5.5.5	Summary	178
CHAPTER SIX CONCLUSION AND FUTURE RESEARCH		179
6.1	Conclusion	179
6.2	Future Research	182
REFERENCES		183

List of Tables

Table 3.1	Comparison between the area/computational time of Bézier, Said/Wang-Ball and DP-Ball by using harmonic condition.	58
Table 3.2	Comparison between the area/computational time of Bézier, Said/Wang-Ball and DP-Ball by using biharmonic condition.	74
Table 3.3	Comparison between the area/computational time of biquartic Bézier, biquartic Said-Ball, biquartic Wang-Ball and biquartic DP-Ball by using biharmonic condition.	97
Table 4.1	Comparison of the interpolating surfaces between bicubic Bézier, bicubic Said/Wang-Ball and bicubic DP-Ball boundary curves for the test function $g(x,y)$	121
Table 4.2	Comparison of the interpolating surfaces between biquintic Bézier, biquintic Said-Ball, biquintic Wang-Ball and biquintic DP-Ball boundary curves for the test function $g(x,y)$	122
Table 4.3	Comparison of the interpolating surfaces between bicubic Bézier, bicubic Said/Wang-Ball and bicubic DP-Ball boundary curves for the test function $f(x,y)$	122
Table 4.4	Comparison of the interpolating surfaces between biquintic Bézier, biquintic Said-Ball, biquintic Wang-Ball and biquintic DP-Ball boundary curves for the test function $f(x,y)$	123
Table 4.5	Comparison between the area/computational time of Bézier, Said/Wang-Ball and DP-Ball by using Dirichlet functional.	139
Table 5.1	Comparison of the interpolating surfaces between bicubic Bézier, bicubic Said/Wang-Ball and bicubic DP-Ball boundary curves for the test function $g(x,y)$	157
Table 5.2	Comparison of the interpolating surfaces between bicubic Bézier and bicubic Said/Wang-Ball boundary curves for the test function $f(x,y)$	158
Table 5.3	Comparison of the interpolating surfaces between biquintic Bézier, biquintic Said-Ball, biquintic Wang-Ball and biquintic DP-Ball boundary curves for the test function $g(x,y)$	161
Table 5.4	Comparison of the interpolating surfaces between biquintic Bézier, biquintic Said-Ball, biquintic Wang-Ball and biquintic DP-Ball boundary curves for the test function $f(x,y)$	162
Table 5.5	Comparison between Said/Wang-Ball and DP-Ball by using PSNR for Rice test image.	168

Table 5.6	Comparison between Said/Wang-Ball and DP-Ball by using PSNR for Cameraman test image.	169
Table 5.7	Comparison between Said/Wang-Ball and DP-Ball by using PSNR for Nuvola test image.	170
Table 5.8	Comparison between Said/Wang-Ball and DP-Ball by using PSNR for Pout test image.	171
Table 5.9	Comparison between Said/Wang-Ball and DP-Ball by using PSNR for Tyre test image.	172
Table 5.10	Comparison between Said/Wang-Ball and DP-Ball by using PSNR for Lena test image.	173
Table 5.11	Comparison between Said/Wang-Ball and DP-Ball by using PSNR for Monkey test image.	174
Table 5.12	Comparison between Said/Wang-Ball and DP-Ball by using PSNR for Pepper test image.	175
Table 5.13	Comparison between Said/Wang-Ball and DP-Ball by using PSNR for Thumb test image.	176

List of Figures

Figure 2.1	The Bernstein polynomials of degree two.	10
Figure 2.2	The Bernstein polynomials of degree three.	10
Figure 2.3	The Bernstein polynomials of degree four.	10
Figure 2.4	The Bernstein polynomials of degree five.	11
Figure 2.5	Degree elevation of Bézier curve from three to six.	12
Figure 2.6	Cubic Ball basis functions.	13
Figure 2.7	Said-Ball basis functions of degree two.	15
Figure 2.8	Said-Ball basis functions of degree three.	15
Figure 2.9	Said-Ball basis functions of degree four.	15
Figure 2.10	Said-Ball basis functions of degree five.	16
Figure 2.11	DP-Ball basis function of degree three.	21
Figure 2.12	DP-Ball basis function of degree four.	21
Figure 2.13	Wang-Ball basis function of degree two.	26
Figure 2.14	Wang-Ball basis function of degree three.	27
Figure 2.15	Wang-Ball basis function of degree four.	27
Figure 2.16	Wang-Ball basis function of degree five.	27
Figure 3.1	(a) Boundary curves of biquadratic Said-Ball generated by dual harmonic mask (b) Surface of biquadratic Said-Ball generated by dual harmonic mask.	45
Figure 3.2	(a) Boundary curves of biquadratic Said-Ball generated by harmonic mask (b) Surface of biquadratic Said-Ball generated by harmonic mask.	45
Figure 3.3	Control points set 1 by harmonic condition on (a) Bézier patch (b) Bézier boundary (c) Said/Wang-Ball patch (d) Said/Wang-Ball boundary (e) DP-Ball patch (f) DP-Ball boundary.	54
Figure 3.4	Control points set 2 by harmonic condition on (a) Bézier patch (b) Bézier boundary (c) Said/Wang-Ball patch (d) Said/Wang-Ball boundary (e) DP-Ball patch (f) DP-Ball boundary.	55
Figure 3.5	Control points set 3 by harmonic condition on (a) Bézier patch (b) Bézier boundary (c) Said/Wang-Ball patch (d) Said/Wang-Ball boundary (e) DP-Ball patch (f) DP-Ball boundary.	56
Figure 3.6	Control points set 4 by harmonic condition on (a) Bézier patch (b) Bézier boundary (c) Said/Wang-Ball patch (d) Said/Wang-Ball boundary (e) DP-Ball patch (f) DP-Ball boundary.	57

Figure 3.7	Control points set 1 by biharmonic condition on (a) Bézier patch (b) Bézier boundary (c) Said/Wang-Ball patch (d) Said/Wang-Ball boundary (e) DP-Ball patch (f) DP-Ball boundary.	70
Figure 3.8	Control points set 2 by biharmonic condition on (a) Bézier patch (b) Bézier boundary (c) Said/Wang-Ball patch (d) Said/Wang-Ball boundary (e) DP-Ball patch (f) DP-Ball boundary.	71
Figure 3.9	Control points set 3 by biharmonic condition on (a) Bézier patch (b) Bézier boundary (c) Said/Wang-Ball patch (d) Said/Wang-Ball boundary (e) DP-Ball patch (f) DP-Ball boundary.	72
Figure 3.10	Control points set 4 by biharmonic condition on (a) Bézier patch (b) Bézier boundary (c) Said/Wang-Ball patch (d) Said/Wang-Ball boundary (e) DP-Ball patch (f) DP-Ball boundary.	73
Figure 3.11	Control points set 1 by biharmonic condition on (a) Bézier patch (b) Said-Ball patch (c) Wang-Ball patch (d) DP-Ball patch (e) Bézier boundary (f) Said-Ball boundary (g) Wang-Ball boundary (h) DP-Ball boundary.	93
Figure 3.12	Control points set 2 by biharmonic condition on (a) Bézier patch (b) Said-Ball patch (c) Wang-Ball patch (d) DP-Ball patch (e) Bézier boundary (f) Said-Ball boundary (g) Wang-Ball boundary (h) DP-Ball boundary.	94
Figure 3.13	Control points set 3 by biharmonic condition on (a) Bézier patch (b) Said-Ball patch (c) Wang-Ball patch (d) DP-Ball patch (e) Bézier boundary (f) Said-Ball boundary (g) Wang-Ball boundary (h) DP-Ball boundary.	95
Figure 3.14	Control points set 4 by biharmonic condition on (a) Bézier patch (b) Said-Ball patch (c) Wang-Ball patch (d) DP-Ball patch (e) Bézier boundary (f) Said-Ball boundary (g) Wang-Ball boundary (h) DP-Ball boundary.	96
Figure 4.1	(a) Unit rectangle and (b) Said-Ball control points.	103
Figure 4.2	(a) 32 rectangles in the rectangular domain (b) 45 data points from positive function, $f(x,y)$	115
Figure 4.3	(a) 16 rectangles in the rectangular domain (b) 45 data points from positive function, $g(x,y)$	116
Figure 4.4	Edges Said/Wang-Ball control points for all rectangles (a) Test function $f(x,y)$ (b) Test function $g(x,y)$	117
Figure 4.5	Boundary curves for all rectangles (a) Test function 1, $f(x,y)$ (b) Test function 2, $g(x,y)$	117

Figure 4.6	Interpolating surface boundary curves (a) Test function 1, $f(x,y)$ (b) Test function 2, $g(x,y)$	117
Figure 4.7	Edges biquintic Said-Ball control points for all rectangles (a) Test function $f(x,y)$ (b) Test function $g(x,y)$	118
Figure 4.8	Quintic Boundary curves for all rectangles (a) Test function 1, $f(x,y)$ (b) Test function 2, $g(x,y)$	118
Figure 4.9	Interpolating biquintic surface boundary curves (a) Test function 1, $f(x,y)$ (b) Test function 2, $g(x,y)$	119
Figure 4.10	(a) Edges DP-Ball control points for all rectangles for test function $g(x,y)$ (b) Interpolating surface boundary curves for test function $g(x,y)$	119
Figure 4.11	(a) Edges biquintic DP-Ball control points for all rectangles for test function $g(x,y)$ (b) Interpolating biquintic surface boundary curves $g(x,y)$	120
Figure 4.12	Edges biquintic Wang-Ball control points for all rectangles (a) Test function $f(x,y)$ (b) Test function $g(x,y)$	120
Figure 4.13	Quintic boundary curves for all rectangles (a) Test function 1, $f(x,y)$ (b) Test function 2, $g(x,y)$	121
Figure 4.14	Interpolating biquintic surface boundary curves (a) Test function 1, $f(x,y)$ (b) Test function 2, $g(x,y)$	121
Figure 4.15	(a) Boundary curves of biquadratic Said-Ball surface generated by an extremal of the Dirichlet condition (b) surface of biquadratic Said-Ball surface generated by an extremal of the Dirichlet condition.	127
Figure 4.16	Control points set 1 by Dirichlet condition on (a) Bézier patch (b) Bézier boundary (c) Said/Wang-Ball patch (d) Said/Wang-Ball boundary (e) DP-Ball patch (f) DP-Ball boundary.	135
Figure 4.17	Control points set 2 by Dirichlet condition on (a) Bézier patch (b) Bézier boundary (c) Said/Wang-Ball patch (d) Said/Wang-Ball boundary (e) DP-Ball patch (f) DP-Ball boundary.	136
Figure 4.18	Control points set 3 by Dirichlet condition on (a) Bézier patch (b) Bézier boundary (c) Said/Wang-Ball patch (d) Said/Wang-Ball boundary (e) DP-Ball patch (f) DP-Ball boundary.	137
Figure 4.19	Control points set 4 by Dirichlet condition on (a) Bézier patch (b) Bézier boundary (c) Said/Wang-Ball patch (d) Said/Wang-Ball boundary (e) DP-Ball patch (f) DP-Ball boundary.	138
Figure 5.1	Function $G(s)$ with $s \geq 0$ for odd degree- n Said-Ball polynomial curve.	145
Figure 5.2	Function $G(s)$ with $s \geq 0$ for odd degree- n DP-Ball polynomial curve.	148

Figure 5.3	(a) Bicubic Said-Ball control points (b) A unit rectangle.	151
Figure 5.4	(a) Bicubic DP-Ball control points (b) A unit rectangle.	152
Figure 5.5	(a) Bicubic Wang-Ball control points (b) A unit rectangle.	153
Figure 5.6	Edges Said/Wang-Ball control points for all rectangles (a) Test function $f(x,y)$ (b) Test function $g(x,y)$	156
Figure 5.7	Boundary curves Said/Wang-Ball for all rectangles (a) Test function 1, $f(x,y)$ (b) Test function 2, $g(x,y)$	156
Figure 5.8	Interpolating Said/Wang-Ball surface boundary curves (a) Test function 1, $f(x,y)$ (b) Test function 2, $g(x,y)$	156
Figure 5.9	Test function $g(x,y)$ (a) Edges DP-Ball control points for all rectangles (b) Interpolating DP-Ball surface boundary curves.	157
Figure 5.10	Biquintic edges Said-Ball control points for all rectangles (a) Test function $f(x,y)$ (b) Test function $g(x,y)$	159
Figure 5.11	Biquintic boundary curves Said-Ball for all rectangles (a) Test function 1, $f(x,y)$ (b) Test function 2, $g(x,y)$	159
Figure 5.12	Interpolating biquintic Said-Ball surface boundary curves (a) Test function 1, $f(x,y)$ (b) Test function 2, $g(x,y)$	159
Figure 5.13	Test function $g(x,y)$ (a) Biquintic edges DP-Ball control points for all rectangles (b) Interpolating biquintic DP-Ball surface boundary curves.	160
Figure 5.14	Biquintic edges Wang-Ball control points for all rectangles (a) Test function $f(x,y)$ (b) Test function $g(x,y)$	160
Figure 5.15	Biquintic boundary curves Wang-Ball for all rectangles (a) Test function 1, $f(x,y)$ (b) Test function 2, $g(x,y)$	160
Figure 5.16	Interpolating biquintic Wang-Ball surface boundary curves (a) Test function 1, $f(x,y)$ (b) Test function 2, $g(x,y)$	161
Figure 5.17	(a) 2 by 2 Input pixels (b) 4 by 4 output pixels of by scaling factor 2 of input pixel.	164
Figure 5.18	(a) Rice (b) Cameraman (c) Nuvola (d) Pout (e) Tyre (f) Lena (g) Monkey Face (h) Pepper (i) Thumb.	167
Figure 5.19	Result using our proposed method for Rice test image (a) Input image (b) Image without interpolation (c) Image with proposed method.	168
Figure 5.20	Result using our proposed method for Cameraman test image (a) Input image (b) Image without interpolation (c) Image with proposed method.	169
Figure 5.21	Result using our proposed method for Nuvola test image (a) Input image (b) Image without interpolation (c) Image with proposed method.	170

Figure 5.22	Result using our proposed method for Pout test image (a) Input image (b) Image without interpolation (c) Image with proposed method.	171
Figure 5.23	Result using our proposed method for Tyre test image (a) Input image (b) Image without interpolation (c) Image with proposed method.	172
Figure 5.24	Result using our proposed method for Lena test image (a) Input image (b) Image without interpolation (c) Image with proposed method.	173
Figure 5.25	Result using our proposed method for Monkey test image (a) Input image (b) Image without interpolation (c) Image with proposed method.	174
Figure 5.26	Result using our proposed method for Pepper test image (a) Input image (b) Image without interpolation (c) Image with proposed method.	175
Figure 5.27	Result using our proposed method for Thumb test image (a) Input image (b) Image without interpolation (c) Image with proposed method.	176
Figure 5.28	Comparison between all image test by PSNR by using the proposed method, nearest neighbor, bilinear and bicubic methods.	177

List of Symbols

$B_i^n(t)$	Bernstein polynomial.
$S_i^n(t)$	Said-Ball basis function.
$D_i^n(t)$	DP-Ball basis function.
$A_i^n(t)$	Wang-Ball basis function.
P_{ij}	Bézier control points.
v_{ij}	Said-Ball control points.
d_{ij}	DP-Ball control points.
w_{ij}	Wang-Ball control points.
$B(u, v)$	Bézier rectangular surface.
$S(u, v)$	Said-Ball rectangular surface.
$D(u, v)$	DP-Ball rectangular surface.
$W(u, v)$	Wang-Ball rectangular surface.
\mathcal{B}	Bézier monomial matrix.
\mathcal{S}	Said-Ball monomial matrix.
\mathcal{C}	DP-Ball monomial matrix.
\mathcal{A}	Wang-Ball monomial matrix.
$\frac{\partial X(u, v)}{\partial u}$	Partial derivatives.
$\sum_{i=0}^n x_i$	The sum $x_0 + x_1 + \cdots + x_n$.
$\binom{n}{i}$	Binomial coefficients.
∇^2	Laplace operator.
∇^4	Bilaplace operator.
$B^n(t)$	Bézier curve on monomial matrix form.
$A^n(t)$	Wang-Ball curve on monomial matrix form.
$D^n(t)$	DP-Ball curve on monomial matrix form.
$S^n(t)$	Said-Ball curve on monomial matrix form.
\langle, \rangle	Inner product.
$\ \vec{X}\ $	Norm of vector \vec{X}
Δ	The usual difference operators.

CHAPTER ONE

INTRODUCTION

1.1 Research Background

Partial differential equations (PDEs) is a large subject with a history that goes back to Newton and Leibnitz. Many mathematical models involve functions which have the property that the value at a point depends on its value in a neighborhood. Dependencies like these can be modeled with a PDE. Famous examples are Newton's second law, Laplace's equation, Schrödinger's equation and Einstein's equations.

Geometric modeling using PDEs have been widely studied in computer graphics for over two decades and was first introduced in blend surface generation by Arnal, Monterde and Ugail (2011), Du and Qin (2004), Monterde (2004), Zhang and You (2004).

Advantages of the PDE methods have been gradually recognized by researchers. A principle advantage comes from the ability that the differential operator of PDEs can ensure the generation of smooth surfaces, where the smoothness is strictly governed by the order of the PDE used. A second advantage of using the PDE method is that the PDE surface can be generated by intuitively manipulating a relative small set of boundary curves. Moreover, the behavior of PDE surfaces has been proven to be compatible with underlying tensor product surfaces, such as Bézier surface (Monterde & Ugail, 2006), B-spline (Bloor & Wilson, 1990) and etc. These advantages have contributed to the widespread adoption of the PDE methods in a wide range of disciplines, such as free-form surface design, solid modeling computer aided manufacturing, shape morphing, web visualization, mesh reconstruct and facial geometry parameterization (Sheng, Sourin, Castro & Ugail, 2010).

Modeling a B-spline, Bézier or Ball surface at high degree is expensive in terms of computational time due to an excessive number of control points. To significantly solve this problem, a new method that can reduce computational time while retaining a highly accurate result will be used instead of all control points of B-spline, Bézier or Ball representations. Therefore the concept of PDE techniques plays a key role in this study.

Ball basis was presented by cubic polynomials over a fine interval. The work of Said (1989) was extended to a polynomial of arbitrary high odd degree and then used Hermite two-point Taylor interpolation theory to generalize the cubic basis functions of the Ball. Hence, the generalization enables higher order curves and surfaces to be defined and also develop a recursive algorithm for efficient computation of the generalized curves and surfaces Said (1989). For the sake of convenience, Hu, Wang and Jin (1996) suggested that the Said-Ball basis should be of arbitrary even degree. Wang (1986) also extended the Ball basis to arbitrary high degree. In 2003, Delgado and Peña (2003) introduced a new parametric curve representation of which the properties are normalized totally positive (NTP) basis functions, corner cutting algorithm and linear computational complexity. Previously, it was called DP-Ball curve (Dejdumrong, 2006; Jiang & Wang, 2005) though it has no relation with any of the generalized Ball curves (Itsariyawanich & Dejdumrong, 2008).

There are many properties of Ball curve and its generalized Said-Ball, DP-Ball and Wang-Ball curves such as positivity, partition of unity, convex hull property, recursive relation, degree elevation, degree reduction, and etc (Goodman & Said 1991; Hu, Wang & Sun, 1998; Hu et al., 1996; Said, 1989).

1.2 Problem Statement

The main point of this work is to show that the harmonic, biharmonic and Dirichlet Bézier surfaces are related to minimal surface, that is, a surface that minimizes the area among all surfaces with the prescribed boundary data. In the harmonic case, two boundary conditions are required to construct the surface, while in the biharmonic case, four boundary conditions are required to satisfy the fourth order elliptic PDE.

In this research, the focus will be on the construction of a generalized Ball surface representation using elliptic PDEs from the boundary curves information because to the best of our knowledge, this representation has not been investigated yet, although the Ball surface also play an important role in the surface modeling which is similar to the Bézier representation. The linear elliptic PDEs are chosen for the proposed method due to the fact that this type of PDEs have been widely used in many areas of sciences (Monterde and Ugail, 2006; Arnal et al., 2011).

1.3 Research Questions

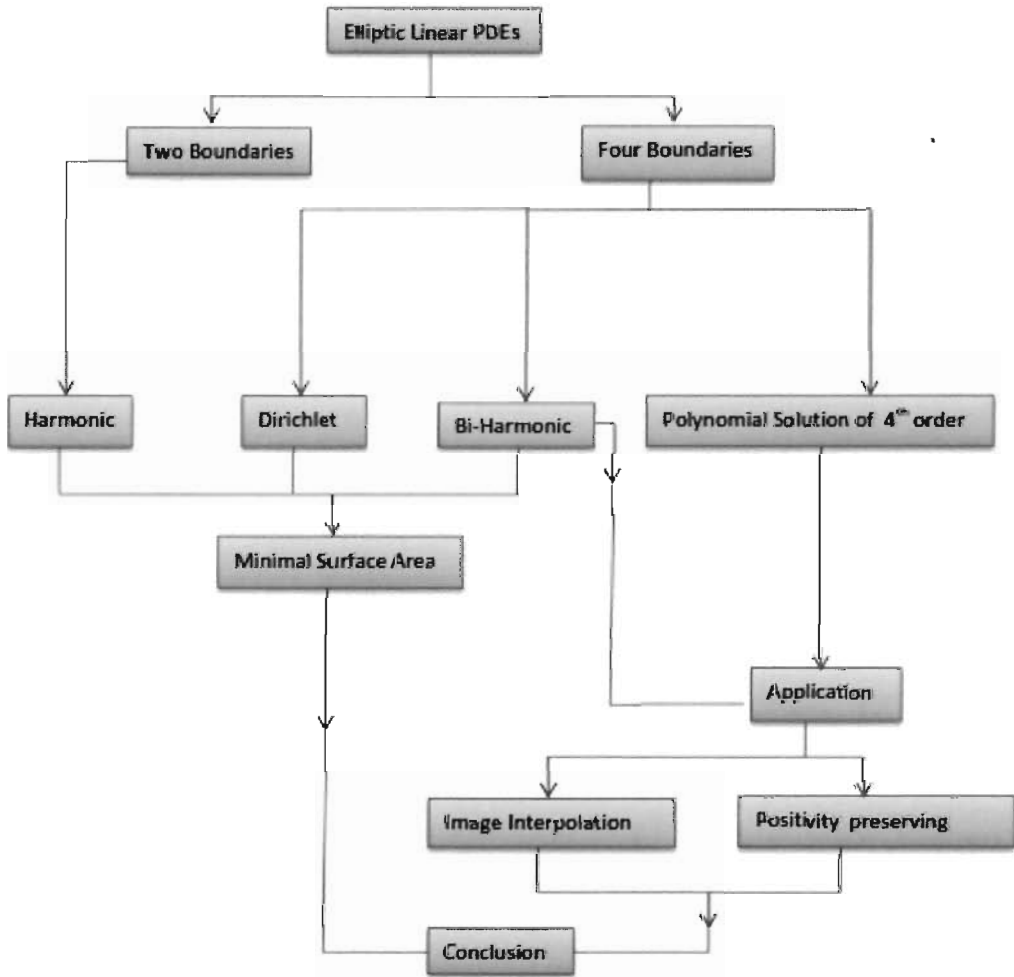
1. Does the concept of PDE techniques play a key role in the generalized Ball surfaces?
2. What is the lowest expense in terms of computational time due to an excessive number of control points for B-spline, Bézier or Ball at high degree?
3. What is the lowest expense in terms of computational time when interpolating an image ?

1.4 Objective of the Research

The main objective of this research is to develop an algorithm for constructing Ball surfaces from the Ball boundary curve of degree n using elliptic PDEs. In order to achieve this objective, we need to do the following:

1. To construct the generalized polynomial solutions, in terms of Ball surface and the different order linear elliptic PDEs satisfying a given the boundary Ball curves.
2. To compare the performance of the proposed algorithm with existing algorithm in terms of smoothness of constructing surface and computational time.
3. To apply the proposed method in the area of image enlargement using different test images.

1.5 Research Framework



1.6 Scope of the study

This study seeks to construct generalized Ball surfaces (Said-Ball, DP-Ball and Wang-Ball) from their boundary curves using fourth order elliptic linear PDEs. Next we compared our result for generalized Ball surface with the existing work for Bézier surface in terms of surface area and computational time. Finally, we applied our algorithm in positivity preserving and image enlargement.

1.7 Significance of the Study

The contributions of this study are twofold. Firstly, the findings of this study contribute towards the body of knowledge in the field of geometric modeling using PDEs. New ideas and concepts are introduced in this study and can be easily extended for future research. Secondly, the proposed method is applicable in the area of surface reconstruction and image processing.

1.8 Thesis Organization

In this thesis, a generalized Ball surface using PDEs is presented. The main contribution is generating Ball surface from their boundaries information. The first part of Chapter One gives a brief introduction of PDEs and Ball surface by explaining the criteria, objectives, and techniques that are used in generalized Ball surface, while the second part of the chapter talks about the problem statement, research questions, objective of the study, scope of the study, research framework, and organization of the thesis. Chapter Two starts with a brief overview of the Ball curves classification and its generalization by the use of PDEs techniques to produce Ball surfaces. The discussion of issues found in prior relation including PDEs adopting boundary value approach is added. This chapter concludes with a summary and justifying the PDEs methods as a theoretical basis for the present study. Chapter Three begins with the general algorithm for harmonic and biharmonic which holds for any surface used in Computer Aided Geometric Design (CAGD), that is applied to Ball surface and our proposed method is compared with the existing method for Bézier surface. Chapter Four begins with a more general polynomial solutions for any fourth-order differential equation and any square surface by using the monomial matrix form which is hold for any surface used in CAGD, which is also applied to Ball surface. This is followed by more general algorithm for Dirichlet functional for any surface used in CAGD, and we applied it to Ball surface. Chapter Five is about the implementations and applications

of our proposed algorithm for the interpolation of the generalized Ball surface with positivity preserving and enlarge images . Finally, Chapter Six concludes the study by addressing several recommendations. It also discusses the possible extensions of the study and scope for further investigation.

CHAPTER TWO

LITERATURE REVIEW

2.1 Introduction

This chapter begins with a brief overview of the classification of the Ball curves and its generalization by using partial differential equations (PDEs) method to generate Ball surfaces. This is followed by a discussion of issues found in prior relation including PDEs adopting boundary value approach. This chapter concludes with a summary and justification of the PDEs methods as a theoretical basis for the present study.

Ball (1974; 1975; 1977) introduced Ball basis function as cubic polynomial, and Said (1989), Delgado and Peña (2003a) and Wang (1987) further extended three different generalizations for high degree n polynomial that have been called the Said-Ball, DP-Ball and Wang-Ball, respectively. Their degree curve and surface can be obtained by overlapping interior control points (Said, 1989). Several researchers (Delgado & Peña, 2003b; Hu et al., 1996; Phien & Dejdumrong, 2000; Said, 1989; Aphirukmatakun & Dejdumrong, 2011; Goodman & Said, 1991) have theoretically come to their calculations, elevation and reduction (Monterde, 2004).

Ball (1974; 1975; 1977) explained lofting surface program CONSURF at British Aircraft Corporation by exploiting various basis functions. The basis functions used are cubic polynomials, but this is distinctive from that used in Bézier method (Bernstein polynomials). The method employed by Ball is comparable to Bézier method though they have the same shape independently. Later, the generalized form for polynomials of higher degree by Wang, Delgado and Peña; and Said namely Wang-Ball, DP-Ball and Said-Ball curves were presented, respectively (Wang, 1987; Delgado & Peña, 2003a; Said, 1989). The effectiveness of Said-Ball, DP-Ball and Wang-Ball basis were described in the works by Hu et al. (1996) and Delgado and Peña (2003a). In addi-

tion, Phien and Dejdumrong (2000) was regarded Said-Ball and Wang-Ball curves as effective methods in evaluating Bézier curves.

Introducing this work in terms of boundary based smooth surface design involves the development of methods for generating Bézier surfaces verifying elliptic boundary value problems with specific applications to boundary value problems associated with the Laplace equation as well as the biharmonic Bézier surfaces (Arnal et al., 2011; Wang & Guo, 2012; Arnal & Monterde, 2014). These surfaces are smooth polynomial surfaces which conforms to the harmonic (degree two) or biharmonic (degree four) PDEs and have the same formulations as Bézier surface.

The chosen fourth-order boundary value problem defines the boundaries of the surface patch alone, which will enable us to fully determine the entire surface. This polynomial solution method has been generalized to satisfy any fourth order biharmonic equation (Monterde & Ugail, 2006). Wang and Guo (2012) further extended the work of Monterde and Ugail (2006) into degree $m \times n$.

2.2 Review on Bézier Curves

Bézier curves of degree n with $n+1$ control points $\{b_i\}_{i=0}^n$ can be defined by (Aphirukmatakun & Dejdumrong, 2007; Farin, 2002)

$$B(t) = \sum_{i=0}^n b_i B_i^n(t), 0 \leq t \leq 1, \quad (2.1)$$

where $B_i^n(t)$ are Bernstein polynomials defined by:

$$B_i^n(t) = \binom{n}{i} t^i (1-t)^{(n-i)}. \quad (2.2)$$

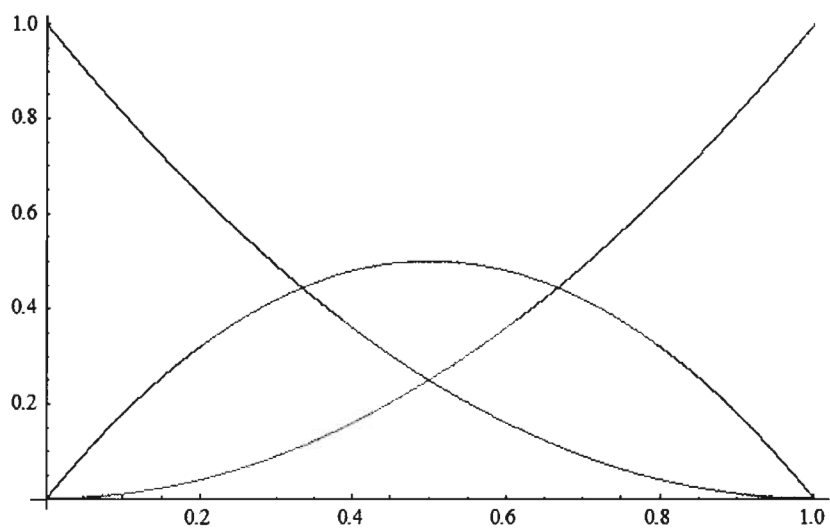


Figure 2.1. The Bernstein polynomials of degree two.

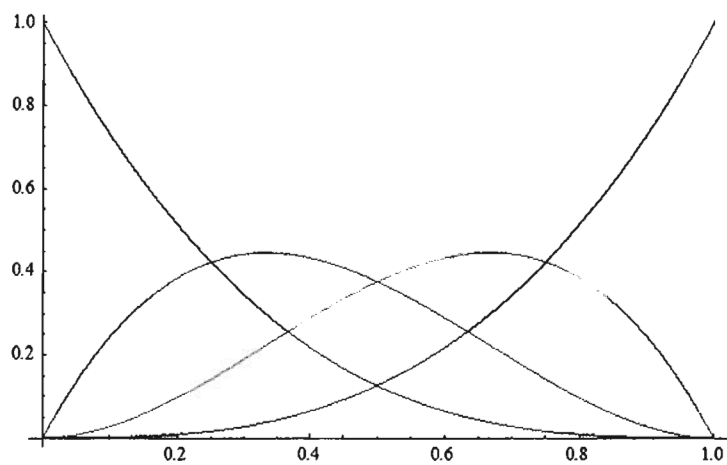


Figure 2.2. The Bernstein polynomials of degree three.

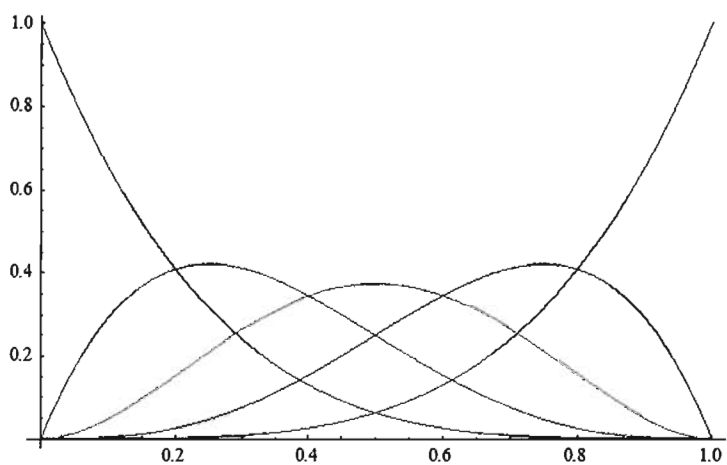


Figure 2.3. The Bernstein polynomials of degree four.

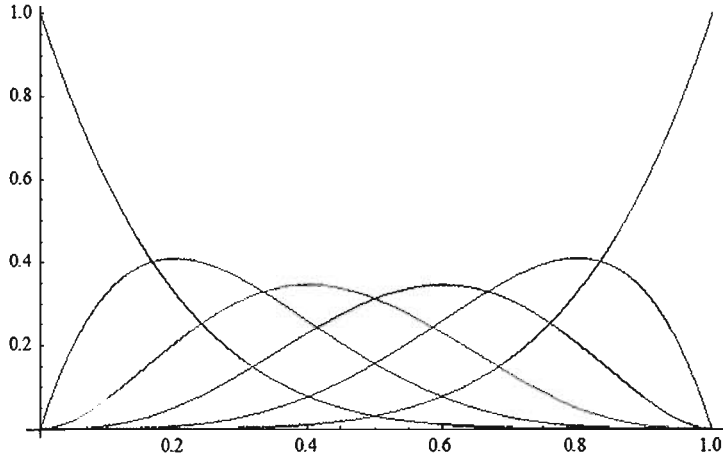


Figure 2.4. The Bernstein polynomials of degree five.

Bernstein basis function satisfies the following properties:

- i. $B_i^n(t) \geq 0, \forall i = 0, 1, \dots, n$.
- ii. $\sum_{i=0}^n B_i^n(t) = 1$.

Since Bernstein polynomials satisfies properties (i) and (ii), it implies the convex combination of its control points. Therefore, the curve lies in the convex hull of its control points (Farin, 2002).

2.2.1 Derivative and Integral of Bernstein Polynomials

The derivative and the integral of Bernstein polynomials are given by Farin (2002):

$$\frac{d}{dt} B_i^n(t) = n(B_{i-1}^{n-1}(t) - B_i^{n-1}(t)), \quad (2.3)$$

and

$$\int_0^1 B_i^n(t) dt = \frac{1}{n+1}. \quad (2.4)$$

2.2.2 Bézier Monomial Form

A Bézier curve of degree n , denoted by $B(t)$, with $n + 1$ control points, denoted by $\{b_i\}_{i=0}^n$, can be written in terms of the power basis as follows

$$B(t) = \sum_{i=0}^n \sum_{j=0}^n b_i m_{i,j} t^j, 0 \leq t \leq 1, \quad (2.5)$$

where

$$m_{ij} = (-1)^{(j-i)} \binom{n}{j} \binom{j}{i}. \quad (2.6)$$

2.2.3 Degree Elevation of Bézier Curves

We can raise the degree of Bézier curves by one by adding one new control point. We are thus looking for a curve with control point $\{b_i^{(1)}\}_{i=0}^{n+1}$ that describes the same curve with the original control points $\{b_i\}_{i=0}^n$. Bézier curve can be defined in terms of its control points by the following formula (Aphirukmatakun & Dejdumrong, 2007; Farin, 2002)

$$b_i^{(1)} = \frac{i}{n+1} b_{i-1} + \left(1 - \frac{i}{n+1}\right) b_i, i = 0, 1, 2, \dots, n = 1. \quad (2.7)$$

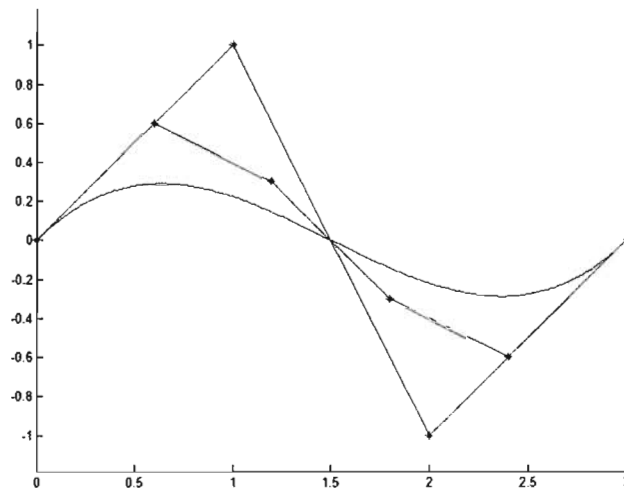


Figure 2.5. Degree elevation of Bézier curve from three to six.

Lemma 3.1: Given a Bernstein polynomial $B_i^n(t)$, we have (Monterde & Ugail, 2004),

$$B_i^{n-k}(t) = \sum_{l=0}^k \frac{\binom{n-i-l}{k-l} \binom{i+l}{l}}{\binom{n}{k}} B_{i+l}^n(t), \quad (2.8)$$

$$\forall n > 0, k \in \{0, 1, \dots, n\} \text{ and } i \in \{0, 1, \dots, n-k\}.$$

2.2.4 Bézier Rectangular Surfaces

The Bézier surfaces of degree $m \times n$ with control points $\{p_{i,j}\}_{i,j=0}^{m,n}$ can be expressed as

$$B(u, v) = \sum_{i=0}^m \sum_{j=0}^n B_i^m(u) B_j^n(v) p_{i,j}, \quad 0 \leq u, v \leq 1, \quad (2.9)$$

where $B_i^m(u)$ and $B_j^n(v)$ are the Bernstein basis (Wang & Cheng, 2001).

2.3 Review on Ball Curves

The curve was declared by A. A. Ball in his well-known aircraft design system CON-SURF in Ball (1974). It is described as a cubic polynomial curve and explained mathematically as:

$$(1-t)^2, 2t(1-t)^2, 2t^2(1-t), t^2. \quad (2.10)$$

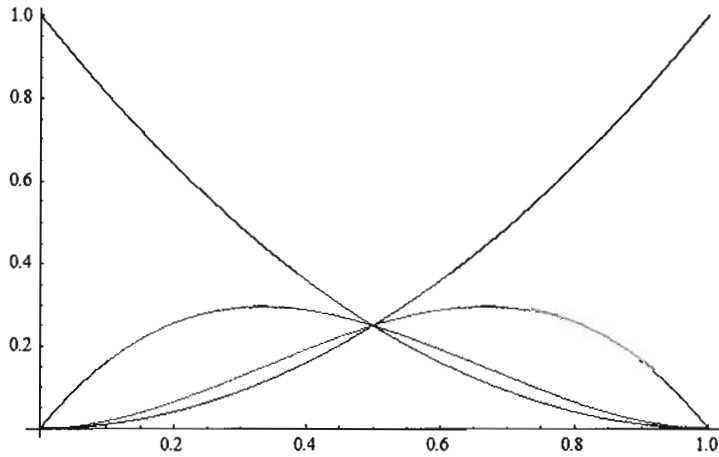


Figure 2.6. Cubic Ball basis functions.

In further research, several studies have discussed about Ball curve's high generalization and its properties. For instance, in the 1980s there were two different Ball curves of arbitrary degree (Hu et al., 1996; Said, 1989; Wang, 1987) and in 2003 there was another generalization of Ball curve called DP-Ball (Delgado & Peña, 2003a).

2.3.1 Said-Ball Representation

The Said-Ball curves of degree n with $n + 1$ control points $\{v_i\}_{i=0}^n$ can be given by:

$$S(t) = \sum_{i=0}^n S_i^n(t) v_i, \quad (2.11)$$

where $S_i^n(t)$ are Said-Ball polynomials defined by:

$$S_i^n(t) = \begin{cases} \binom{\frac{n-1}{2}+i}{i} t^i (1-t)^{\frac{n-1}{2}+1} & , \text{for } 0 \leq i \leq \frac{n-1}{2}, \\ \binom{\frac{n-1}{2}+n-i}{n-i} t^{\frac{n-1}{2}+1} (1-t)^{n-i} & , \text{for } \frac{n+1}{2} \leq i \leq n, \end{cases} \quad (2.12)$$

when n is odd, and

$$S_i^n(t) = \begin{cases} \binom{\frac{n}{2}+i}{i} t^i (1-t)^{\frac{n}{2}+1} & , \text{for } 0 \leq i \leq \frac{n}{2} - 1, \\ \binom{\frac{n}{2}}{\frac{n}{2}} t^{\frac{n}{2}} (1-t)^{\frac{n}{2}} & , \text{for } i = \frac{n}{2}, \\ \binom{\frac{n}{2}+n-i}{n-i} t^{\frac{n}{2}+1} (1-t)^{n-i} & , \text{for } \frac{n}{2} \leq i \leq n, \end{cases} \quad (2.13)$$

when n is even (Aphirukmatakun & Dejdumrong, 2007; Dan & Xinmeng, 2007; Hu et al., 1996; Said, 1989).

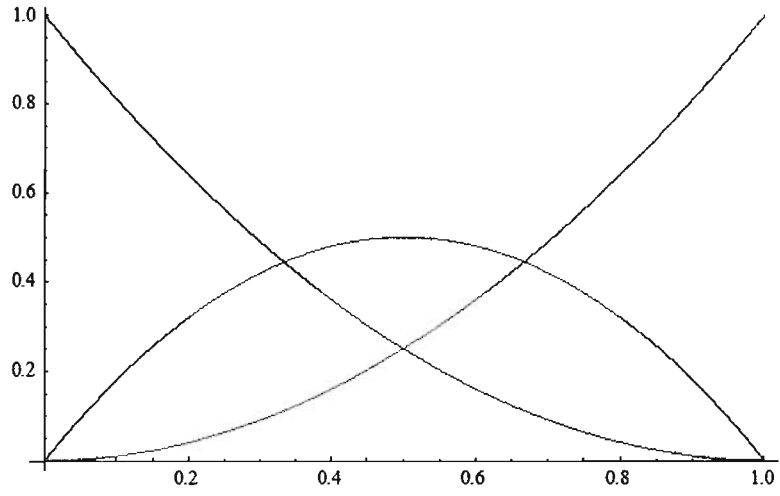


Figure 2.7. Said-Ball basis functions of degree two.

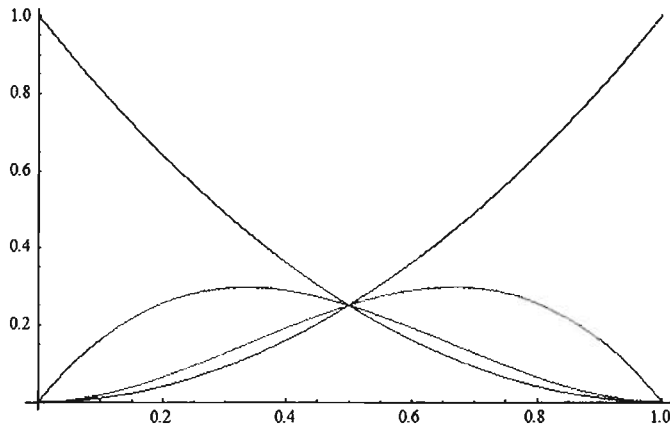


Figure 2.8. Said-Ball basis functions of degree three.

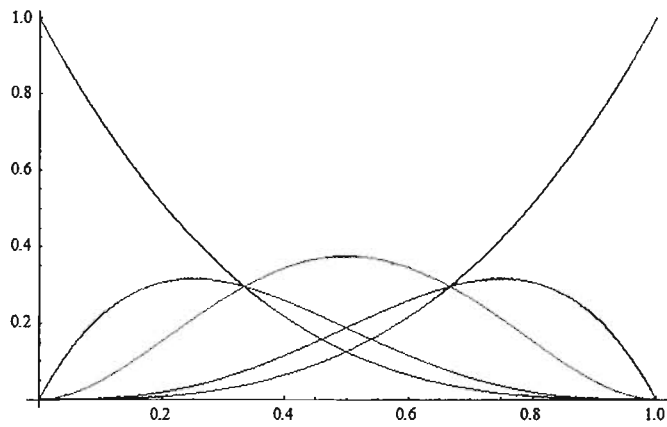


Figure 2.9. Said-Ball basis functions of degree four.

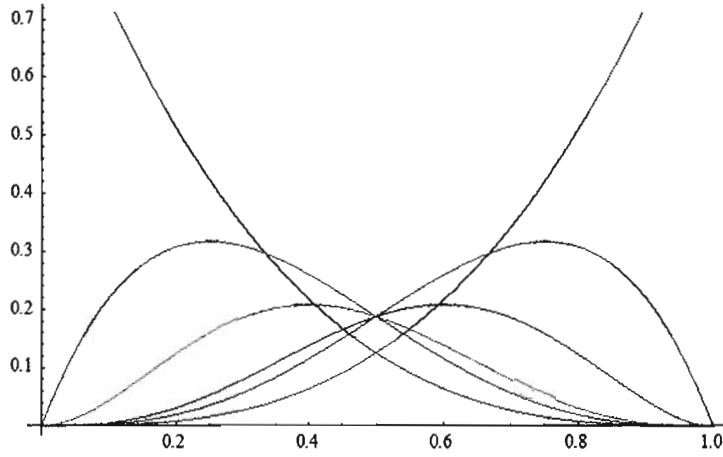


Figure 2.10. Said-Ball basis functions of degree five.

The Said-Ball basis function satisfies the following properties:

- i. The Said-Ball basis function is non-negative, that is,

$$S_i^n(t) \geq 0, \forall i = 0, 1, \dots, n. \quad (2.14)$$

- ii. The partition of unity, that is,

$$\sum_{i=0}^n S_i^n(t) = 1. \quad (2.15)$$

The fact that the Said-Ball basis fulfills the above properties implies the convex combination of its control points. Hence, the curve lies in the convex hull of its control points (Hu et al., 1996).

2.3.1.1 Said-Ball Monomial Form

A Said-Ball curve of degree n , denoted by $S(t)$, with $n + 1$ control points, denoted by $\{v_i\}_{i=0}^n$, can be written in terms of the power basis as follows

$$S(t) = \sum_{i=0}^n \sum_{j=0}^n v_i s_{i,j} t^j, 0 \leq t \leq 1, \quad (2.16)$$

where

$$s_{ij} = \begin{cases} (-1)^{(j-i)} \binom{i+\lfloor \frac{n}{2} \rfloor}{i} \binom{\lfloor \frac{n}{2} \rfloor + 1}{j-i}, & \text{for } 0 \leq i \leq \lfloor \frac{n}{2} \rfloor, \\ (-1)^{(j-i)} \binom{n}{i} \binom{i}{j-i}, & \text{for } i = \frac{n}{2}, \\ (-1)^{(j-\lfloor \frac{n}{2} \rfloor - i)} \binom{\lfloor \frac{n}{2} \rfloor + n - i}{n-i} \binom{n-i}{j-\lfloor \frac{n}{2} \rfloor - 1}, & \text{for } \lfloor \frac{n}{2} \rfloor + 1 \leq i \leq n, \end{cases} \quad (2.17)$$

and $\lfloor x \rfloor$ and $\lceil x \rceil$ denote the greatest integer less than or equal to x , and the least integer greater than or equal to x , respectively.

2.3.1.2 Conversion of Said-Ball Curve to Bézier Curve

The converting formula for basis from Said-Ball to Bézier is given as follows (Hu et al., 1996; Aphirukmatakun & Dejdumrong, 2007):

$$\begin{bmatrix} S_0^n(t) \\ S_1^n(t) \\ \vdots \\ S_i^n(t) \\ \vdots \\ S_n^n(t) \end{bmatrix} = \begin{bmatrix} c_{00} & c_{01} & \cdots & \cdots & \cdots & c_{0n} \\ c_{10} & c_{11} & \ddots & & & c_{1n} \\ \vdots & \vdots & \ddots & \ddots & & \vdots \\ c_{i0} & c_{i1} & \cdots & \ddots & & c_{in} \\ \vdots & \vdots & & & \ddots & \ddots \\ c_{n0} & c_{n1} & \cdots & \cdots & \cdots & c_{nn} \end{bmatrix} \begin{bmatrix} B_0^n(t) \\ B_1^n(t) \\ \vdots \\ B_i^n(t) \\ \vdots \\ B_n^n(t) \end{bmatrix}, \quad (2.18)$$

where $S_i^n(t), B_i^n(t), i \in \{0, 1, \dots, n\}$ are Said-Ball basis functions and Bernstein basis functions, respectively. Thus from (2.18), we have

$$S_i^n(u) = \sum_{f=0}^n c_{if} B_f^n(u). \quad (2.19)$$

A Said-Ball control point can be written as an associate Bézier control point as follows:

$$[b_0 \ b_1 \ \dots \ b_n] = [v_0 \ v_1 \ \dots \ v_n] \begin{bmatrix} c_{00} & c_{01} & \dots & \dots & \dots & c_{0n} \\ c_{10} & c_{11} & \ddots & & & c_{1n} \\ \vdots & \vdots & \ddots & \ddots & & \vdots \\ c_{i0} & c_{i1} & \dots & \ddots & & c_{in} \\ \vdots & \vdots & & & \ddots & \ddots \\ c_{n0} & c_{n1} & \dots & \dots & \dots & c_{nn} \end{bmatrix}. \quad (2.20)$$

and

$$c_{i,j} = \begin{cases} \frac{\binom{\frac{n}{2}+i}{i} \binom{\frac{n}{2}-i-1}{j-i}}{\binom{n}{j}}, & \text{for } i \leq j \leq \frac{n}{2} - 1, \\ \frac{\binom{\frac{3}{2}n-i}{n-i} \binom{i-1-\frac{n}{2}}{i-j}}{\binom{n}{j}}, & \text{for } i \geq j \geq \frac{n}{2} + 1, \\ 1 & \text{for } i = j = \frac{n}{2}, \\ 0 & \text{otherwise,} \end{cases} \quad (2.21)$$

when n is even, and

$$c_{i,j} = \begin{cases} \frac{\binom{\frac{n-1}{2}+i}{i} \binom{\frac{n-1}{2}-i}{j-i}}{\binom{n}{j}}, & \text{for } i \leq j \leq \frac{n-1}{2}, \\ \frac{\binom{\frac{3n-1}{2}-i}{n-i} \binom{i-\frac{n+1}{2}}{i-j}}{\binom{n}{j}}, & \text{for } i \geq j \geq \frac{n+1}{2}, \end{cases} \quad (2.22)$$

when n is odd.

2.3.1.3 Said-Ball Rectangular Surfaces

The Said-Ball surfaces of degree $m \times n$ with control points $\{v_{i,j}\}_{i,j=0}^{m,n}$ can be expressed as

$$S(u, v) = \sum_{i=0}^m \sum_{j=0}^n S_i^m(u) S_j^n(v) v_{i,j}, \quad 0 \leq u, v \leq 1, \quad (2.23)$$

where $S_i^m(u)$ and $S_j^n(v)$ are the Said-Ball basis (Wang & Cheng, 2001).

2.3.1.4 Converting Said-Ball Surface into Bézier Surface

The Said-Ball surface of degree $m \times n$ in (2.23) can be written in matrix form as

$$X(u, v) = S_u V S_v, \quad (2.24)$$

where $S_u = [S_0^m(u) \ S_1^m(u) \ \cdots \ S_m^m(u)]$, $S_v = [S_0^n(v) \ S_1^n(v) \ \cdots \ S_n^n(v)]^T$,

$$V = \begin{bmatrix} v_{00} & v_{01} & \cdots & v_{0n} \\ v_{10} & v_{11} & \cdots & v_{1n} \\ \vdots & \vdots & \ddots & \cdots \\ v_{m0} & v_{m1} & \cdots & v_{mn} \end{bmatrix},$$

and $v_{ij}, i \in \{0, 1, \dots, m\}, j \in \{0, 1, \dots, n\}$ are the control points of the Said-Ball surface. By using (2.18) in (2.24) we get

$$\begin{aligned} X(u, v) &= (CB_u)^t V (HB_v) \\ &= (B_u^t C^t) V (HB_v) \\ &= B_u^t (C^t V H) B_v \\ &= B_u^t P B_v \end{aligned} \quad (2.25)$$

where $P = FVH$, $F = C^t$ and F, H are square matrices of order m and n , respectively, given by (2.21) and (2.22). Now, we rewrite (2.25) as

$$X(u, v) = \sum_{i=0}^m \sum_{j=0}^n B_i^m(u) B_j^n(v) P_{ij}, \quad (2.26)$$

where

$$P_{ij} = \sum_{r=0}^m \sum_{s=0}^n f_{ir} v_{rs} h_{sj}, \quad i \in \{0, 1, \dots, m\}, \quad j \in \{0, 1, \dots, n\}, \quad (2.27)$$

which is the Bézier surface of degree $m \times n$, where v_{ij} are Said-Ball control points.

2.3.2 DP-Ball Curves Representation

The degree n DP-Ball curves with $n + 1$ control points $\{d_i\}_{i=0}^n$, is defined by

$$D(t) = \sum_{i=0}^n d_i D_i^n(t), \quad 0 \leq t \leq 1, \quad (2.28)$$

where $D_i^n(t)$ are DP-Ball polynomials (Delgado & Peña, 2003a) defined by:

$$D_i^n(t) = \begin{cases} (1-t)^n & , \text{for } i = 0, \\ t(1-t)^{n-i} & , \text{for } 1 \leq i \leq \lfloor \frac{n}{2} \rfloor - 1, \\ K_1^n(t) + K_2^n(t) & , \text{for } i = \lfloor \frac{n}{2} \rfloor, \\ K_1^n(t) + K_3^n(t) & , \text{for } i = \lceil \frac{n}{2} \rceil, \\ D_{n-i}^n(1-t) & , \text{for } \lfloor \frac{n}{2} \rfloor + 1 \leq i \leq n, \end{cases} \quad (2.29)$$

and

$$\begin{aligned} K_1^n(t) &= \left(\frac{1}{2}\right)^{\lceil \frac{1}{2} \rceil - \lfloor \frac{1}{2} \rfloor} \left(1 - t^{\lfloor \frac{1}{2} \rfloor + 1} - (1-t)^{\lfloor \frac{1}{2} \rfloor + 1}\right), \\ K_2^n(t) &= \left(\lceil \frac{1}{2} \rceil - \lfloor \frac{1}{2} \rfloor\right) t(1-t)^{\lfloor \frac{1}{2} \rfloor + 1}, \\ K_3^n(u) &= \left(\lceil \frac{1}{2} \rceil - \lfloor \frac{1}{2} \rfloor\right) t^{\lfloor \frac{1}{2} \rfloor + 1} (1-t). \end{aligned}$$

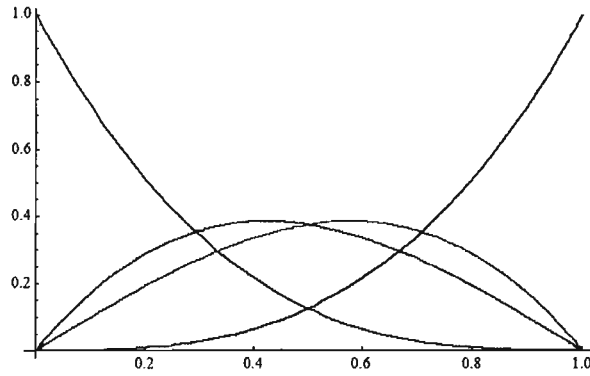


Figure 2.11. DP-Ball basis function of degree three.

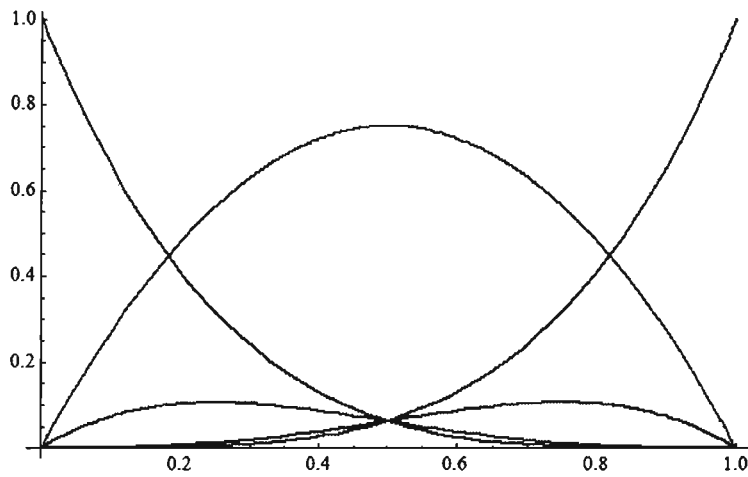


Figure 2.12. DP-Ball basis function of degree four.

The DP-Ball basis function satisfies the following properties:

- i. $D_i^n(t) \geq 0, \forall i = 0, 1, \dots, n.$
- ii. $\sum_{i=0}^n D_i^n(t) = 1.$

Since the DP-Ball satisfies properties (i) and (ii), it implies the convex combination of its control points. Therefore, the curve lies in the convex hull of its control points.

2.3.2.1 DP Monomial Form

An n^{th} -degree DP curve, denoted by $D(t)$, given by a set of $n + 1$ control points, denoted by $\{d_i\}_{i=0}^n$ can be formulated in power basis form by

$$D(t) = \sum_{i=0}^n \sum_{j=0}^n d_i c_{ij} t^j, \quad (2.30)$$

where

$$c_{ij} = \begin{cases} (-1)^j \binom{n}{j}, & \text{for } i = 0, \\ (-1)^{j-1} \binom{n-i}{j-1}, & \text{for } 0 < i \leq \lfloor \frac{n}{2} \rfloor - 1, \\ (-1)^{j-1} (n-2i) \binom{i+1}{j-1} + \frac{1}{2} n^{-2i} \left(\binom{0}{j} - \binom{0}{j-i-1} - (-1)^j \binom{i+1}{j} \right), & \text{for } i = \lfloor \frac{n}{2} \rfloor, \\ (-1)^{j-n+i} (n-2i) \binom{1}{j-n+i-1} + \frac{1}{2} 2^{i-n} \left(\binom{0}{j} - \binom{0}{j-n+i-1} - (-1)^j \binom{n-i+1}{j} \right), & \text{for } i = \lceil \frac{n}{2} \rceil, \\ (-1)^{(j-i)} \binom{1}{j-i}, & \text{for } \lceil \frac{n}{2} \rceil + 1 \leq i \leq n-1, \\ \binom{0}{j-n}, & \text{for } i = n, \end{cases} \quad (2.31)$$

$\lfloor x \rfloor$ and $\lceil x \rceil$ denotes the greatest integer less than or equal to x , and the least integer greater than or equal to x , respectively.

2.3.2.2 Conversion of DP-Ball Curve to Bézier Curve

The formula for converting between DP-Ball Curve and Bézier curve (Aphirukmatakun & Dejdumrong, 2007) are given as follows

$$\begin{bmatrix} D_0^n(t) \\ D_1^n(t) \\ \vdots \\ D_i^n(t) \\ \vdots \\ D_n^n(t) \end{bmatrix} = \begin{bmatrix} c_{00} & c_{01} & \cdots & \cdots & \cdots & c_{0n} \\ c_{10} & c_{11} & \ddots & & & c_{1n} \\ \vdots & \vdots & \ddots & \ddots & & \vdots \\ c_{i0} & c_{i1} & \cdots & \ddots & & c_{in} \\ \vdots & \vdots & & & \ddots & \ddots \\ c_{n0} & c_{n1} & \cdots & \cdots & \cdots & c_{nn} \end{bmatrix} \begin{bmatrix} B_0^n(t) \\ B_1^n(t) \\ \vdots \\ B_i^n(t) \\ \vdots \\ B_n^n(t) \end{bmatrix}. \quad (2.32)$$

Thus we have,

$$D_i^n(t) = \sum_{f=0}^n \sum_{i=0}^n c_{if} B_f^n(t). \quad (2.33)$$

A DP-Ball control point can be written as an associate Bézier control point as follows:

$$[b_0 \ b_1 \ \cdots \ b_n] = [d_0 \ d_1 \ \cdots \ d_n] \begin{bmatrix} c_{00} & c_{01} & \cdots & \cdots & \cdots & c_{0n} \\ c_{10} & c_{11} & \ddots & & & c_{1n} \\ \vdots & \vdots & \ddots & \ddots & & \vdots \\ c_{i0} & c_{i1} & \cdots & \ddots & & c_{in} \\ \vdots & \vdots & & & \ddots & \ddots \\ c_{n0} & c_{n1} & \cdots & \cdots & \cdots & c_{nn} \end{bmatrix}, \quad (2.34)$$

where $D_i^n(t), B_i^n(t), i \in \{0, 1, \dots, n\}$ are DP-Ball basis functions and Bernstein basis functions, respectively, while C is the convert matrix given by:

$$c_{ij} = \begin{cases} 1 & , \text{for } i = j = 0 \text{ or } i = j = n, \\ \frac{j \binom{n-j}{n-i}}{n \binom{n-i}{n-i}} & , \text{for } 1 \leq j \leq i, 1 \leq i \leq \lfloor \frac{n}{2} \rfloor - 1, \\ \frac{(n-j) \binom{j}{i}}{(n-i) \binom{n}{i}} & , \text{for } i \leq j \leq n-1, \lfloor \frac{n}{2} \rfloor + 1 \leq i \leq n-1. \end{cases} \quad (2.35)$$

If n is even, then

$$c_{ij} = \begin{cases} 1 - \frac{\binom{n-j}{\lfloor \frac{n}{2} \rfloor + 1} - \binom{j}{\lfloor \frac{n}{2} \rfloor + 1}}{\binom{n}{\lfloor \frac{n}{2} \rfloor + 1}} & , \text{for } 1 \leq j \leq \lfloor \frac{n}{2} \rfloor \text{ and } i = \lfloor \frac{n}{2} \rfloor, \\ 1 - \frac{\binom{j}{\lfloor \frac{n}{2} \rfloor + 1} - \binom{n-j}{\lfloor \frac{n}{2} \rfloor + 1}}{\binom{n}{\lfloor \frac{n}{2} \rfloor + 1}} & , \text{for } \lceil \frac{n}{2} \rceil \leq j \leq n-1 \text{ and } i = \lfloor \frac{n}{2} \rfloor, \\ 0 & , \text{otherwise;} \end{cases} \quad (2.36)$$

but if n is odd,

$$c_{ij} = \begin{cases} \frac{1}{2} \left[1 - \frac{\binom{n-j}{\lfloor \frac{n}{2} \rfloor + 1} - \binom{j}{\lfloor \frac{n}{2} \rfloor + 1}}{\binom{n}{\lfloor \frac{n}{2} \rfloor + 1}} \right] + \frac{2j \binom{n-j}{\lfloor \frac{n}{2} \rfloor + 1}}{(n-1) \binom{n}{\lfloor \frac{n}{2} \rfloor + 1}} \\ \text{for } 1 \leq j \leq \lfloor \frac{n}{2} \rfloor \text{ and } i = \lfloor \frac{n}{2} \rfloor, \\ \frac{1}{2} \left[1 - \frac{\binom{n-j}{\lfloor \frac{n}{2} \rfloor + 1} - \binom{j}{\lfloor \frac{n}{2} \rfloor + 1}}{\binom{n}{\lfloor \frac{n}{2} \rfloor + 1}} \right] + \frac{(n-j) \binom{j}{\lfloor \frac{n}{2} \rfloor + 1}}{n \binom{n-1}{\lfloor \frac{n}{2} \rfloor + 1}} \\ \text{for } 1 \leq j \leq \lfloor \frac{n}{2} \rfloor \text{ and } i = \lceil \frac{n}{2} \rceil, \\ \frac{1}{2} \left[1 - \frac{\binom{j}{\lfloor \frac{n}{2} \rfloor + 1} - \binom{n-j}{\lfloor \frac{n}{2} \rfloor + 1}}{\binom{n}{\lfloor \frac{n}{2} \rfloor + 1}} \right] + \frac{j \binom{n-j}{\lfloor \frac{n}{2} \rfloor + 1}}{n \binom{n-1}{\lfloor \frac{n}{2} \rfloor + 1}} \\ \text{for } \lceil \frac{n}{2} \rceil \leq j \leq n-1 \text{ and } i = \lfloor \frac{n}{2} \rfloor, \\ \frac{1}{2} \left[1 - \frac{\binom{j}{\lfloor \frac{n}{2} \rfloor + 1} - \binom{n-j}{\lfloor \frac{n}{2} \rfloor + 1}}{\binom{n}{\lfloor \frac{n}{2} \rfloor + 1}} \right] + \frac{2(n-j) \binom{j}{\lfloor \frac{n}{2} \rfloor + 1}}{(n-1) \binom{n}{\lfloor \frac{n}{2} \rfloor + 1}} \\ \text{for } \lceil \frac{n}{2} \rceil \leq j \leq n-1 \text{ and } i = \lceil \frac{n}{2} \rceil, \\ 0, \text{ otherwise.} \end{cases} \quad (2.37)$$

2.3.2.3 DP-Ball Rectangular Surfaces

The DP-Ball surfaces of degree $m \times n$ with control points $\{d_{i,j}\}_{i,j=0}^{m,n}$ can be expressed as

$$D(u, v) = \sum_{i=0}^m \sum_{j=0}^n D_i^m(u) D_j^n(v) d_{i,j}, \quad 0 \leq u, v \leq 1, \quad (2.38)$$

where $D_i^m(u)$ and $D_j^n(v)$ are the DP-Ball basis (Wang & Cheng, 2001).

2.3.2.4 Converting DP-Ball Surface into Bézier Surface

The DP-Ball surface of degree $m \times n$ in (2.38) can be written in matrix form as

$$X(u, v) = D_u D D_v \quad (2.39)$$

where $D_u = [D_0^m(u) D_1^m(u) \cdots D_m^m(u)]$, $D_v = [D_0^n(v) D_1^n(v) \cdots D_n^n(v)]^T$,

$$D = \begin{bmatrix} d_{00} & d_{01} & \cdots & d_{0n} \\ d_{10} & d_{11} & \cdots & d_{1n} \\ \cdots & \cdots & \cdots & \cdots \\ d_{m0} & d_{m1} & \cdots & d_{mn} \end{bmatrix},$$

and $d_{ij}, i \in \{0, 1, \dots, m\}, j \in \{0, 1, \dots, n\}$ are the control points of the DP-Ball surface.

By using (2.28) in (2.39) we get

$$\begin{aligned} X(u, v) &= (CB_u)^t D(HB_v) \\ &= (B_u^t C^t) D(HB_v) \\ &= B_u^t (C^t D H) B_v \\ &= B_u^t P B_v \end{aligned} \tag{2.40}$$

where $P = FDH$, $F = C^t$ and F, H are square matrices of order m and n , respectively, given by (2.35), (2.36) and (2.37). Now, we rewrite (2.40) as

$$X(u, v) = \sum_{i=0}^m \sum_{j=0}^n B_i^m(u) B_j^n(v) P_{ij}, \tag{2.41}$$

where

$$P_{ij} = \sum_{r=0}^m \sum_{s=0}^n f_{ir} d_{rs} h_{sj}, \quad i \in \{0, 1, \dots, m\}, \quad j \in \{0, 1, \dots, n\}, \tag{2.42}$$

which is the Bézier surface of degree $m \times n$, where d_{ij} are DP-Ball control points.

2.3.3 Wang-Ball Curves

Wang-Ball curves of degree n with $n + 1$ control points, $\{w_i\}_{i=0}^n$ (Aphirukmatakun & Dejdumrong, 2007; Hu et al., 1996; Wang, 1987) can be defined by:

$$A(t) = \sum_{i=0}^n w_i A_i^n(t), \quad 0 \leq t \leq 1, \quad (2.43)$$

where $A(t)$ are Wang-Ball polynomials defined by:

$$A_i^n(t) = \begin{cases} (1-t)^{2+i}(2t)^i & , 0 \leq i \leq \frac{n-3}{2}, \\ (1-t)^{\frac{n+1}{2}}(2t)^{\frac{n-1}{2}} & , i = \frac{n-1}{2}, \\ (2(1-t)^{\frac{n-1}{2}}t^{\frac{n+1}{2}} & , i = \frac{n+1}{2}, \\ (2t(1-t))^{n-i}t^{n-i+2} & , \frac{n+3}{2} \leq i \leq n, \end{cases} \quad (2.44)$$

when n is odd, and

$$A_i^n(t) = \begin{cases} (1-t)^{2+i}(2t)^i & , 0 \leq i \leq \frac{n}{2} - 1, \\ (2t(1-t))^{\frac{n}{2}} & , i = \frac{n}{2}, \\ (2(1-t))^{n-i}t^{n-i+2} & , \frac{n+3}{2} \leq i \leq n, \end{cases} \quad (2.45)$$

when n is even.

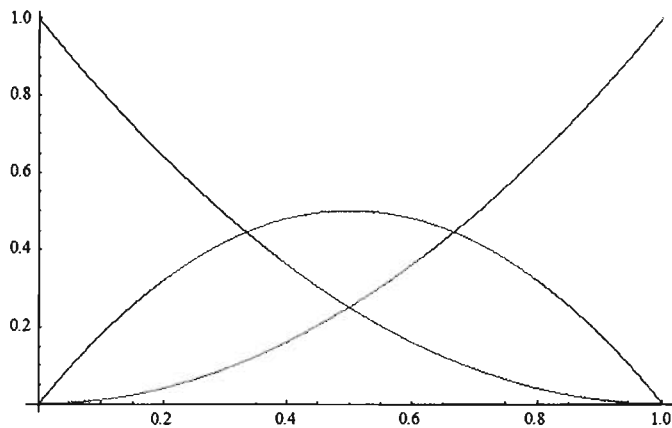


Figure 2.13. Wang-Ball basis function of degree two.

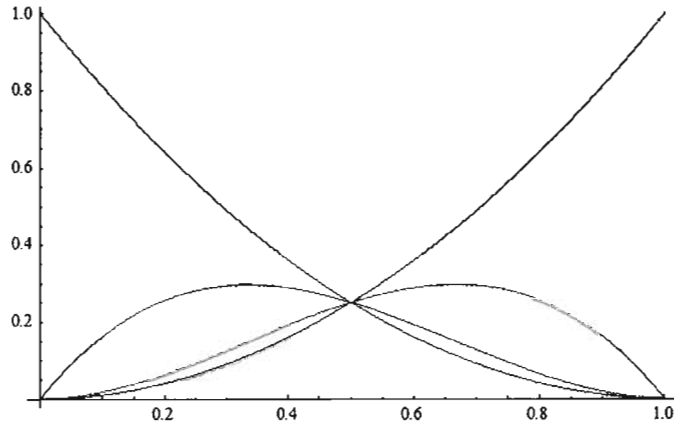


Figure 2.14. Wang-Ball basis function of degree three.

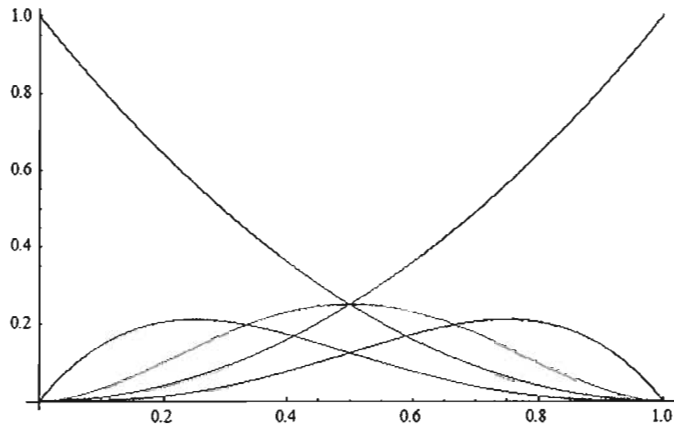


Figure 2.15. Wang-Ball basis function of degree four.

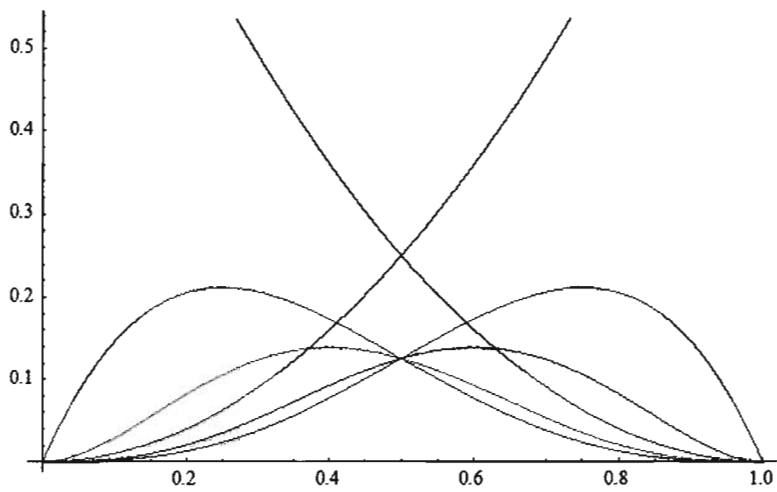


Figure 2.16. Wang-Ball basis function of degree five.

The Wang-Ball basis function satisfies the following properties:

i. Each term is positive, that is,

$$A_i^n(t) \geq 0, \forall i = 0, 1, \dots, n. \quad (2.46)$$

ii. Partition of unity, that is,

$$\sum_{i=0}^n A_i^n(t) = 1. \quad (2.47)$$

Since Wang-Ball satisfies properties (i) and (ii), it implies the convex combination of its control points. Therefore, the curve lies in the convex hull of its control points (Hu et al., 1996).

2.3.3.1 Wang-Ball Monomial Form

A Wang-Ball curve, denoted by $A(t)$, provided with $n + 1$ control points, denoted by $\{w_i\}_{i=0}^n$, can be shown as

$$A(t) = \sum_{i=0}^n \sum_{j=0}^n w_i a_{i,j} t^j, 0 \leq t \leq 1, \quad (2.48)$$

where

$$a_{ij} = \begin{cases} (-1)^{(j-i)} 2^i \binom{i+2}{j-i}, & \text{for } 0 \leq i \leq \lfloor \frac{n}{2} \rfloor - 1, \\ (-1)^{(j-i)} 2^i \binom{n-i}{j-i}, & \text{for } i = \lfloor \frac{n}{2} \rfloor, \\ (-1)^{(j-i)} 2^{n-i} \binom{n-i}{j-i}, & \text{for } i = \lceil \frac{n}{2} \rceil, \\ (-1)^{(j-n+i)} 2^{n-i} \binom{n-i}{j-n+i-2}, & \text{for } \lceil \frac{n}{2} \rceil + 1 \leq i \leq n, \end{cases} \quad (2.49)$$

and $\lfloor x \rfloor$ and $\lceil x \rceil$ denote the greatest integer less than or equal to x , and the least integer greater than or equal to x , respectively.

2.3.3.2 Conversion of Wang-Ball Curve to Bézier Curve

The converting formula for basis from Wang-Ball to Bézier is given as follows (Aphirukmatakun & Dejdumrong, 2007; Hu et al., 1996):

$$\begin{bmatrix} A_0^n(t) \\ A_1^n(t) \\ \vdots \\ A_i^n(t) \\ \vdots \\ A_n^n(t) \end{bmatrix} = \begin{bmatrix} c_{00} & c_{01} & \cdots & \cdots & \cdots & c_{0n} \\ c_{10} & c_{11} & \ddots & & & c_{1n} \\ \vdots & \vdots & \ddots & \ddots & & \vdots \\ c_{i0} & c_{i1} & \cdots & \ddots & & c_{in} \\ \vdots & \vdots & & & \ddots & \ddots \\ c_{n0} & c_{n1} & \cdots & \cdots & \cdots & c_{nn} \end{bmatrix} \begin{bmatrix} B_0^n(t) \\ B_1^n(t) \\ \vdots \\ B_i^n(t) \\ \vdots \\ B_n^n(t) \end{bmatrix}. \quad (2.50)$$

Thus we have,

$$A_i^n(t) = \sum_{i=0}^n \sum_{f=0}^n c_{if} B_f^n(t). \quad (2.51)$$

A Wang-Ball control point can be written as an associate Bézier control point as follows:

$$[b_0 \ b_1 \ \cdots \ b_n] = [w_0 \ w_1 \ \cdots \ w_n] \begin{bmatrix} c_{00} & c_{01} & \cdots & \cdots & \cdots & c_{0n} \\ c_{10} & c_{11} & \ddots & & & c_{1n} \\ \vdots & \vdots & \ddots & \ddots & & \vdots \\ c_{i0} & c_{i1} & \cdots & \ddots & & c_{in} \\ \vdots & \vdots & & & \ddots & \ddots \\ c_{n0} & c_{n1} & \cdots & \cdots & \cdots & c_{nn} \end{bmatrix}, \quad (2.52)$$

where $A_i^n(t), B_i^n(t), i \in \{0, 1, \dots, n\}$ are Wang-Ball basis functions and Bernstein basis functions, respectively, and C is the convert matrix given by:

$$c_{ij} = \begin{cases} 2^i \frac{\binom{n-2-2i}{j-i}}{\binom{n}{j}} & , \text{ for } i < \lfloor \frac{n}{2} \rfloor, \\ 2^{n-i} \frac{\binom{2i-2-n}{j-i}}{\binom{n}{j}} & , \text{ for } i > \lceil \frac{n}{2} \rceil, \\ \frac{2^j}{\binom{n}{j}} & , \text{ for } i = j = \lfloor \frac{n}{2} \rfloor, \\ \frac{2^{n-j}}{\binom{n}{j}} & , \text{ for } i = j = \lceil \frac{n}{2} \rceil, \\ 0 & , \text{ otherwise,} \end{cases} \quad (2.53)$$

where $\lfloor \frac{n}{2} \rfloor$ and $\lceil \frac{n}{2} \rceil$ denote the greatest integer less than or equal to $\frac{n}{2}$, and the least integer greater than or equal to $\frac{n}{2}$, respectively.

2.3.3.3 Wang-Ball Rectangular Surfaces

The Wang-Ball surfaces of degree $m \times n$ with control points $\{w_{i,j}\}_{i,j=0}^{m,n}$ can be expressed as

$$W(u, v) = \sum_{i=0}^m \sum_{j=0}^n A_i^m(u) A_j^n(v) w_{i,j}, \quad 0 \leq u, v \leq 1, \quad (2.54)$$

where $W_i^m(u)$ and $W_j^n(v)$ are the Wang-Ball basis (Wang & Cheng, 2001).

2.3.3.4 Converting Wang-Ball Surface into Bézier Surface

The Wang-Ball surface of degree $m \times n$ in (2.54) can be written in matrix form as

$$X(u, v) = A_u W A_v \quad (2.55)$$

where $A_u = [A_0^m(u) \ A_1^m(u) \ \cdots \ A_m^m(u)]$, $A_v = [A_0^n(v) \ A_1^n(v) \ \cdots \ A_n^n(v)]^T$,

$$W = \begin{bmatrix} w_{00} & w_{01} & \cdots & w_{0n} \\ w_{10} & w_{11} & \cdots & w_{1n} \\ \vdots & \vdots & \ddots & \vdots \\ w_{m0} & w_{m1} & \cdots & w_{mn} \end{bmatrix},$$

and $w_{ij}, i \in \{0, 1, \dots, m\}, j \in \{0, 1, \dots, n\}$ are the control points of the Wang-Ball surface. By using (2.50) in (2.55), we get

$$\begin{aligned}
X(u, v) &= (CB_u)^t V (HB_v) \\
&= (B_u^t C^t) V (HB_v) \\
&= B_u^t (C^t V H) B_v \\
&= B_u^t P B_v
\end{aligned} \tag{2.56}$$

where $P = FVH$, $F = C^t$ and F, H are square matrices of order m and n , respectively, given by (2.53). Now we rewrite (2.56) as

$$X(u, v) = \sum_{i=0}^m \sum_{j=0}^n B_i^m(u) B_j^n(v) P_{ij}, \tag{2.57}$$

where

$$P_{ij} = \sum_{r=0}^m \sum_{s=0}^n f_{ir} w_{rs} h_{sj}, \quad i \in \{0, 1, \dots, m\}, \quad j \in \{0, 1, \dots, n\}, \tag{2.58}$$

which is the Bézier surface of degree $m \times n$, where w_{ij} are Wang-Ball control points.

2.4 Parametric Surface

The general form of a parametric surface is $P(u, v) = (f_1(u, v), f_2(u, v), f_3(u, v))$. The surface depends on two parameters, u and v , that vary independently in some interval $[a, b]$ (normally, but not always, limited to $[0, 1]$). For each pair (u, v) , the expression above produces the three coordinates of a point on the surface.

2.5 Harmonic and Biharmonic Surface

Let $f : [u, v] \mapsto \mathbb{R}^3$ be a parametric surface patch, then \vec{X} is harmonic if $\nabla^2 \vec{X} = 0$ and biharmonic if $(\nabla^2 \vec{X})^2 = 0$, where ∇^2 is the Laplace operator defined by $\nabla^2 = \left(\frac{\partial^2}{\partial u^2} + \frac{\partial^2}{\partial v^2} \right)$.

Harmonic surfaces are related to minimal surfaces, that is, surfaces that minimize the area among all surfaces with prescribed boundary conditions introduced by Monterde (2004). Arnal and Monterde (2014) introduced a method for generating harmonic tensor product Bézier surfaces, and the explicit expression of each point in the control net is provided as a linear combination of prescribed boundary control points. Zhange, Cai and Wang (2011) introduced a new effective approach to construct rational Bézier harmonic surfaces over rectangular or triangular domain, and Xua and Wang (2010) proposed the sufficient condition of quintic harmonic polynomial parametric surface being a minimal surface. Yang and Wang (2015) studied the constructing polynomial Bézier surface that interpolates a Bézier curvilinear quadrilateral as boundary geodesics, while Zhanga et al. (2011) presented a new effective approach to construct rational Bézier harmonic surfaces over rectangular or triangular domain. Arnal et al. (2011) also presented an explicit polynomial solution method for surface generation by some boundary configuration whereby the resulting surface conforms to a fourth order linear elliptic partial differential equation, and the Euler–Lagrange equation of a quadratic functional defined by a norm.

2.5.1 The First Fundamental Form

Given a parametric surface $\vec{X}(u, v)$, we define the quantities $E = \vec{X}_u \cdot \vec{X}_u$, $F = \vec{X}_u \cdot \vec{X}_v$ and $G = \vec{X}_v \cdot \vec{X}_v$. Then, the first fundamental form, I of the surface is the quadratic expression defined as,

$$I = Edu^2 + 2Fdudv + Gdv^2, \quad (2.59)$$

where $\vec{X}_u = \frac{\partial}{\partial u}\vec{X}$ and $\vec{X}_v = \frac{\partial}{\partial v}\vec{X}$ (Ugail, 2011). The surface area can also be expressed in terms of the coefficients of the first fundamental form (Ugail, 2011)

$$A(\vec{X}) = \iint_R \sqrt{EG - F^2} dudv. \quad (2.60)$$

2.5.2 Monomial Matrix Form

A simple approach to represent polynomial curves is provided in the form of monomial matrices because it is more convenient to code and implement matrix operations than to solve for symbolic computations. The monomial form of Bézier curves was first investigated by Faux and Pratt (1979), Mortenson and Micheal (1985), and Chang (1982), although it was obvious that the formula for Bézier curve was very simple. Dejdumrong (2014) suggested the monomial functions for the Said-Ball, Wang-Ball, DP-Ball, Dejdumrong and NB1 curves and these functions are less complicated and more efficient for constructing curves and surfaces in CAGD applications. Furthermore, the conversions among polynomial curves can be readily obtained from their monomial matrices.

There are many applications for monomial matrix form such as the use of the monomial form of DP-Ball to get a simple and efficient algorithm for approximating conic sections by DP-Ball curves of arbitrary degree with endpoint interpolation (Bakhshesh & Davoodi, 2014). Rewriting the monomial matrix form for the curves given in equations (2.6), (2.31), (2.17) and (2.49) give the following.

2.5.2.1 Bézier Monomial Matrix

The definition of Bézier monomial matrix is

$$\mathcal{B} = \begin{bmatrix} m_{00} & m_{01} & \cdots & \cdots & m_{0n} \\ m_{10} & m_{11} & \cdots & \cdots & m_{1n} \\ \vdots & \vdots & \ddots & & \vdots \\ \vdots & \vdots & \ddots & \ddots & \vdots \\ m_{n0} & m_{n1} & \cdots & \cdots & m_{nn} \end{bmatrix}_{(n+1) \times (n+1)}, \quad (2.61)$$

where $m_{i,j}$ is given as defined in (2.6).

2.5.2.2 Said-Ball Monomial Matrix

The definition of Said-Ball monomial matrix is

$$\mathcal{S} = \begin{bmatrix} s_{00} & s_{01} & \cdots & \cdots & s_{0n} \\ s_{10} & s_{11} & \cdots & \cdots & s_{1n} \\ \vdots & \vdots & \ddots & & \vdots \\ \vdots & \vdots & \ddots & \ddots & \vdots \\ s_{n0} & s_{n1} & \cdots & \cdots & s_{nn} \end{bmatrix}_{(n+1) \times (n+1)}, \quad (2.62)$$

where $s_{i,j}$ is given as defined in (2.17).

2.5.2.3 DP-Ball Monomial Matrix

The definition of DP-Ball monomial matrix is

$$\mathcal{C} = \begin{bmatrix} c_{00} & c_{01} & \cdots & \cdots & c_{0n} \\ c_{10} & c_{11} & \cdots & \cdots & c_{1n} \\ \vdots & \vdots & \ddots & & \vdots \\ \vdots & \vdots & \ddots & \ddots & \vdots \\ c_{n0} & c_{n1} & \cdots & \cdots & c_{nn} \end{bmatrix}_{(n+1) \times (n+1)}, \quad (2.63)$$

where $c_{i,j}$ is given as defined in (2.31).

2.5.2.4 Wang-Ball Monomial Matrix

The definition of Wang-Ball monomial matrix is

$$\mathcal{A} = \begin{bmatrix} a_{00} & a_{01} & \cdots & \cdots & a_{0n} \\ a_{10} & a_{11} & \cdots & \cdots & a_{1n} \\ \vdots & \vdots & \ddots & & \vdots \\ \vdots & \vdots & \ddots & \ddots & \vdots \\ a_{n0} & a_{n1} & \cdots & \cdots & a_{nn} \end{bmatrix}, \quad (2.64)$$

$(n+1) \times (n+1)$

where $a_{i,j}$ is given as defined in (2.49).

2.5.2.5 Converting the Control Points of Bézier Surface into Control Points of Ball Surface using Monomial Matrix

We rewrite the Bézier surface of degree $m \times n$ in power basis (Dejdumrong, 2011) as follows:

$$\begin{aligned} B(u, w) &= (U\mathcal{B}^t)P(W\mathcal{B}^t)^t \\ &= U(\mathcal{B}^tP\mathcal{B})W^t \\ &= UKW^t \end{aligned} \quad (2.65)$$

where \mathcal{B} is Bézier monomial matrix form given in (2.61), $U = [1 \ u \ u^2 \ \dots \ u^m]$, $W = [1 \ w \ w^2 \ \dots \ w^n]$, P is the control points of Bézier surface and $K = \mathcal{B}^tP\mathcal{B}$. In the same manner, we can rewrite $X(u, w)$ surface of degree $m \times n$ where $X(u, w)$ represents Said-Ball or DP-Ball or Wang-Ball surfaces of degree $m \times n$ as follows:

$$\begin{aligned} X(u, w) &= (U\mathcal{M}^t)V(W\mathcal{M}^t)^t \\ &= U(\mathcal{M}^tV\mathcal{M})W^t \\ &= ULW^t \end{aligned} \quad (2.66)$$

where \mathcal{M} is $X(u, w)$ monomial matrix form given in (2.61), $U = [1 \ u \ u^2 \dots u^m]$, $W = [1 \ w \ w^2 \dots w^n]$, V is the control points of $X(u, w)$ surface and $L = \mathcal{M}'V\mathcal{M}$. Suppose $X(u, w) = B(u, w)$, and by using (2.66) and (2.65), we have

$$\begin{aligned} ULW &= UKW \\ 0(\text{Zero matrix}) &= ULW - UKW \\ &= U(LW - KW) \\ &= U(L - K)W \end{aligned}$$

Since U and W are different from zero, then we must have $L - K = 0$, i.e. $L = K$.

Using the values of L and K we have

$$\begin{aligned} \mathcal{M}'V\mathcal{M} &= \mathcal{B}'P\mathcal{B} \\ V\mathcal{M} &= (\mathcal{M}')^{-1} \mathcal{B}'P\mathcal{B} \\ V &= (\mathcal{M}')^{-1} \mathcal{B}'P\mathcal{B}(\mathcal{M})^{-1}. \end{aligned} \quad (2.67)$$

2.6 Definition of Isothermal Surface

A regular parametric surfaces $\mathbf{x} = \mathbf{x}(u, v)$ is said to be isothermal (Do Carmo & Perdigao, 1976) if

$$\langle \mathbf{x}_u, \mathbf{x}_u \rangle = \langle \mathbf{x}_v, \mathbf{x}_v \rangle \text{ and } \langle \mathbf{x}_u, \mathbf{x}_v \rangle = 0.$$

We shall study some second order functionals defined on the space of smooth patches $\vec{\mathbf{x}} : R \rightarrow \mathbb{R}^3$, where $R = [0, 1] \times [0, 1]$. The Lagrangian is given as follows

$$L(\vec{\mathbf{x}}) = L(\vec{\mathbf{x}}, \vec{\mathbf{x}}_u, \vec{\mathbf{x}}_v, \vec{\mathbf{x}}_{uu}, \vec{\mathbf{x}}_{uv}, \vec{\mathbf{x}}_{vv}). \quad (2.68)$$

We take the functional I to be such that,

$$I(\vec{\mathbf{x}}) = \iint_R L(\vec{\mathbf{x}}) dudv. \quad (2.69)$$

Minimizing the functional I is equivalent to requiring that the first variation of I is zero which then gives rise to the corresponding Euler–Lagrange equations. For instance, the Lagrange functional generating the Laplacian operator is

$$\mathcal{D}(\mathbf{x}) = \frac{1}{2} \iint_R (\|\vec{\mathbf{x}}_u\|^2 + \|\vec{\mathbf{x}}_v\|^2) dudv, \quad (2.70)$$

which is also known as the Dirichlet functional in the theory of minimal surfaces.

In a similar fashion to the harmonic functional, the Lagrange functional defining the biharmonic Laplacian operator, which we shall refer to as the biharmonic functional (Monterde, 2004) is

$$\mathcal{B}(\mathbf{x}) = \frac{1}{2} \iint_R (\|\vec{\mathbf{x}}_u\|^2 + 2\|\vec{\mathbf{x}}\| + \|\vec{\mathbf{x}}_v\|^2) dudv. \quad (2.71)$$

A surface is called minimal if its mean curvature vanishes everywhere. Ahmad and Masud (2014) presented an algorithm to reduce the area of a surface spanned by a finite number of boundary curves by initiating a variational improvement in the surface. Also, Chen, Xua and Wanga (2009) presented two other simple methods by using the extended stretching energy functional and the extended bending energy functional such that the resulting surface obtained by this new methods will have a smaller area obtained by using the Dirichlet functional. Ugail, Márquez and Yılmaz (2011) studied the Plateau-Bézier problem in three-dimensional Minkowski space (Kahyaolu & Emin, 2014) and derived the necessary and sufficient condition for minimal surface by using the Frenet frame of a given curve and isothermal parameter. Li et al. (1996) studied the approximation of minimal surface with geodesics by using Dirichlet functional, while Tråsdahl and Rønquist (2011) derived an algorithm for finding high order numerical

approximations of minimal surfaces with a fixed boundary.

2.7 Estimate the Partial Derivative with respect to x and y for the Control Points at the Boundary Curves

With the use of first order partial derivatives of interpolating surface S , where $S(V_i) = f(V_i)$ with $f(V_i)$ is the functional value at node $V_i(x_i, y_j)$, $i = 1, 2, 3, 4$, we can calculate the initial value of v_{10}, v_{20}, v_{13} ,

$v_{23}, v_{01}, v_{02}, v_{31}$ and v_{32} as follows Saaban, Man and Karim (2013)

$$v_{10} = v_{00} + \frac{1}{3}(\Delta x) \frac{\partial S}{\partial x}(v_1),$$

$$v_{01} = v_{00} + \frac{1}{3}(\Delta y) \frac{\partial S}{\partial y}(v_1),$$

$$v_{20} = v_{30} + \frac{1}{3}(\Delta x) \frac{\partial S}{\partial x}(v_2),$$

$$v_{31} = v_{30} + \frac{1}{3}(\Delta y) \frac{\partial S}{\partial y}(v_2),$$

$$v_{23} = v_{33} + \frac{1}{3}(\Delta x) \frac{\partial S}{\partial x}(v_3),$$

$$v_{32} = v_{33} + \frac{1}{3}(\Delta y) \frac{\partial S}{\partial y}(v_3),$$

$$v_{13} = v_{03} + \frac{1}{3}(\Delta x) \frac{\partial S}{\partial x}(v_4),$$

$$v_{02} = v_{03} + \frac{1}{3}(\Delta y) \frac{\partial S}{\partial y}(v_4),$$

where $\Delta x = x_2 - x_1 = x_3 - x_4$ and $\Delta y = y_4 - y_1 = y_3 - y_1$.

CHAPTER THREE

HARMONIC AND BIHARMONIC SURFACE

In this chapter, we discuss about the harmonic and biharmonic surface. All these surfaces will give us the minimal surface areas. To compare our purposed method with the existing method for Bézier surface, we must have surface with the same boundary i.e. two opposite boundaries for harmonic and four boundaries for biharmonic . To do this, we must convert Bézier surface control points into generalization Ball surface control points. i.e. different surface with same boundary curves.

3.1 Harmonic of $X(u, v)$ Surface

The Harmonic equation for the parametric surface $X(u, v)$ (Said-Ball, DP-Ball and Wang-Ball) is defined as the differential equation obtained by applying the Laplace operator that is defined by

$$\nabla^2 X(u, v) = 0. \quad (3.1)$$

Theorem 3.1. *Given the control net of points in \mathbb{R}^3 , $\{q_{i,j}\}_{i,j=0}^{n,m}$, the associate $X(u, v)$ surface, $\vec{X} : [0, 1] \times [0, 1] \rightarrow \mathbb{R}^3$ is harmonic, i.e. $\nabla^2 \vec{X} = 0$ if and only if*

$$\begin{aligned} 0 = \sum_{r,s=0}^{m,n} & \left(m(m-1) \left(f_{i+2,r} q_{rs} h_{sj} a_{i,m} + f_{i+1,r} q_{rs} h_{sj} (b_{i-1,m} - 2a_{i,m}) \right. \right. \\ & \left. \left. + f_{i-1,r} q_{rs} h_{sj} (b_{i-1,m} - 2c_{i-2,m}) + f_{i-2,r} q_{rs} h_{sj} c_{i-2,m} \right) \right. \\ & \left. + n(n-1) \left(f_{ir} q_{rs} h_{s,j+2} c_{j,n} + f_{ir} q_{rs} h_{s,j+1} (b_{j-1,n} - 2a_{j,n}) \right. \right. \\ & \left. \left. + f_{ir} q_{rs} h_{s,j-1} (b_{j-1,n} - 2c_{j-2,n}) + f_{ir} q_{rs} h_{s,j-2} c_{j-2,n} \right) \right. \\ & \left. + f_{ir} q_{rs} h_{sj} \left(m(m-1) a_{i,m} - 2b_{i-1,m} \right. \right. \\ & \left. \left. + c_{i-2,m} \right) + n(n-1) (a_{j,n} - 2b_{j-1,n} + c_{j-2,n}) \right). \end{aligned}$$

Proof. By using (2.26), we can write the $X(u, v)$ surface of degree $m \times n$ as the Bézier surface of degree $m \times n$ as follows:

$$X(u, v) = \sum_{i=0}^m \sum_{j=0}^n B_i^m(u) B_j^n(v) P_{ij}, \quad (3.2)$$

where

$$P_{ij} = \sum_{r=0}^m \sum_{s=0}^n f_{ir} q_{rs} h_{sj}, \quad i \in \{0, 1, \dots, m\}, \quad j \in \{0, 1, \dots, n\}. \quad (3.3)$$

The Laplace of the $X(u, v)$ surface is

$$\begin{aligned} \nabla^2 X(u, v) &= \left(\frac{\partial^2}{\partial u^2} + \frac{\partial^2}{\partial v^2} \right) X(u, v) \\ &= \sum_{i=0}^m \sum_{j=0}^n \left(\frac{\partial^2}{\partial u^2} + \frac{\partial^2}{\partial v^2} \right) B_i^m(u) B_j^n(v) P_{ij} \\ &= m(m-1) \sum_{i=0}^{m-2} \sum_{j=0}^n B_i^{m-2}(u) B_j^n(v) \Delta^{20} P_{ij} \\ &\quad + n(n-1) \sum_{i=0}^m \sum_{j=0}^{n-2} B_i^m(u) B_j^{n-2}(v) \Delta^{02} P_{ij} \end{aligned} \quad (3.4)$$

where

$$\left. \begin{aligned} \Delta^{20} P_{i,j} &= P_{i+2,j} - 2P_{i+1,j} + P_{i,j} = \sum_{r=0}^m \sum_{s=0}^n (f_{i+2,r} - 2f_{i+1,r} + f_{ir}) q_{rs} h_{sj}, \\ \Delta^{02} P_{i,j} &= P_{i,j+2} - 2P_{i,j+1} + P_{i,j} = \sum_{r=0}^m \sum_{s=0}^n f_{ir} q_{rs} (h_{s,j+2} - 2h_{s,j+1} + h_{sj}). \end{aligned} \right\} \quad (3.5)$$

Now, we rewrite (3.4) as the Bézier surface of degree $m \times n$. To do this, we use the following relation (Cosín & Monterde, 2002)

$$\begin{aligned} B_i^{n-2}(t) &= \frac{1}{n(n-1)} \left((n-i)(n-i-1) B_i^n(t) \right. \\ &\quad \left. + 2(i+1)(n-i-1) B_{i+1}^n(t) + (i+1)(i+2) B_{i+2}^n(t) \right). \end{aligned} \quad (3.6)$$

Then we define

$$\left. \begin{aligned} a_{in} &= (n-i)(n-i-1), \\ b_{in} &= 2(i+1)(n-i-1), \\ c_{in} &= (i+1)(i+2) \text{ for } i \in \{0, 1, \dots, n-2\}, \text{ and} \\ a_{in} &= b_{in} = c_{in} = 0, \text{ otherwise.} \end{aligned} \right\} \quad (3.7)$$

By using (3.6) in (3.4), we get

$$\begin{aligned} \nabla^2 X(u, v) &= \sum_{i=0}^n \sum_{j=0}^m B_i^m(u) B_j^n(v) \\ &\quad \left(m(m-1)(a_{i,m} \Delta^{20} P_{i,j} + b_{i-1,m} \Delta^{20} P_{i-1,j} + c_{i-2,j} \Delta^{20} P_{i-2,j}) \right. \\ &\quad \left. + n(n-1)(a_{j,n} \Delta^{02} P_{i,j} + b_{j-1,n} \Delta^{02} P_{i,j-1} + c_{j-2,n} \Delta^{02} P_{i,j-2}) \right). \end{aligned} \quad (3.8)$$

Expression (3.8) is the Bézier surface of degree $m \times n$ associated with the new control points $\{\mathcal{F}_{i,j}\}_{i,j=0}^{m,n}$, where

$$\begin{aligned} \{\mathcal{F}_{i,j}\}_{i,j=0}^{m,n} &= \left(m(m-1)(a_{i,m} \Delta^{20} P_{i,j} + b_{i-1,m} \Delta^{20} P_{i-1,j} + c_{i-2,j} \Delta^{20} P_{i-2,j}) + \right. \\ &\quad \left. n(n-1)(a_{j,n} \Delta^{02} P_{i,j} + b_{j-1,n} \Delta^{02} P_{i,j-1} + c_{j-2,n} \Delta^{20} P_{i,j-2}) \right) \\ &= \sum_{r,s=0}^{m,n} \left(m(m-1) \left(a_{i,m} ((f_{i+2,r} - f_{i+1,r} + f_{i,r}) q_{rs} h_{sj}) \right. \right. \\ &\quad \left. \left. + b_{i-1,m} ((f_{i+1,r} - f_{i,r} + f_{i-1,r}) q_{rs} h_{sj}) \right. \right. \\ &\quad \left. \left. + c_{i-2,j} ((f_{i,r} - f_{i-1,r} + f_{i-2,r}) q_{rs} h_{sj}) \right) \right. \\ &\quad \left. + n(n-1) \left(a_{j,n} f_{i,r} q_{rs} (h_{sj} - 2h_{s,j+1} + h_{sj}) \right. \right. \\ &\quad \left. \left. + b_{j-1,n} f_{i,r} q_{rs} (h_{s,j+1} - 2h_{s,j} + h_{s,j-1}) \right. \right. \\ &\quad \left. \left. + c_{j-2,n} f_{i,r} q_{rs} (h_{s,j} - 2h_{s,j-1} + h_{s,-2j}) \right) \right). \end{aligned} \quad (3.9)$$

Hence, as we know that $\{B_i^m(u) B_j^n(v)\}_{i,j=0}^{m,n}$ is the basis of polynomials, it must not be equal to zero, we showed that $X(u, v)$ is harmonic if and only if

$$\mathcal{F}_{i,j} = 0, \quad \forall i, j. \quad (3.10)$$

Now, we use the value of the operators Δ^{20} and Δ^{02} from (3.5) and (3.3) in (3.9) to get

$$\begin{aligned} 0 = \sum_{r,s=0}^{m,n} & \left(m(m-1) \left(f_{i+2,r} q_{rs} h_{sj} a_{i,m} + f_{i+1,r} q_{rs} h_{sj} (b_{i-1,m} - 2a_{i,m}) \right. \right. \\ & \left. \left. + f_{i-1,r} q_{rs} h_{sj} (b_{i-1,m} - 2c_{i-2,m}) + f_{i-2,r} q_{rs} h_{sj} c_{i-2,m} \right) \right. \\ & \left. + n(n-1) \left(f_{ir} q_{rs} h_{s,j+2} c_{j,n} + f_{ir} q_{rs} h_{s,j+1} (b_{j-1,n} - 2a_{j,n}) \right. \right. \\ & \left. \left. + f_{ir} q_{rs} h_{s,j-1} (b_{j-1,n} - 2c_{j-2,n}) + f_{ir} q_{rs} h_{s,j-2} c_{j-2,n} \right) \right. \\ & \left. + f_{ir} q_{rs} h_{sj} \left(m(m-1) a_{i,m} - 2b_{i-1,m} \right) \right. \\ & \left. \left. + c_{i-2,m} \right) + n(n-1) (a_{j,n} - 2b_{j-1,n} + c_{j-2,n}) \right). \quad \square \end{aligned} \quad (3.11)$$

If we let $n = m$ in (3.11) i.e. the quadratic case, we have the following theorem.

Theorem 3.2. *Given the quadratic net of points in \mathbb{R}^3 , $\{q_{i,j}\}_{i,j=0}^{n,n}$ the associate $\vec{X}(u, v)$ surface, $\vec{X} : [0, 1] \times [0, 1] \rightarrow \mathbb{R}^3$ is harmonic, i.e. $\nabla^2 \vec{X} = 0$ if and only if*

$$\begin{aligned} 0 = \sum_{r,s=0}^{n,n} & \left(f_{i+2,j} q_{rs} h_{sj} c_{i,n} + f_{i+1,j} q_{rs} h_{sj} (b_{i-2,n} - 2a_{i,n}) \right. \\ & \left. + f_{i-1,j} q_{rs} h_{sj} (b_{i-1,n} - 2c_{i-2,n}) + f_{i-2,j} q_{rs} h_{sj} c_{i-2,n} \right. \\ & \left. + f_{ij} q_{rs} h_{s,j+1} a_{j,n} + f_{ij} q_{rs} h_{s,j+1} (b_{j-1,n} - 2a_{j,n}) \right. \\ & \left. + f_{ij} q_{rs} h_{s,j-1} (b_{j-1,n} - 2c_{j-2,n}) + f_{ij} q_{rs} h_{s,j-2} c_{j-2,n} \right. \\ & \left. \left. + f_{ij} q_{rs} h_{sj} (a_{i,n} - 2b_{i-1,n} + c_{i-2,n} + a_{j,n} - 2b_{j-1,n} + c_{j-2,n}) \right) \right). \end{aligned} \quad (3.12)$$

Remark 3.1. *Theorem 3.2 holds for Bézier if the control points $\{q_{i,j}\}_{i,j=0}^{n,n}$ of the $X(u, v)$ surface is replaced by the Bézier control points $\{P_{i,j}\}_{i,j=0}^{n,n}$ and also if the convert matrices F and H are being replaced by the identity matrix.*

Corollary 3.1. *If we replace the convert matrices f, h by the convert matrices from (Said-Ball, DP-Ball, Wang-Ball) to Bézier as in (Said-Ball 2.21, 2.22, DP-Ball 2.35, 2.36, 2.37, Wang-Ball 2.53) and the control points $\{q_{i,j}\}_{i=0, j=0}^{m,n}$ of the $X(u, v)$ surface by the (Said-Ball $\{v_{i,j}\}_{i=0, j=0}^{m,n}$, DP-Ball $\{d_{i,j}\}_{i=0, j=0}^{m,n}$, Wang-Ball $\{w_{i,j}\}_{i=0, j=0}^{m,n}$) control points respectively. Then Theorem 3.1 and Theorem 3.2 gives us the harmonic condition for Said-Ball surface, DP-Ball surface and Wang-Ball surface.*

Let us study equation (3.12) in the simplest case: biquadratic and bicubical generalized Ball patches, i.e. Said-Ball, DP-Ball and Wang-Ball patches.

3.1.1 Biquadratic Harmonic Patches

In the case $n = m = 2$ from equation (3.12), it is possible to find an expression for four of the control points in terms of the other five. In fact, we have obtained that the null space of the coefficient matrix of (3.12) is of dimension four. Moreover, it is possible to choose free variables points in the first and last column of the control net.

3.1.1.1 Said-Ball Patch

Corollary 3.2. *The biquadratic Said-Ball surface is harmonic if and only if*

$$v_{01} = \frac{1}{2}(2v_{00} + v_{02} - 2v_{10} + v_{20}), \quad (3.13)$$

$$v_{11} = \frac{1}{4}(v_{00} + v_{02} + v_{20} + v_{22}), \quad (3.14)$$

$$v_{21} = \frac{1}{2}(v_{00} - 2v_{10} + 2v_{20} + v_{22}), \quad (3.15)$$

$$v_{12} = \frac{1}{2}(-v_{00} + v_{02} + 2v_{10} - v_{20} + v_{22}). \quad (3.16)$$

A way of writing a sample equation involving the inner control point v_{11} is by using the following mask

$$v_{11} = \frac{1}{4} \begin{array}{ccc} 1 & 0 & 1 \\ 0 & \bullet & 0 \\ 1 & 0 & 1 \end{array} \quad (3.17)$$

Since the Said-Ball and Bézier basis functional for degree two are the same, then we use the dual of the mask (3.17) associated to the Laplace operator. It can be found in Farin and Hansford (1999) that the mask

$$v_{11} = \frac{1}{4} \begin{array}{ccc} 0 & 1 & 0 \\ 1 & \bullet & 1 \\ 0 & 1 & 0 \end{array} \quad (3.18)$$

is the discrete form of the Laplace operator.

In general, the notation of permanent patches (3.17) and (3.18) is generated by the mask of the form

$$v_{11} = \begin{array}{ccc} \alpha & \beta & \alpha \\ \beta & \bullet & \beta \\ \alpha & \beta & \alpha \end{array} \quad (3.19)$$

with $4\alpha + 4\beta = 1$ (Farin & Hansford, 1999). Thus, the mask (3.17) is a particular case with $\alpha = 0.25$ while the mask (3.18) corresponds to $\alpha = 0$.

In order to obtain a minimal patch, we have to impose the isothermal conditions.

Example 3.1. Given the control points of a biquadratic Said-Ball as follows:

$v_{00} = (0, 0, 1)$, $v_{10} = (1, 0, 0)$, $v_{20} = (2, 0, 1)$, $v_{01} = (0, 1, 0)$, $v_{21} = (2, 1, 0)$, $v_{02} = (0, 2, 1)$, $v_{12} = (1, 2, 0)$, $v_{22} = (2, 2, 1)$. Then, by using the mask (3.17), we have the inner control point as $v_{11} = (1, 1, 1)$, and we get $v_{11} = (1, 1, 0)$ by using the dual mask (3.18).

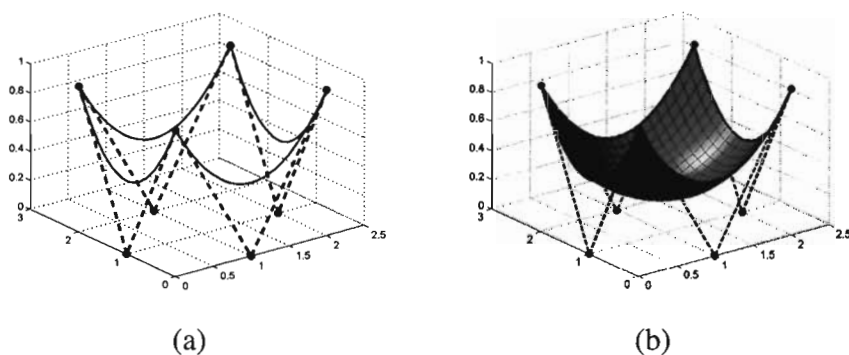


Figure 3.1. (a) Boundary curves of biquadratic Said-Ball generated by dual harmonic mask (b) Surface of biquadratic Said-Ball generated by dual harmonic mask.

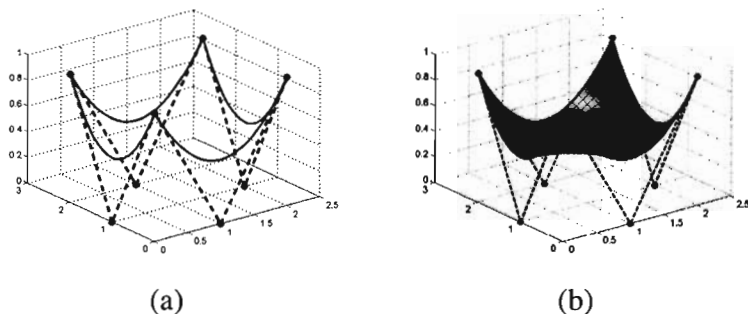


Figure 3.2. (a) Boundary curves of biquadratic Said-Ball generated by harmonic mask (b) Surface of biquadratic Said-Ball generated by harmonic mask.

Remark 3.2. Since the Said-Ball surface, DP-Ball surface and Wang-Ball surface of degree two are the same, then Corollary 3.2 holds on DP-Ball surface and Wang-Ball surface of degree two.

3.1.2 Bicubical Harmonic Patches

In the case $n = m = 3$ from equation (3.12), it is possible to write half of the control points in terms of the other eight. We obtained that the null space of the coefficient matrix of (3.12) is of dimension eight. Moreover, it is possible to choose free variables for the exact eight points in the first and last column of the control net.

3.1.2.1 Bicubical Harmonic Said-Ball Patches

Corollary 3.3. *A bicubic Said-Ball surface is harmonic if and only if*

$$v_{11} = \frac{1}{6}(2v_{00} + v_{01} - 2v_{02} + 2v_{03} + v_{30} + 2v_{31} - v_{32} + v_{33}), \quad (3.20)$$

$$v_{21} = \frac{1}{6}(v_{00} + 2v_{01} - v_{02} + v_{03} + 2v_{30} + v_{31} - 2v_{32} + 2v_{33}), \quad (3.21)$$

$$v_{12} = \frac{1}{6}(2v_{00} - 2v_{01} + v_{02} + 2v_{03} + v_{30} - v_{31} + 2v_{32} + v_{33}), \quad (3.22)$$

$$v_{22} = \frac{1}{6}(v_{00} - v_{01} + 2v_{02} + v_{03} + 2v_{30} - 2v_{31} + v_{32} + 2v_{33}), \quad (3.23)$$

$$v_{10} = \frac{1}{6}(5v_{00} - 8v_{01} + 4v_{02} + 2v_{03} + 4v_{30} - 4v_{31} + 2v_{32} + v_{33}), \quad (3.24)$$

$$v_{20} = \frac{1}{6}(4v_{00} - 4v_{01} + 2v_{02} + v_{03} + 5v_{30} - 8v_{31} + 4v_{32} + 2v_{33}), \quad (3.25)$$

$$v_{13} = \frac{1}{6}(2v_{00} + 4v_{01} - 8v_{02} + 5v_{03} + v_{30} + 2v_{31} - 4v_{32} + 4v_{33}), \quad (3.26)$$

$$v_{23} = \frac{1}{6}(v_{00} + 2v_{01} - 4v_{02} + 4v_{03} + 2v_{30} + v_{31} - 8v_{32} + 5v_{33}). \quad (3.27)$$

Remark 3.3. *This means that, given the first and last columns of the control net (eight control points in total), the other eight control points are fully determined by the harmonic condition. In other words, any pair of two opposed borders of an harmonic Ball surface determines the rest of the control points. There are two different kind of masks depending whether the point is an inner control point or not.*

Remark 3.4. *Since the Said-Ball patch of degree 3×3 and Wang-Ball patch of degree 3×3 are the same, then Corollary 3.3 holds on Wang-Ball patch of degree 3×3 .*

3.1.2.2 Bicubical Harmonic DP-Ball Patches

Corollary 3.4. *A bicubic DP-Ball surface is harmonic if and only if*

$$d_{11} = d_{00}, \quad (3.28)$$

$$d_{12} = d_{03}, \quad (3.29)$$

$$d_{21} = d_{30}, \quad (3.30)$$

$$d_{22} = d_{33}, \quad (3.31)$$

$$d_{10} = 2d_{00} - d_{01}, \quad (3.32)$$

$$d_{20} = 2d_{30} - d_{31}, \quad (3.33)$$

$$d_{13} = 2d_{03} - d_{02}, \quad (3.34)$$

$$d_{23} = 2d_{33} - d_{32}. \quad (3.35)$$

Remark 3.5. *This means that given the first and last columns of the control net (eight control points in total), the other eight control points are fully determined by the harmonic condition. In other words, any pair of two opposed borders of the harmonic DP-Ball surface determines the rest of the control points.*

Remark 3.6. *Equations (3.28) to (3.31) imply that the inner control points are fully determined by the four corner points and the two neighbor control points that lies on the boundaries. There are two different kind of masks depending whether the point is an inner control point or not.*

The masks displayed below show the bicubic harmonic condition: the first column represents Bézier, second column meant for Said/Wang-Ball, while the third column is for DP-Ball.

$$\begin{array}{ccc}
\begin{array}{c} 0 \quad \bullet \quad \bullet \quad 0 \\ 2 \quad \bullet \quad \bullet \quad 1 \\ -4 \quad \bullet \quad \bullet \quad -2 \\ 4 \quad \bullet \quad \bullet \quad 2 \end{array} &
\begin{array}{c} v_{10} = \frac{1}{6} \\ 4 \quad \bullet \quad \bullet \quad 2 \\ -8 \quad \bullet \quad \bullet \quad -4 \\ 5 \quad \bullet \quad \bullet \quad 4 \end{array} &
\begin{array}{c} d_{10} = \\ 0 \quad \bullet \quad \bullet \quad 0 \\ 1 \quad \bullet \quad \bullet \quad 0 \\ 2 \quad \bullet \quad \bullet \quad 0 \end{array}
\end{array}$$

$$\begin{array}{ccc}
\begin{array}{c} 0 \quad \bullet \quad \bullet \quad 0 \\ 1 \quad \bullet \quad \bullet \quad 2 \\ -2 \quad \bullet \quad \bullet \quad -4 \\ 2 \quad \bullet \quad \bullet \quad 4 \end{array} &
\begin{array}{c} v_{20} = \frac{1}{6} \\ 1 \quad \bullet \quad \bullet \quad 2 \\ 2 \quad \bullet \quad \bullet \quad 4 \\ -4 \quad \bullet \quad \bullet \quad -8 \\ 4 \quad \bullet \quad \bullet \quad 5 \end{array} &
\begin{array}{c} d_{20} = \\ 0 \quad \bullet \quad \bullet \quad 0 \\ 0 \quad \bullet \quad \bullet \quad 0 \\ 0 \quad \bullet \quad \bullet \quad -2 \\ 0 \quad \bullet \quad \bullet \quad 2 \end{array}
\end{array}$$

$$\begin{array}{ccc}
\begin{array}{c} 4 \quad \bullet \quad \bullet \quad 2 \\ -4 \quad \bullet \quad \bullet \quad 2 \\ 2 \quad \bullet \quad \bullet \quad 1 \\ 0 \quad \bullet \quad \bullet \quad 0 \end{array} &
\begin{array}{c} v_{13} = \frac{1}{6} \\ 5 \quad \bullet \quad \bullet \quad 4 \\ -8 \quad \bullet \quad \bullet \quad -4 \\ 4 \quad \bullet \quad \bullet \quad 2 \\ 2 \quad \bullet \quad \bullet \quad 1 \end{array} &
\begin{array}{c} d_{13} = \\ 2 \quad \bullet \quad \bullet \quad 0 \\ -1 \quad \bullet \quad \bullet \quad 0 \\ 0 \quad \bullet \quad \bullet \quad 0 \\ 0 \quad \bullet \quad \bullet \quad 0 \end{array}
\end{array}$$

$$\begin{array}{ccc}
\begin{array}{c} 2 \quad \bullet \quad \bullet \quad 4 \\ -2 \quad \bullet \quad \bullet \quad -4 \\ 1 \quad \bullet \quad \bullet \quad 2 \\ 0 \quad \bullet \quad \bullet \quad 0 \end{array} &
\begin{array}{c} v_{23} = \frac{1}{6} \\ 4 \quad \bullet \quad \bullet \quad 5 \\ -4 \quad \bullet \quad \bullet \quad -8 \\ 2 \quad \bullet \quad \bullet \quad 4 \\ 1 \quad \bullet \quad \bullet \quad 2 \end{array} &
\begin{array}{c} d_{23} = \\ 0 \quad \bullet \quad \bullet \quad 2 \\ 0 \quad \bullet \quad \bullet \quad -1 \\ 0 \quad \bullet \quad \bullet \quad 0 \\ 0 \quad \bullet \quad \bullet \quad 0 \end{array}
\end{array}$$

$$\begin{array}{ccc}
\begin{array}{c} P_{11} = \frac{1}{9} \\ 2 \bullet \bullet 1 \\ 0 \bullet \bullet 0 \\ 0 \bullet \bullet 0 \\ 4 \bullet \bullet 2 \end{array} &
\begin{array}{c} v_{11} = \frac{1}{6} \\ -2 \bullet \bullet -1 \\ 1 \bullet \bullet 2 \\ 2 \bullet \bullet 1 \end{array} &
\begin{array}{c} d_{11} = \\ 0 \bullet \bullet 0 \\ 0 \bullet \bullet 0 \\ 0 \bullet \bullet 0 \\ 1 \bullet \bullet 0 \end{array}
\end{array}$$

$$\begin{array}{ccc}
\begin{array}{c} P_{12} = \frac{1}{9} \\ 1 \bullet \bullet 2 \\ 0 \bullet \bullet 0 \\ 0 \bullet \bullet 0 \\ 2 \bullet \bullet 4 \end{array} &
\begin{array}{c} v_{12} = \frac{1}{6} \\ 2 \bullet \bullet 1 \\ 1 \bullet \bullet 2 \\ -2 \bullet \bullet -1 \\ 2 \bullet \bullet 1 \end{array} &
\begin{array}{c} d_{12} = \\ 1 \bullet \bullet 0 \\ 0 \bullet \bullet 0 \\ 0 \bullet \bullet 0 \\ 0 \bullet \bullet 0 \end{array}
\end{array}$$

$$\begin{array}{ccc}
\begin{array}{c} P_{21} = \frac{1}{9} \\ 1 \bullet \bullet 2 \\ 0 \bullet \bullet 0 \\ 0 \bullet \bullet 0 \\ 2 \bullet \bullet 4 \end{array} &
\begin{array}{c} v_{13} = \frac{1}{6} \\ 1 \bullet \bullet 2 \\ -1 \bullet \bullet -2 \\ 2 \bullet \bullet 2 \\ 1 \bullet \bullet 2 \end{array} &
\begin{array}{c} d_{13} = \\ 0 \bullet \bullet 0 \\ 0 \bullet \bullet 0 \\ 0 \bullet \bullet 0 \\ 0 \bullet \bullet 1 \end{array}
\end{array}$$

$$\begin{array}{ccc}
\begin{array}{c} P_{22} = \frac{1}{9} \\ 2 \bullet \bullet 4 \\ 0 \bullet \bullet 0 \\ 0 \bullet \bullet 0 \\ 1 \bullet \bullet 2 \end{array} &
\begin{array}{c} v_{22} = \frac{1}{6} \\ 1 \bullet \bullet 2 \\ 2 \bullet \bullet 1 \\ -1 \bullet \bullet -2 \\ 1 \bullet \bullet 2 \end{array} &
\begin{array}{c} d_{22} = \\ 0 \bullet \bullet 1 \\ 0 \bullet \bullet 0 \\ 0 \bullet \bullet 0 \\ 0 \bullet \bullet 0 \end{array}
\end{array}$$

3.1.3 Graphical Examples for Harmonic Bicubic Surface

Here we give some graphical examples for bicubic Said/Wang-Ball and bicubic DP-Ball, generated by four sets of control points such that the surface with the same two opposite boundaries are the same.

3.1.3.1 Graphical Examples for Harmonic Bicubic Said/Wang-Ball Surface

To generate the harmonic Said-Ball surface, we have chosen four sets of boundary curves.

Example 3.2. Given the boundary control points set 1 of the bicubic Said-Ball surface as follows

$$v_{00} = (0, 0, 1), v_{01} = (0, 18/5, -491/625), v_{02} = (0, 14/5, -71/625), v_{03} = (0, 4, 1), \\ v_{30} = (4, 0, 1), v_{31} = (4, 9/5, -885/1687), v_{32} = (4, 11/5, -885/1687), v_{33} = (4, 4, 1).$$

Then, the inner control points of the bicubic Said-Ball surface by harmonic condition are

$$v_{11} = (2, 19/10, 622/759), v_{12} = (2, 17/10, 1397/1209), \\ v_{21} = (2, 23/10, 1021/1209), v_{22} = (2, 21/10, 896/759), v_{10} = (2, -7/5, 601/191), \\ v_{20} = (2, -2/5, 2294/809), v_{13} = (2, 19/5, 1525/846), \\ \text{and } v_{23} = (0, 27/10, 1686/695). \text{ The graph of the above surface is in Figure 3.3(c)} \\ \text{while its boundary with control points is in Figure 3.3(d).}$$

Example 3.3. Given the boundary control points set 2 of the bicubic Said-Ball surface as follows

$$v_{00} = (0, 0, 0), v_{01} = (0, 9/4, -9/2), v_{02} = (0, 3/4, 9/2), v_{03} = (0, 3, 0), v_{30} = (3, 0, 0), \\ v_{31} = (3, 3/2, 3/2), v_{32} = (3, 3/2, 3/2), v_{33} = (3, 3, 0).$$

Then, the inner control points of the bicubic Said-Ball surface by harmonic condition are

$$v_{11} = (3/2, 15/8, -2), v_{12} = (3/2, 15/8, -5/2), v_{21} = (3/2, 15/8, -5/2), \\ v_{22} = (3/2, 9/8, 2), v_{10} = (3/2, -3/2, 17/2), v_{20} = (3/2, -3/4, 7/2), \\ v_{13} = (3/2, 9/2, -19/2), \text{ and } v_{23} = (0, 3, -25/4). \text{ The graph of the above surface is in} \\ \text{Figure 3.4(c) while its boundary with control points is in Figure 3.4(d).}$$

Example 3.4. Given the boundary control points set 3 of the bicubic Said-Ball surface as follows

$$\begin{aligned} v_{00} &= (1/2, 0, 0), v_{01} = (31/80, 0, 27/40), v_{02} = (29/80, 0, 5/8), \\ v_{03} &= (1, 0, 1), v_{30} = (-1/2, 0, 0), v_{31} = (-31/80, 0, 27/40), v_{32} = (-29/80, 0, 5/8), \\ v_{33} &= (-1, 0, 1). \end{aligned}$$

Then, the inner control points of the bicubic Said-Ball surface by harmonic condition are

$$\begin{aligned} v_{11} &= (1/8, 0, 21/40), v_{12} = (1/8, 0, 19/40), v_{21} = (-1/8, 0, 21/40) \\ v_{22} &= (-1/8, 0, 19/40), v_{10} = (9/80, 0, -9/40), v_{20} = (9/80, 0, -9/40), \\ v_{13} &= (11/80, 0, 37/40),, \text{ and } v_{23} = (9/160, 0, 47/80). \end{aligned}$$

The graph of the above surface is in Figure 3.5(c) while its boundary with control points in is Figure 3.5(d).

Example 3.5. Given the boundary control points set 4 of the bicubic Said-Ball surface as follows

$$\begin{aligned} v_{00} &= (-585/631, 1378/483, 0),, v_{01} = (-111/581, 2342/3983, 21/40), \\ v_{02} &= (-327/3697, 457/1674, 2/5), v_{03} = (-585/631, 1378/483, 1), \\ v_{30} &= (585/631 - 1378/4830), v_{31} = (512/1599, -1699/1724, 9/20), \\ v_{32} &= (161/7124, -173/2475, 13/40), v_{33} = (585/631, -1378/483, 1). \end{aligned}$$

Then, the inner control points of the bicubic Said-Ball surface by harmonic condition are

$$\begin{aligned} v_{11} &= (-475/2279, 1047/1633, 11/20), v_{12} = (-253/827, 2219/2357, 17/40), \\ v_{21} &= (253/827, -2219/2357, 23/40), v_{22} = (475/2279, -1047/1633, 9/20), \\ v_{10} &= (-527/1651, 1761/1792, -1/8), v_{20} = (-644/130087, 84/5455, -1/10), \\ v_{13} &= (-501/2209, 481/690, 5/4), \text{ and } v_{23} = (472/1441, -626/621, 21/20). \end{aligned}$$

The graph of the above surface is in Figure 3.6(c) while its boundary with control points is in Figure 3.6(d).

3.1.3.2 Graphical Examples for Harmonic Bicubic DP-Ball Surface

To generate the harmonic DP-Ball surface, we have chosen four sets of boundary curves.

Example 3.6. Given the boundary control points set 1 of the bicubic DP-Ball surface as follows

$$d_{00} = (0, 0, 1), d_{30} = (4, 0, 1), d_{01} = (08/5 - 399/625), d_{02} = (0, 4, 441/625),$$
$$d_{03} = (0, 4, 1), d_{31} = (4, -2/5, -41/2500), d_{32} = (422/5 - 41/2500), d_{33} = (4, 4, 1).$$

Then, the inner control points of the bicubic DP-Ball surface by harmonic condition are

$$d_{11} = (0, 0, 1), d_{12} = (0, 4, 1), d_{21} = (4, 0, 1), d_{22} = (4, 4, 1), d_{10} = (0, -8/5, 1649/625),$$
$$d_{20} = (4, 2/5, 5041/2500), d_{13} = (0, 4, 809/625),, \text{ and } d_{23} = (4, 18/5, 5041/2500).$$

The graph of the above surface is in Figure 3.3(e) while its boundary with control points is in Figure 3.3(f).

Example 3.7. Given the boundary control points set 2 of the bicubic DP-Ball surface as follows

$$d_{00} = (0, 0, 0), d_{30} = (3, 0, 0), d_{01} = (0, 3/2, -9), d_{02} = (0, 3/2, 9), d_{03} = (0, 3, 0),$$
$$d_{31} = (3, 0, 1), d_{32} = (3, 3, 1), d_{33} = (3, 3, 0).$$

Then, the inner control points of the bicubic DP-Ball surface by harmonic condition are

$$d_{11} = (0, 0, 0), d_{12} = (0, 3, 0), d_{21} = (3, 0, 0), d_{22} = (3, 3, 0), d_{10} = (0, -3/2, 9),$$
$$d_{20} = (3, 0, -1), d_{13} = (0, 9/2, -9), d_{23} = (3, 3, -1).$$

The graph of the above surface is in Figure 3.4(e) while its boundary with control points is in Figure 3.4(f).

Example 3.8. Given the boundary control points set 3 of the bicubic DP-Ball surface as follows

$$d_{00} = (1/2, 0, 0), d_{30} = (-1/2, 0, 0), d_{01} = (11/40, 0, 3/20), d_{02} = (29/40, 0, 21/20),$$
$$d_{03} = (1, 0, 1), d_{31} = (-11/40, 0, 3/20), d_{32} = (-29/40, 0, 21/20), d_{33} = (-1, 0, 1).$$

Then, the inner control points of the bicubic DP-Ball surface by harmonic condition are

$$d_{11} = (1/2, 0, 0), d_{12} = (1, 0, 1), d_{21} = (-1/2, 0, 0), d_{22} = (-1, 0, 1), d_{10} = (29/40, 0, -3/20),$$

$$d_{20} = (-29/40, 0, -3/20), d_{13} = (51/40, 0, 19/20), \text{ and } d_{23} = (-51/40, 0, 19/20).$$

The graph of the above surface is in Figure 3.5(e) while its boundary with control points is in Figure 3.5(f).

Example 3.9. Given the boundary control points set 4 of the bicubic DP-Ball surface as follows

$$d_{00} = (-585/631, 1378/483, 0), d_{30} = (585/631, -1378/483, 0),$$

$$d_{01} = (-631/1250, 1553/1000, 1/10), d_{02} = (-749/2500, 923/1000, 17/20),$$

$$d_{03} = (-585/631, 1378/483, 1), d_{31} = (1121/1555, -2773/1250, 1/20),$$

$$d_{32} = (292/2323, -242/625, 4/5), d_{33} = (585/631, -1378/483, 1).$$

Then, the inner control points of the bicubic DP-Ball surface by an extremal of the Dirichlet condition are

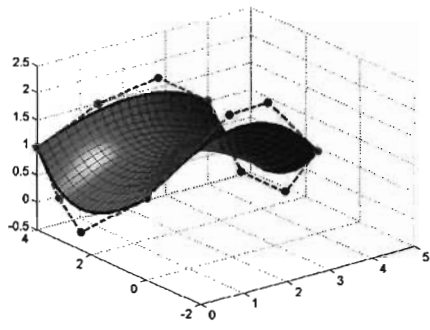
$$d_{11} = (-585/631, 1378/483, 0), d_{12} = (-585/631, 1378/483, 1),$$

$$d_{21} = (585/631, -1378/483, 0), d_{22} = (585/631, -1378/483, 1),$$

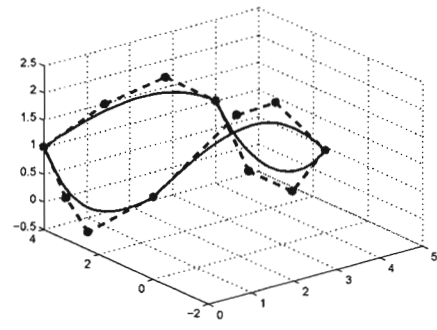
$$d_{10} = (-7755/5747, 760/183, -1/10), d_{20} = (2219/1958, -422/121, -1/20),$$

$$d_{13} = (-2349/1511, 3152/659, 23/20), \text{ and } d_{23} = (2219/1958, -422/121, -1/20).$$

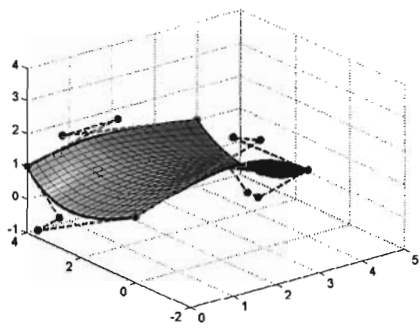
The graph of the above surface is in Figure 3.6(e) while its boundary with control points is in Figure 3.6(f).



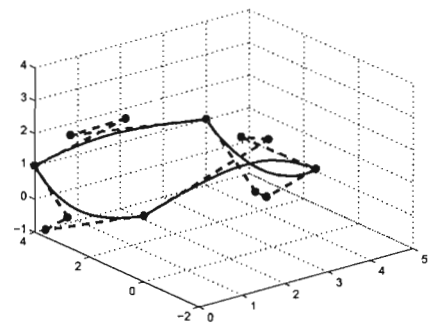
(a)



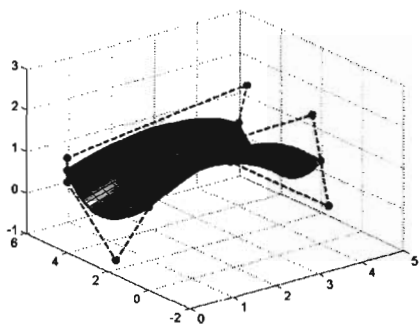
(b)



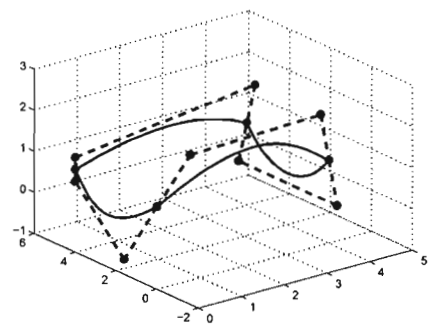
(c)



(d)

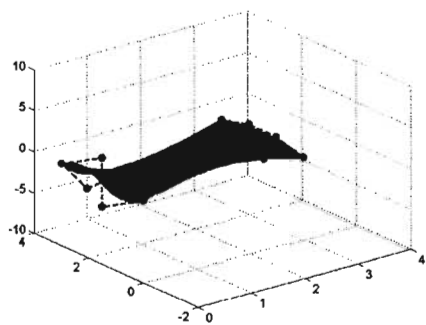


(e)

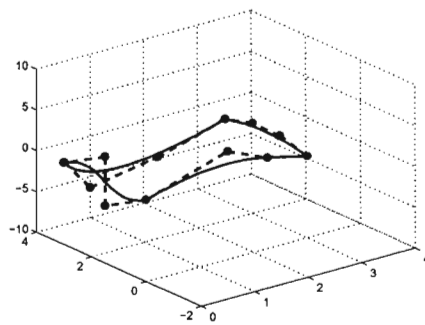


(f)

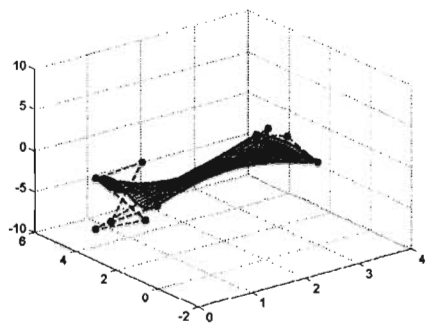
Figure 3.3. Control points set 1 by harmonic condition on (a) Bézier patch (b) Bézier boundary (c) Said/Wang-Ball patch (d) Said/Wang-Ball boundary (e) DP-Ball patch (f) DP-Ball boundary.



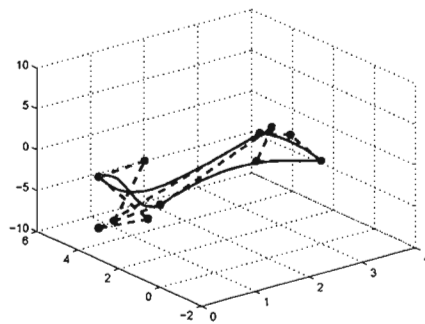
(a)



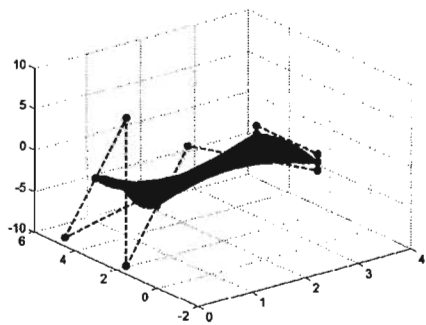
(b)



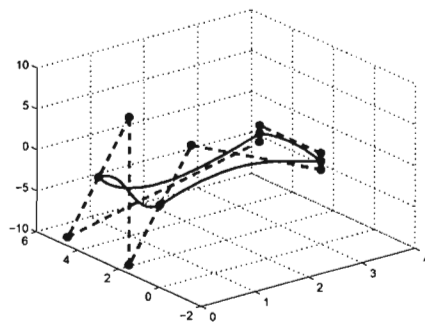
(c)



(d)

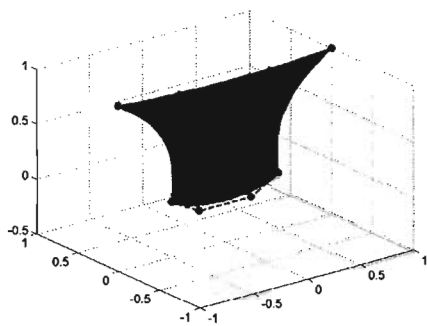


(e)

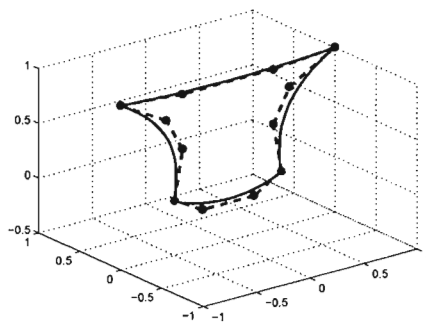


(f)

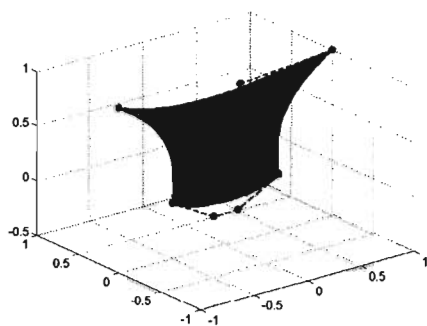
Figure 3.4. Control points set 2 by harmonic condition on (a) Bézier patch (b) Bézier boundary (c) Said/Wang-Ball patch (d) Said/Wang-Ball boundary (e) DP-Ball patch (f) DP-Ball boundary.



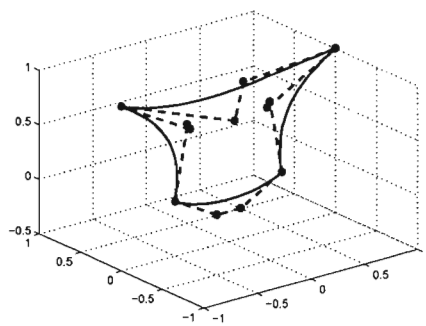
(a)



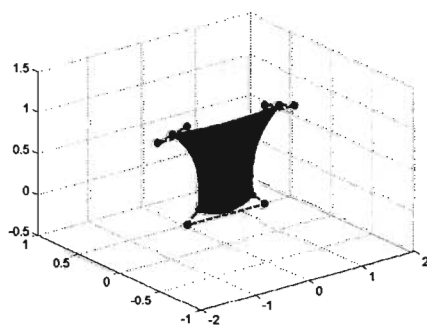
(b)



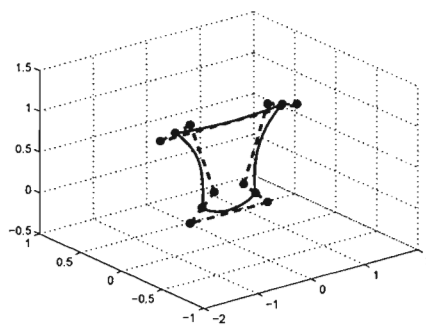
(c)



(d)

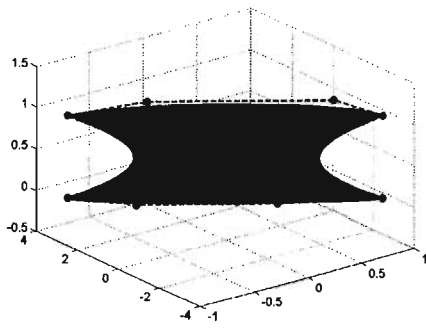


(e)

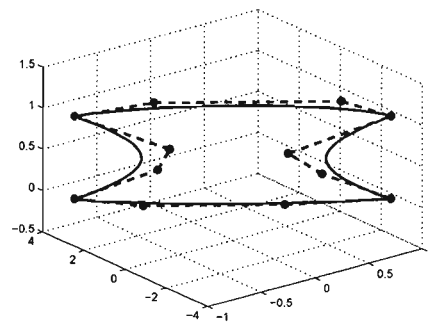


(f)

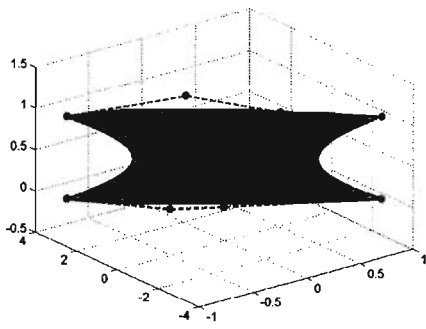
Figure 3.5. Control points set 3 by harmonic condition on (a) Bézier patch (b) Bézier boundary (c) Said/Wang-Ball patch (d) Said/Wang-Ball boundary (e) DP-Ball patch (f) DP-Ball boundary.



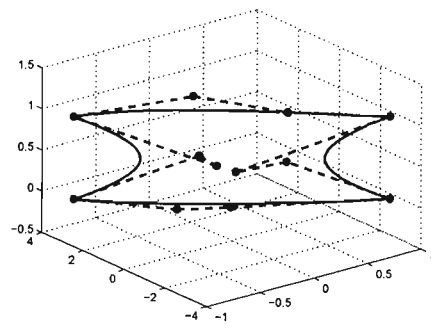
(a)



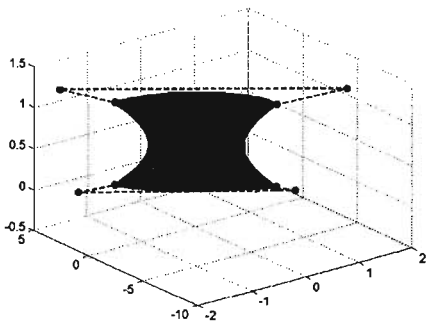
(b)



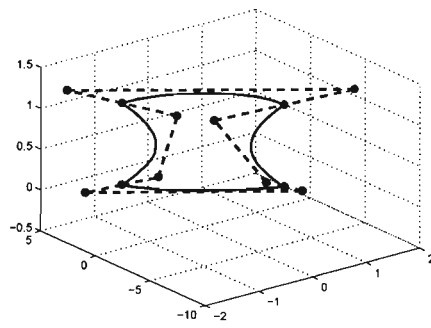
(c)



(d)



(e)



(f)

Figure 3.6. Control points set 4 by harmonic condition on (a) Bézier patch (b) Bézier boundary (c) Said/Wang-Ball patch (d) Said/Wang-Ball boundary (e) DP-Ball patch (f) DP-Ball boundary.

The following comparisons between Bézier surface, Said/Wang-Ball surface and DP-Ball surface was made using harmonic condition. We note that all surfaces have the same two boundary curves.

Table 3.1

Comparison between the area/computational time of Bézier, Said/Wang-Ball and DP-Ball by using harmonic condition.

	Control Points	Bézier	Said/Wang-Ball	DP-Ball
Set 1	Area	19.396724	18.941272	19.372356
	Computational time	0.10468	0.0933	0.10549
Set 2	Area	22.959153	22.579643	23.022066
	Computational time	0.10837	0.0922	0.11019
Set 3	Area	1.230625	1.116308	1.230625
	Computational time	0.10665	0.0907	0.10939
Set 4	Area	5.166923	4.923110	5.166923
	Computational time	0.10594	0.0939	0.10614

From Table 3.1, the harmonic condition is applied to the bicubic patches of Said-Ball surface, Wang-Ball surface and DP-Ball surface, and compared with the existing work for bicubic patch of Bézier surface. It is discovered that the bicubic Said/Wang-Ball are better than the bicubic Bézier and bicubic DP-Ball in terms of the minimal surface area and computational time required to construct the surfaces by harmonic condition. On the other hand, if we compare bicubic Bézier with bicubic DP-Ball by using harmonic condition, we see that the surface area for Bézier and DP-Ball are almost comparable but Bézier needs less computational time than DP-Ball.

3.2 Biharmonic of $X(u, v)$ Patch

The biharmonic equation for the parametric surface $X(u, v)$ is defined as the differential equation obtained by applying the biharmonic operator also known as the bilaplace, that is, the differential operator defined by $\nabla^4 = (\nabla^2)^2$ where

$$\nabla^2 = \frac{\partial^2}{\partial u^2} + \frac{\partial^2}{\partial v^2}, \quad (3.36)$$

is the Laplace and setting them to zeros. In general, for a rectangular system of coordinates, it can be written as,

$$\left(\frac{\partial^2}{\partial u^2} + \frac{\partial^2}{\partial v^2} \right)^2 X(u, v) = 0, \quad (3.37)$$

or

$$\frac{\partial^4 X}{\partial u^4} + 2 \frac{\partial^4 X}{\partial u^2 \partial v^2} + \frac{\partial^4 X}{\partial v^4} = 0. \quad (3.38)$$

We discuss the two solutions of equation (3.38), that are, the solutions on the rectangular grid.

Theorem 3.3. *Given a control net in \mathbb{R}^3 , $\{q_{i,j}\}_{i,j=0}^{m,n}$, the associated $X(u, v)$ surface $X : [0, 1] \times [0, 1] \rightarrow \mathbb{R}^3$, is biharmonic, $\nabla^4 X = 0$ if and only if $\forall i \in \{1, 2, \dots, m\}$ and $j \in \{1, 2, \dots, n\}$*

$$\begin{aligned} 0 &= \sum_{k=0}^4 \sum_{r,s=0}^{m,n} b_{m,i-k,k} \left((f_{i-k+4,r} - 4f_{i-k+3,r} + 6f_{i-k+2,r} - 4f_{i-k+1,r} + f_{i-kr}) q_{rs} h_{sj} \right) \\ &+ 2 \sum_{k,l=0}^2 \sum_{r,s=0}^{m,n} a_{m,i-k,k} a_{n,j-l,l} \left((f_{i-k+2,r} - 2f_{i-k+1,r} + f_{i-k,r}) q_{rs} \times \right. \\ &\quad \left. (h_{s,j-l+2} - 2h_{s,j-l+1} + h_{s,j-l}) \right) \\ &+ \sum_{l=0}^4 \sum_{r,s=0}^{m,n} b_{n,j-l,l} \left(f_{i-k,r} q_{rs} \times \right. \\ &\quad \left. (h_{s,j+4} - 4h_{s,j+3} + 6h_{s,j+2} - 4h_{s,j+1} + h_{sj}) \right), \end{aligned} \quad (3.39)$$

where for $i \in \{0, 1, \dots, m-2\}$,

$$\begin{aligned}
 a_{mi0} &= (m-i)(m-i-1), \\
 a_{mi1} &= 2(i+1)(m-i-1), \\
 a_{mi2} &= (i+1)(i+2), \text{ and} \\
 a_{mik} &= 0, \text{ otherwise;}
 \end{aligned} \tag{3.40}$$

and for $i \in \{0, 1, \dots, m-4\}$,

$$\begin{aligned}
 b_{mi0} &= (m-i)(m-i-1)(m-i-2)(m-i-3), \\
 b_{mi1} &= 4(i+1)(m-i-1)(m-i-2)(m-i-3), \\
 b_{mi2} &= 6(i+1)(i+2)(m-i-2)(m-i-3), \\
 b_{mi3} &= 4(i+1)(i+2)(i+3)(m-i-3), \\
 b_{mi4} &= (i+1)(i+2)(i+3)(i+4), \\
 b_{mik} &= 0, \text{ otherwise.}
 \end{aligned}$$

F and H are convert matrices from the curve $X(u), X(v)$ into the Bézier curve.

Proof. The $X(u, v)$ surface of degree $m \times n$ can be written as the Bézier surface of degree $m \times n$ as follows

$$X(u, v) = \sum_{i=0}^m \sum_{j=0}^n B_i^m(u) B_j^n(v) P_{ij}, \tag{3.41}$$

where

$$P_{ij} = \sum_{r,s=0}^{m,n} f_{ir} q_{rs} h_{sj}, \quad q_{rs} \text{ are the contol points of the surface, } X(u, v),$$

$$\begin{aligned}
\nabla^4 X(u, v) &= \left(\frac{\partial^2}{\partial u^2} + \frac{\partial^2}{\partial v^2} \right)^2 X(u, v) \\
&= \left(\frac{\partial^2}{\partial u^2} + \frac{\partial^2}{\partial v^2} \right) \left(\frac{\partial^2}{\partial u^2} + \frac{\partial^2}{\partial v^2} \right) X(u, v) \\
&= \left(\frac{\partial^2}{\partial u^2} + \frac{\partial^2}{\partial v^2} \right) \left(m(m-1) \sum_{i,j=0}^{m-2,n} B_i^{m-2}(u) B_j^n(v) \Delta^{2,0} P_{i,j} \right. \\
&\quad \left. + n(n-1) \sum_{i,j=0}^{m,n-2} B_i^m(u) B_j^{n-2}(v) \Delta^{0,2} P_{i,j} \right) \\
&= \left(m(m-1)(m-2)(m-3) \sum_{i,j=0}^{m-4,n} B_i^{m-4}(u) B_j^n(v) \Delta^{4,0} P_{i,j} \right. \\
&\quad + 2m(m-1)n(n-1) \sum_{i,j=0}^{m-2,n-2} B_i^{m-2}(u) B_j^{n-2}(v) \Delta^{2,2} P_{i,j} \\
&\quad \left. + n(n-1)(n-2)(n-3) \sum_{i,j=0}^{m,n-4} B_i^m(u) B_j^{n-4}(v) \Delta^{0,4} P_{i,j} \right), \quad (3.42)
\end{aligned}$$

where $\Delta^{4,0}$, $\Delta^{2,2}$ and $\Delta^{0,4}$ are the usual forward difference operators given as:

$$\begin{aligned}
\Delta^{4,0} P_{ij} &= \sum_{r,s=0}^{m,n} \left((\Delta^{4,0} f_{i,r}) q_{rs} h_{s,j} \right) \\
&= \sum_{r,s=0}^{m,n} \left((f_{i+4,r} - 4f_{i+3,r} + 6f_{i+2,r} - 4f_{i+1,r} + f_{i,r}) q_{rs} h_{s,j} \right), \quad (3.43)
\end{aligned}$$

$$\begin{aligned}
\Delta^{2,2} P_{ij} &= \sum_{r,s=0}^{m,n} \left((\Delta^{2,0} f_{i,r}) q_{rs} (\Delta^{0,2} h_{s,j}) \right) \\
&= \left((f_{i+2,r} - 2f_{i+1,r} + f_{i,r}) q_{rs} (h_{s,j+2} - 2h_{s,j+1} + h_{s,j}) \right), \quad (3.44)
\end{aligned}$$

$$\begin{aligned}
\Delta^{0,4} P_{ij} &= \sum_{r,s=0}^{m,n} \left(f_{i,s} q_{rs} (\Delta^{0,4} h_{s,j}) \right) \\
&= \sum_{r,s=0}^{m,n} \left(f_{i,r} q_{rs} (h_{s,j+4} - 4h_{s,j+3} + 6h_{s,j+2} - 4h_{s,j+1} + h_{s,j}) \right). \quad (3.45)
\end{aligned}$$

Now, we want to raise the degree of equation (3.42) as the Bezier surface of degree $m \times n$. We need to use the formula given in Monterde and Ugail (2004) i.e.,

$$B_i^{n-k}(t) = \sum_{l=0}^k \frac{\binom{n-i-l}{k-l} \binom{i+l}{l}}{\binom{n}{k}} B_{i+l}^n(t). \quad (3.46)$$

Thus we have,

$$\begin{aligned} B_i^{n-2}(t) &= \binom{n-2}{i} \sum_{k=0}^2 \frac{\binom{2}{k}}{\binom{n}{i+k}} B_{i+k}^n(t) \\ &= \frac{1}{n(n-1)} ((n-i)(n-i-1)B_i^n(t) \\ &\quad + 2(i+1)(n-i-1)B_{i+1}^n(t) + (i+1)(i+2)B_{i+2}^n(t)) \\ &= \frac{1}{n(n-1)} (a_{ni0}B_i^n(t) + a_{ni1}B_{i+1}^n(t) + a_{ni2}B_{i+2}^n(t)), \end{aligned} \quad (3.47)$$

$\forall i \in \{0, 1, \dots, n-2\}$ and

$$\begin{aligned} B_i^{n-4}(t) &= \binom{n-4}{i} \sum_{k=0}^4 \frac{\binom{4}{k}}{\binom{n}{i+k}} B_{i+k}^n(t) \\ &= \frac{1}{n(n-1)(n-2)(n-3)} ((n-i)(n-i-1)(n-i-2)(n-i-3)B_i^n(t) \\ &\quad + 4(i+1)(n-i-1)(n-i-2)(n-i-3)B_{i+1}^n(t) \\ &\quad + 6(i+1)(i+2)(n-i-2)(n-i-3)B_{i+2}^n(t) \\ &\quad + 4(i+1)(i+2)(i+3)(n-i-3)B_{i+3}^n(t) \\ &\quad + (i+1)(i+2)(i+3)(i+4)B_{i+4}^n(t)) \\ &= \frac{1}{n(n-1)(n-2)(n-3)} (b_{ni0}B_i^n(t) + b_{ni1}B_{i+1}^n(t) \\ &\quad + b_{ni2}B_{i+2}^n(t) + b_{ni3}B_{i+3}^n(t) + b_{ni4}B_{i+4}^n(t)), \end{aligned} \quad (3.48)$$

$\forall i \in \{0, 1, \dots, n-4\}$.

By using (3.47) and (3.48) in (3.42), we get

$$\nabla^4 X(u, v) = \sum_{i=0}^m \sum_{j=0}^n B_i^m(u) B_j^n(v) \times \{\mathcal{F}_{ij}\}, \quad (3.49)$$

where

$$\begin{aligned}
\{\mathcal{F}_{ij}\}_{i,j=0}^{m,n} &= \sum_{k=0}^4 b_{m,i-k,k} \Delta^{4,0} P_{i-k,j} + 2 \sum_{k,l=0}^2 a_{m,i-k,k} a_{n,j-l,l} \Delta^{2,2} P_{i-k,j-l} \\
&\quad + \sum_{l=0}^4 b_{n,j-l,l} \Delta^{0,4} P_{i,j-l} \\
&= \sum_{k=0}^4 \sum_{r,s=0}^{m,n} b_{m,i-k,k} \left((f_{i-k+4,r} - 4f_{i-k+3,r} + 6f_{i-k+2,r} - 4f_{i-k+1,r} + f_{i-kr}) \times \right. \\
&\quad \left. q_{rs} h_{sj} \right) + 2 \sum_{k,l=0}^2 \sum_{r,s=0}^{m,n} \left((f_{i-k+2,r} - 2f_{i-k+1,r} + f_{i-k,r}) \times \right. \\
&\quad \left. q_{rs} (h_{s,j-l+2} - 2h_{s,j-l+1} + h_{s,j-l}) \right) a_{m,i-k,k} a_{n,j-l,l} + \sum_{l=0}^4 \sum_{r,s=0}^{m,n} b_{n,j-l,l} \times \\
&\quad \left(f_{ir} q_{rs} (h_{s,j-l+4} - 4h_{s,j-l+3} + 6h_{s,j-l+2} - 4h_{s,j-l+1} + h_{s,j-l}) \right). \quad (3.50)
\end{aligned}$$

Due to the fact that $\{B_i^m(u)B_j^n(v)\}_{i,j=0}^{m,n}$ is a basis of bivariated polynomials, we get $X(u, v)$ to be biharmonic if and only if $\{\mathcal{F}_{i,j}\}_{i,j=0}^{m,n} = 0$, for all i, j . \square

Corollary 3.5. *If we replace the convert matrix and the control points in Theorem 3.3 of the $X(u, v)$ surface by the Said-Ball, DP-Ball, Wang-Ball convert matrix and control points $\{q_{ij}\}_{i,j=0}^{m,n}$ by $\{v_{ij}\}_{i,j=0}^{m,n}$, $\{d_{ij}\}_{i,j=0}^{m,n}$, $\{w_{ij}\}_{i,j=0}^{m,n}$, we get the biharmonic condition for Said-Ball, DP-Ball and Wang-Ball surface of degree $m \times n$.*

Remark 3.7. *Theorem 3.3 holds for Bézier if the control points $\{q_{i,j}\}_{i,j=0}^{n,n}$ of the $X(u, v)$ surface is replaced by the Bézier control points $\{P_{i,j}\}_{i,j=0}^{n,n}$ and also if the convert matrices F and H are being replaced by the identity matrix.*

3.2.1 Bicubic Biharmonic Patch

In the case $n = m = 3$ from equation (3.39), it is possible to find an expression of four of the control points in terms of the other twelve. In fact, we have obtained that the null space of the coefficient matrix of (3.3) is of dimension four. Moreover, it is possible to choose free variables points in the four boundaries of the control net.

3.2.1.1 Bicubic Said/Wang-Ball Biharmonic Equation

We note that the first case where the biharmonic equation makes sense is for $n = m = 3$. In this case, the solution of equation (3.39) exists. Then, the inner control points by biharmonic condition for the bicubic Said-Ball surface are:

$$v_{11} = (1/4)(-v_{00} + 2v_{01} - v_{03} + 2v_{10} + 2v_{13} - v_{30} + 2v_{31} - v_{33}), \quad (3.51)$$

$$v_{12} = (1/4)(-v_{00} + 2v_{02} - v_{03} + 2v_{10} + 2v_{13} - v_{30} + 2v_{32} - v_{33}), \quad (3.52)$$

$$v_{21} = (1/4)(-v_{00} + 2v_{01} - v_{03} + 2v_{20} + 2v_{23} - v_{30} + 2v_{31} - v_{33}), \quad (3.53)$$

$$v_{22} = (1/4)(-v_{00} + 2v_{02} - v_{03} + 2v_{20} + 2v_{23} - v_{30} + 2v_{32} - v_{33}). \quad (3.54)$$

3.2.1.2 DP-Ball Biharmonic Equation

If we replace the convert matrix and the control points in Theorem 3.3 of the $X(u, v)$ surface by the DP-Ball convert matrix and control points $\{D_{ij}\}_{i,j=0}^{m,n}$, we get the biharmonic condition for the DP-Ball surface of degree $m \times n$.

We note that the first case where the biharmonic equation makes sense is for $n = m = 3$. In this case, the solution of equation (3.39) exists. Then, the inner control points by biharmonic condition for the bicubic DP-Ball surface are:

$$d_{11} = d_{01} - d_{00} + d_{10}, \quad (3.55)$$

$$d_{12} = d_{02} - d_{03} + d_{13}, \quad (3.56)$$

$$d_{21} = d_{20} - d_{30} + d_{31}, \quad (3.57)$$

$$d_{22} = d_{23} + d_{32} - d_{33}. \quad (3.58)$$

The masks represented below are for the bicubic biharmonic condition where the left represents Bézier, the middle denotes Said/Wang-Ball, while the right signifies DP-Ball.

	$\begin{matrix} -2 & 3 & 0 & -1 \\ 0 & \bullet & \bullet & 0 \\ 6 & \bullet & \bullet & 3 \\ -4 & 6 & 0 & -2 \end{matrix}$	$\begin{matrix} -1 & 2 & 0 & -1 \\ 0 & \bullet & \bullet & 0 \\ 2 & \bullet & \bullet & 2 \\ -1 & 2 & 0 & -1 \end{matrix}$	$\begin{matrix} 0 & 0 & 0 & 0 \\ 0 & \bullet & \bullet & 0 \\ 1 & \bullet & \bullet & 0 \\ -1 & 1 & 0 & 0 \end{matrix}$
$P_{11} = \frac{1}{9}$	$v_{11} = \frac{1}{4}$	$d_{11} =$	
	$\begin{matrix} -4 & 6 & 0 & -2 \\ 6 & \bullet & \bullet & 3 \\ 0 & \bullet & \bullet & 0 \\ -2 & 3 & 0 & -1 \end{matrix}$	$\begin{matrix} -1 & 2 & 0 & -1 \\ 2 & \bullet & \bullet & 2 \\ 0 & \bullet & \bullet & 0 \\ -1 & 2 & 0 & -1 \end{matrix}$	$\begin{matrix} -1 & 1 & 0 & 0 \\ 1 & \bullet & \bullet & 0 \\ 0 & \bullet & \bullet & 0 \\ 0 & 0 & 0 & 0 \end{matrix}$
$P_{12} = \frac{1}{9}$	$v_{12} = \frac{1}{4}$	$d_{12} =$	
	$\begin{matrix} -1 & 0 & 3 & -2 \\ 0 & \bullet & \bullet & 0 \\ 3 & \bullet & \bullet & 6 \\ -2 & 0 & 6 & -4 \end{matrix}$	$\begin{matrix} -1 & 0 & 2 & -1 \\ 0 & \bullet & \bullet & 0 \\ 2 & \bullet & \bullet & 2 \\ -1 & 0 & 2 & -1 \end{matrix}$	$\begin{matrix} 0 & 0 & 0 & 0 \\ 0 & \bullet & \bullet & 0 \\ 0 & \bullet & \bullet & 1 \\ 0 & \bullet & 1 & -1 \end{matrix}$
$P_{21} = \frac{1}{9}$	$v_{21} = \frac{1}{4}$	$d_{21} =$	
	$\begin{matrix} -4 & 6 & 0 & -2 \\ 6 & \bullet & \bullet & 3 \\ 0 & \bullet & \bullet & 0 \\ -2 & 3 & 0 & 1 \end{matrix}$	$\begin{matrix} -1 & 0 & 2 & -1 \\ 2 & \bullet & \bullet & 2 \\ 0 & \bullet & \bullet & 0 \\ -1 & 0 & 2 & -1 \end{matrix}$	$\begin{matrix} 0 & 0 & 1 & -1 \\ 0 & \bullet & \bullet & 1 \\ 0 & \bullet & \bullet & 0 \\ 0 & 0 & 0 & 0 \end{matrix}$
$P_{22} = \frac{1}{9}$	$v_{22} = \frac{1}{4}$	$d_{22} =$	

3.2.2 Graphical Examples for Biharmonic Bicubic Patch

Here we give some graphical examples for bicubic Said/Wang-Ball and bicubic DP-Ball generated by four sets of control points such that the surface have the same boundaries.

3.2.2.1 Graphical Examples for Biharmonic Bicubic Said/Wang-Ball Patch

To generate the Biharmonic Said-Ball surface, we have chosen four sets of boundary curves.

Example 3.10. Given the boundary control points set 1 of the bicubic Said-Ball surface as follows

$$\begin{aligned}v_{00} &= (0, 0, 1), v_{01} = (0, 18/5, -491/625), v_{02} = (0, 14/5, -71/625), v_{03} = (0, 4, 1), \\v_{10} &= (6/5, 0, 2113/1000), v_{20} = (1, 0, 23/8), v_{13} = (9/5, 4, 631/250), \\v_{23} &= (11/5, 4, 631/250), v_{30} = (4, 0, 1), v_{31} = (4, 9/5, -885/1687), \text{ and} \\v_{32} &= (4, 11/5, -885/1687), v_{33} = (4, 4, 1).\end{aligned}$$

Then, the inner control points of the bicubic Said-Ball surface by biharmonic condition are

$$\begin{aligned}v_{11} &= (3/2, 27/10, 1557/2347), v_{12} = (3/2, 5/2, 1666/1667), \\v_{21} &= (8/5, 27/10, 1576/1509), v_{22} = (8/5, 5/2, 1310/949).\end{aligned}$$

The graph of the above surface is in Figure 3.7(c) while its boundary with control points is in Figure 3.7(c).

Example 3.11. Given the boundary control points set 2 of the bicubic Said-Ball surface as follows

$$\begin{aligned}v_{00} &= (0, 0, 0), v_{01} = (0, 9/4, -9/2), v_{02} = (0, 3/4, 9/2), v_{03} = (0, 3, 0) \\v_{10} &= (9/4, 0, -9/2), v_{20} = (3/4, 0, 9/2), v_{13} = (3/2, 3, -3/2), v_{23} = (3/2, 3, -3/2), \\v_{30} &= (3, 0, 0) v_{31} = (3, 3/2, 3/2), v_{32} = (3, 3/2, 3/2), v_{33} = (3, 3, 0).\end{aligned}$$

Then, the inner control points of the bicubic Said-Ball surface by biharmonic condition are $v_{11} = (15/8, 15/8, -9/2)$, $v_{12} = (15/8, 9/8, 0)$, $v_{21} = (9/8, 15/8, 0)$, and $v_{22} = (9/8, 9/8, 9/2)$. The graph of the above surface is in Figure 3.8(c) while its boundary with control points is in Figure 3.8(c).

Example 3.12. Given the boundary control points set 3 of the bicubic Said-Ball surface as follows

$$\begin{aligned} v_{00} &= (1/2, 0, 0), v_{10} = (433/3171, 3/5, 0), v_{20} = (-1/2, 27/50, 0), v_{30} = (-1/2, 0, 0), \\ v_{01} &= (31/80, 0, 27/40), v_{02} = (29/80, 0, 5/8), v_{03} = (1, 0, 1), v_{13} = (223/817, 3/2, 1), \\ v_{23} &= (-1, 27/25, 1), v_{31} = (-31/80, 0, 27/40), v_{32} = (-29/80, 0, 5/8), v_{33} = (-1, 0, 1). \end{aligned}$$

Then, the inner control points of the bicubic Said-Ball surface by biharmonic condition are

$$\begin{aligned} v_{11} &= (569/2779, 21/20, 27/40), v_{12} = (569/2779, 21/20, 5/8), \\ v_{21} &= (-3/4, 81/100, 27/40), \text{ and } v_{22} = (-3/4, 81/100, 5/8). \end{aligned}$$

The graph of the above surface is in Figure 3.9(c) while its boundary with control points is in Figure 3.9(c).

Example 3.13. Given the boundary control points set 4 of the bicubic Said-Ball surface as follows

$$\begin{aligned} v_{00} &= (-585/631, 1378/483, 0), v_{10} = (-2547/631, -689/483, 0), \\ v_{20} &= (-710/173, -609/500, 0), v_{30} = (585/631, -1378/483, 0), \\ v_{01} &= (-111/581, 2342/3983, 21/40), v_{02} = (-327/3697, 457/1674.2/5), \\ v_{03} &= (-585/631, 1378/483, 1), v_{13} = (-622/163, -2234/793, 1), v_{23} = (-1170/631, -1378/483, 1), \\ v_{31} &= (512/1599, -1699/1724, 9/20), \\ v_{32} &= (161/7124, -173/2475, 13/40), v_{33} = (585/631, -1378/483, 1). \end{aligned}$$

Then, the inner control points of the bicubic Said-Ball surface by biharmonic condition are

$$\begin{aligned} v_{11} &= (-2707/701, -485/209, 39/80), v_{12} = (-1453/367, -2491/1233, 29/80), \\ v_{21} &= (-1262/433, -1135/508, 39/80), \text{ and } v_{22} = (-250/83, -1669/863, 29/80). \end{aligned}$$

The graph of the above surface is in Figure 3.10(c) while its boundary with control points is in Figure 3.10(c).

3.2.2.2 Graphical Examples for Biharmonic Bicubic DP-Ball Surface

To generate the biharmonic DP-Ball surface, we have chosen four sets of boundary curves.

Example 3.14. Given the boundary control points set 1 of the bicubic DP-Ball surface as follows

$$\begin{aligned}d_{00} &= (0, 0, 1), d_{30} = (4, 0, 1), d_{01} = (0, 18/5, -491/625), d_{31} = (4, -2/5, -41/2500), \\d_{02} &= (0, 4, 441/625), d_{32} = (4, 11/5, -885/1687), d_{03} = (0, 4, 1), d_{33} = (4, 4, 1), \\d_{10} &= (-2/5, 0, 617/500), d_{20} = (16/5, 0, 1379/500), d_{13} = (-2/5, 4, 252/125) \text{ and} \\d_{23} &= (4, 22/5, -41/2500).\end{aligned}$$

Then, the inner control points of the bicubic DP-Ball surface by biharmonic condition are

$$\begin{aligned}d_{11} &= (2/5, -8/5, 1011/2500), d_{12} = (2/5, -4, -1076/625), \\d_{21} &= (-16/5, 2/5, -2177/1250), d_{22} = (-22/5, -22/5, -2499/2500).\end{aligned}$$

The graph of the above surface is in Figure 3.7(e) while its boundary with control points is in Figure 3.7(f).

Example 3.15. Given the boundary control points set 2 of the bicubic DP-Ball surface as follows

$$\begin{aligned}d_{00} &= (0, 0, 0), d_{10} = (3/2, 0, -9), d_{20} = (3/4, 0, 9/2), d_{30} = (3, 0, 0), d_{01} = (0, 3/2, -9), \\d_{02} &= (0, 3/2, 9), d_{03} = (0, 3, 0), d_{13} = (0, 3, -1), d_{23} = (3, 3, -1), d_{31} = (3, 0, 1), \\d_{32} &= (3, 3, 1), d_{33} = (3, 3, 0).\end{aligned}$$

Then, the inner control points of the bicubic DP-Ball surface by biharmonic condition are

$$\begin{aligned}d_{11} &= (-3/2, -3/2, 18), d_{12} = (0, -3/2, -8), d_{21} = (-3/2, 0, -10), \text{ and} \\d_{22} &= (-3, -3, 0).\end{aligned}$$

The graph of the above surface is in Figure 3.8(e) while its boundary with control points is in Figure 3.8(f).

Example 3.16. Given the boundary control points set 3 of the bicubic DP-Ball surface as follows

$$\begin{aligned} d_{00} &= (1/2, 0, 0), d_{10} = (989/974, 11/25, 0), d_{20} = (-1225/974, 8/25, 0), \\ d_{30} &= (-1/2, 0, 0), d_{01} = (11/40, 0, 3/20), d_{02} = (29/40, 0, 21/20), d_{03} = (1, 0, 1), \\ d_{13} &= (1659/817, 32/25, 1), d_{23} = (-2055/817, 11/25, 1), d_{31} = (-11/40, 0, 3/20), \\ d_{32} &= (-29/40, 0, 21/20), d_{33} = (-1, 0, 1). \end{aligned}$$

Then, the inner control points of the bicubic DP-Ball surface by biharmonic condition are

$$\begin{aligned} d_{11} &= (-494/625, -11/25, -3/20), d_{12} = (-862/491, -32/25, -21/20), \\ d_{21} &= (979/948, -8/25, -3/20), \text{ and } d_{22} = (1790/799, -11/25, -21/20). \end{aligned}$$

The graph of the above surface is in Figure 3.9(e) while its boundary with control points is in Figure 3.9(f).

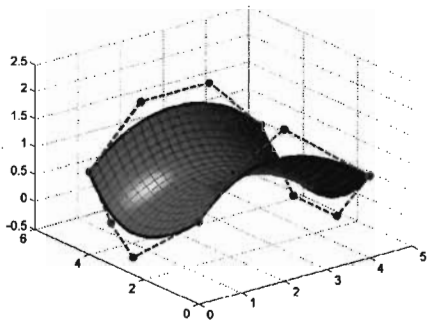
Example 3.17. Given the boundary control points set 4 of the bicubic DP-Ball surface as follows

$$\begin{aligned} d_{00} &= (-585/631, 1378/483, 0), d_{10} = (-1297/363, 1763/1000, 0), \\ d_{20} &= (-927/500, -1763/500, 0), d_{30} = (585/631, -1378/483, 0), \\ d_{01} &= (-631/1250, 1553/1000, 1/10), d_{02} = (-749/2500, 923/1000, 17/20), \\ d_{03} &= (-585/631, 1378/483, 1), d_{13} = (-2356/493, 834/835, 1), \\ d_{23} &= (834/835, -2356/493, 1), d_{31} = (1121/1555, -2773/1250, 1/20), \\ d_{32} &= (292/2323, -242/625, 4/5), d_{33} = (585/631, -1378/483, 1). \end{aligned}$$

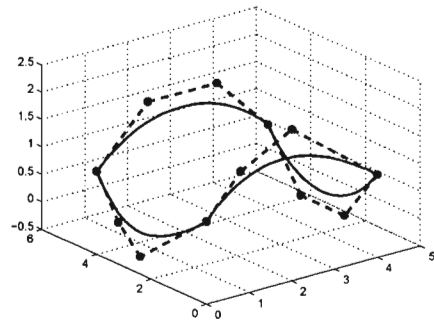
Then, the inner control points of the bicubic DP-Ball surface by biharmonic condition are

$$\begin{aligned} d_{11} &= (2467/783, -244/527, -1/10), d_{12} = (1179/284, 582/625, -17/20), \\ d_{21} &= (616/299, 2689/930, -1/20), \text{ and } d_{22} = (-1003/5081, 2401/1038, -4/5). \end{aligned}$$

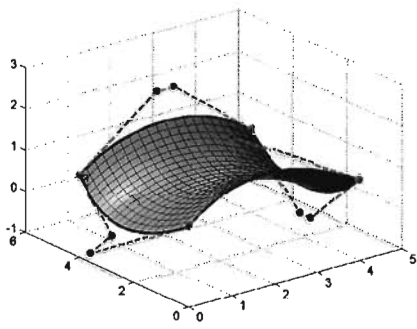
The graph of the above surface is in Figure 3.10(e) while its boundary with control points is in Figure 3.10(f).



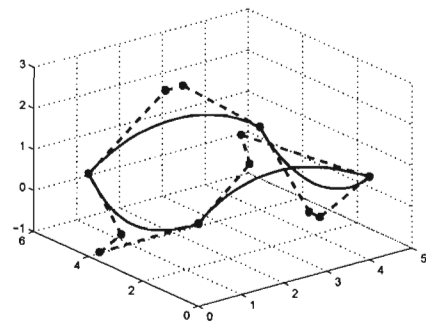
(a)



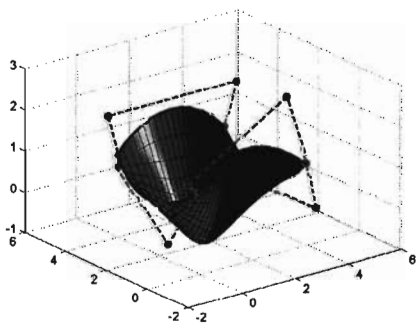
(b)



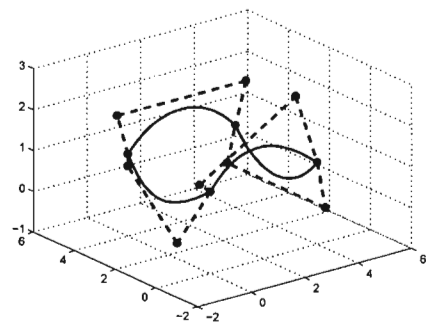
(c)



(d)

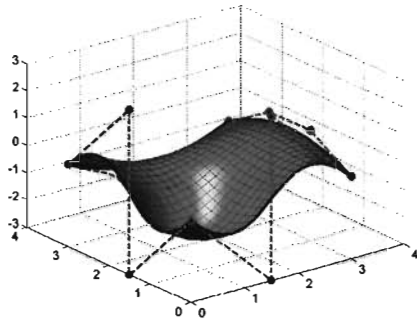


(e)

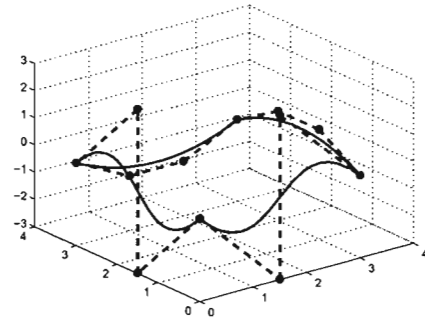


(f)

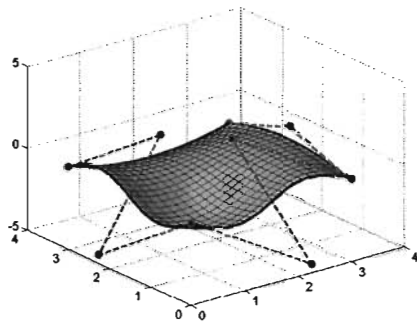
Figure 3.7. Control points set 1 by biharmonic condition on (a) Bézier patch (b) Bézier boundary (c) Said/Wang-Ball patch (d) Said/Wang-Ball boundary (e) DP-Ball patch (f) DP-Ball boundary.



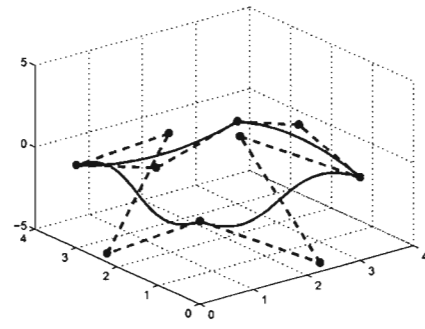
(a)



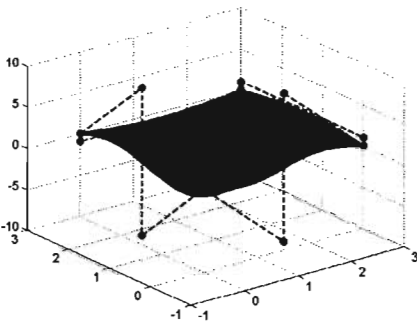
(b)



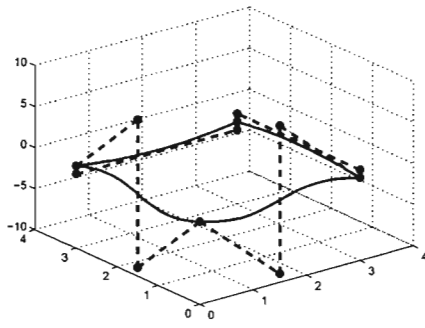
(c)



(d)

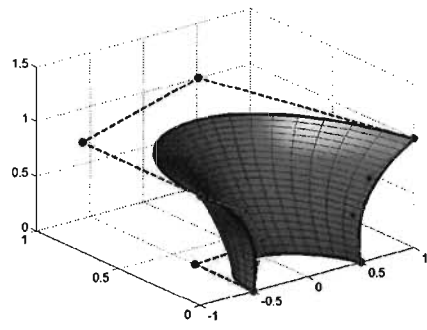


(e)

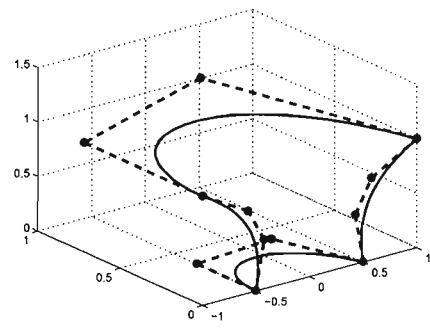


(f)

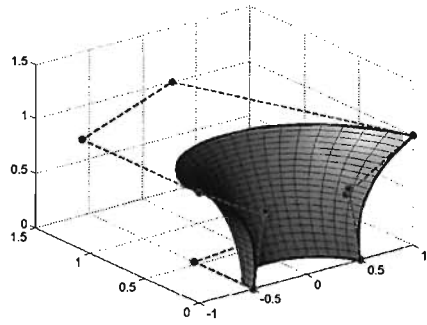
Figure 3.8. Control points set 2 by biharmonic condition on (a) Bézier patch (b) Bézier boundary (c) Said/Wang-Ball patch (d) Said/Wang-Ball boundary (e) DP-Ball patch (f) DP-Ball boundary.



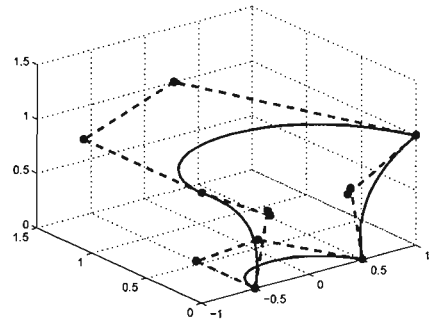
(a)



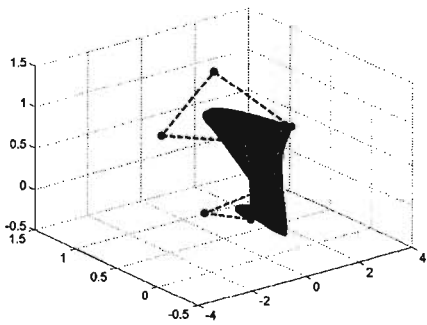
(b)



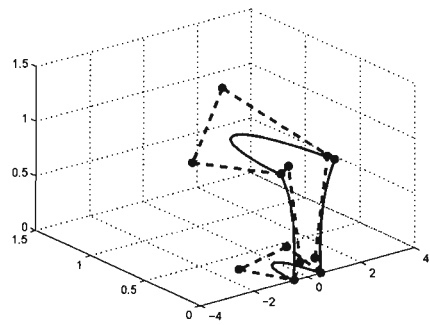
(c)



(d)



(e)



(f)

Figure 3.9. Control points set 3 by biharmonic condition on (a) Bézier patch (b) Bézier boundary (c) Said/Wang-Ball patch (d) Said/Wang-Ball boundary (e) DP-Ball patch (f) DP-Ball boundary.

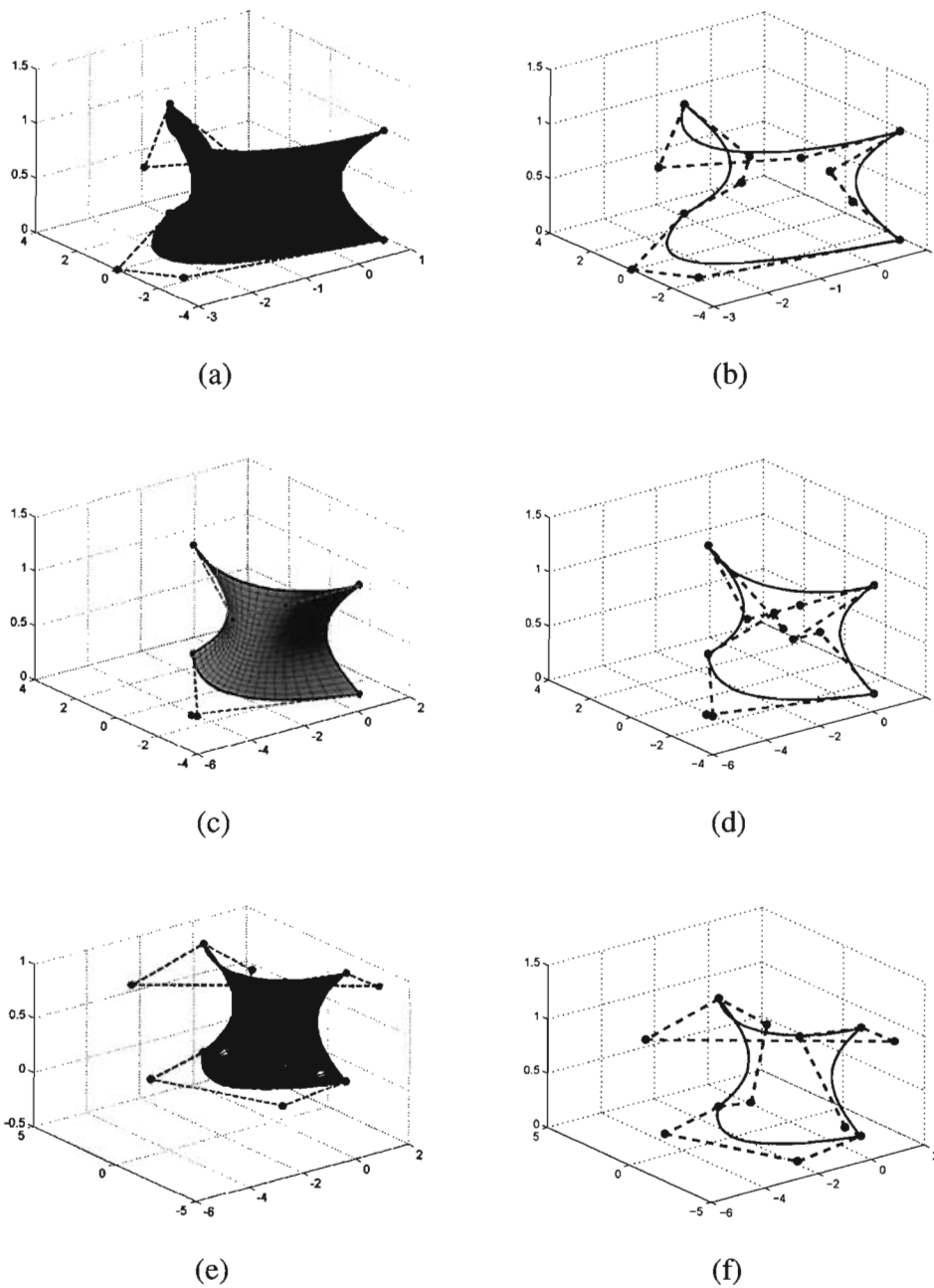


Figure 3.10. Control points set 4 by biharmonic condition on (a) Bézier patch (b) Bézier boundary (c) Said/Wang-Ball patch (d) Said/Wang-Ball boundary (e) DP-Ball patch (f) DP-Ball boundary.

The following comparisons between Bézier surface, Said/Wang-Ball surface and DP-Ball surface was made using biharmonic condition. We note that all surfaces have the same four boundary curves.

Table 3.2

Comparison between the area/computational time of Bézier, Said/Wang-Ball and DP-Ball by using biharmonic condition.

	Control Points	Bézier	Said/Wang-Ball	DP-Ball
Set 1	Area	18.765491	18.765491	26.738931
	Computational time	0.0933	0.0924	0.10538
Set 2	Area	14.064599	14.064599	17.723976
	Computational time	0.0952	0.0936	0.10994
Set 3	Area	1.867949	1.867949	2.282157
	Computational time	0.10458	0.0937	0.11671
Set 4	Area	10.045463	10.045461	21.665577
	Computational time	0.0932	0.0927	0.10517

From Table 3.2 , the biharmonic condition is applied to the bicubic patches of Said-Ball surface, Wang-Ball surface and DP-Ball surface, and compared with the existing work for bicubic patch of Bézier surface. It is discovered that the bicubic Said/Wang-Ball surface and bicubic Bézier surface have the same surface area but bicubic Said/Wang-Ball surface is better than the bicubic Bézier surface in terms of the computational time required to construct the surfaces by biharmonic condition. On the other hand, if we compare bicubic Bézier with bicubic DP-Ball by using the biharmonic condition, we see that the Bézier is better than DP-Ball in terms of minimal surface area and computational time.

3.2.3 Biquartic Biharmonic Equation

We note that the second case where the biharmonic equation makes sense is for $n = m = 4$. In this case, the solution of equation (3.39) exists. Then, the inner control points by biharmonic condition for the biquartic surface are given in Sections 3.2.3.1 until 3.2.3.3.

3.2.3.1 Biquartic Said-Ball Biharmonic Equation

Corollary 3.6. *The biquartic Said-Ball surface is biharmonic if and only if*

$$\begin{aligned} v_{11} = & \frac{-1}{252}(37v_{00} + 39v_{01} + 36v_{02} - 18v_{03} + 6v_{04} + 39v_{10} \\ & - 18v_{14} + 36v_{20} + 18v_{24} - 18v_{30} - 9v_{34} + 6v_{40} \\ & - 18v_{41} + 18v_{42} - 9v_{43} + 3v_{44}), \end{aligned} \quad (3.59)$$

$$\begin{aligned} v_{12} = & \frac{1}{451584}(89v_{00} + 227v_{01} - 92v_{02} - 178v_{03} + 134v_{04} + 3v_{10} \\ & - 402v_{14} + 132v_{20} + 402v_{24} - 66v_{30} - 201v_{34} + 22v_{40} \\ & + 46v_{41} - 46v_{42} - 89v_{43} + 67v_{44}), \end{aligned} \quad (3.60)$$

$$\begin{aligned} v_{13} = & \frac{-1}{2016}(13v_{00} + 831v_{01} + 948v_{02} - 1818v_{03} + 606v_{04} \\ & + 831v_{10} - 1818v_{14} - 396v_{20} + 1818v_{24} + 198v_{30} - 909v_{34} \\ & - 66v_{40} + 198v_{41} + 474v_{42} - 909v_{43} + 303v_{44}), \end{aligned} \quad (3.61)$$

$$\begin{aligned} v_{21} = & \frac{-1}{672}(89v_{00} + 3v_{01} + 132v_{02} - 66v_{03} + 22v_{04} + 227v_{10} \\ & + 46v_{14} - 92v_{20} - 46v_{24} - 178v_{30} - 89v_{34} + 134v_{40} \\ & - 402v_{41} + 402v_{42} - 201v_{43} + 67v_{44}), \end{aligned} \quad (3.62)$$

$$\begin{aligned} v_{22} = & \frac{-1}{896}(89v_{00} + 227v_{01} - 92v_{02} - 178v_{03} + 134v_{04} + 227v_{10} \\ & - 178v_{14} - 92v_{20} + 178v_{24} - 178v_{30} - 313v_{34} + 134v_{40} \\ & - 178v_{41} + 178v_{42} - 313v_{43} + 179v_{44}), \end{aligned} \quad (3.63)$$

$$\begin{aligned} v_{23} = & \frac{-1}{96}(v_{00} + 27v_{01} + 36v_{02} - 66v_{03} + 22v_{04} + 43v_{10} \\ & - 34v_{14} - 28v_{20} + 34v_{24} - 2v_{30} - 49v_{34} + 6v_{40} \\ & - 18v_{41} + 66v_{42} - 81v_{43} + 27v_{44}), \end{aligned} \quad (3.64)$$

$$\begin{aligned} v_{31} = & \frac{-1}{2016}(13v_{00} + 831v_{01} - 396v_{02} + 198v_{03} - 66v_{04} \\ & + 831v_{10} + 198v_{14} + 948v_{20} + 474v_{24} - 1818v_{30} - 909v_{34} \\ & + 606v_{40} - 1818v_{41} + 1818v_{42} - 909v_{43} + 303v_{44}), \end{aligned} \quad (3.65)$$

$$\begin{aligned}
v_{32} = & \frac{-1}{96}(v_{00} + 43v_{01} - 28v_{02} - 2v_{03} + 6v_{04} + 27v_{10} \\
& -18v_{14} + 36v_{20} + 66v_{24} - 66v_{30} - 81v_{34} + 22v_{40} \\
& -34v_{41} + 34v_{42} - 49v_{43} + 27v_{44}), \tag{3.66}
\end{aligned}$$

$$\begin{aligned}
v_{33} = & \frac{-1}{1008}(-53v_{00} + 489v_{01} + 12v_{02} - 342v_{03} + 114v_{04} + 489v_{10} \\
& -342v_{14} + 12v_{20} + 1014v_{24} - 342v_{30} - 1179v_{34} + 114v_{40} \\
& -342v_{41} + 1014v_{42} - 1179v_{43} + 393v_{44}). \tag{3.67}
\end{aligned}$$

The masks below show the biharmonic conditions for degree 4. The first column represents the Bézier, while the second column denotes Said-Ball.

$P_{11} = \frac{1}{448}$	$v_{11} = \frac{1}{525}$																																																		
<table style="margin: auto; border-collapse: collapse;"> <tr><td>-18</td><td>24</td><td>-18</td><td>12</td><td>-9</td></tr> <tr><td>24</td><td>•</td><td>•</td><td>•</td><td>12</td></tr> <tr><td>-36</td><td>•</td><td>•</td><td>•</td><td>-18</td></tr> <tr><td>60</td><td>•</td><td>•</td><td>•</td><td>24</td></tr> <tr><td>-39</td><td>60</td><td>-36</td><td>24</td><td>-18</td></tr> </table>	-18	24	-18	12	-9	24	•	•	•	12	-36	•	•	•	-18	60	•	•	•	24	-39	60	-36	24	-18	<table style="margin: auto; border-collapse: collapse;"> <tr><td>-6</td><td>18</td><td>-18</td><td>9</td><td>-3</td></tr> <tr><td>18</td><td>•</td><td>•</td><td>•</td><td>9</td></tr> <tr><td>-36</td><td>•</td><td>•</td><td>•</td><td>-18</td></tr> <tr><td>-39</td><td>•</td><td>•</td><td>•</td><td>18</td></tr> <tr><td>-37</td><td>-39</td><td>-36</td><td>18</td><td>-6</td></tr> </table>	-6	18	-18	9	-3	18	•	•	•	9	-36	•	•	•	-18	-39	•	•	•	18	-37	-39	-36	18	-6
-18	24	-18	12	-9																																															
24	•	•	•	12																																															
-36	•	•	•	-18																																															
60	•	•	•	24																																															
-39	60	-36	24	-18																																															
-6	18	-18	9	-3																																															
18	•	•	•	9																																															
-36	•	•	•	-18																																															
-39	•	•	•	18																																															
-37	-39	-36	18	-6																																															
$P_{12} = \frac{1}{2688}$	$v_{12} = \frac{1}{451584}$																																																		
<table style="margin: auto; border-collapse: collapse;"> <tr><td>-982</td><td>1608</td><td>-1206</td><td>804</td><td>-49</td></tr> <tr><td>712</td><td>•</td><td>•</td><td>•</td><td>356</td></tr> <tr><td>948</td><td>•</td><td>•</td><td>•</td><td>138</td></tr> <tr><td>-908</td><td>•</td><td>•</td><td>•</td><td>-184</td></tr> <tr><td>-37</td><td>-12</td><td>-396</td><td>264</td><td>-86</td></tr> </table>	-982	1608	-1206	804	-49	712	•	•	•	356	948	•	•	•	138	-908	•	•	•	-184	-37	-12	-396	264	-86	<table style="margin: auto; border-collapse: collapse;"> <tr><td>134</td><td>-402</td><td>402</td><td>-201</td><td>67</td></tr> <tr><td>-178</td><td>•</td><td>•</td><td>•</td><td>-89</td></tr> <tr><td>-92</td><td>•</td><td>•</td><td>•</td><td>-46</td></tr> <tr><td>227</td><td>•</td><td>•</td><td>•</td><td>46</td></tr> <tr><td>89</td><td>3</td><td>132</td><td>-66</td><td>22</td></tr> </table>	134	-402	402	-201	67	-178	•	•	•	-89	-92	•	•	•	-46	227	•	•	•	46	89	3	132	-66	22
-982	1608	-1206	804	-49																																															
712	•	•	•	356																																															
948	•	•	•	138																																															
-908	•	•	•	-184																																															
-37	-12	-396	264	-86																																															
134	-402	402	-201	67																																															
-178	•	•	•	-89																																															
-92	•	•	•	-46																																															
227	•	•	•	46																																															
89	3	132	-66	22																																															
$P_{13} = \frac{1}{3584}$	$v_{13} = \frac{1}{2016}$																																																		
<table style="margin: auto; border-collapse: collapse;"> <tr><td>-2042</td><td>3320</td><td>-1818</td><td>1212</td><td>-909</td></tr> <tr><td>3320</td><td>•</td><td>•</td><td>•</td><td>1212</td></tr> <tr><td>-948</td><td>•</td><td>•</td><td>•</td><td>-474</td></tr> <tr><td>-1108</td><td>•</td><td>•</td><td>•</td><td>-264</td></tr> <tr><td>541</td><td>-1108</td><td>396</td><td>-264</td><td>198</td></tr> </table>	-2042	3320	-1818	1212	-909	3320	•	•	•	1212	-948	•	•	•	-474	-1108	•	•	•	-264	541	-1108	396	-264	198	<table style="margin: auto; border-collapse: collapse;"> <tr><td>-606451584</td><td>1818</td><td>1818</td><td>909</td><td>-303</td></tr> <tr><td>1818</td><td>•</td><td>•</td><td>•</td><td>909</td></tr> <tr><td>-948</td><td>•</td><td>•</td><td>•</td><td>-474</td></tr> <tr><td>-831</td><td>•</td><td>•</td><td>•</td><td>-198</td></tr> <tr><td>-13</td><td>-831</td><td>396</td><td>198</td><td>66</td></tr> </table>	-606451584	1818	1818	909	-303	1818	•	•	•	909	-948	•	•	•	-474	-831	•	•	•	-198	-13	-831	396	198	66
-2042	3320	-1818	1212	-909																																															
3320	•	•	•	1212																																															
-948	•	•	•	-474																																															
-1108	•	•	•	-264																																															
541	-1108	396	-264	198																																															
-606451584	1818	1818	909	-303																																															
1818	•	•	•	909																																															
-948	•	•	•	-474																																															
-831	•	•	•	-198																																															
-13	-831	396	198	66																																															

	198	-264	-747	1212	-909		66	-198	-474	909	-303
	-264	•	•	•	1212		-198	•	•	•	909
$P_{31} = \frac{1}{3584}$	396	•	•	•	-1818	$v_{31} = \frac{1}{2016}$	-396	•	•	•	-1818
	-1108	•	•	•	3320		-831	•	•	•	1818
	541	-1108	-948	3320	-2042		-13	-831	-948	1818	-606
	-38	72	-198	324	-211		-6	18	-66	81	-27
	8	•	•	•	196		2	•	•	•	49
$P_{32} = \frac{1}{384}$	48	•	•	•	-6	$v_{32} = \frac{1}{96}$	28	•	•	•	-34
	-172	•	•	•	136		-43	•	•	•	34
	67	-108	-108	264	-166		-1	-27	-36	66	-22
	-342	456	-1014	2020	-1291		-114	342	-1014	1179	-393
	456	•	•	•	2020		342	•	•	•	1179
$P_{33} = \frac{1}{1792}$	-12	•	•	•	-1014	$v_{33} = \frac{1}{1008}$	-12	•	•	•	-1014
	-652	•	•	•	456		-489	•	•	•	342
	379	-652	-12	567	0342		53	-489	-12	342	-114
	-86	-184	138	356	-491		-22	-46	46	89	-67
	264	•	•	•	804		66	•	•	•	201
$P_{21} = \frac{1}{2688}$	-396	•	•	•	-1206	$v_{21} = \frac{1}{672}$	-132	•	•	•	-402
	-12	•	•	•	1608		-3	•	•	•	402
	-37	-908	948	712	-982		-89	-227	92	178	-134
	-758	712	-534	1252	-1163		-134	178	-178	313	-179
	712	•	•	•	1252		178	•	•	•	313
$P_{22} = \frac{1}{2688}$	276	•	•	•	-534	$v_{22} = \frac{1}{896}$	92	•	•	•	-178
	-908	•	•	•	712		-227	•	•	•	178
	187	-908	276	712	-758		-89	-227	92	178	-134

$P_{23} = \frac{1}{384}$	$v_{23} = \frac{1}{96}$																																																		
<table style="width: 100%; border-collapse: collapse;"> <tr><td style="padding: 2px 10px;">-166</td><td style="padding: 2px 10px;">136</td><td style="padding: 2px 10px;">-6</td><td style="padding: 2px 10px;">196</td><td style="padding: 2px 10px;">-211</td></tr> <tr><td style="padding: 2px 10px;">264</td><td style="padding: 2px 10px;">•</td><td style="padding: 2px 10px;">•</td><td style="padding: 2px 10px;">•</td><td style="padding: 2px 10px;">324</td></tr> <tr><td style="padding: 2px 10px;">-108</td><td style="padding: 2px 10px;">•</td><td style="padding: 2px 10px;">•</td><td style="padding: 2px 10px;">•</td><td style="padding: 2px 10px;">-198</td></tr> <tr><td style="padding: 2px 10px;">-108</td><td style="padding: 2px 10px;">•</td><td style="padding: 2px 10px;">•</td><td style="padding: 2px 10px;">•</td><td style="padding: 2px 10px;">72</td></tr> <tr><td style="padding: 2px 10px;">67</td><td style="padding: 2px 10px;">-172</td><td style="padding: 2px 10px;">84</td><td style="padding: 2px 10px;">8</td><td style="padding: 2px 10px;">-38</td></tr> </table>	-166	136	-6	196	-211	264	•	•	•	324	-108	•	•	•	-198	-108	•	•	•	72	67	-172	84	8	-38	<table style="width: 100%; border-collapse: collapse;"> <tr><td style="padding: 2px 10px;">-22</td><td style="padding: 2px 10px;">34</td><td style="padding: 2px 10px;">-34</td><td style="padding: 2px 10px;">49</td><td style="padding: 2px 10px;">-27</td></tr> <tr><td style="padding: 2px 10px;">66</td><td style="padding: 2px 10px;">•</td><td style="padding: 2px 10px;">•</td><td style="padding: 2px 10px;">•</td><td style="padding: 2px 10px;">81</td></tr> <tr><td style="padding: 2px 10px;">-36</td><td style="padding: 2px 10px;">•</td><td style="padding: 2px 10px;">•</td><td style="padding: 2px 10px;">•</td><td style="padding: 2px 10px;">-66</td></tr> <tr><td style="padding: 2px 10px;">-27</td><td style="padding: 2px 10px;">•</td><td style="padding: 2px 10px;">•</td><td style="padding: 2px 10px;">•</td><td style="padding: 2px 10px;">18</td></tr> <tr><td style="padding: 2px 10px;">-1</td><td style="padding: 2px 10px;">-43</td><td style="padding: 2px 10px;">28</td><td style="padding: 2px 10px;">2</td><td style="padding: 2px 10px;">-6</td></tr> </table>	-22	34	-34	49	-27	66	•	•	•	81	-36	•	•	•	-66	-27	•	•	•	18	-1	-43	28	2	-6
-166	136	-6	196	-211																																															
264	•	•	•	324																																															
-108	•	•	•	-198																																															
-108	•	•	•	72																																															
67	-172	84	8	-38																																															
-22	34	-34	49	-27																																															
66	•	•	•	81																																															
-36	•	•	•	-66																																															
-27	•	•	•	18																																															
-1	-43	28	2	-6																																															

3.2.3.2 Biquartic DP-Ball Biharmonic Equation

Corollary 3.7. *The biquartic DP-Ball surface is biharmonic if and only if*

$$\begin{aligned}
 d_{11} = & \frac{1}{896}(391d_{00} - 719d_{01} + 1125d_{02} + 250d_{03} - 1422d_{04} - 719d_{10} \\
 & + 698d_{14} + 1125d_{20} + 375d_{24} + 250d_{30} + 125d_{34} - 1422d_{40} \\
 & + 698d_{41} + 375d_{42} + 125d_{43} - 151d_{44}), \tag{3.68}
 \end{aligned}$$

$$\begin{aligned}
 d_{12} = & \frac{1}{2688}(709d_{00} + 227d_{01} - 2817d_{02} - 178d_{03} + 1654d_{04} - 669d_{10} \\
 & - 1074d_{14} + 1215d_{20} + 405d_{24} + 270d_{30} + 135d_{34} - 1930d_{40} \\
 & + 718d_{41} + 1749d_{42} + 583d_{43} - 1525d_{44}), \tag{3.69}
 \end{aligned}$$

$$\begin{aligned}
 d_{13} = & \frac{-1}{896}(997d_{00} - 125d_{01} - 225d_{02} + 1294d_{03} - 1866d_{04} - 573d_{10} \\
 & + 1294d_{14} - 225d_{20} - 75d_{24} - 50d_{30} - 25d_{34} - 74d_{40} \\
 & - 50d_{41} - 75d_{42} - 473d_{43} + 747d_{44}), \tag{3.70}
 \end{aligned}$$

$$\begin{aligned}
 d_{21} = & \frac{1}{2688}(709d_{00} - 669d_{01} + 1215d_{02} + 270d_{03} - 1930d_{04} + 227d_{10} \\
 & + 718d_{14} - 2817d_{20} + 1749d_{24} - 178d_{30} + 583d_{34} + 1654d_{40} \\
 & - 1074d_{41} + 405d_{42} + 135d_{43} - 1525d_{44}), \tag{3.71}
 \end{aligned}$$

$$\begin{aligned}
 d_{22} = & \frac{-1}{2688}(187d_{00} - 227d_{01} + 129d_{02} + 178d_{03} - 758d_{04} - 227d_{10} \\
 & + 178d_{14} + 129d_{20} + 939d_{24} + 178d_{30} + 313d_{34} - 758d_{40} \\
 & + 178d_{41} + 939d_{42} + 313d_{43} - 1163d_{44}), \tag{3.72}
 \end{aligned}$$

$$\begin{aligned}
d_{23} = & \frac{-1}{2688}(1315d_{00} - 75d_{01} - 135d_{02} + 1314d_{03} - 2374d_{04} - 523d_{10} \\
& + 418d_{14} - 1479d_{20} + 3987d_{24} - 478d_{30} + 433d_{34} + 1210d_{40} \\
& - 30d_{41} - 45d_{42} + 1329d_{43} - 2419d_{44}), \tag{3.73}
\end{aligned}$$

$$\begin{aligned}
d_{31} = & \frac{-1}{2688}(997d_{00} - 573d_{01} - 225d_{02} - 50d_{03} - 74d_{04} - 125d_{10} \\
& - 50d_{14} - 225d_{20} - 75d_{24} + 1294d_{30} - 473d_{34} - 1866d_{40} \\
& + 1294d_{41} - 75d_{42} - 25d_{43} + 747d_{44}), \tag{3.74}
\end{aligned}$$

$$\begin{aligned}
d_{32} = & \frac{-1}{2688}(1315d_{00} - 523d_{01} - 1479d_{02} - 478d_{03} + 1210d_{04} - 75d_{10} \\
& - 30d_{14} - 135d_{20} - 45d_{24} + 1314d_{30} + 1329d_{34} - 2374d_{40} \\
& + 418d_{41} + 3987d_{42} + 433d_{43} - 2419d_{44}), \tag{3.75}
\end{aligned}$$

$$\begin{aligned}
d_{33} = & \frac{1}{896}(159d_{00} + 25d_{01} + 45d_{02} + 458d_{03} - 702d_{04} + 25d_{10} \\
& + 10d_{14} + 45d_{20} + 15d_{24} + 458d_{30} - 1339d_{34} - 702d_{40} \\
& + 10d_{41} + 15d_{42} - 1339d_{43} + 2001d_{44}). \tag{3.76}
\end{aligned}$$

The masks below show the biharmonic conditions for degree 4. The first column represents the Bézier, while the second column denotes for DP-Ball.

$P_{11} = \frac{1}{448}$	
$\begin{matrix} -18 & 24 & -18 & 12 & -9 \\ 24 & \bullet & \bullet & \bullet & 12 \\ -36 & \bullet & \bullet & \bullet & -18 \\ 60 & \bullet & \bullet & \bullet & 24 \\ -39 & 60 & -36 & 24 & -18 \end{matrix}$	$d_{11} = \frac{1}{896}$
	$\begin{matrix} 1422 & -698 & -375 & -125 & 151 \\ -250 & \bullet & \bullet & \bullet & -125 \\ -1125 & \bullet & \bullet & \bullet & -375 \\ 719 & \bullet & \bullet & \bullet & -698 \\ -391 & 719 & -1125 & -250 & 1422 \end{matrix}$
$P_{12} = \frac{1}{2688}$	
$\begin{matrix} -982 & 1608 & -1206 & 804 & -49 \\ 712 & \bullet & \bullet & \bullet & 356 \\ 948 & \bullet & \bullet & \bullet & 138 \\ -908 & \bullet & \bullet & \bullet & -184 \\ -37 & -12 & -396 & 264 & -86 \end{matrix}$	$d_{12} = \frac{1}{2688}$
	$\begin{matrix} -1654 & 1074 & -405 & -135 & 1525 \\ 178 & \bullet & \bullet & \bullet & -583 \\ 2817 & \bullet & \bullet & \bullet & -1749 \\ -227 & \bullet & \bullet & \bullet & -718 \\ -709 & 669 & -1215 & -270 & 1930 \end{matrix}$

	-2042	3320	-1818	1212	-909		-1866	1294	-75	-25	747	
		3320	•	•	•	1212		1294	•	•	•	-473
$P_{13} = \frac{1}{3584}$	-948	•	•	•	-474		$d_{13} = \frac{1}{896}$	-225	•	•	•	-75
	-1108	•	•	•	-264			-125	•	•	•	50
	541	-1108	396	-264	198			997	-573	-225	-50	-74
	198	-264	-747	1212	-909		-74	-50	-75	-473	747	
	-264	•	•	•	1212		-50	•	•	•	-25	
$P_{31} = \frac{1}{3584}$	396	•	•	•	-1818		$d_{31} = \frac{1}{896}$	-225	•	•	•	-75
	-1108	•	•	•	3320			-573	•	•	•	1294
	541	-1108	-948	3320	-2042			997	-125	-225	129	-1866
	-38	72	-198	324	-211		1210	30	-45	1329	-2419	
	8	•	•	•	196		-478	•	•	•	433	
$P_{32} = \frac{1}{384}$	48	•	•	•	-6		$d_{32} = \frac{1}{2688}$	-1479	•	•	•	3987
	-172	•	•	•	136			-532	•	•	•	418
	67	-108	-108	264	-166			1315	-75	-135	131	-2374
	-342	456	-1014	2020	-1291		-702	10	15	-1339	2001	
	456	•	•	•	2020		458	•	•	•	-1889	
$P_{33} = \frac{1}{1792}$	-12	•	•	•	-1014		$d_{33} = \frac{-1}{896}$	45	•	•	•	15
	-652	•	•	•	456			25	•	•	•	10
	379	-652	-12	567	0342			159	25	45	458	-702
	-86	-184	138	356	-491		1930	-718	-1749	-583	1525	
	264	•	•	•	804		-270	•	•	•	-135	
$P_{21} = \frac{1}{2688}$	-396	•	•	•	-1206		$d_{21} = \frac{1}{2688}$	-1215	•	•	•	-405
	-12	•	•	•	1608			669	•	•	•	1074
	-37	-908	948	712	-982			-709	-227	2817	178	-1654

$P_{22} = \frac{1}{2688}$ <table style="width: 100%; border-collapse: collapse;"> <tr><td style="padding: 2px 10px;">-758</td><td style="padding: 2px 10px;">712</td><td style="padding: 2px 10px;">-534</td><td style="padding: 2px 10px;">1252</td><td style="padding: 2px 10px;">-1163</td></tr> <tr><td style="padding: 2px 10px;">712</td><td style="padding: 2px 10px;">•</td><td style="padding: 2px 10px;">•</td><td style="padding: 2px 10px;">•</td><td style="padding: 2px 10px;">1252</td></tr> <tr><td style="padding: 2px 10px;">276</td><td style="padding: 2px 10px;">•</td><td style="padding: 2px 10px;">•</td><td style="padding: 2px 10px;">•</td><td style="padding: 2px 10px;">-534</td></tr> <tr><td style="padding: 2px 10px;">-908</td><td style="padding: 2px 10px;">•</td><td style="padding: 2px 10px;">•</td><td style="padding: 2px 10px;">•</td><td style="padding: 2px 10px;">712</td></tr> <tr><td style="padding: 2px 10px;">187</td><td style="padding: 2px 10px;">-908</td><td style="padding: 2px 10px;">276</td><td style="padding: 2px 10px;">712</td><td style="padding: 2px 10px;">-758</td></tr> </table>	-758	712	-534	1252	-1163	712	•	•	•	1252	276	•	•	•	-534	-908	•	•	•	712	187	-908	276	712	-758	$d_{22} = \frac{1}{2688}$ <table style="width: 100%; border-collapse: collapse;"> <tr><td style="padding: 2px 10px;">-758</td><td style="padding: 2px 10px;">178</td><td style="padding: 2px 10px;">939</td><td style="padding: 2px 10px;">313</td><td style="padding: 2px 10px;">-1163</td></tr> <tr><td style="padding: 2px 10px;">178</td><td style="padding: 2px 10px;">•</td><td style="padding: 2px 10px;">•</td><td style="padding: 2px 10px;">•</td><td style="padding: 2px 10px;">313</td></tr> <tr><td style="padding: 2px 10px;">129</td><td style="padding: 2px 10px;">•</td><td style="padding: 2px 10px;">•</td><td style="padding: 2px 10px;">•</td><td style="padding: 2px 10px;">939</td></tr> <tr><td style="padding: 2px 10px;">-227</td><td style="padding: 2px 10px;">•</td><td style="padding: 2px 10px;">•</td><td style="padding: 2px 10px;">•</td><td style="padding: 2px 10px;">178</td></tr> <tr><td style="padding: 2px 10px;">187</td><td style="padding: 2px 10px;">-227</td><td style="padding: 2px 10px;">129</td><td style="padding: 2px 10px;">178</td><td style="padding: 2px 10px;">-758</td></tr> </table>	-758	178	939	313	-1163	178	•	•	•	313	129	•	•	•	939	-227	•	•	•	178	187	-227	129	178	-758
-758	712	-534	1252	-1163																																															
712	•	•	•	1252																																															
276	•	•	•	-534																																															
-908	•	•	•	712																																															
187	-908	276	712	-758																																															
-758	178	939	313	-1163																																															
178	•	•	•	313																																															
129	•	•	•	939																																															
-227	•	•	•	178																																															
187	-227	129	178	-758																																															
$P_{23} = \frac{1}{384}$ <table style="width: 100%; border-collapse: collapse;"> <tr><td style="padding: 2px 10px;">-166</td><td style="padding: 2px 10px;">136</td><td style="padding: 2px 10px;">-6</td><td style="padding: 2px 10px;">196</td><td style="padding: 2px 10px;">-211</td></tr> <tr><td style="padding: 2px 10px;">264</td><td style="padding: 2px 10px;">•</td><td style="padding: 2px 10px;">•</td><td style="padding: 2px 10px;">•</td><td style="padding: 2px 10px;">324</td></tr> <tr><td style="padding: 2px 10px;">-108</td><td style="padding: 2px 10px;">•</td><td style="padding: 2px 10px;">•</td><td style="padding: 2px 10px;">•</td><td style="padding: 2px 10px;">-198</td></tr> <tr><td style="padding: 2px 10px;">-108</td><td style="padding: 2px 10px;">•</td><td style="padding: 2px 10px;">•</td><td style="padding: 2px 10px;">•</td><td style="padding: 2px 10px;">72</td></tr> <tr><td style="padding: 2px 10px;">67</td><td style="padding: 2px 10px;">-172</td><td style="padding: 2px 10px;">84</td><td style="padding: 2px 10px;">8</td><td style="padding: 2px 10px;">-38</td></tr> </table>	-166	136	-6	196	-211	264	•	•	•	324	-108	•	•	•	-198	-108	•	•	•	72	67	-172	84	8	-38	$d_{23} = \frac{1}{2688}$ <table style="width: 100%; border-collapse: collapse;"> <tr><td style="padding: 2px 10px;">-2374</td><td style="padding: 2px 10px;">418</td><td style="padding: 2px 10px;">3987</td><td style="padding: 2px 10px;">433</td><td style="padding: 2px 10px;">-2419</td></tr> <tr><td style="padding: 2px 10px;">1314</td><td style="padding: 2px 10px;">•</td><td style="padding: 2px 10px;">•</td><td style="padding: 2px 10px;">•</td><td style="padding: 2px 10px;">1329</td></tr> <tr><td style="padding: 2px 10px;">-135</td><td style="padding: 2px 10px;">•</td><td style="padding: 2px 10px;">•</td><td style="padding: 2px 10px;">•</td><td style="padding: 2px 10px;">-45</td></tr> <tr><td style="padding: 2px 10px;">-75</td><td style="padding: 2px 10px;">•</td><td style="padding: 2px 10px;">•</td><td style="padding: 2px 10px;">•</td><td style="padding: 2px 10px;">-30</td></tr> <tr><td style="padding: 2px 10px;">1315</td><td style="padding: 2px 10px;">-523</td><td style="padding: 2px 10px;">-1497</td><td style="padding: 2px 10px;">-478</td><td style="padding: 2px 10px;">1210</td></tr> </table>	-2374	418	3987	433	-2419	1314	•	•	•	1329	-135	•	•	•	-45	-75	•	•	•	-30	1315	-523	-1497	-478	1210
-166	136	-6	196	-211																																															
264	•	•	•	324																																															
-108	•	•	•	-198																																															
-108	•	•	•	72																																															
67	-172	84	8	-38																																															
-2374	418	3987	433	-2419																																															
1314	•	•	•	1329																																															
-135	•	•	•	-45																																															
-75	•	•	•	-30																																															
1315	-523	-1497	-478	1210																																															

3.2.3.3 Biquartic Wang-Ball Biharmonic Equation

Corollary 3.8. *The biquartic Wang-Ball surface is biharmonic if and only if*

$$\begin{aligned}
 w_{11} = & \frac{-1}{112} (103w_{00} + 82w_{01} + 24w_{02} - 12w_{03} + 3w_{04} + 82w_{10} \\
 & - 12w_{14} + 24w_{20} + 12w_{24} - 12w_{30} - 6w_{34} + 3w_{40} \\
 & - 12w_{41} + 12w_{42} - 6w_{43} + 3w_{44}), \tag{3.77}
 \end{aligned}$$

$$\begin{aligned}
 w_{12} = & \frac{-1}{896} (629w_{00} + 454w_{01} + 264w_{02} - 356w_{03} + 89w_{04} + 230w_{10} \\
 & - 580w_{14} + 264w_{20} + 804w_{24} - 132w_{30} - 402w_{34} + 89w_{40} \\
 & + 92w_{41} - 92w_{42} - 178w_{43} + 89w_{44}), \tag{3.78}
 \end{aligned}$$

$$\begin{aligned}
 w_{13} = & \frac{-1}{896} (59w_{00} + 554w_{01} + 632w_{02} - 764w_{03} + 79w_{04} + 554w_{10} \\
 & - 764w_{14} - 264w_{20} + 1212w_{24} + 132w_{30} - 606w_{34} + 79w_{40} \\
 & + 132w_{41} + 316w_{42} - 606w_{43} + 79w_{44}), \tag{3.79}
 \end{aligned}$$

$$\begin{aligned}
w_{21} = & \frac{-1}{896}(629w_{00} + 230w_{01} + 264w_{02} - 132w_{03} + 89w_{04} + 454w_{10} \\
& + 92w_{14} + 264w_{20} - 92w_{24} - 356w_{30} - 178w_{34} + 89w_{40} \\
& - 580w_{41} + 804w_{42} - 402w_{43} + 89w_{44}), \tag{3.80}
\end{aligned}$$

$$\begin{aligned}
w_{22} = & \frac{-1}{3584}(2111w_{00} + 1362w_{01} + 344w_{02} - 1068w_{03} + 491w_{04} + 1362w_{10} \\
& - 1068w_{14} + 344w_{20} + 1964w_{24} - 1068w_{30} - 1878w_{34} + 491w_{40} \\
& - 1068w_{41} + 1964w_{42} - 1878w_{43} + 491w_{44}), \tag{3.81}
\end{aligned}$$

$$\begin{aligned}
w_{23} = & \frac{-1}{128}(77w_{00} + 54w_{01} + 72w_{02} - 100w_{03} + 17w_{04} + 86w_{10} \\
& - 68w_{14} - 56w_{20} + 132w_{24} - 4w_{30} - 98w_{34} + 17w_{40} \\
& - 36w_{41} + 132w_{42} - 130w_{43} + 17w_{44}), \tag{3.82}
\end{aligned}$$

$$\begin{aligned}
w_{31} = & \frac{-1}{896}(659w_{00} + 554w_{01} - 264w_{02} + 132w_{03} + 79w_{04} + 554w_{10} \\
& + 132w_{14} + 632w_{20} + 316w_{24} - 764w_{30} - 606w_{34} + 79w_{40} \\
& - 764w_{41} + 1212w_{42} - 606w_{43} + 79w_{44}), \tag{3.83}
\end{aligned}$$

$$\begin{aligned}
w_{32} = & \frac{-1}{128}(77w_{00} + 86w_{01} - 56w_{02} - 4w_{03} + 17w_{04} + 54w_{10} \\
& - 36w_{14} + 72w_{20} + 132w_{24} - 100w_{30} - 130w_{34} + 17w_{40} \\
& - 68w_{41} + 132w_{42} - 98w_{43} + 17w_{44}), \tag{3.84}
\end{aligned}$$

$$\begin{aligned}
w_{33} = & \frac{-1}{448}(277w_{00} + 326w_{01} + 8w_{02} - 228w_{03} + 57w_{04} + 326w_{10} \\
& - 228w_{14} + 8w_{20} + 676w_{24} - 228w_{30} - 562w_{34} + 57w_{40} \\
& - 228w_{41} + 676w_{42} - 562w_{43} + 57w_{44}). \tag{3.85}
\end{aligned}$$

The masks below show the biharmonic conditions for degree 4. The first column represents the Bézier, while Wang-Ball is shown in the second column.

$$P_{11} = \frac{1}{448} \begin{pmatrix} -18 & 24 & -18 & 12 & -9 \\ 24 & \bullet & \bullet & \bullet & 12 \\ -36 & \bullet & \bullet & \bullet & -18 \\ 60 & \bullet & \bullet & \bullet & 24 \\ -39 & 60 & -36 & 24 & -18 \end{pmatrix}$$

$$W_{11} = \frac{1}{112} \begin{pmatrix} -3 & 12 & -12 & 6 & -3 \\ 12 & \bullet & \bullet & \bullet & 6 \\ -24 & \bullet & \bullet & \bullet & -12 \\ -82 & \bullet & \bullet & \bullet & 12 \\ -103 & -82 & -24 & 12 & -3 \end{pmatrix}$$

$$P_{12} = \frac{1}{2688} \begin{pmatrix} -982 & 1608 & -1206 & 804 & -49 \\ 712 & \bullet & \bullet & \bullet & 356 \\ 948 & \bullet & \bullet & \bullet & 138 \\ -908 & \bullet & \bullet & \bullet & -184 \\ -37 & -12 & -396 & 264 & -86 \end{pmatrix}$$

$$W_{12} = \frac{1}{896} \begin{pmatrix} -89 & 580 & -804 & 402 & -89 \\ 35 & \bullet & \bullet & \bullet & 178 \\ -264 & \bullet & \bullet & \bullet & 92 \\ -454 & \bullet & \bullet & \bullet & -92 \\ -629 & -230 & -264 & 132 & -89 \end{pmatrix}$$

$$P_{13} = \frac{1}{3584} \begin{pmatrix} -2042 & 3320 & -1818 & 1212 & -909 \\ 3320 & \bullet & \bullet & \bullet & 1212 \\ -948 & \bullet & \bullet & \bullet & -474 \\ -1108 & \bullet & \bullet & \bullet & -264 \\ 541 & -1108 & 396 & -264 & 198 \end{pmatrix}$$

$$W_{13} = \frac{1}{896} \begin{pmatrix} -79 & 764 & -1212 & -606 & -79 \\ 764 & \bullet & \bullet & \bullet & 606 \\ -632 & \bullet & \bullet & \bullet & -316 \\ -554 & \bullet & \bullet & \bullet & -132 \\ -59 & -554 & 264 & -132 & -79 \end{pmatrix}$$

$$P_{31} = \frac{1}{3584} \begin{pmatrix} 198 & -264 & -747 & 1212 & -909 \\ -264 & \bullet & \bullet & \bullet & 1212 \\ 396 & \bullet & \bullet & \bullet & -1818 \\ -1108 & \bullet & \bullet & \bullet & 3320 \\ 541 & -1108 & -948 & 3320 & -2042 \end{pmatrix}$$

$$W_{31} = \frac{-1}{896} \begin{pmatrix} 79 & 132 & 316 & -606 & 79 \\ 132 & \bullet & \bullet & \bullet & -606 \\ -264 & \bullet & \bullet & \bullet & 1212 \\ 554 & \bullet & \bullet & \bullet & -764 \\ 659 & 554 & 632 & -764 & 79 \end{pmatrix}$$

$$P_{32} = \frac{1}{384} \begin{pmatrix} -38 & 72 & -198 & 324 & -211 \\ 8 & \bullet & \bullet & \bullet & 196 \\ 48 & \bullet & \bullet & \bullet & -6 \\ -172 & \bullet & \bullet & \bullet & 136 \\ 67 & -108 & -108 & 264 & -166 \end{pmatrix}$$

$$W_{12} = \frac{1}{128} \begin{pmatrix} -17 & 36 & -132 & 130 & -17 \\ 4 & \bullet & \bullet & \bullet & 98 \\ 56 & \bullet & \bullet & \bullet & -132 \\ -86 & \bullet & \bullet & \bullet & 68 \\ -77 & -54 & -72 & 100 & -17 \end{pmatrix}$$

$$P_{33} = \frac{1}{1792} \begin{pmatrix} -342 & 456 & -1014 & 2020 & -1291 \\ 456 & \bullet & \bullet & \bullet & 2020 \\ -12 & \bullet & \bullet & \bullet & -1014 \\ -652 & \bullet & \bullet & \bullet & 456 \\ 379 & -652 & -12 & 567 & 0342 \end{pmatrix}$$

$$W_{22} = \frac{-1}{448} \begin{pmatrix} 57 & -228 & 676 & -562 & 57 \\ -228 & \bullet & \bullet & \bullet & -562 \\ 8 & \bullet & \bullet & \bullet & 676 \\ 326 & \bullet & \bullet & \bullet & -228 \\ 227 & 326 & 8 & -228 & 57 \end{pmatrix}$$

$$P_{21} = \frac{1}{2688} \begin{pmatrix} -86 & -184 & 138 & 356 & -491 \\ 264 & \bullet & \bullet & \bullet & 804 \\ -396 & \bullet & \bullet & \bullet & -1206 \\ -12 & \bullet & \bullet & \bullet & 1608 \\ -37 & -908 & 948 & 712 & -982 \end{pmatrix}$$

$$W_{21} = \frac{1}{896} \begin{pmatrix} -89 & -92 & 92 & 178 & -89 \\ 132 & \bullet & \bullet & \bullet & 402 \\ -264 & \bullet & \bullet & \bullet & -804 \\ -230 & \bullet & \bullet & \bullet & 580 \\ -629 & -454 & -264 & 356 & 89 \end{pmatrix}$$

$$P_{22} = \frac{1}{2688} \begin{pmatrix} -758 & 712 & -534 & 1252 & -1163 \\ 712 & \bullet & \bullet & \bullet & 1252 \\ 276 & \bullet & \bullet & \bullet & -534 \\ -908 & \bullet & \bullet & \bullet & 712 \\ 187 & -908 & 276 & 712 & -758 \end{pmatrix}$$

$$W_{22} = \frac{1}{3584} \begin{pmatrix} -491 & 1068 & -1964 & 1878 & -491 \\ 1068 & \bullet & \bullet & \bullet & 1878 \\ -344 & \bullet & \bullet & \bullet & -1964 \\ -1362 & \bullet & \bullet & \bullet & 1068 \\ -2111 & -1362 & -344 & 1068 & -491 \end{pmatrix}$$

$$P_{23} = \frac{1}{384} \begin{pmatrix} -166 & 136 & -6 & 196 & -211 \\ 264 & \bullet & \bullet & \bullet & 324 \\ -108 & \bullet & \bullet & \bullet & -198 \\ -108 & \bullet & \bullet & \bullet & 72 \\ 67 & -172 & 84 & 8 & -38 \end{pmatrix}$$

$$W_{23} = \frac{1}{128} \begin{pmatrix} -17 & 68 & -132 & 98 & -17 \\ 100 & \bullet & \bullet & \bullet & 130 \\ -72 & \bullet & \bullet & \bullet & -132 \\ -54 & \bullet & \bullet & \bullet & 36 \\ -77 & -86 & 56 & 4 & -17 \end{pmatrix}$$

3.2.4 Graphical Examples for Biharmonic Biquartic Patch

Here we give some graphical examples for biquartic Said/Wang-Ball and biquartic DP-Ball generated by four sets of control points such that the surface have the same boundaries.

3.2.4.1 Graphical Examples for Biharmonic Biquartic Said-Ball Patch

To generate the biharmonic Said-Ball surface, we have chosen four sets of boundary curves.

Example 3.18. Given the boundary control points set 1 of the biquartic Said-Ball surface as follows

$$\begin{aligned}v_{00} &= (0, 0, 1), v_{01} = (0, 12/5, -119/625), v_{02} = (0, 14/5, 21/625), \\v_{03} &= (0, 16/5, 161/625), v_{04} = (0, 4, 1), v_{10} = (4/5, 0, 871/500), \\v_{20} &= (7/5, 0, 499/250), v_{30} = (2, 0, 9/4), v_{40} = (4, 0, 1), v_{41} = (4, 6/5, -41/2500), \\v_{42} &= (4, 2, -41/2500), v_{43} = (4, 14/5, -41/2500), v_{44} = (4, 4, 1), \text{ and } v_{04} = (0, 4, 1), \\v_{14} &= (6/5, 4, 252/125), v_{24} = (24252/125), v_{34} = (14/5, 4, 252/125).\end{aligned}$$

Then, the inner control points of the biquartic Said-Ball surface by biharmonic condition are

$$\begin{aligned}v_{11} &= (-0.1381, -0.5000, -0.4859), v_{12} = (-0.0004, -0.0013, -0.0001), \\v_{13} &= (0.2899, 1.2542, 0.2305), v_{21} = (0.8768, 0.1125, 0.0982), \\v_{22} &= (1.1576, 1.1344, 0.4138), v_{23} = (1.2375, 1.6875, 0.5069), \\v_{31} &= (1.4899, -0.2125, 0.2372), v_{32} = (1.2375, 1.6875, 0.5069), \\v_{33} &= (1.9440, 1.5583, 0.5162). \text{ The graph of the above surface is in Figure 3.11(b)} \\&\text{while its boundary with control points is in Figure 3.11(f).}\end{aligned}$$

Example 3.19. Given the boundary control points set 2 of the biquartic Said-Ball surface as follows

$$\begin{aligned} v_{00} &= (1/2, 0, 0), v_{01} = (17/40, 0, 9/20), v_{02} = (1/2, 0, 3/5), v_{03} = (23/40, 0, 3/4), \\ v_{04} &= (1, 0, 1), v_{10} = (251/974, 2/5, 0), v_{20} = (-59/487, 19/50, 0), \\ v_{30} &= (-1/2, 9/25, 0), v_{40} = (-1/2, 0, 0), v_{41} = (-17/40, 0, 9/20), \\ v_{42} &= (-1/2, 0, 3/5), v_{43} = (-23/40, 0, 3/4), v_{44} = (-1, 0, 1), \text{ and} \\ v_{04} &= (1, 0, 1), v_{14} = (421/817, 1, 1), v_{24} = (-198/817, 43/50, 1), v_{34} = (-1, 18/25, 1). \end{aligned}$$

Then, the inner control points of the biquartic Said-Ball surface by biharmonic condition are

$$\begin{aligned} v_{11} &= (-0.2246, -0.0548, -0.0857), v_{12} = (0.0387, -0.3840, -0.3548), \\ v_{13} &= (-0.0102, 0.3253, 0.3616), v_{21} = (-0.4907, 0.0980, 0.0884), \\ v_{22} &= (-0.4286, 0.2885, 0.3288), v_{23} = (-0.4580, 0.3563, 0.4688), \\ v_{31} &= (-0.9396, 0.0053, 0.0616), v_{32} = (-0.9227, 0.1963, 0.3187), \\ v_{33} &= (-1.0154, 0.2399, 0.4554). \end{aligned}$$

The graph of the above surface is in Figure 3.12(b) while its boundary with control points is in Figure 3.12(f).

Example 3.20. Given the boundary control points set 3 of the biquartic Said-Ball surface as follows

$$\begin{aligned} v_{00} &= (-585/631, 1378/483, 0), v_{01} = (-1091/2500, 1343/1000, 7/20), \\ v_{02} &= (-1170/2909, 619/500, 19/40), v_{03} = (-46/125, 1133/1000, 3/5), \\ v_{04} &= (-585/631, 1378/483, 1), v_{10} = (-450001/150000, 0, 0), \\ v_{20} &= (-985/363, -729/827, 0), v_{30} = (-665/274, -1763/1000, 0), \\ v_{40} &= (585/631, -1378/483, 0), v_{41} = (209/400, -201/125, 3/10), \\ v_{42} &= (803/1897, -512/393, 17/40), v_{43} = (117/361, -1247/1250, 11/20), \\ v_{44} &= (585/631, -1378/483, 1), \text{ and } v_{04} = (-585/631, 1378/483, 1), \\ v_{14} &= (-1281/449, -585/631, 1), v_{24} = (-4160/2201, -4160/2201, 1), \\ v_{34} &= (-585/631, -1378/483, 1). \end{aligned}$$

Then, the inner control points of the biquartic Said-Ball surface by biharmonic condi-

tion are

$v_{11} = (0.8191, -0.7792, -0.0685)$, $v_{12} = (0.0005, 0.0014, -0.0003)$,
 $v_{13} = (-0.1363, -1.0582, 0.2920)$, $v_{21} = (0.0191, -1.2682, 0.0538)$,
 $v_{22} = (-0.4799, -1.3567, 0.2466)$, $v_{23} = (-0.3081, -1.4224, 0.3641)$,
 $v_{31} = (0.3251, -1.7593, 0.3457)$, $v_{32} = (0.0404, -1.7491, 0.2307)$,
 $v_{33} = (0.3251, -1.7593, 0.3457)$. The graph of the above surface is in Figure 3.13(b)
 while its boundary with control points is in Figure 3.13(f).

Example 3.21. Given the boundary control points set 4 of the biquartic Said-Ball surface as follows

$v_{00} = (0, 0, 1)$, $v_{01} = (0, 0.6667, 0.3333)$, $v_{02} = (0, 1, 0.3333)$, $v_{03} = (0, 1.3333, 0.3333)$,
 $v_{04} = (0, 2, 1)$, $v_{10} = (0.6667, 0, 0.3333)$, $v_{20} = (1, 0, 0.3333)$, $v_{30} = (1.3333, 0, 0.3333)$,
 $v_{40} = (2, 0, 1)$, $v_{41} = (2, 0.6667, 0.3333)$, $v_{42} = (2, 1, 0.3333)$, $v_{43} = (2, 1.3333, 0.3333)$,
 $v_{44} = (2, 2, 1)$, and $v_{04} = (0, 2, 1)$, $v_{14} = (0.6667, 2, 0.3333)$, $v_{24} = (1, 2, 0.3333)$,
 $v_{34} = (1.3333, 2, 0.3333)$.

Then, the inner control points of the biquartic Said-Ball surface by biharmonic condition are $v_{11} = (-0.1270, -0.1270, -0.3333)$, $v_{12} = (-0.1949, -0.6909, 0.4961)$,
 $v_{13} = (0.0913, 0.7579, -0.3333)$, $v_{21} = (0.4643, 0.1310, -0.3333)$,
 $v_{22} = (0.5982, 0.5982, -0.3334)$, $v_{23} = (0.5833, 0.9166, -0.3334)$,
 $v_{31} = (0.7579, 0.0913, -0.3333)$, $v_{32} = (0.9166, 0.5833, -0.3334)$,
 $v_{33} = (0.8968, 0.8968, -0.3334)$. The graph of the above surface is in Figure 3.14(b)
 while its boundary with control points is in Figure 3.14(f).

3.2.4.2 Graphical Examples for Biharmonic Biquartic DP-Ball Patch

To generate the biharmonic DP-Ball surface, we have chosen four sets of boundary curves.

Example 3.22. Given the boundary control points set 1 of the biquartic DP-Ball surface as follows

$$\begin{aligned} d_{00} &= (0, 0, 1), d_{01} = (0, -1.2, 0.3280), d_{02} = (0, 2.8, 0.0336), d_{03} = (0, 5.2, 1.6720), \\ d_{04} &= (0, 4, 1), d_{10} = (-2, -1, 1.3110), d_{20} = (2, -0.6, 2.3274), d_{30} = (6, 1, 0.6890), \\ d_{40} &= (4, 0, 1), d_{41} = (4, -2.4, 1), d_{42} = (4, 2, -0.0164), d_{43} = (4, 6.4, 1), d_{44} = (4, 4, 1), \\ \text{and } d_{04} &= (0, 4, 1), d_{14} = (-2, 4.2, 0.6390), d_{24} = (2, 3.8, 1.6554), \\ d_{34} &= (6, 3.8, 1.3610). \end{aligned}$$

Then, the inner control points of the biquartic DP-Ball surface by biharmonic condition are

$$\begin{aligned} d_{11} &= (-4.2321, -4.4879, -1.6939), d_{12} = (-2.8036, 1.9763, -0.8062), \\ d_{13} &= (-2.4464, 4.9424, 0.8444), d_{21} = (1.1964, -3.4237, 1.4876), \\ d_{22} &= (1.1964, 1.1763, 0.1602), d_{23} = (1.9107, 5.7085, 1.5621), \\ d_{31} &= (5.5536, -1.8576, 0.2224), d_{32} = (5.9107, 1.9085, -0.1097), \\ d_{33} &= (5.9107, 6.1085, 1.2677). \end{aligned}$$

The graph of the above surface is in Figure 3.11(d) while its boundary with control points is in Figure 3.11(h).

Example 3.23. Given the boundary control points set 2 of the biquartic DP-Ball surface as follows

$$\begin{aligned} d_{00} &= (0.5000, 0, 0), d_{01} = (0.2748, 0, -0.4500), d_{02} = (0.5000, 0, 0.6000), \\ d_{03} &= (1.2248, 0, 1.4500), d_{04} = (1.0000, 0, 1.0000), d_{10} = (1.6365, 0.0600, 0), \\ d_{20} &= (-0.1211, 0.3800, 0), d_{30} = (-1.6367, -0.0600, 0), d_{40} = (-0.5000, 0, 0), \\ d_{41} &= (-0.2748, 0, -0.4500), d_{42} = (-0.5000, 0, 0.6000), d_{43} = (-1.2248, 0, 1.4500), \\ d_{44} &= (-1.0000, 0, 1.0000), \text{ and } d_{04} = (1.0000, 0, 1.0000), d_{14} = (3.2732, 0.4200, 1), \\ d_{24} &= (-0.2424, 0.8600, 1.0000), d_{34} = (-3.2728, -0.4200, 1.0000). \end{aligned}$$

Then, the inner control points of the biquartic DP-Ball surface by biharmonic condition are

$$\begin{aligned}
d_{11} &= (0.1821, -1.0408, -1.2033), d_{12} = (1.7079, -0.0915, 0.3288), \\
d_{13} &= (3.9040, 0.4158, 1.2993), d_{21} = (-0.3074, -0.1915, -0.7212), \\
d_{22} &= (-0.4286, 0.2885, 0.3288), d_{23} = (-0.3304, 1.0632, 1.4199), \\
d_{31} &= (-1.0054, -0.0642, -0.6007), d_{32} = (-1.9820, -0.2768, 0.5699), \\
d_{33} &= (-4.0679, -0.6368, 1.4199). \text{ The graph of the above surface is in Figure 3.12(d)} \\
&\text{while its boundary with control points is in Figure 3.12(h).}
\end{aligned}$$

Example 3.24. Given the boundary control points set 3 of the biquartic DP-Ball surface as follows

$$\begin{aligned}
d_{00} &= (-0.9271, 2.8530, 0), d_{01} = (-1.0298, 3.1680, -0.3750), \\
d_{02} &= (-0.4022, 1.2380, 0.4750), d_{03} = (-0.8246, 2.5380, 1.3750), \\
d_{04} &= (-0.9271, 2.8530, 1.0000), d_{10} = (-1.7867, 5.4977, 0), \\
d_{20} &= (-2.7135, -0.8815, 0), d_{30} = (1.7865, -5.4975, 0), d_{40} = (0.9271, -2.8530, 0), \\
d_{41} &= (1.2245, -3.7688, -0.3750), d_{42} = (0.4233, -1.3028, 0.4250), \\
d_{43} &= (0.6293, -1.9376, 1.3750), d_{44} = (0.9271, -2.8530, 1.0000), \text{ and } d_{04} = (-0.9271, 2.8530, 1.00 \\
&(-3.8160, 5.7416, 1.0000), \\
d_{24} &= (-1.8900, -1.8900, 1.0000), d_{34} = (3.8160, -5.7420, 1.0000).
\end{aligned}$$

Then, the inner control points of the biquartic DP-Ball surface by biharmonic condition are

$$\begin{aligned}
d_{11} &= (3.9568, 6.4770, -0.9400), d_{12} = (0.0493, 2.4836, 0.2966), \\
d_{13} &= (-3.5217, 4.9675, 1.2620), d_{21} = (-1.2165, -0.6161, -0.5784), \\
d_{22} &= (-0.4799, -1.3568, 0.2466), d_{23} = (-1.3746, -2.0873, 1.3524), \\
d_{31} &= (2.2755, -6.8723, -0.4880), d_{32} = (1.9843, -2.4802, 0.3774), \\
d_{33} &= (4.5341, -4.3268, 1.3524). \text{ The graph of the above surface is in Figure 3.13(d)} \\
&\text{while its boundary with control points is in Figure 3.13(h).}
\end{aligned}$$

Example 3.25. Given the boundary control points set 4 of the biquartic DP-Ball surface as follows

$$\begin{aligned} d_{00} &= (0, 0, 1), d_{01} = (0, -1, 1), d_{02} = (0, 1, 0.3333), d_{03} = (0, 3, 1), d_{04} = (0, 2, 1), \\ d_{10} &= (-1, 0, 1), d_{20} = (1, 0, 0.3333), d_{30} = (3.0000, 0, 1.0000), d_{40} = (2, 0, 1), \\ d_{41} &= (2, -1, 1), d_{42} = (2, 1, 0.3333), d_{43} = (2, 3, 1), d_{44} = (2, 2, 1), \text{ and } d_{04} = (0, 2, 1), \\ d_{14} &= (-1, 2, 1), d_{24} = (1, 2, 0.3333), d_{34} = (3, 2, 1). \end{aligned}$$

Then, inner control points of the biquartic DP-Ball surface by biharmonic condition are

$$\begin{aligned} d_{11} &= (-2.1161, -2.1161, 1.0001), d_{12} = (-1.4018, 0.5982, 0.3333), \\ d_{13} &= (-1.2232, 2.7768, 1.0000), d_{21} = (0.5982, -1.4018, 0.3333), \\ d_{22} &= (0.5982, 0.5982, -0.3334), d_{23} = (0.9554, 2.9554, 0.3333), \\ d_{31} &= (2.7768, -1.2232, 1.0000), d_{32} = (2.9554, 0.9554, 0.3333), \\ d_{33} &= (2.9554, 2.9554, 1.0000). \end{aligned}$$

The graph of the above surface is in Figure 3.14(d) while its boundary with control points is in Figure 3.14(h).

3.2.4.3 Graphical Examples for Biharmonic Biquartic Wang-Ball Patch

To generate the biharmonic Wang-Ball surface, we have chosen four sets of boundary curves.

Example 3.26. Given the boundary control points set 1 of the biquartic Wang-Ball surface as follows

$$\begin{aligned} w_{00} &= (0, 0, 1), w_{01} = (0, 3.6, -0.7856), w_{02} = (0, 3.2, -0.4496), \\ w_{03} &= (0, 2.8, -0.1136), w_{04} = (0, 4, 1), w_{10} = (1.2, 0, 2.1130), w_{20} = (1.1, 0, 2.4940), \\ w_{30} &= (1, 0, 2.8750), w_{40} = (4, 0, 1), w_{41} = (4, 1.8, -0.5246), w_{42} = (4, 2, -0.5246), \\ w_{43} &= (4, 2, -0.5246), w_{44} = (4, 4, 1), \text{ and } w_{04} = (0, 4, 1), w_{14} = (1.8, 4, 2.5240), \\ w_{24} &= (2, 4, 2.5240), w_{34} = (2.2, 4, 2.5240). \end{aligned}$$

Then, the inner control points of the biquartic Wang-Ball surface by biharmonic condition are

$w_{11} = (-0.9107, -2.9250, -2.0070)$, $w_{12} = (-0.1272, -1.1969, -0.9711)$,
 $w_{13} = (-0.2478, -1.5781, -0.2670)$, $w_{21} = (-0.0772, -1.0969, -0.9486)$,
 $w_{22} = (0.3296, -0.2477, -0.3300)$, $w_{23} = (0.2844, -0.4531, -0.2120)$,
 $w_{31} = (-0.1478, -1.3781, -0.8916)$, $w_{32} = (0.3344, -0.3531, -0.1895)$,
 $w_{33} = (0.2741, -0.5938, -0.0883)$. The graph of the above surface is in Figure 3.11(c)
 while its boundary with control points is in Figure 3.11(g).

Example 3.27. Given the boundary control points set 2 of the biquartic Wang-Ball surface as follows

$w_{00} = (0.5000, 0, 0)$, $w_{01} = (0.3875, 0, 0.6750)$, $w_{02} = (0.3750, 0, 0.6500)$,
 $w_{03} = (0.3625, 0, 0.6250)$, $w_{04} = (1.0000, 0, 1.0000)$, $w_{10} = (0.1365, 0.6000, 0)$,
 $w_{20} = (-0.1817, 0.5700, 0)$, $w_{30} = (-0.5000, 0.5400, 0)$, $w_{40} = (-0.5000, 0, 0)$,
 $w_{41} = (-0.3875, 0, 0.6750)$, $w_{42} = (-0.3750, 0, 0.6500)$, $w_{43} = (-0.3625, 0, 0.6250)$,
 $w_{44} = (-1.0000, 0, 1.0000)$, and $w_{04} = (1.0000, 0, 1.0000)$, $w_{14} = (0.2730, 1.5000, 1)$,
 $w_{24} = (-0.3635, 1.2900, 1.0000)$, $w_{34} = (-1.0000, 1.0800, 1.0000)$.

Then, the inner control points of the biquartic Wang-Ball surface by biharmonic condition are

$w_{11} = (-0.8924, -0.4232, -0.5304)$, $w_{12} = (-0.5358, 0.0556, -0.1636)$,
 $w_{13} = (-0.2558, -0.0181, -0.2489)$, $w_{21} = (-1.0132, -0.0644, -0.1386)$,
 $w_{22} = (-0.8280, 0.1842, 0.0398)$, $w_{23} = (-0.8486, 0.1566, -0.0078)$,
 $w_{31} = (-1.5454, -0.2581, -0.1989)$, $w_{32} = (-1.3260, 0.0366, 0.0172)$,
 $w_{33} = (-1.3534, -0.0003, -0.0379)$. The boundary with control points of the above
 surface is in Figure 3.12(g) while its graph is in Figure 3.12(c).

Example 3.28. Given the boundary control points set 3 of the biquartic Wang-Ball surface as follows

$w_{00} = (-0.9271, 2.8530, 0)$, $w_{01} = (-0.1910, 0.5880, 0.5250)$,
 $w_{02} = (-0.1397, 0.4305, 0.4625)$, $w_{03} = (-0.0884, 0.2730, 0.4000)$,

$$\begin{aligned}
w_{04} &= (-0.9271, 2.853, 1), w_{10} = (-4.0365, -1.4265, 0), w_{20} = (-4.0702, -1.3222, 0), \\
w_{30} &= (-4.1041, -1.218, 0), w_{40} = (0.9271, -2.853, 0), w_{41} = (0.3202, -0.9855, 0.45), \\
w_{42} &= (0.1714, -0.5277, 0.3875), w_{43} = (0.0226, -0.0699, 0.325), \\
w_{44} &= (0.9271, -2.853, 1), \text{ and } w_{04} = (-0.9271, 2.853, 1), w_{14} = (-3.816, -2.8172, 1) \\
, w_{24} &= (-2.8351, -2.8351, 1), w_{34} = (-1.8542, -2.8530, 1).
\end{aligned}$$

Then, the inner control points of the biquartic Wang-Ball surface by biharmonic condition are

$$\begin{aligned}
w_{11} &= (4.1886, -2.0473, -0.4165), w_{12} = (1.5235, -1.9860, -0.1852), \\
w_{13} &= (1.2565, 0.0884, -0.2929), w_{21} = (2.0458, -2.0930, -0.1227), \\
w_{22} &= (0.6386, -1.9889, -0.0327), w_{23} = (0.7408, -1.8336, -0.1121), \\
w_{31} &= (2.9218, -2.0361, -0.1679), w_{32} = (1.2630, -1.9406, -0.0496), \\
w_{33} &= (1.4156, -1.7836, -0.1347). \text{ The graph of the above surface is in Figure 3.13(c),} \\
&\text{while its boundary with control points is in Figure 3.13(g).}
\end{aligned}$$

Example 3.29. Given the boundary control points set 4 of the biquartic Wang-Ball surface as follows

$$\begin{aligned}
w_{00} &= (0, 0, 1), w_{01} = (0, 1, 0), w_{02} = (0, 1, 0), w_{03} = (0, 1, 0), w_{04} = (0, 2, 1), \\
w_{10} &= (1, 0, 0), w_{20} = (1, 0, 0), w_{30} = (1, 0, 0), w_{40} = (2, 0, 1), w_{41} = (2, 1, 0), \\
w_{42} &= (2, 1, 0), w_{43} = (2, 1, 0), w_{44} = (2, 2, 1), \text{ and } w_{04} = (0, 2, 1), w_{14} = (1, 2, 0), \\
w_{24} &= (1, 2, 0), w_{34} = (1, 2, 0).
\end{aligned}$$

Then, inner control points of the biquartic Wang-Ball surface by biharmonic condition are

$$\begin{aligned}
w_{11} &= (-0.7857, -0.7857, -1.0000), w_{12} = (-0.2054, -0.2054, -1.0000), \\
w_{13} &= (-0.2946, -0.2946, -0.3304), w_{21} = (-0.2054, -0.2054, -1.0000), \\
w_{22} &= (0.0960, 0.0960, -1.0000), w_{23} = (0.0625, 0.0625, -1.0000), \\
w_{31} &= (-0.2946, -0.2946, -1.0000), w_{32} = (0.0625, 0.0625, -1.0000), \\
w_{33} &= (0.0179, 0.0179, -1.0000). \text{ The graph of the above surface is in Figure 3.14(c)} \\
&\text{while its boundary with control points is in Figure 3.14(g).}
\end{aligned}$$

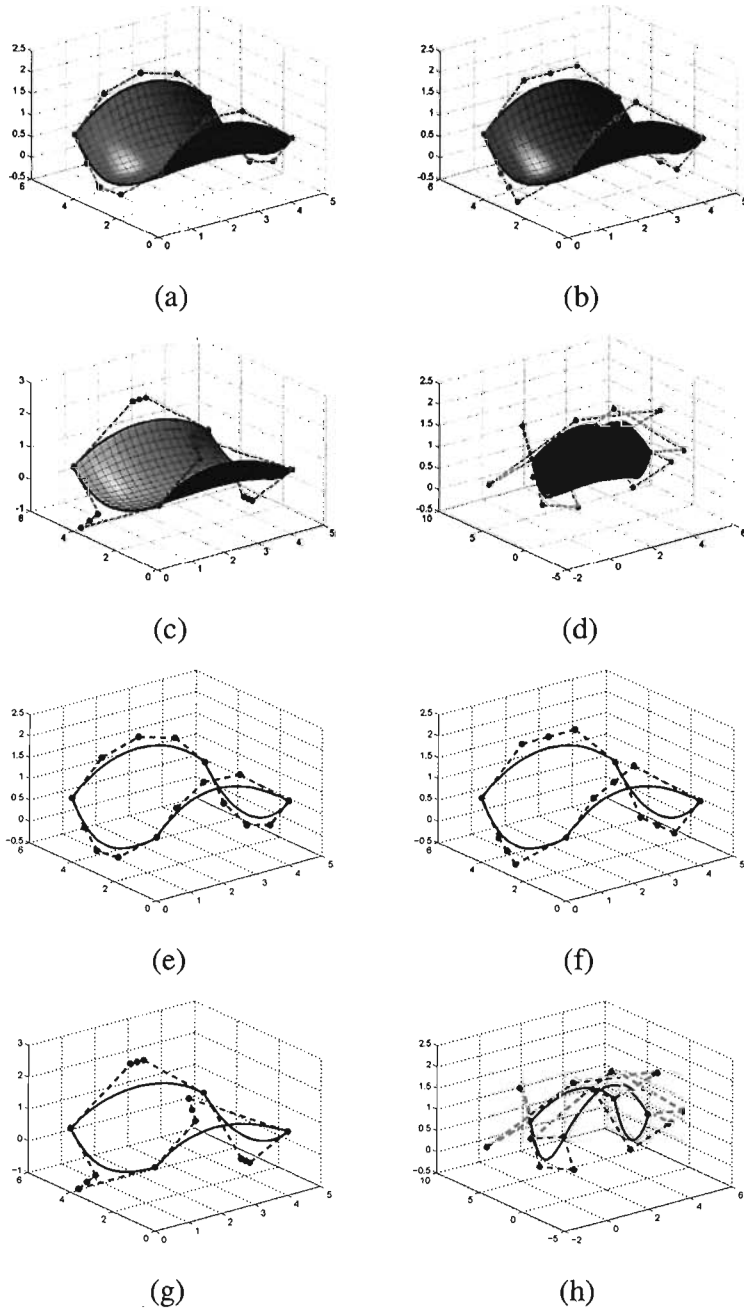


Figure 3.11. Control points set 1 by biharmonic condition on (a) Bézier patch (b) Said-Ball patch (c) Wang-Ball patch (d) DP-Ball patch (e) Bézier boundary (f) Said-Ball boundary (g) Wang-Ball boundary (h) DP-Ball boundary.

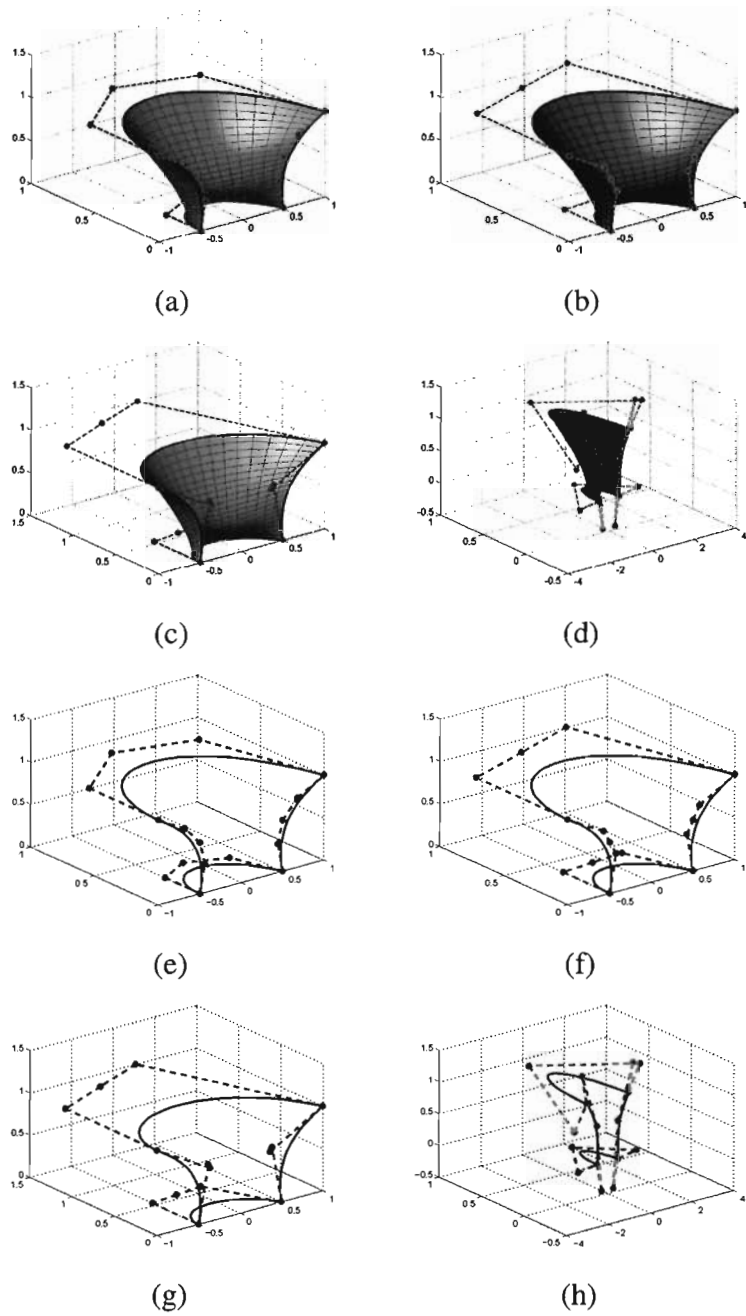
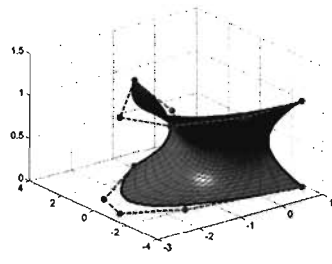
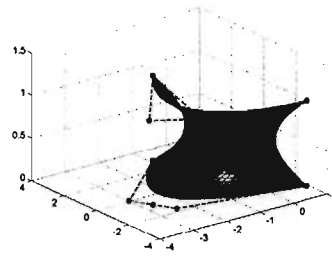


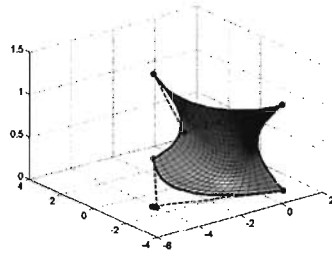
Figure 3.12. Control points set 2 by biharmonic condition on (a) Bézier patch (b) Said-Ball patch (c) Wang-Ball patch (d) DP-Ball patch (e) Bézier boundary (f) Said-Ball boundary (g) Wang-Ball boundary (h) DP-Ball boundary.



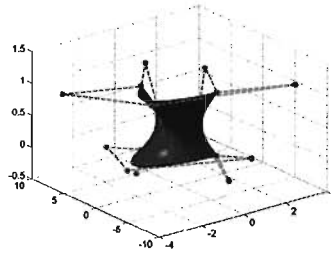
(a)



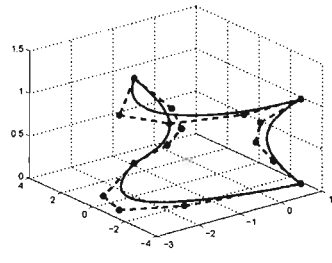
(b)



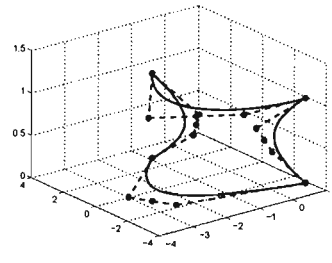
(c)



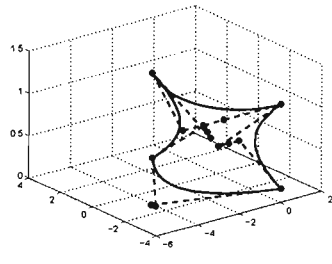
(d)



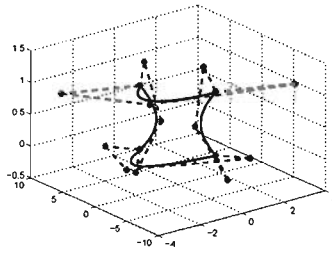
(e)



(f)



(g)



(h)

Figure 3.13. Control points set 3 by biharmonic condition on (a) Bézier patch (b) Said-Ball patch (c) Wang-Ball patch (d) DP-Ball patch (e) Bézier boundary (f) Said-Ball boundary (g) Wang-Ball boundary (h) DP-Ball boundary.

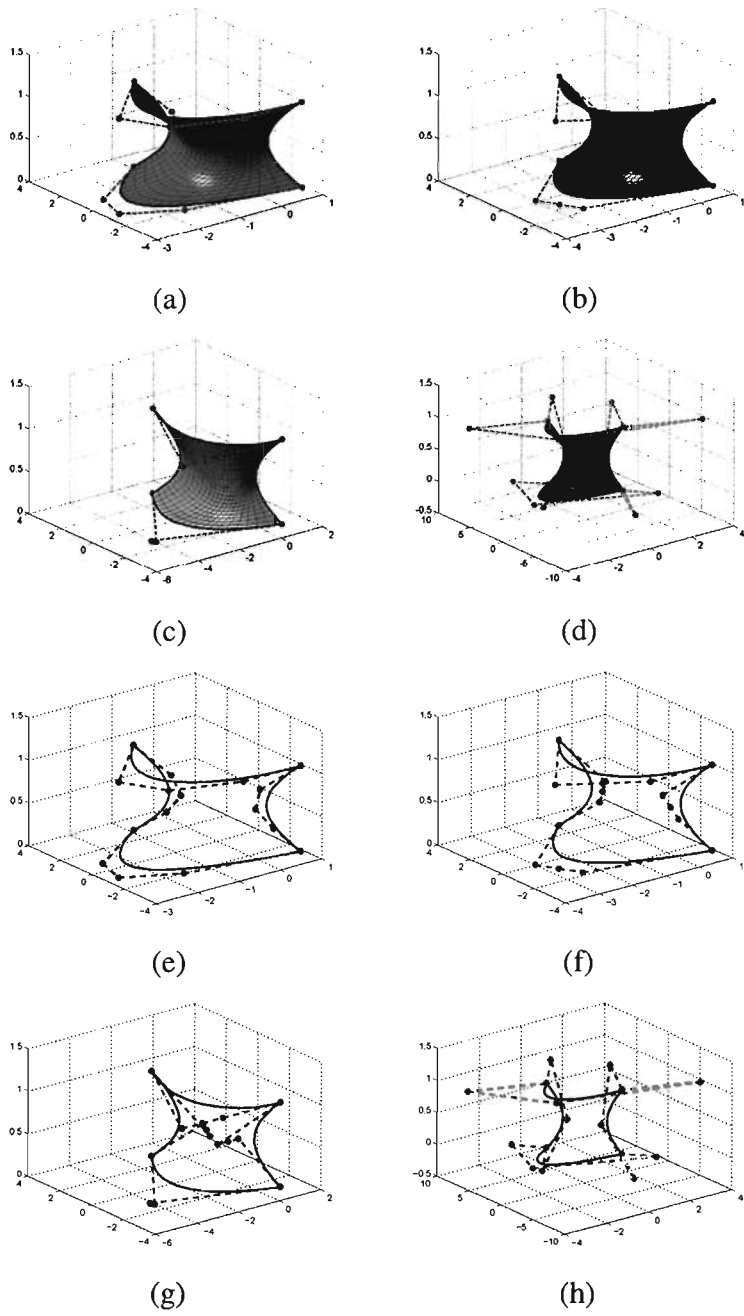


Figure 3.14. Control points set 4 by biharmonic condition on (a) Bézier patch (b) Said-Ball patch (c) Wang-Ball patch (d) DP-Ball patch (e) Bézier boundary (f) Said-Ball boundary (g) Wang-Ball boundary (h) DP-Ball boundary.

Table 3.3

Comparison between the area/computational time of biquartic Bézier, biquartic Said-Ball, biquartic Wang-Ball and biquartic DP-Ball by using biharmonic condition.

Control Points		Bézier	Said-Ball	Wang-Ball	DP-Ball
Set 1	Area	19.455817	19.516096	19.462083	20.147274
	Computational time	0.1938	0.1417	0.1343	0.1320
Set 2	Area	1.896763	1.904573	1.896150	1.896763
	Computational time	0.1938	0.1416	0.1344	0.1334
Set 3	Area	14.012209	14.202749	13.960906	14.012209
	Computational time	0.1878	0.1414	0.1365	0.1329
Set 4	Area	5.201627	5.247477	5.207346	5.247499
	Computational time	0.1891	0.1411	0.1356	0.1330

From Table 3.3, the biharmonic condition is applied to the biquartic patches of Said-Ball surface, Wang-Ball surface and DP-Ball surface, and compared with the existing work for biquartic patch of Bézier surface. It is discovered that the biquartic Bézier surface is better than biquartic Wang-Ball, followed by biquartic Said-Ball and then biquartic DP-Ball in terms of surface area for control points Set 1 and Set 4. We also discovered that the biquartic Wang-Ball is better than biquartic Bézier and biquartic DP-Ball, followed by biquartic Said-Ball in terms of surface area for control points Set 2 and Set 3. On the other hand, biquartic DP-Ball requires the least computational time for all control point sets.

3.3 Summary

In this chapter, we derived a general algorithm for harmonic and biharmonic patches. These algorithms hold for Bézier if the control points $\{q_{i,j}\}_{i,j=0}^{m,n}$ of the $X(u, v)$ surface is replaced by the Bézier control points $\{P_{i,j}\}_{i,j=0}^{m,n}$ and also if the convert matrices F and H are being replaced by the identity matrix.

The harmonic and biharmonic conditions are applied to the Said-Ball surface, DP-Ball surface and Wang-Ball surface. The computational time for Said-Ball surface, DP-Ball surface and Wang-Ball surface are compared with Bézier surface. In Table 3.1 and Table 3.2, the results show that the bicubic patch for Said/Wang-Ball are better than Bézier patch in terms of computational time. However, the DP-Ball consumed the most computational time. On the other hand for biquartic biharmonic, it is seen in Table 3.3 that the DP-Ball takes lesser time than the others while Bézier requires much more computational time. The calculation of the area of each surface is also considered.

CHAPTER FOUR
POLYNOMIAL SOLUTIONS OF FOURTH ORDER LINEAR
ELLIPTIC PARTIAL DIFFERENTIAL EQUATIONS AND
EXTREMAL OF THE DIRICHLET FUNCTIONAL IN TERMS
OF BALL SURFACE

In this chapter, we derived two general algorithms to generate any surface used in CAGD from their four boundary curves, where the first algorithm used the polynomial solutions of fourth order linear elliptic PDEs, while the second algorithm used the extremal of the Dirichlet functional.

4.1 Polynomial Solutions of Fourth Order Linear Elliptic PDEs in terms of Ball Surface

Consider the fourth order PDE in the form of

$$A \frac{\partial^4 X}{\partial u^4} + B \frac{\partial^4 X}{\partial u^3 \partial v} + C \frac{\partial^4 X}{\partial u^2 \partial v^2} + D \frac{\partial^4 X}{\partial u \partial v^3} + E \frac{\partial^4 X}{\partial v^4} = 0, \quad (4.1)$$

where $A, B, C, D, E \in \mathbb{R}$ are constants.

We present a general algorithm to compute the polynomial solutions of any fourth-order differential equation and any square surface $X(u, v)$.

First, we note that the boundary control points of surface $X(u, v)$ determine the first column and the first row of the coefficients of the polynomial expression, as described below.

Let

$$X(u, v) = \sum_{i,j=0}^n X_i^n(u)X_j^n(v)b_{ij} = \sum_{i,j=0}^n \frac{a_{ij}}{i!j!}u^i v^j, \quad (4.2)$$

where b_{ij} are control points of surface $X(u, v)$; $X_i^n(u), X_j^n(v)$ are basis functions of surface $X(u, v)$ and $a_{ij} \in \mathbb{R}^3$. The relation between the first row of polynomial coefficients $\{a_{0j}\}_{j=0}^n$ with boundary control points $\{b_{0j}\}_{j=0}^n$ can be defined as follows. On substituting $u = 0$ in (4.2), we get

$$X(0, v) = \sum_{j=0}^n X_j^n(v)b_{0j} = \sum_{j=0}^n \left(\frac{a_{0j}}{j!}\right)v^j, \quad (4.3)$$

so that

$$X(0, v) = \sum_{j=0}^n X_j^n(v)b_{0j} \quad (4.4)$$

is a curve of degree n , Then, we can write equation (4.4) in monomial matrix form as follows

$$X(0, v) = \sum_{j=0}^n \left(\sum_{k=0}^n c_{kj}b_{0k}\right)v^j, \quad (4.5)$$

where c_{kj} is a monomial matrix form of curve $X_j^n(v)$. On applying (4.5) in (4.3) we have

$$X(0, v) = \sum_{j=0}^n \left(\sum_{k=0}^n c_{kj}b_{0k}\right)v^j = \sum_{j=0}^n \left(\frac{a_{0j}}{j!}\right)v^j, \quad (4.6)$$

where

$$a_{0j} = j! \left(\sum_{k=0}^n c_{kj}b_{0k}\right), j = 0, 1, \dots, n. \quad (4.7)$$

Similarly, substituting $v = 0$ in (4.2) yields

$$a_{i0} = i! \left(\sum_{k=0}^n c_{ki}b_{k0}\right), i = 0, 1, \dots, n. \quad (4.8)$$

Next, we shall calculate the second row $\{a_{i1}\}_{i=0}^n$, and the second column $\{a_{1j}\}_{j=0}^n$ of

coefficients $\{a_{ij}\}_{i,j=0}^{n,n}$ in the same manner. We note that coefficients a_{01} and a_{10} are already computed. Next, we substitute $u = 1$ in (4.2) to obtain

$$X(1, v) = \sum_{j=0}^n X_j^n(v) b_{nj} = \sum_{j=0}^n \frac{1}{j!} \left(\sum_{i=0}^n \frac{a_{ij}}{i!} \right) v^j. \quad (4.9)$$

We can write (4.9) in monomial matrix form as

$$X(1, v) = \sum_{j=0}^n \left(\sum_{k=0}^n c_{kj} b_{nk} \right) v^j = \sum_{j=0}^n \frac{1}{j!} \left(\sum_{i=0}^n \frac{a_{ij}}{i!} \right) v^j. \quad (4.10)$$

Hence

$$\sum_{k=0}^n c_{kj} b_{nk} = \frac{1}{j!} \sum_{i=0}^n \frac{a_{ij}}{i!}, j = 0, \dots, n. \quad (4.11)$$

Thus, we have

$$a_{1j} = j! \left(\sum_{k=0}^n c_{kj} b_{nk} \right) - \sum_{\substack{i=0, \\ i \neq 1}}^n \frac{a_{ij}}{i!}, j > 0. \quad (4.12)$$

We note that a_{1j} can be obtained from the boundary control points of $X(u, v)$ by using the coefficients a_{0j} and the coefficients $\{a_{ij}\}_{i>1}$.

Similarly, we substitute $v = 1$ in (4.2) to obtain

$$a_{i1} = i! \left(\sum_{k=0}^n c_{ki} b_{kn} \right) - \sum_{\substack{j=0, \\ j \neq 1}}^n \frac{a_{ij}}{j!}, i > 0. \quad (4.13)$$

The technique applied to compute the coefficients in the polynomial expression is by solving a set of systems of linear equations recursively. Each system corresponds to a line parallel to the transverse diagonal of the following scheme.

$$\begin{array}{cccccccccc}
a_{00} & a_{10} & a_{20} & \dots & * & * & \mathbf{a}_{k0} & \dots & a_{n-1,0} & a_{n0} \\
a_{01} & a_{11} & a_{21} & \dots & * & \mathbf{a}_{k-1,1} & * & \dots & a_{n-1,1} & a_{n1} \\
a_{02} & a_{12} & a_{22} & \dots & \mathbf{a}_{k-2,2} & * & * & \dots & a_{n-2,2} & 0 \\
\vdots & \vdots & \vdots & \ddots & \vdots & \vdots & \vdots & \ddots & \vdots & \vdots \\
* & * & \mathbf{a}_{2,k-2} & \dots & * & * & * & \vdots & 0 & 0 \\
* & \mathbf{a}_{1,k-1} & * & \dots & * & * & 0 & \dots & 0 & 0 \\
\mathbf{a}_{0,k} & * & * & \dots & * & 0 & 0 & \dots & 0 & 0 \\
\vdots & \vdots & \vdots & \ddots & \vdots & \vdots & \vdots & \ddots & \vdots & \vdots \\
a_{0,n-1} & a_{1,n-1} & a_{2,n-1} & \dots & 0 & 0 & 0 & \dots & 0 & 0 \\
a_{0n} & a_{1n} & 0 & \dots & 0 & 0 & 0 & \dots & 0 & 0
\end{array} \tag{4.14}$$

We note that the coefficient a_{kl} with $k+l > n+1$ belongs to a homogeneous system. Observe that the only solution is the trivial one. This implies that $a_{kl} = 0$ if $k+l > n+1$.

The first non homogeneous system corresponds to the line defined by $k+l = n+1$. The coefficients $a_{0,n+1}$ and $a_{n+1,0}$ are zeros, but the coefficients $a_{1,n}$ and $a_{n,1}$ can be computed using (4.12) and (4.13). Once the coefficients $a_{1,n}$ and $a_{n,1}$ are computed, we can assume that the linear system for $k+l = n+1$ has an associated coefficient matrix with non vanishing determinant. In this case, there is a unique solution and we can compute all the unknowns $a_{k,l}$ with $k+l = n+1$.

We can now proceed with the line defined by $k+l = n$. Coefficients $a_{0,n}$ and $a_{n,0}$ can be computed in terms of control points using (4.7) and (4.8), while coefficients $a_{1,n-1}$ and $a_{n-1,1}$ are computed using (4.12) and (4.13). Note that $a_{2,n-2}$ and $a_{n-2,2}$ have been computed in the previous step since they are more to the right, are needed to compute $a_{1,n-1}$ and $a_{n-1,1}$.

Remark 4.1. *If we replace the monomial matrix form c_{ij} and the control points in equations (4.7), (4.8), (4.12) and (4.13) of the surface $X(u, v)$ by the Bézier monomial matrix form and Bézier control points, we obtain the result which similar as in Monterde and Ugail (2006).*

For the purpose of our numerical examples of uniform scattered data, we will consider the fourth order PDE in the form of

$$A \frac{\partial^4 X}{\partial u^3 \partial v} + B \frac{\partial^4 X}{\partial u^2 \partial v^2} + C \frac{\partial^4 X}{\partial u \partial v^3} = 0, \quad (4.15)$$

with the degree-3 and degree-5 boundary curves.

Let R be a rectangle with vertices $V_1(x_1, y_1)$, $V_2(x_2, y_1)$, $V_3(x_2, y_2)$ and $V_4(x_1, y_2)$. The edges along V_1V_2 , V_4V_3 , V_1V_4 and V_2V_3 is respectively denoted by e_1, e_2, e_3 and e_4 as shown in Figure 4.1.

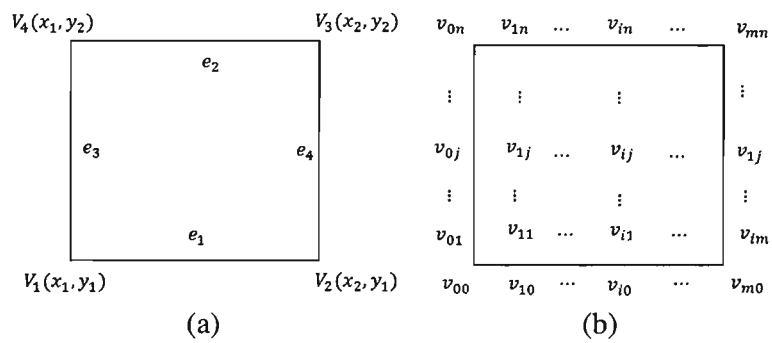


Figure 4.1. (a) Unit rectangle and (b) Said-Ball control points.

4.1.1 Said-Ball Polynomial Solutions for Fourth Order Partial Differential Equations

If we replace the monomial matrix form c_{ij} in (4.7), (4.8), (4.12) and (4.13) by the Said-Ball monomial matrix form (2.62), and the control points b_{ij} by the Said-Ball control points v_{ij} , we get the Said-Ball polynomial solution.

4.1.1.1 Odd Degree- n Said-Ball Boundary Curves Defined on Rectangular Grid

The four Said-Ball boundary curves along the edges e_1, e_2, e_3 and e_4 are given by $C_1(u), C_2(u), C_3(v)$ and $C_4(v)$, respectively with

$$\left. \begin{aligned} C_1(u) &= S(u, 0) = \sum_{i=0}^m v_{i0} S_i^m(u), \\ C_2(u) &= S(u, 1) = \sum_{i=0}^m v_{in} S_i^m(u), \\ C_3(v) &= S(0, v) = \sum_{i=0}^n v_{0i} S_i^m(v), \\ C_4(v) &= S(1, v) = \sum_{i=0}^n v_{mi} S_i^m(v). \end{aligned} \right\} \quad (4.16)$$

4.1.1.2 Relation Between Cubic Said-Ball Boundary Coefficients and Polynomial Coefficients Using Fourth Order PDEs

The relationship between the first row of polynomial coefficients, $\{a_{0j}\}_{j=0}^3$ and the boundary control points $\{v_{0j}\}_{j=0}^3$, are obtained by letting $n = 3$ in equation (4.7) and this gives

$$\left. \begin{aligned} a_{00} &= v_{00}, \\ a_{01} &= 2(v_{01} - v_{00}), \\ a_{02} &= 2(v_{00} - 4v_{01} + 2v_{02} + v_{03}), \\ a_{03} &= 12(v_{01} - v_{02}). \end{aligned} \right\} \quad (4.17)$$

In a similar way, the relationship between the first column of polynomial coefficients, $\{a_{j0}\}_{j=0}^3$ and the boundary control points $\{v_{j0}\}_{j=0}^3$, are obtained by letting $n = 3$ in equation (4.8) and this gives

$$\left. \begin{aligned} a_{10} &= 2(v_{10} - v_{00}), \\ a_{20} &= 2(v_{00} - 4v_{10} + 2v_{20} + v_{30}), \\ a_{30} &= 12(v_{10} - v_{20}) \end{aligned} \right\} \quad (4.18)$$

Next, we calculate of the second row $\{a_{j3}\}_{j=1}^3$, the second column $\{v_{j3}\}_{j=1}^3$ and the coefficients remained of polynomial coefficients in terms of boundary control point of Said-Ball patch with the use of expression (4.15) and by letting $n = 3$ in the expression (4.12) and (4.13) respectively. The following expressions are obtained

$$\left. \begin{aligned} a_{33} &= a_{32} = a_{23} = 0, \\ a_{31} &= -a_{30} + 12(v_{13} - v_{23}), \\ a_{21} &= -a_{20} - \frac{a_{22}}{2} + 2(v_{03} - 4v_{13} + 2v_{23} + v_{33}), \\ a_{11} &= -a_{01} - \frac{a_{21}}{2} - \frac{a_{31}}{6} - 2v_{30} + 2v_{31}, \\ a_{13} &= -a_{03} + 12(v_{31} - v_{32}), \\ a_{12} &= -a_{02} - \frac{a_{22}}{2} + 2(v_{30} - 4v_{31} + 2v_{32} + v_{33}), \end{aligned} \right\} \quad (4.19)$$

with $a_{22} = \frac{a_{31}A + a_{13}C}{B}$, where A, B , and C , ($B \neq 0$) are free parameters from equation (4.15).

4.1.1.3 Relation Between Quintic Said-Ball Boundary Coefficients and Polynomial Coefficients Using Fourth Order PDEs

The relationship between the first row of polynomial coefficients, $\{a_{0j}\}_{j=0}^5$ and the boundary control points $\{v_{0j}\}_{j=0}^5$, are obtained by letting $n = 5$ in equation (4.7) and this gives

$$\left. \begin{aligned}
a_{ij} &= 0, \forall i + j > 6, \\
a_{00} &= v_{00}, a_{01} = -3(v_{00} - v_{01}), \\
a_{02} &= 6(v_{00} - 3v_{01} + 2v_{02}), \\
a_{03} &= -6(v_{00} - 9v_{01} + 18v_{02} - 6v_{03} - 3v_{04} - v_{05}), \\
a_{04} &= -72(v_{01} - 6v_{02} + 4v_{03} + v_{04}), \\
a_{05} &= -720(v_{02} - v_{03}).
\end{aligned} \right\} \quad (4.20)$$

In a similar way, the relationship between the first row of polynomial coefficients, $\{a_{j0}\}_{j=0}^5$ and the boundary control points $\{v_{j0}\}_{j=0}^5$, are obtained by letting $n = 5$ in equation (4.8) and this gives

$$\left. \begin{aligned}
a_{10} &= -3(v_{00} - v_{01}), \\
a_{20} &= 6(v_{00} - 3v_{10} + 2v_{20}), \\
a_{30} &= -6(v_{00} - 9v_{10} + 18v_{20} - 6v_{30} - 3v_{40} - v_{50}), \\
a_{40} &= -72(v_{10} - 6v_{20} + 4v_{30} + v_{40}), \\
a_{50} &= -720(v_{20} - v_{30}).
\end{aligned} \right\} \quad (4.21)$$

Next, we calculate the second row $\{a_{j5}\}_{j=1}^5$, the second column $\{v_{j5}\}_{j=1}^5$ and the coefficients remained of polynomial coefficients in terms of boundary control point of Said-Ball patch with the use of expression (4.15) and by letting $n = 5$ in the expression (4.12) and (4.13) respectively. The following expressions are obtained

$$\left. \begin{aligned}
a_{15} &= -a_{05} - 720(v_{52} - v_{53}), \\
a_{51} &= -a_{50} - 720(v_{25} - v_{35}), \\
a_{14} &= -a_{04} - \frac{a_{24}}{2} - 72(v_{51} - 6v_{52} + 4v_{53} + v_{54}), \\
a_{41} &= -a_{40} - \frac{a_{42}}{2} - 72(v_{15} - 6v_{25} + 4v_{35} + v_{45}), \\
a_{13} &= -a_{03} - \frac{a_{23}}{2} - \frac{a_{33}}{6} - 6(v_{50} - 9v_{51} + 18v_{52} - 6v_{53} - 3v_{54} - v_{55}), \\
a_{31} &= -a_{30} - \frac{a_{32}}{2} - \frac{a_{33}}{6} - 6(v_{05} - 9v_{15} + 18v_{25} - 6v_{35} - 3v_{45} - v_{55}), \\
a_{12} &= -a_{02} - \frac{a_{22}}{2} - \frac{a_{32}}{6} - \frac{a_{42}}{24} + 6(v_{50} - 3v_{51} + 2v_{52}), \\
a_{21} &= -a_{20} - \frac{a_{22}}{2} - \frac{a_{23}}{6} - \frac{a_{24}}{24} + 6(v_{05} - 3v_{15} + 2v_{25}), \\
a_{11} &= -a_{01} - \frac{a_{21}}{2} - \frac{a_{31}}{6} - \frac{a_{41}}{24} - \frac{a_{51}}{120} - 3(v_{50} - v_{51}),
\end{aligned} \right\} \quad (4.22)$$

with

$$\begin{aligned}
a_{24} &= \frac{(A^3 a_{51} + C(B^2 - AC)a_{15})}{(B(2AC - B^2))}, \\
a_{42} &= \frac{(C^3 a_{15} + A(B^2 - AC)a_{51})}{B(2AC - B^2)}, \\
a_{22} &= \frac{a_{31}A + a_{13}C}{B}, \\
a_{33} &= (A^2 a_{51} + C^2 a_{15}) / (B^2 - 2AC), \\
a_{23} &= (BCa_{14} - A^2 a_{41}) / (B^2 - AC), \\
a_{32} &= (C^2 a_{14} - ABA_{41}) / (AC - B^2),
\end{aligned}$$

where A, B , and C , ($B \neq 0$) are free parameters from equation (4.15).

4.1.2 DP-Ball Polynomial Solutions for Fourth-Order Partial Differential Equations

If we replace the monomial matrix form c_{ij} in (4.7), (4.8), (4.12) and (4.13) by the DP-Ball monomial matrix form, and the control points b_{ij} by DP-Ball control points d_{ij} , we get the DP-Ball polynomial solution.

4.1.3 Odd Degree- n DP-Ball Boundary Curves Defined on Rectangular Grid

The four DP-Ball boundary curves along the edges e_1, e_2, e_3 and e_4 are given by $C_1(u), C_2(u), C_3(v)$ and $C_4(v)$, respectively with

$$\left. \begin{aligned} C_1(u) &= D(u, 0) = \sum_{i=0}^m d_{i0} D_i^m(u), \\ C_2(u) &= D(u, 1) = \sum_{i=0}^m d_{i1} D_i^m(u), \\ C_3(v) &= D(0, v) = \sum_{i=0}^n d_{0i} D_i^n(v), \\ C_4(v) &= D(1, v) = \sum_{i=0}^n d_{1i} D_i^n(v). \end{aligned} \right\} \quad (4.23)$$

4.1.3.1 Relation Between Cubic DP-Ball Boundary Coefficients and Polynomial Coefficients Using Fourth Order PDEs

The relationship between the first row of polynomial coefficients, $\{a_{0j}\}_{j=0}^3$ and the boundary control points $\{d_{0j}\}_{j=0}^3$, are obtained by letting $n = 3$ in equation (4.7) and this gives

$$\left. \begin{aligned} a_{00} &= d_{00}, \\ a_{01} &= -3d_{00} + 2d_{01} + d_{02}, \\ a_{02} &= 2(3d_{00} - 3d_{01}), \\ a_{03} &= 6(-d_{00} + d_{01} - d_{02} + d_{03}). \end{aligned} \right\} \quad (4.24)$$

In a similar way, the relationship between the first column of polynomial coefficients, $\{a_{j0}\}_{j=0}^3$ and the boundary control points $\{d_{j0}\}_{j=0}^3$, are obtained by letting $n = 3$ in equation (4.8) and this gives

$$\left. \begin{aligned} a_{10} &= -3d_{00} + 2d_{10} + d_{20}, \\ a_{20} &= 2(3d_{00} - 3d_{10}), \\ a_{30} &= 6(-d_{00} + d_{10} - d_{20} + d_{30}). \end{aligned} \right\} \quad (4.25)$$

Next, we calculate the second row $\{a_{j3}\}_{j=1}^3$, the second column $\{d_{j3}\}_{j=1}^3$ and the coefficients remained of polynomial coefficients in terms of boundary control point of Said-Ball patch with the use of expression (4.15) and by letting $n = 3$ in the expression (4.12) and (4.13) respectively. The following expressions are obtained

$$\left. \begin{aligned} a_{33} &= a_{23} = a_{32} = 0, \\ a_{31} &= a_{30} - 6(d_{03} - d_{13} + d_{23} - d_{33}), \\ a_{21} &= -a_{20} - \frac{a_{22}}{2} + 6(d_{03} - d_{13}), \\ a_{11} &= -a_{01} - \frac{a_{21}}{2} - \frac{a_{31}}{6} - 3d_{30} + 2d_{31} + d_{32}, \\ a_{13} &= -a_{03} - 6(d_{30} - d_{31} + d_{32} - d_{33}), \\ a_{12} &= -a_{02} - \frac{a_{22}}{2} + 6(d_{30} - d_{31}), \end{aligned} \right\} \quad (4.26)$$

with $a_{22} = \frac{a_{31}A + a_{13}C}{B}$, where A, B , and C , ($B \neq 0$) are free parameters from equation (4.15).

4.1.3.2 Relation Between Quintic DP-Ball Boundary Coefficients and Polynomial Coefficients Using Fourth Order PDEs

The relationship between the first row of polynomial coefficients, $\{a_{0j}\}_{j=0}^5$ and the boundary control points $\{d_{0j}\}_{j=0}^5$, are obtained by letting $n = 5$ in equation (4.7) and this gives

$$\left. \begin{aligned} a_{ij} &= 0, \forall i + j > 6, \\ a_{00} &= d_{00}, \\ a_{01} &= \frac{1}{2}(-10d_{00} + 2d_{01} + 5d_{02} + 3d_{03}), \\ a_{02} &= 20d_{00} - 8d_{01} - 9d_{02} - 3d_{03}, \\ a_{03} &= -6(10d_{00} - 6d_{01} - 3d_{02} - d_{03}), \\ a_{04} &= 24(5d_{00} - 4d_{01} - d_{02} - d_{03} + d_{04}), \\ a_{05} &= -120(d_{00} - d_{01} + d_{04} - d_{05}). \end{aligned} \right\} \quad (4.27)$$

In a similar way, the relationship between the first row of polynomial coefficients, $\{a_{j0}\}_{j=0}^5$ and the boundary control points $\{d_{j0}\}_{j=0}^5$, are obtained by letting $n = 5$ in equation (4.8) and this gives

$$\left. \begin{aligned} a_{10} &= \frac{1}{2}(-10d_{00} + 2d_{10} + 5d_{20} + 3d_{30}), \\ a_{20} &= 20d_{00} - 8d_{10} - 9d_{20} - 3d_{30}, \\ a_{30} &= -6(10d_{00} - 6d_{10} - 3d_{20} - d_{30}), \\ a_{40} &= 24(5d_{00} - 4d_{10} - d_{20} - d_{30} + d_{40}), \\ a_{50} &= -120(d_{00} - d_{10} + d_{40} - d_{50}). \end{aligned} \right\} \quad (4.28)$$

Next, we calculate the second row $\{a_{j5}\}_{j=1}^5$, the second column $\{d_{j5}\}_{j=1}^5$ and the coefficients remained of polynomial coefficients in terms of boundary control point of Said-Ball patch with the use of expression (4.15) and by letting $n = 5$ in the expression (4.12) and (4.13) respectively. The following expressions are obtained

$$\left. \begin{aligned}
 a_{15} &= -a_{05} - 120(d_{50} - d_{51} + d_{54} - d_{55}), \\
 a_{51} &= -a_{50} - 120(d_{05} - d_{15} + d_{45} - d_{55}), \\
 a_{24} &= (A^3 a_{51} + C(B^2 - AC)a_{15}) / (B(2AC - B^2)), \\
 a_{33} &= (A^2 a_{51} + C^2 a_{15}) / (B^2 - 2AC), \\
 a_{42} &= (A(B^2 - AC)a_{51} + C^3 a_{15}) / B(2AC - B^2), \\
 a_{14} &= -a_{04} - \frac{a_{24}}{2} + 24(5d_{50} - 4d_{51} - d_{52} - d_{53} + d_{54}), \\
 a_{41} &= -a_{40} - \frac{a_{42}}{2} + 24(5d_{05} - 4d_{15} - d_{25} - d_{35} + d_{45}), \\
 a_{13} &= -a_{03} - \frac{a_{23}}{2} - \frac{a_{33}}{6} - 6(10d_{50} - 6d_{51} - 3d_{52} - d_{53}), \\
 a_{31} &= -a_{30} - \frac{a_{32}}{2} - \frac{a_{33}}{6} - 6(10d_{05} - 6d_{15} - 3d_{25} - d_{35}), \\
 a_{22} &= -(Aa_{31} + Ca_{13}) / B, \\
 a_{21} &= -a_{20} - \frac{a_{22}}{2} - \frac{a_{23}}{6} - \frac{a_{24}}{24} + 20d_{05} - 8d_{15} - 9d_{25} - 3d_{35}, \\
 a_{12} &= -a_{02} - \frac{a_{22}}{2} - \frac{a_{32}}{6} - \frac{a_{42}}{24} + 20d_{50} - 8d_{51} - 9d_{52} - 3d_{53}, \\
 a_{11} &= -a_{01} - \frac{a_{21}}{2} - \frac{a_{31}}{6} - \frac{a_{41}}{24} - \frac{a_{51}}{120} + \frac{1}{2}(-10d_{50} + 2d_{51} \\
 &\quad + 5d_{52} + 3d_{53}),
 \end{aligned} \right\} \quad (4.29)$$

with $a_{22} = \frac{a_{31}A + a_{13}C}{B}$, where d_{ij} are control points of DP-Ball surface of degree 5×5 , and $A, B, (B \neq 0)$ and C are free parameters (4.15).

4.1.4 Wang-Ball Polynomial Solutions for Fourth Order Partial Differential Equations

If we replace the monomial matrix form c_{ij} in (4.7), (4.8), (4.12) and (4.13) by the Wang-Ball monomial matrix form, and the control points b_{ij} by Wang-Ball control points w_{ij} , we get the Wang-Ball polynomial solution.

4.1.4.1 Odd Degree- n Wang-Ball Boundary Curves Defined on Rectangular Grid

The four Wang-Ball boundary curves along the edges e_1, e_2, e_3 and e_4 are given by $C_1(u), C_2(u), C_3(v)$ and $C_4(v)$, respectively with

$$\left. \begin{aligned} C_1(u) &= D(u, 0) = \sum_{i=0}^m w_{i0} A_i^m(u), \\ C_2(u) &= D(u, 1) = \sum_{i=0}^m w_{in} A_i^n(u), \\ C_3(v) &= D(0, v) = \sum_{i=0}^n w_{0i} A_i^m(v), \\ C_4(v) &= D(1, v) = \sum_{i=0}^n w_{mi} A_i^m(v). \end{aligned} \right\} \quad (4.30)$$

4.1.4.2 Relation Between Cubic Wang-Ball Boundary Coefficients and Polynomial Coefficients Using Fourth Order PDEs

Since in application to degree three, cubic Said-Ball curve and Wang-Ball curve generate the same results, it is however not necessary to express solutions for both, but it is sufficient to show the results for only bicubic Said-Ball as given in Section 4.1.1.2.

4.1.4.3 Relation Between quintic Wang-Ball Boundary Coefficients and Polynomial Coefficients Using Fourth Order PDEs

The relationship between the first row of polynomial coefficients, $\{a_{0j}\}_{j=0}^5$ and boundary control points $\{w_{0j}\}_{j=0}^5$, are obtained by letting $n = 5$ in equation (4.7) and this gives

$$\left. \begin{aligned} a_{ij} &= 0, \forall i + j > 6, \\ a_{00} &= w_{00}, \\ a_{01} &= -2(w_{00} - w_{01}), \\ a_{02} &= 2(w_{00} - 6w_{01} + 4w_{02} + w_{05}), \\ a_{03} &= 12(3w_{01} - 6w_{02} + 2w_{03} + w_{04}), \\ a_{04} &= -48(w_{01} - 6w_{02} + 4w_{03} + w_{04}), \\ a_{05} &= -480(w_{02} - w_{03}). \end{aligned} \right\} \quad (4.31)$$

In a similar way, the relationship between the first row of polynomial coefficients, $\{a_{j0}\}_{j=0}^5$ and boundary control points $\{w_{j0}\}_{j=0}^5$, are obtained by letting $n = 5$ in equation (4.8) and this gives

$$\left. \begin{aligned} a_{10} &= -2(w_{00} - w_{10}), \\ a_{20} &= 2(w_{00} - 6w_{10} + 4w_{20} + w_{50}), \\ a_{30} &= 12(3w_{10} - 6w_{20} + 2w_{30} + w_{40}), \\ a_{40} &= -48(w_{10} - 6w_{20} + 4w_{30} + w_{40}), \\ a_{50} &= -480(w_{20} - w_{30}). \end{aligned} \right\} \quad (4.32)$$

Next, we calculate of the second row $\{a_{j5}\}_{j=1}^5$, the second column $\{w_{j5}\}_{j=1}^5$ and the coefficients remained of polynomial coefficients in terms of boundary control point of Wang-Ball patch with the use of expression (4.15) and by letting $n = 5$ in the expression (4.12) and (4.13) respectively. The following expressions are obtained

$$\left. \begin{aligned}
 a_{ij} &= 0, \forall i + j > 6, \\
 a_{51} &= a_{50} - 480(d_{25} - d_{35}), \\
 a_{15} &= -a_{05} - 480(d_{52} - d_{53}), \\
 a_{14} &= -a_{04} - \frac{a_{24}}{2} - 48(d_{51} - 6d_{52} + 4d_{53} + d_{54}), \\
 a_{41} &= -a_{40} - \frac{a_{42}}{2} - 48(d_{15} - 6d_{25} + 4d_{35} + d_{45}), \\
 a_{13} &= -a_{03} - \frac{a_{23}}{2} - \frac{a_{33}}{6} + 12(3d_{51} - 6d_{52} + 2d_{53} + d_{54}), \\
 a_{31} &= -a_{30} - \frac{a_{32}}{2} - \frac{a_{33}}{6} + 12(3d_{15} - 6d_{25} + 2d_{35} + d_{45}), \\
 a_{22} &= -\frac{(Aa_{31} + Ca_{31})}{B}, \\
 a_{21} &= -a_{20} - \frac{a_{22}}{2} - \frac{a_{23}}{6} - \frac{a_{24}}{24} + 2(d_{05} - 6d_{15} + 4d_{25} + d_{55}), \\
 a_{12} &= -a_{02} - \frac{a_{22}}{2} - \frac{a_{32}}{6} - \frac{a_{42}}{24} + 2(d_{50} - 6d_{51} + 4d_{52} + d_{55}), \\
 a_{11} &= -a_{10} - \frac{a_{12}}{2} - \frac{a_{13}}{6} - \frac{a_{14}}{24} - 2(d_{05} - d_{15}), \\
 a_{24} &= (A^3a_{51} + C(B^2 - AC)a_{15}) / (B(2AC - B^2)), \\
 a_{33} &= (A^2a_{51} + C^2a_{15}) / (B^2 - 2AC), \\
 a_{42} &= (A(B^2 - AC)a_{51} + C^3a_{15}) / B(2AC - B^2), \\
 a_{23} &= (BCa_{41} - A^2a_{41}) / (B^2 - AC), \\
 a_{32} &= (B^2a_{14} - ABa_{41}) / (AC - B^2),
 \end{aligned} \right\} \quad (4.33)$$

with $a_{22} = \frac{a_{31}A + a_{13}C}{B}$, where A, B , and C , ($B \neq 0$) are free parameters from equation (4.15).

4.1.5 Surface Construction

To generate a surface which interpolates some given functional values at the vertices of the rectangular, we also need to estimate the partial derivatives with respect to x and y at these vertices. Partial derivatives are estimated using well-known methods for uniform grid, that are forward, central and backward difference methods. Then, the surface interpolation defined with boundary curves will be generated by using polynomial form (4.2) with all coefficients a_{ij} calculated as the above method. To visualize our proposed method, we have chosen two datasets taken from well known test functions as follows:

$$f(x,y) = \begin{cases} 0.1, & \text{if } (y-x) \geq 0, \\ 2(y-x), & \text{if } -0.5 \geq (y-x) \geq 0.5, \\ \frac{\cos(4\pi\sqrt{(x-1.5)^2+(y-0.5)^2+1})}{2}, & \text{if } (x-1.5)^2 + (y-0.5)^2 \leq \frac{1}{16}, \\ 0, & \text{otherwise,} \end{cases} \quad (4.34)$$

where $0 \leq x \leq 2, 0 \leq y \leq 1$, and

$$g(x,y) = 1 + 3e^{(-3(9\sqrt{x^2+y^2}-6.7))^{-0.5}}, \quad 0 < x < 1, \quad 0 < y < 1. \quad (4.35)$$

We obtain the first dataset from $f(x,y)$ and it comprises 45 data points with 32 rectangles in a rectangular domain as in Figure 4.2.

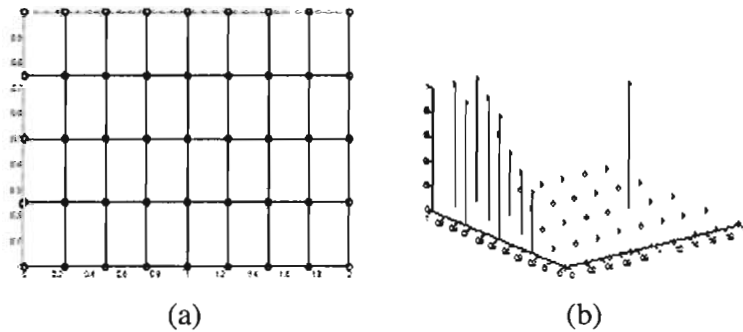


Figure 4.2. (a) 32 rectangles in the rectangular domain (b) 45 data points from positive function, $f(x,y)$.

The second dataset is taken from $g(x,y)$ which consists of 25 data points with 16 rectangles as in Figure 4.3.

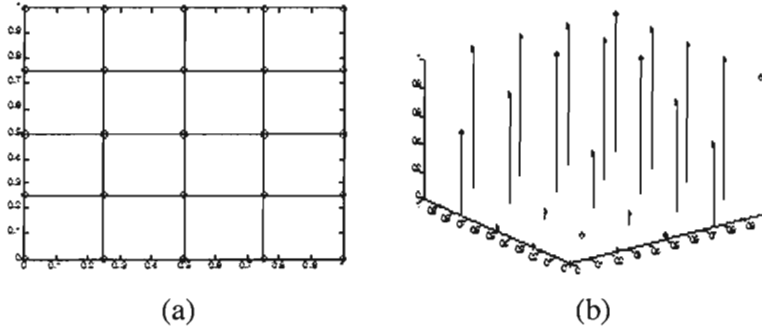


Figure 4.3. (a) 16 rectangles in the rectangular domain (b) 45 data points from positive function, $g(x,y)$.

After several numbers of experimentation, the values of the free parameters A, B and C in (4.15) are set to be 0.0003, 2 and 0.005, respectively, which produced good quality of interpolating surfaces for all the datasets.

4.1.6 Graphical Examples

Here we give some graphical examples to illustrate the interpolations of the surfaces using the bicubic and biquintic Said-Ball, Wang-Ball and DP-Ball by using the test function $f(x,y)$ and $g(x,y)$.

4.1.6.1 Bicubic Said/Wang-Ball

Figure 4.4 shows the initial value for the edge bicubic Said/Wang-Ball control points for the datasets in Figure 4.2 (test function $f(x,y)$) and Figure 4.3 (test function $g(x,y)$). Figure 4.5 shows the boundary curves for each rectangle for the edge control points, while the results for the interpolating surfaces cubic boundary curves for each test functions are shown in Figure 4.6. The summaries of these results is given in Table 4.1 and Table 4.3.

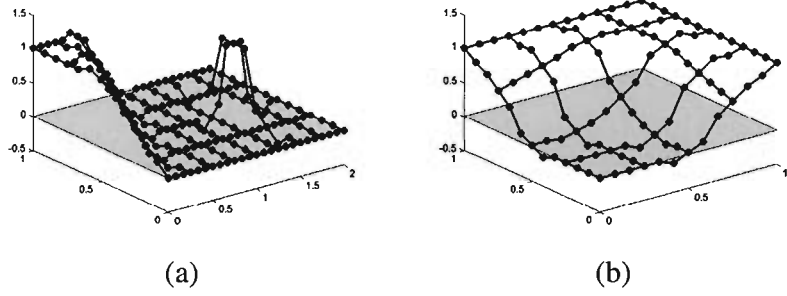


Figure 4.4. Edges Said/Wang-Ball control points for all rectangles (a) Test function $f(x,y)$ (b) Test function $g(x,y)$.

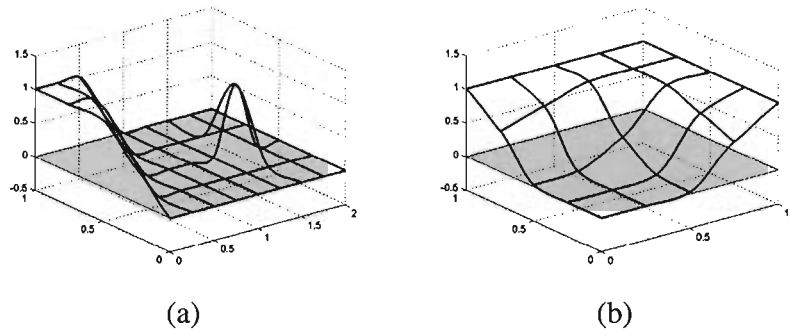


Figure 4.5. Boundary curves for all rectangles (a) Test function 1, $f(x,y)$ (b) Test function 2, $g(x,y)$.

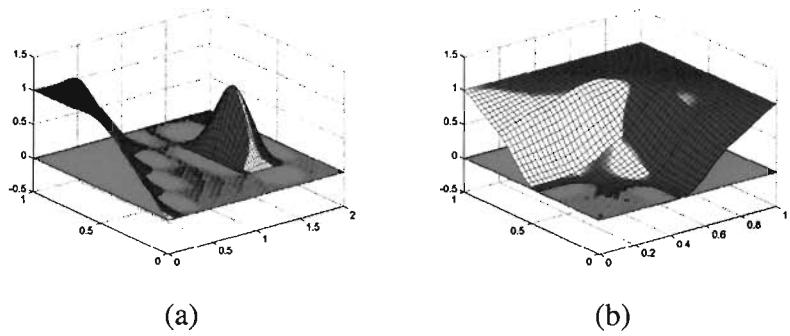


Figure 4.6. Interpolating surface boundary curves (a) Test function 1, $f(x,y)$ (b) Test function 2, $g(x,y)$.

4.1.6.2 Biquintic Said-Ball

Following the same approach from the bicubic Said-Ball, Figure 4.7 displays the initial value for the edge biquintic Said-Ball control points for the datasets in Figure 4.2 (test function $f(x,y)$) and Figure 4.3 (test function $g(x,y)$).

Also, Figure 4.8 shows the boundary curves for each rectangle for the edge control points, while the results for the interpolating surfaces cubic boundary curves for each test functions are shown in Figure 4.9. Table 4.2 and Table 4.4 give the summaries of these results.

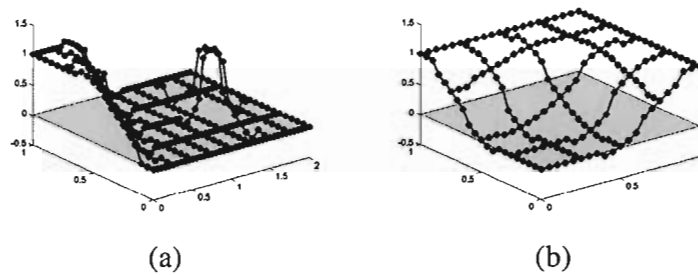


Figure 4.7. Edges biquintic Said-Ball control points for all rectangles (a) Test function $f(x,y)$ (b) Test function $g(x,y)$.

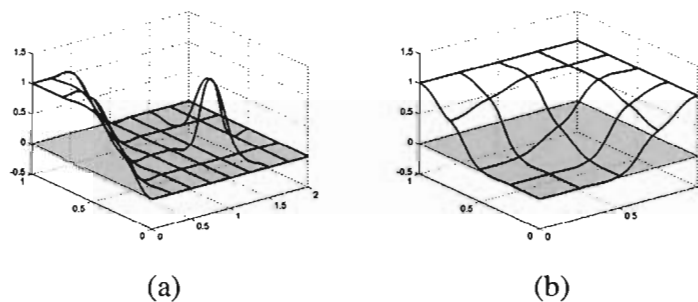


Figure 4.8. Quintic Boundary curves for all rectangles (a) Test function 1, $f(x,y)$ (b) Test function 2, $g(x,y)$.

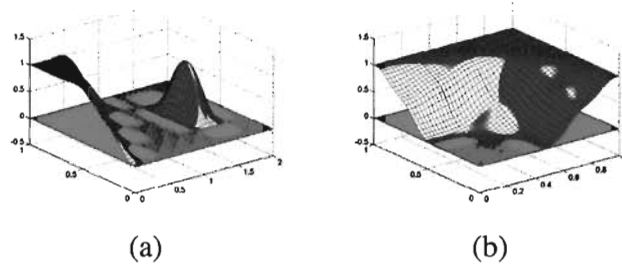


Figure 4.9. Interpolating biquintic surface boundary curves (a) Test function 1, $f(x,y)$ (b) Test function 2, $g(x,y)$.

4.1.6.3 Bicubic DP-Ball

Figure 4.10(b) shows the generated surface from the test function $g(x,y)$, while Figure 4.10(a) presents the initial value for the edge bicubic DP-Ball control points for the test function $g(x,y)$.

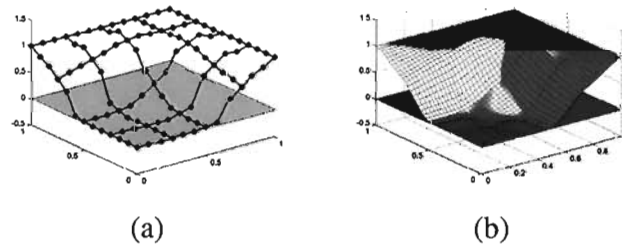


Figure 4.10. (a) Edges DP-Ball control points for all rectangles for test function $g(x,y)$ (b) Interpolating surface boundary curves for test function $g(x,y)$.

4.1.6.4 Biquintic DP-Ball

Following the same approach in Section 4.1.6.3, we show in Figure 4.11, the initial value for the edge biquintic DP-Ball control points for the dataset in Figure 4.3 (test function $g(x,y)$).

Also in Figure 4.11(a), we show the boundary curves for each rectangle for the edge control points, while the result for the interpolating surface quintic boundary curves for test function $g(x,y)$ is shown in Figure 4.11(b). The summaries of these results are given in Table 4.2 and Table 4.4.

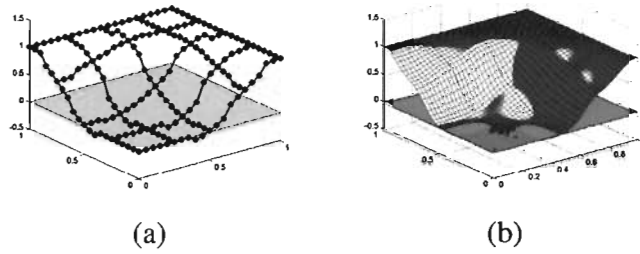


Figure 4.11. (a) Edges biquintic DP-Ball control points for all rectangles for test function $g(x,y)$ (b) Interpolating biquintic surface boundary curves $g(x,y)$.

4.1.6.5 Biquintic Wang-Ball

Following the same approach from the bicubic Wang-Ball, the initial value for the edge biquintic Wang-Ball control points for the datasets in Figure 4.2 (test function $f(x,y)$) and Figure 4.3 (test function $g(x,y)$) respectively, is shown in Figure 4.12.

The boundary curves for each rectangle for the edge control points in Figure 4.12 is also shown in Figure 4.13, while the results for the interpolating surfaces cubic boundary curves for each test functions are shown in Figure 4.14. Table 4.2 and Table 4.4 gives the summaries of these results.

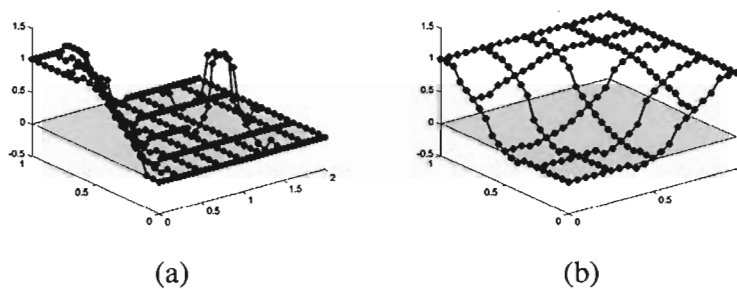


Figure 4.12. Edges biquintic Wang-Ball control points for all rectangles (a) Test function $f(x,y)$ (b) Test function $g(x,y)$.

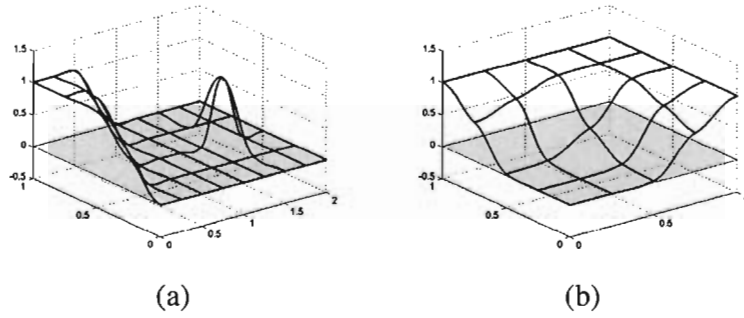


Figure 4.13. Quintic boundary curves for all rectangles (a) Test function 1, $f(x,y)$ (b) Test function 2, $g(x,y)$.

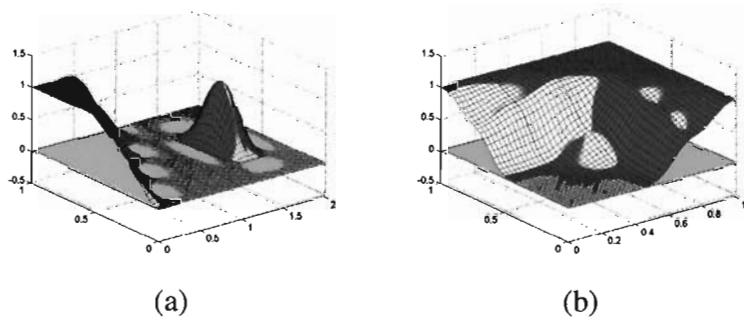


Figure 4.14. Interpolating biquintic surface boundary curves (a) Test function 1, $f(x,y)$ (b) Test function 2, $g(x,y)$.

Table 4.1

Comparison of the interpolating surfaces between bicubic Bézier, bicubic Said/Wang-Ball and bicubic DP-Ball boundary curves for the test function $g(x,y)$.

Surface	Number of evaluation points	Number of points below XY -plane and percentage	Minimum value of function
Bézier	1681	291 17.31 %	-0.012363
Said/Wang-Ball	1681	231 13.7419 %	-0.012736
DP-Ball	1707	292 17.1060%	-0.072144

Table 4.1 showed that our proposed method for bicubic Said/Wang-Ball and bicubic DP-Ball representations are better than the bicubic Bézier representation in terms of the percentage of number of points below XY -plane.

Table 4.2

Comparison of the interpolating surfaces between biquintic Bézier, biquintic Said-Ball, biquintic Wang-Ball and biquintic DP-Ball boundary curves for the test function $g(x,y)$.

Surface	Number of evaluation points	Number of points below XY -plane and percentage	Minimum value of function
Bézier	1681	291 17.014 %	-0.039003
Said-Ball	1681	246 14.634 %	-0.019917
Wang-Ball	1681	151 8.9827 %	-0.0050132
DP-Ball	1681	312 18.56%	-0.037932

Table 4.2 showed that our proposed method for biquintic Wang-Ball and biquintic Said-Ball representations are better than biquintic Bézier representation in terms of the percentage of number of points below the XY -plane. However, our proposed method for the biquintic DP-Ball is not as good as the biquintic Sais-Ball and biquintic Wang-Ball representations.

Table 4.3

Comparison of the interpolating surfaces between bicubic Bézier, bicubic Said/Wang-Ball and bicubic DP-Ball boundary curves for the test function $f(x,y)$.

Surface	Number of evaluation points	Number of points below XY -plane and percentage	Minimum value of function
Bézier	3321	1134 34.146 %	-0.08232
Said/Wang-Ball	3321	1118 33.6646 %	-0.04900

As demonstrated in Table 4.3, we found out that our proposed method for bicubic Said/Wang-Ball representation performed slightly better than the bicubic Bézier representation in terms of the percentage of number of points below XY -plane.

Table 4.4

Comparison of the interpolating surfaces between biquintic Bézier, biquintic Said-Ball, biquintic Wang-Ball and biquintic DP-Ball boundary curves for the test function $f(x, y)$.

Surface	Number of evaluation points	Number of points below XY -plane and percentage	Minimum value of function
Bézier	3321	1134 34.146 %	-0.08232
Said-Ball	3322	1147 34.527 %	-0.058653
Wang-Ball	3324	1136 34.176 %	-0.039102

Table 4.4 showed that the biquintic Bézier representation performed better than our proposed method for biquintic Said-Ball and biquintic Wang-Ball representations in terms of the percentage of number of points below XY -plane.

4.2 Dirichlet Functional

In this section, we present a more general algorithm to compute an extremal of the Dirichlet functional in terms of Ball surface. All these surfaces will give us the minimal surface areas. To compare our purposed method with the existing method for Bézier surface, we must have surface with the same four boundary curves. To do this, we must convert Bézier surface control points into generalization Ball surface control points, i.e. different surface with same boundary curves.

Theorem 4.1. A square control net, $P = \{P_{ij}\}_{i,j=0}^{n,n}$ of surface $X(u, v)$, is an extremal of the Dirichlet functional with prescribed border if and only if

$$\begin{aligned} \frac{\partial \mathcal{D}(P)}{\partial x_{ij}^a} &= \sum_{k=1}^n \sum_{l=0}^n \sum_{r=0}^n \sum_{s=0}^n \sum_{f=1}^n \sum_{h=0}^n c_{ik} c_{lj} c_{rf} c_{sh} A_{fk} P_{rs} \\ &+ \sum_{k=0}^n \sum_{l=1}^n \sum_{r=0}^n \sum_{s=0}^n \sum_{f=0}^n \sum_{h=1}^n c_{ik} c_{lj} c_{rf} c_{sh} A_{lh} P_{rs}, \end{aligned} \quad (4.36)$$

for any $i \in \{1, \dots, n-1\}$, and $j \in \{1, \dots, m-1\}$, where c_{ij} is the monomial matrix form of the curve $X(u), X(v)$ and $A_{fk} = \frac{fk}{(k+f-1)(l+h)}$.

Proof. Let us compute the gradient of the Dirichlet functional with respect to the coordinates of the control points $P_{ij} = (x_{ij}^1, x_{ij}^2, x_{ij}^3)$ of $X(u, v)$. For any $i \in \{1, \dots, n-1\}$, and $j \in \{1, \dots, m-1\}$, $a \in \{1, 2, 3\}$, $e^1 = (1, 0, 0)$, $e^2 = (0, 1, 0)$ and $e^3 = (0, 0, 1)$, we have

$$\frac{\partial \mathcal{D}(P)}{\partial x_{ij}^a} = \iint_R \left(\left\langle \frac{\partial \vec{X}_u}{\partial x_{ij}^a}, \vec{X}_u \right\rangle + \left\langle \frac{\partial \vec{X}_v}{\partial x_{ij}^a}, \vec{X}_v \right\rangle \right) dudv. \quad (4.37)$$

Compute the partial derivatives

$$\frac{\partial \vec{X}_u(u, v)}{\partial x_{ij}^a} = \frac{\partial}{\partial x_{ij}^a} \frac{\partial}{\partial u} \vec{X}(u, v) = \frac{\partial}{\partial u} \frac{\partial}{\partial x_{ij}^a} \vec{X}(u, v), \quad (4.38)$$

so that the surface $X(u, v)$ can be written in monomial matrix form as follows

$$\vec{X}(u, v) = \sum_{r=0}^n \sum_{s=0}^n \sum_{f=0}^n \sum_{h=0}^n c_{rf} c_{sh} u^f v^h P_{rs}, \quad (4.39)$$

where c_{rf} is the monomial matrix form of the curve $X(u)$, and c_{sh} is the monomial matrix form of the curve $X(v)$. Now, we apply (4.39) in (4.38) to obtain

$$\begin{aligned}
\frac{\partial \vec{X}_u(u, v)}{\partial x_{ij}^a} &= \frac{\partial}{\partial u} \sum_{k=0}^n \sum_{l=0}^n c_{rf} c_{sh} u^k v^l e^a \\
&= \sum_{k=1}^n \sum_{l=0}^n k c_{rf} c_{sh} u^{k-1} v^l e^a.
\end{aligned} \tag{4.40}$$

Similarly, we have

$$\frac{\partial \vec{X}_v(u, v)}{\partial x_{ij}^a} = \sum_{k=0}^n \sum_{l=1}^n l c_{rf} c_{sh} u^k v^{l-1} e^a. \tag{4.41}$$

On applying (4.40) and (4.41) in (4.37), we obtain

$$\begin{aligned}
\frac{\partial \mathcal{D}(D)}{\partial x_{ij}^a} &= \iint_R \left(\left\langle \sum_{k=1}^n \sum_{l=0}^n k c_{ik} c_{lj} u^{k-1} v^l e^a, \vec{X}_u(u, v) \right\rangle + \right. \\
&\quad \left. \left\langle \sum_{k=0}^n \sum_{l=1}^n l c_{ik} c_{jl} u^k v^{l-1} e^a, \vec{X}_v(u, v) \right\rangle \right) dudv \\
&= \int_R \left(\left\langle \sum_{k=1}^n \sum_{l=0}^n k c_{ik} c_{lj} u^{k-1} v^l e^a, \right. \right. \\
&\quad \left. \left. \sum_{r=0}^n \sum_{s=0}^n \sum_{f=1}^n \sum_{h=0}^n f c_{rf} c_{sh} u^{f-1} v^h P_{rs} \right\rangle + \right. \\
&\quad \left. \left\langle \sum_{k=0}^n \sum_{l=1}^n l c_{ik} c_{jl} u^k v^{l-1} e^a, \right. \right. \\
&\quad \left. \left. \sum_{r=0}^n \sum_{s=0}^n \sum_{f=0}^n \sum_{h=1}^n l c_{rf} c_{sh} u^f v^{h-1} P_{rs} \right\rangle \right) dudv \\
&= \int_R \sum_{k=1}^n \sum_{l=0}^n \sum_{r=0}^n \sum_{s=0}^n \sum_{f=1}^n \sum_{h=0}^n k f c_{ik} c_{lj} c_{rf} c_{sh} \times \\
&\quad u^{k+f-2} v^{l+h} \langle e^a, P_{rs} \rangle dudv + \\
&\quad \int_R \sum_{k=0}^n \sum_{l=1}^n \sum_{r=0}^n \sum_{s=0}^n \sum_{f=0}^n \sum_{h=1}^n k f c_{ik} c_{lj} c_{rf} c_{sh} \times \\
&\quad u^{k+f} v^{l+h-2} \langle e^a, P_{rs} \rangle dudv,
\end{aligned} \tag{4.42}$$

so that

$$\int_0^1 \int_0^1 u^{k+f-2} v^{l+h} dudv = \frac{1}{(k+f-1)(l+h)}. \tag{4.43}$$

On applying (4.43) in (4.42), we obtain

$$\begin{aligned}
\frac{\partial \mathcal{D}(P)}{\partial x_{ij}^a} &= \sum_{k=1}^n \sum_{l=0}^n \sum_{r=0}^n \sum_{s=0}^n \sum_{f=1}^n \sum_{h=0}^n c_{ik} c_{lj} c_{rf} c_{sh} \frac{fk}{(k+f-1)(l+h)} \langle e^a, P_{rs} \rangle + \\
&\quad \sum_{k=0}^n \sum_{l=1}^n \sum_{r=0}^n \sum_{s=0}^n \sum_{f=0}^n \sum_{h=1}^n c_{ik} c_{lj} c_{rf} c_{sh} \frac{lh}{(k+f)(l+h-1)} \langle e^a, P_{rs} \rangle \\
&= \sum_{k=1}^n \sum_{l=0}^n \sum_{r=0}^n \sum_{s=0}^n \sum_{f=1}^n \sum_{h=0}^n c_{ik} c_{lj} c_{rf} c_{sh} A_{fk} \langle e^a, P_{rs} \rangle + \\
&\quad \sum_{k=0}^n \sum_{l=1}^n \sum_{r=0}^n \sum_{s=0}^n \sum_{f=0}^n \sum_{h=1}^n c_{ik} c_{lj} c_{rf} c_{sh} A_{lh} \langle e^a, P_{rs} \rangle, \tag{4.44}
\end{aligned}$$

Where $A_{fk} = \frac{fk}{(k+f-1)(l+h)}$. □

Remark 4.1. *If we replace the monomial matrix form c_{ij} and the control points of the surface $X(u, v)$ in Theorem 4.1 by the Bézier monomial matrix form and Bézier control points, we have the result similar as in Monterde (2004).*

4.2.1 Biquadratic Dirichlet Surface

If we substitute $m = n = 2$ in (4.36), this give us the biquadratic case. Since Said-Ball, DP-Ball and Wang-Ball surfaces are identical at degree 2, then it is enough to consider examples from biquadratic Said-Ball.

If we replace the monomial matrix form c_{ij} in Theorem 4.1 by the Said-Ball monomial matrix form, and the control points b_{ij} by Said-Ball control points v_{ij} , we obtain the Dirichlet functional of Said-Ball polynomial solution. In this case, there are only one interior control point namely v_{11} .

Proposition 4.1. A biquadratic Said-Ball surface is an extremal of the Dirichlet functional with prescribed border if and only if

$$v_{11} = \frac{1}{8}(3v_{00} - v_{01} + 3v_{02} - v_{10} - v_{12} + 3v_{20} - v_{21} + 3v_{22}). \quad (4.45)$$

Example 4.1. Given the control points as follows: $v_{00} = (0, 0, 1)$, $v_{10} = (1, 0, 0)$, $v_{20} = (2, 0, 1)$, $v_{01} = (0, 1, 0)$, $v_{21} = (2, 1, 0)$, $v_{02} = (0, 2, 1)$, $v_{12} = (1, 2, 0)$, $v_{22} = (2, 2, 1)$. (Monterde & Ugail, 2009).

By using equation (4.45), we have $v_{11} = (1, 1, 1.5)$.

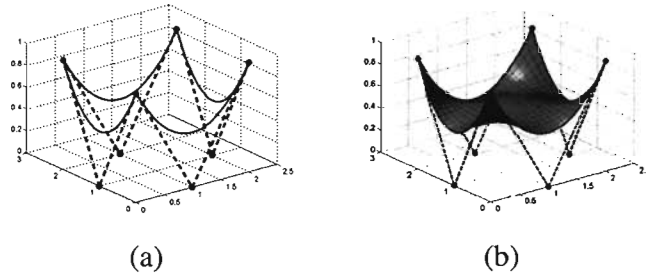


Figure 4.15. (a) Boundary curves of biquadratic Said-Ball surface generated by an extremal of the Dirichlet condition (b) surface of biquadratic Said-Ball surface generated by an extremal of the Dirichlet condition.

4.2.2 Bicubic Dirichlet Surface

If we substitute $n = m = 3$ in Theorem 4.1, we obtain the bicubic case. In this case, there are four equations corresponding to the inner control points.

4.2.2.1 Said-Ball and Wang-Ball

If we replace the monomial matrix form c_{ij} in Theorem 4.1 by the Said-Ball monomial matrix form, and the control points b_{ij} by Said-Ball control points w_{ij} , we obtain the Dirichlet functional of Said-Ball polynomial solution.

Since in application to degree three, cubic Said-Ball curve and Wang-Ball curve generate the same results, it is however not necessary to express solutions for both, but it is sufficient to show the results for only bicubic Said-Ball as given in Proposition 4.2.

Proposition 4.2. *A bicubic Said-Ball surface is an extremal of the Dirichlet functional with prescribed border if and only if*

$$v_{11} = \frac{1}{104}(74v_{00} - 96v_{01} + 48v_{02} + 39v_{03} - 96v_{10} + 30v_{13} + 48v_{20} - 8v_{23} + 39v_{30} + 30v_{31} - 8v_{32} + 4v_{33}), \quad (4.46)$$

$$v_{12} = \frac{1}{104}(39v_{00} + 48v_{01} - 96v_{02} + 74v_{03} + 30v_{10} - 96v_{13} - 8v_{20} + 48v_{23} + 4v_{30} - 8v_{31} + 30v_{32} + 39v_{33}), \quad (4.47)$$

$$v_{21} = \frac{1}{104}(39v_{00} + 30v_{01} - 8v_{02} + 4v_{03} + 48v_{10} - 8v_{13} - 96v_{20} + 30v_{23} + 74v_{30} - 96v_{31} + 48v_{32} + 39v_{33}), \quad (4.48)$$

$$v_{22} = \frac{1}{104}(4v_{00} - 8v_{01} + 30v_{02} + 39v_{03} - 8v_{10} + 48v_{13} + 30v_{20} - 96v_{23} + 39v_{30} + 48v_{31} - 96v_{32} + 74v_{33}). \quad (4.49)$$

4.2.2.2 DP-Ball

If $n = m = 3$, there are four equations corresponding to the inner control points d_{11} , d_{12} , d_{21} , d_{22} .

Proposition 4.3. *A bicubic DP-Ball surface is an extremal of the Dirichlet functional with prescribed border if and only if*

$$d_{11} = \frac{1}{78}(196d_{00} - 59d_{01} + 52d_{02} - 104d_{03} - 59d_{10} + 52d_{13} + 52d_{20} - 32d_{23} - 104d_{30} + 52d_{31} - 32d_{32} + 64d_{33}), \quad (4.50)$$

$$d_{12} = \frac{1}{78} - (104d_{00} - 52d_{01} + 59d_{02} - 196d_{03} - 52d_{10} + 59d_{13} + 32d_{20} - 52d_{23} - 64d_{30} + 32d_{31} - 52d_{32} + 104d_{33}) \quad (4.51)$$

$$d_{21} = \frac{1}{78} - (104d_{00} - 52d_{01} + 32d_{02} - 64d_{03} - 52d_{10} + 32d_{13} + 59d_{20} - 52d_{23} - 196d_{30} + 59d_{31} - 52d_{32} + 104d_{33}), \quad (4.52)$$

$$d_{22} = \frac{1}{78}(64d_{00} - 32d_{01} + 52d_{02} - 104d_{03} - 32d_{10} + 52d_{13} + 52d_{20} - 59d_{23} - 104d_{30} + 52d_{31} - 59d_{32} + 196d_{33}). \quad (4.53)$$

4.2.3 Dirichlet Mask for Bicubic Pathes

The following masks for the bicubic Dirichlet functional, where the masks on the left side for bicubic Bézier, on the middle side for bicubic Said/Wang-Ball, and on the right side for bicubic DP-Ball.

$$P_{11} = \frac{1}{78} \begin{array}{cccc} 0 & 15 & -4 & 4 \\ 24 & \bullet & \bullet & -4 \\ -22 & \bullet & \bullet & 15 \\ 48 & -22 & 24 & 0 \end{array} \quad w_{11} = \frac{1}{104} \begin{array}{cccc} 39 & 30 & -8 & 4 \\ 48 & \bullet & \bullet & -8 \\ -96 & \bullet & \bullet & 30 \\ 74 & -96 & 48 & 39 \end{array} \quad d_{11} = \frac{1}{78} \begin{array}{cccc} -10 & 52 & -32 & 64 \\ 52 & \bullet & \bullet & -32 \\ -59 & \bullet & \bullet & 52 \\ 196 & -59 & 52 & -104 \end{array}$$

$$P_{12} = \frac{1}{78} \begin{array}{cccc} 48 & -22 & 24 & 0 \\ -22 & \bullet & \bullet & 15 \\ 24 & \bullet & \bullet & -4 \\ 0 & 3 & 0 & 4 \end{array} \quad w_{12} = \frac{1}{104} \begin{array}{cccc} 4 & -8 & 30 & 39 \\ -8 & \bullet & \bullet & 48 \\ 30 & \bullet & \bullet & -96 \\ 39 & 48 & -96 & 74 \end{array} \quad d_{12} = \frac{1}{78} \begin{array}{cccc} 64 & -32 & 52 & -104 \\ -32 & \bullet & \bullet & 52 \\ 52 & \bullet & \bullet & -59 \\ -104 & 52 & -59 & 196 \end{array}$$

$$P_{21} = \frac{1}{78} \begin{array}{cccc} 4 & -4 & -15 & 0 \\ -4 & \bullet & \bullet & 24 \\ 15 & \bullet & \bullet & -22 \\ 0 & 24 & -22 & 48 \end{array} \quad w_{21} = \frac{1}{104} \begin{array}{cccc} 47 & -96 & 48 & 39 \\ -96 & \bullet & \bullet & 30 \\ 48 & \bullet & \bullet & -8 \\ 39 & 30 & -8 & 4 \end{array} \quad d_{21} = \frac{1}{78} \begin{array}{cccc} 196 & -59 & 52 & -104 \\ -59 & \bullet & \bullet & 52 \\ 52 & \bullet & \bullet & -32 \\ -104 & 52 & -32 & 64 \end{array}$$

$$\begin{array}{cccc}
0 & 24 & -22 & 48 \\
15 & \bullet & \bullet & -22 \\
-4 & \bullet & \bullet & 24 \\
4 & -4 & 15 & 0
\end{array}
\quad
\begin{array}{cccc}
39 & 48 & -96 & 74 \\
30 & \bullet & \bullet & -96 \\
-8 & \bullet & \bullet & 48 \\
4 & -8 & 30 & 39
\end{array}
\quad
\begin{array}{cccc}
-104 & 52 & -59 & 196 \\
52 & \bullet & \bullet & -59 \\
-32 & \bullet & \bullet & 52 \\
64 & -32 & 52 & -104
\end{array}$$

$P_{22} = \frac{1}{78}$ $w_{22} = \frac{1}{104}$ $d_{22} = \frac{1}{78}$

4.2.4 Graphical Examples for Extremal of the Dirichlet Bicubic Surface

Here are some graphical examples of surfaces generated by extremals of the Dirichlet functional by using four different sets of control points such that each set has similar four boundaries for the surface.

4.2.4.1 Graphical Examples for Extremal of the Dirichlet Bicubic Wang-Ball Surface

Example 4.2. Given the boundary control points set 1 of bicubic Wang-Ball surface as follows

$$\begin{aligned}
w_{00} &= (0, 0, 1), w_{10} = (6/5, 0, 2113/1000), w_{20} = (1, 0, 23/8), w_{30} = (4, 0, 1), \\
w_{01} &= (0, 18/5, -491/625), w_{02} = (0, 14/5, -71/625), w_{03} = (0, 4, 1), \\
w_{13} &= (9/5, 4, 631/250), w_{23} = (11/5, 4, 631/250), w_{31} = (4, 9/5, -885/1687), \\
w_{32} &= (4, 11/5, -885/1687), w_{33} = (4, 4, 1).
\end{aligned}$$

The inner control points of bicubic Wang-Ball surface by an extremal of the Dirichlet condition are

$$\begin{aligned}
w_{11} &= (573/260, 213/260, 779/395), w_{12} = (138/65, 539/260, 370/1043), \\
w_{21} &= (53/260, -51/65, -1219/893), \text{ and } w_{22} = (389/260, 119/65, 1395/1097).
\end{aligned}$$

The graph of the above surface is in Figure 4.16(c), while the boundary curves and its control points in Figure 4.16(d).

Example 4.2. Given the boundary control points set 2 of bicubic Wang-Ball surface as follows

$$w_{00} = (0, 0, 0), w_{10} = (9/4, 0, -9/2), w_{20} = (3/4, 0, 9/2), w_{30} = (3, 0, 0),$$

$$w_{01} = (0, 9/4, -9/2), w_{02} = (0, 3/4, 9/2), w_{03} = (0, 3, 0), w_{13} = (3/2, 3, -3/2),$$

$$w_{23} = (3/2, 3, -3/2), w_{31} = (3, 3/2, 3/2), w_{32} = (3, 3/2, 3/2), w_{33} = (3, 3, 0).$$

The inner control points of bicubic Wang-Ball surface by an extremal of the Dirichlet condition are

$$w_{11} = (6/13, 6/13, 162/13), w_{12} = (369/208, 33/13, -357/52),$$

$$w_{21} = (21/26, -171/208, -417/52), \text{ and}$$

$$w_{22} = (255/208, 255/208, 171/52). \text{ The graph of the above surface is in Figure 4.17(c),}$$

while the boundary curves and its control points in Figure 4.17(d).

Example 4.3. Given the boundary control points set 3 of bicubic Wang-Ball surface as follows

$$w_{00} = (0.5, 0, 0), w_{10} = (0.2577, 0.4, 0), w_{20} = (-0.5, 0.36, 0), w_{30} = (-0.5, 0, 0),$$

$$w_{01} = (0.425, 0, 0.45), w_{02} = (0.575, 0, 0.75), w_{03} = (1, 0, 1), w_{13} = (0.5153, 1, 1),$$

$$w_{23} = (-1, 0.72, 1), w_{31} = (-0.425, 0, 0.45), w_{32} = (-0.575, 0, 0.75), w_{33} = (-1, 0, 1).$$

The inner control points of bicubic Wang-Ball surface by an extremal of the Dirichlet condition are

$$w_{11} = (283/9635, 9/200, 909/2080), w_{12} = (-679/1879, -981/1300, 203/416),$$

$$w_{21} = (1048/1233, -843/1300, -891/2080), \text{ and } w_{22} = (922/1487, -39/200, 203/416).$$

The graph of the above surface is in Figure 4.18(c), while the boundary curves and its control points in Figure 4.18(d).

Example 4.4. Given the boundary control points set 4 of bicubic Wang-Ball surface as follows

$$\begin{aligned} w_{00} &= (-585/631, 1378/483, 0), w_{10} = (-2547/631, -689/483, 0), \\ w_{20} &= (-710/173, -609/500, 0), w_{30} = (585/631 - 1378/4830), \\ w_{01} &= (-111/581, 2342/3983, 21/40), w_{02} = (-327/3697, 457/1674, 2/5), \\ w_{03} &= (-585/631, 1378/483, 1), w_{13} = (-622/163, -2234/793, 1), \\ w_{23} &= (-1170/631, -1378/483, 1), w_{31} = (512/1599, -1699/1724, 9/20), \\ w_{32} &= (161/7124, -173/2475, 13/40), w_{33} = (585/631, -1378/483, 1). \end{aligned}$$

The inner control points of bicubic Wang-Ball surface by an extremal of the Dirichlet condition are

$$\begin{aligned} w_{11} &= (993/2087, 517/373, 447/1040), w_{12} = (1913/1636, 2671/902, 1159/2080), \\ w_{21} &= (1048/1233, -843/1300, -891/2080), \text{ and} \\ w_{22} &= (-171/935, -211/178, 79/130). \end{aligned}$$

The graph of the above surface is in Figure 4.19(c), while the boundary curves and its control points in Figure 4.19(d).

4.2.4.2 Graphical Examples for Extremal of the Dirichlet Bicubic DP-Ball Surface

Example 4.6. Given the boundary control points set 1 of bicubic DP-Ball surface as follows

$$\begin{aligned} d_{00} &= (0, 0, 1), d_{10} = (-2/5, 0, 617/500), d_{20} = (16/5, 0, 1379/500), d_{30} = (4, 0, 1), \\ d_{01} &= (0, 8/5, -399/625), d_{02} = (0, 4, 441/625), d_{03} = (0, 4, 1), \\ d_{13} &= (-2/5, 4, 252/125), d_{23} = (22/5, 4, 252/125), d_{31} = (4, -2/5, -41/2500), \\ d_{32} &= (4, 22/5, -41/2500), d_{33} = (4, 4, 1). \end{aligned}$$

The inner control points of bicubic DP-Ball surface by an extremal of the Dirichlet condition are

$$\begin{aligned} d_{11} &= (97/65, 56/39, 5199/1133), d_{12} = (-29/65, 772/195, -2104/1347), \\ d_{21} &= (6/13, -881/195, -4974/1277), \text{ and } d_{22} = (339/65, 1141/195, 759/185). \end{aligned}$$

The graph of the above surface is in Figure 4.16(e), while the boundary curves and its control points in Figure 4.16(f).

Example 4.5. Given the boundary control points set 2 of bicubic DP-Ball surface as follows

$$\begin{aligned} d_{00} &= (0, 0, 0), d_{10} = (3/2, 0, -9), d_{20} = (3/2, 0, 9), d_{30} = (3, 0, 0), d_{01} = (0, 3/2, -9), \\ d_{02} &= (0, 3/2, 9), d_{03} = (0, 3, 0), d_{13} = (0, 3, -1), \\ d_{23} &= (3, 3, -1), d_{31} = (3, 0, 1), d_{32} = (3, 3, 1), d_{33} = (3, 3, 0). \end{aligned}$$

The inner control points of bicubic DP-Ball surface by an extremal of the Dirichlet condition are

$$\begin{aligned} d_{11} &= (-31/52, 9/52, 323/13), d_{12} = (11/13, 207/52, -283/13), \\ d_{21} &= (107/52, -3, -277/13), \text{ and } d_{22} = (38/13, 48/13, 242/13). \end{aligned}$$

The graph of the above surface is in Figure 4.17(e), while the boundary curves and its control points in Figure 4.17(f).

Example 4.6. Given the boundary control points set 3 of bicubic DP-Ball surface as follows

$$\begin{aligned} d_{00} &= (1/2, 0, 0), d_{10} = (989/974, 11/25, 0), d_{20} = (-1225/974, 8/25, 0), \\ d_{30} &= (-1/2, 0, 0), d_{01} = (11/40, 0, 3/20), d_{02} = (29/40, 0, 21/20), d_{03} = (1, 0, 1), \\ d_{13} &= (1659/817, 32/25, 1), d_{23} = (-2055/817, 11/25, 1), d_{31} = (-11/40, 0, 3/20), \\ d_{32} &= (-29/40, 0, 21/20), d_{33} = (-1, 0, 1). \end{aligned}$$

The inner control points of bicubic DP-Ball surface by an extremal of the Dirichlet condition are

$$\begin{aligned} d_{11} &= (433/2569, 1095/989, 1199/1560), d_{12} = (531/1333, -154/195, 1013/1560), \\ d_{21} &= (403/809, -1256/975, -925/601), \text{ and} \\ d_{22} &= (-905/1129, 1095/989, 788/437). \end{aligned}$$

The graph of the above surface is in Figure 4.18(e), while the boundary curves and its control points in Figure 4.18(f).

Example 4.7. Given the boundary control points set 4 of bicubic DP-Ball surface as follows

$$d_{00} = (-585/631, 1378/483, 0), d_{10} = (-1297/363, 1763/1000, 0),$$

$$d_{20} = (-927/500, -1763/500, 0), d_{30} = (585/631, -1378/483, 0),$$

$$d_{01} = (-631/1250, 1553/1000, 1/10), d_{02} = (-749/2500, 923/1000, 17/20),$$

$$d_{03} = (-585/631, 1378/483, 1), d_{13} = (-2356/493, 834/835, 1),$$

$$d_{23} = (834/835, -2356/493, 1), d_{31} = (1121/1555, -2773/1250, 1/20),$$

$$d_{32} = (292/2323, -242/625, 4/5), d_{33} = (585/631, -1378/483, 1).$$

The inner control points of bicubic DP-Ball surface by an extremal of the Dirichlet condition are

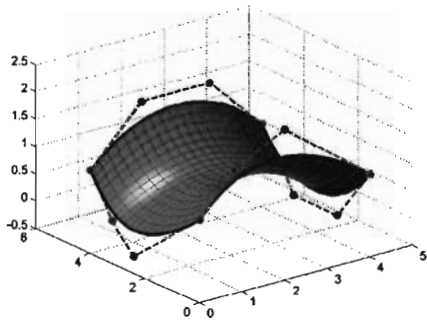
$$d_{11} = (-196673/51756, -1219/4014, 553/780),$$

$$d_{12} = (2132/1895, 1589/284, 77/120),$$

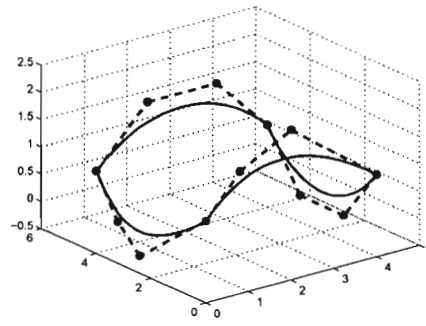
$$d_{21} = (2281/575, 1157/614, -2467/1560), \text{ and}$$

$$d_{22} = (-1229/499, -2058/293, 707/390).$$

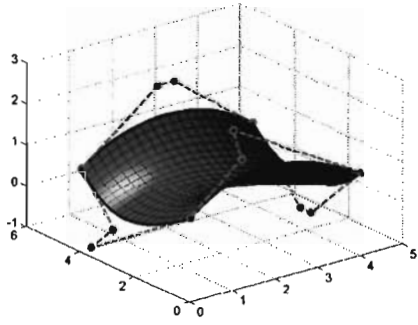
The graph of the above surface is in Figure 4.19(e), while the boundary curves and its control points in Figure 4.19(f).



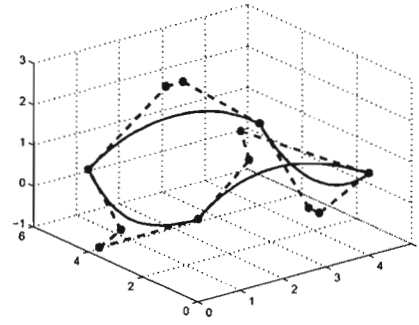
(a)



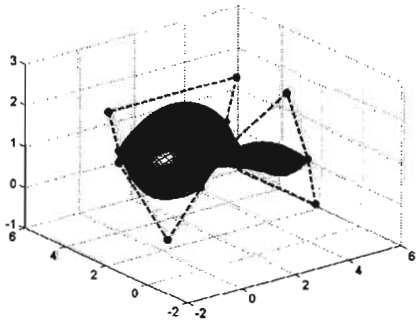
(b)



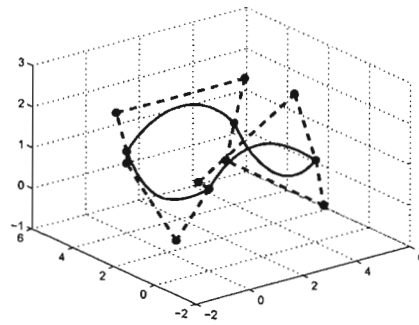
(c)



(d)

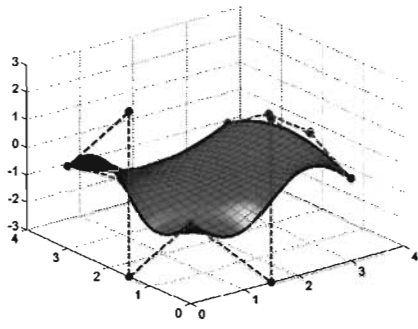


(e)

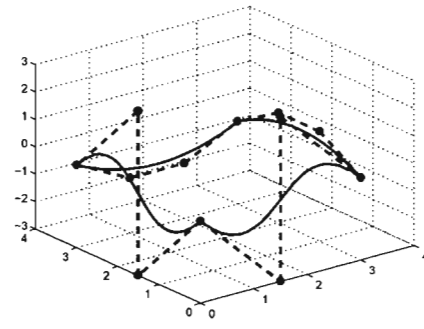


(f)

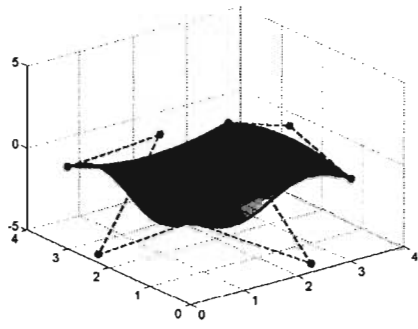
Figure 4.16. Control points set 1 by Dirichlet condition on (a) Bézier patch (b) Bézier boundary (c) Said/Wang-Ball patch (d) Said/Wang-Ball boundary (e) DP-Ball patch (f) DP-Ball boundary.



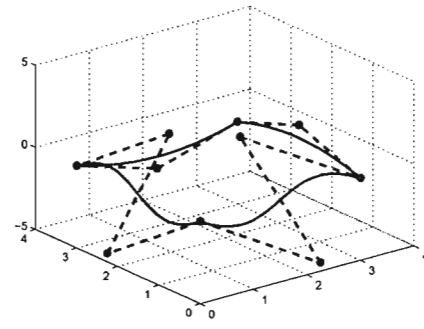
(a)



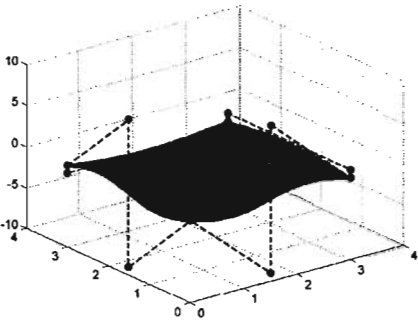
(b)



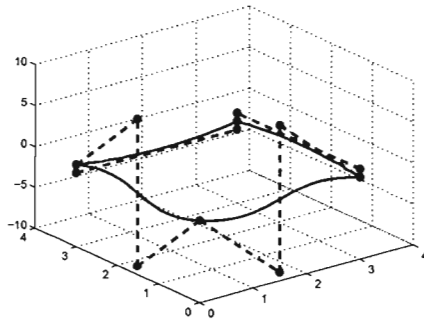
(c)



(d)

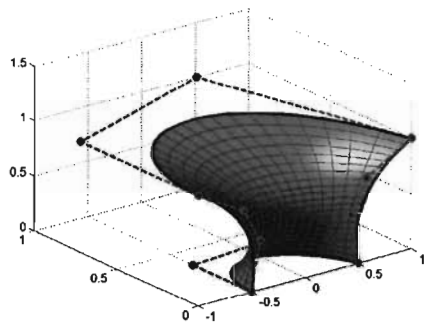


(e)

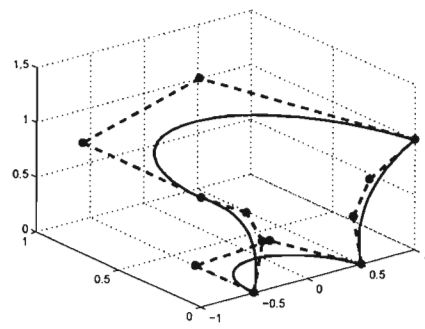


(f)

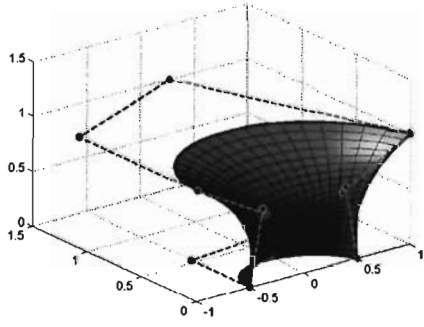
Figure 4.17. Control points set 2 by Dirichlet condition on (a) Bézier patch (b) Bézier boundary (c) Said/Wang-Ball patch (d) Said/Wang-Ball boundary (e) DP-Ball patch (f) DP-Ball boundary.



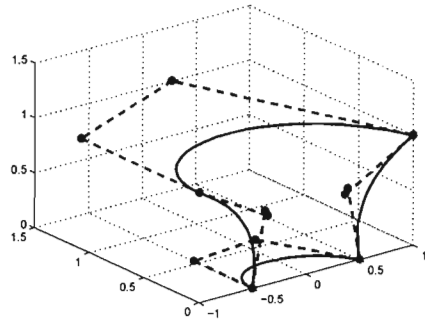
(a)



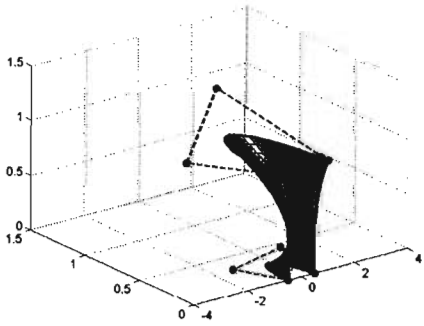
(b)



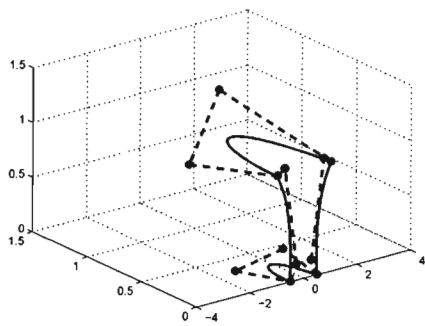
(c)



(d)

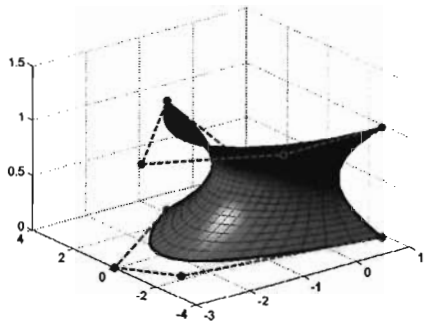


(e)

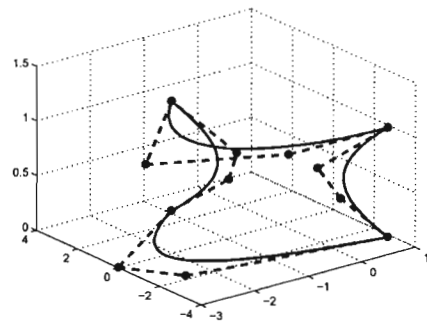


(f)

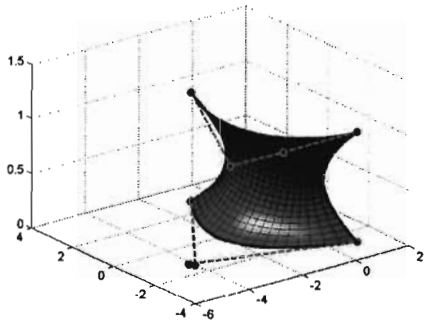
Figure 4.18. Control points set 3 by Dirichlet condition on (a) Bézier patch (b) Bézier boundary (c) Said/Wang-Ball patch (d) Said/Wang-Ball boundary (e) DP-Ball patch (f) DP-Ball boundary.



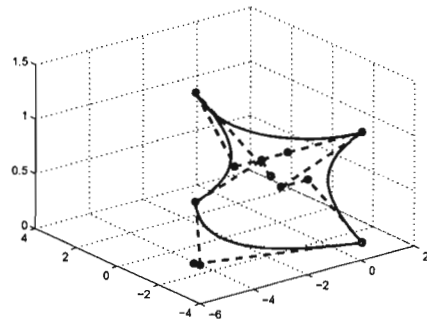
(a)



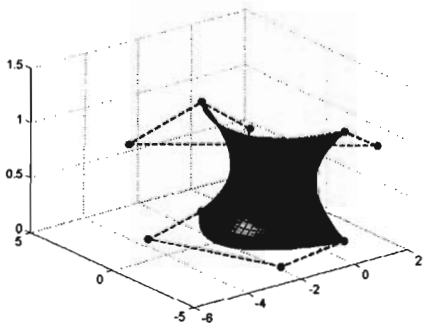
(b)



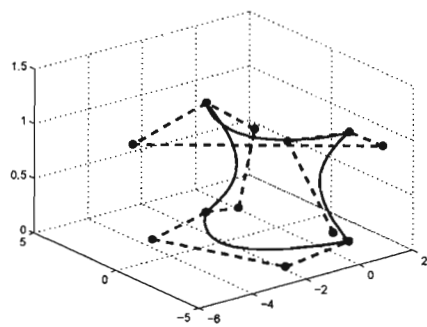
(c)



(d)



(e)



(f)

Figure 4.19. Control points set 4 by Dirichlet condition on (a) Bézier patch (b) Bézier boundary (c) Said/Wang-Ball patch (d) Said/Wang-Ball boundary (e) DP-Ball patch (f) DP-Ball boundary.

The following comparison between Bézier surface, Said/Wang-Ball surface and DP-Ball surface was made by using Dirichlet functional. All surface have the same four boundary curves.

Table 4.5
Comparison between the area/computational time of Bézier, Said/Wang-Ball and DP-Ball by using Dirichlet functional.

	Control Points	Bézier	Said/Wang-Ball	DP-Ball
Set 1	Area	18.757105	18.945053	18.945053
	Computational time	0.0959	0.090818	0.1113
Set 2	Area	11.766806	11.809898	11.809898
	Computational time	0.0919	0.0914	0.10439
Set 3	Area	1.796075	1.806860	1.806860
	Computational time	0.0932	0.0909	0.10575
Set 4	Area	13.668435	14.2352	14.2352
	Computational time	0.0950	0.0906	0.10307

From Table 4.5, the Dirichlet functional is applied to the bicubic patches of Said/Wang-Ball surface and DP-Ball surface, and compared with the existing work for bicubic patch of Bézier surface. It is discovered that the bicubic Bézier surface is better than bicubic Said/Wang-Ball surface in terms of minimal surface area. The bicubic Said/Wang-Ball surface is better than the bicubic Bézier surface in terms of the computational time required to construct the surface by Dirichlet functional. On the other hand, if we compare bicubic Bézier with bicubic DP-Ball by using Dirichlet functional, we see that Bézier is better than DP-Ball in terms of minimal surface area but vice versa for computational time.

4.3 Summary

In this chapter, we have presented a more general algorithm for the polynomial solution method of generating any surface used in CAGD based on the Euler-Lagrange equation arises from the most quadratic functional by using the monomial matrix form. Also, we derived a more generalized algorithm to find the Dirichlet functional for any surface used in CAGD.

CHAPTER FIVE

IMPLEMENTATION AND APPLICATIONS

In this chapter, we derived and discussed the sufficient condition for the positive preservation of boundary curves for each edge of rectangular Said-Ball, DP-Ball and Wang-Ball patches of odd degree- n . With the use of polynomial solution of fourth order linear elliptic PDEs, these curves are defined on rectangular grid for the purpose of enhancing the positivity preservation of the interpolating surface. We also apply the polynomial solution of fourth order linear elliptic PDEs to image enlargement using cubic Said-Ball, Wang-Ball and DP-Ball boundary curves with PDEs.

5.1 An Improved Positivity Preserving Said-Ball, DP-Ball and Wang-Ball Curves of Odd Degree- n

In this section, we will propose sufficient conditions for positivity preserving odd degree- n boundary curves defined on rectangular grid.

5.1.1 Sufficient Condition for Positivity Preserving Odd Degree- n Said-Ball Curves

Proposition 5.1. *Consider the Said-Ball polynomial curve odd degree- n ($n \geq 3$),*

$$r(x) = \sum_{i=0}^n S_i^n(x) v_i, \quad (5.1)$$

where v_i represents control points of Said-Ball and $S_i^n(x)$ are Said-Ball basis functions of odd degree- n , for all $0 \leq x \leq 1$. If $v_0, v_n > 0$, $M = \max(v_0, v_n)$, $N = \min(v_0, v_n)$ and $v_i \geq -t_0 = \frac{-1}{s_0}, i \neq 0, i \neq n$, such that s_0 in $\left[\frac{2^{\frac{n-1}{2}}-1}{M}, \frac{2^{\frac{n-1}{2}}-1}{N} \right]$ is the unique solution of $G(s) = 1$ with $G(s) = \frac{1}{(v_0 s + 1)^{\frac{n-1}{2}}} + \frac{1}{(v_n s + 1)^{\frac{n-1}{2}}}$, then $r(x) \geq 0, \forall x \in [0, 1]$.

Proof. Let all Said-Ball ordinates of Said-Ball polynomial curve of odd degree- n except of v_0 and v_n , are equal to $-t$ ($t > 0$). From (5.1) we get

$$r(x) = v_0(1-x)^{\frac{n+1}{2}} - t \sum_{i=1}^{n-1} S_i^n(x) + v_n x^{\frac{n+1}{2}}. \quad (5.2)$$

Recall that

$$\sum_{i=0}^n S_i^n(x) = (1-x)^{\frac{n+1}{2}} + \sum_{i=1}^{n-1} S_i^n(x) + x^{\frac{n+1}{2}} = 1,$$

that is equivalent to

$$\sum_{i=1}^{n-1} S_i^n(x) = 1 - (1-x)^{\frac{n+1}{2}} - x^{\frac{n+1}{2}}. \quad (5.3)$$

On applying (5.3) in (5.2), we obtain

$$r(x) = (v_0 + t)(1-x)^{\frac{n+1}{2}} + (v_n + t)x^{\frac{n+1}{2}} - t. \quad (5.4)$$

Assume that t is fixed. Then, the first and second derivatives of r with respect to x are

$$r'(x) = -\frac{n+1}{2}(v_0 + t)(1-x)^{\frac{n-1}{2}} + \frac{n+1}{2}(v_n + t)x^{\frac{n-1}{2}},$$

and

$$r''(x) = \frac{(n+1)(n-1)}{4} \left((v_0 + t)(1-x)^{\frac{n-3}{2}} + (v_n + t)x^{\frac{n-3}{2}} \right).$$

On setting $r'(x) = 0$, this gives

$$\frac{(1-x)^{\frac{n-1}{2}}}{x^{\frac{n-1}{2}}} = \frac{(v_n + t)}{(v_0 + t)}, x \neq 0, \text{ or } \frac{1-x}{x} = \left(\frac{(v_n + t)}{(v_0 + t)} \right)^{\frac{2}{n-1}}, x \neq 0.$$

Thus, we obtain

$$x = \frac{(v_0 + t)^{\frac{2}{n-1}}}{(v_0 + t)^{\frac{2}{n-1}} + (v_n + t)^{\frac{2}{n-1}}}.$$

It follows that $v_0 > 0$ and $v_n > 0, 0 < x \leq 1$, implies that $r''(x) > 0$, then the minimum value of r occurs when $x = \frac{(v_0 + t)^{\frac{2}{n-1}}}{(v_0 + t)^{\frac{2}{n-1}} + (v_n + t)^{\frac{2}{n-1}}}$, that is

$$r_{min}(x) = \frac{(v_0 + t)(v_n + t)}{\left((v_0 + t)^{\frac{2}{n-1}} + (v_n + t)^{\frac{2}{n-1}} \right)^{\frac{n-1}{2}}} - t. \quad (5.5)$$

Observe that if $t = 0, r_{min} > 0$. Now, we describe how to obtain the value of $t_0 > 0$, to ensure that $r(x)$ preserved the positivity for all $0 \leq x \leq 1$. We rewrite (5.5) to obtain

$$r_{min}(x) = \frac{1}{\left(\frac{1}{(v_0 + t)^{\frac{2}{n-1}}} + \frac{1}{(v_n + t)^{\frac{2}{n-1}}} \right)^{\frac{n-1}{2}}} - t,$$

which equivalent to

$$r_{min}(x) = \frac{t}{\left(\frac{1}{(\frac{v_0}{t} + 1)^{\frac{2}{n-1}}} + \frac{1}{(\frac{v_n}{t} + 1)^{\frac{2}{n-1}}} \right)^{\frac{n-1}{2}}} - t, \quad t > 0. \quad (5.6)$$

The Said-Ball polynomial curve $r(x)$ is positive for all x if $r_{min} > 0$. Thus, the lower bound of $t = t_0$ occurs when $r_{min} = 0$, and this can be achieved by setting the denominator of (5.6) equal to 1. Therefore,

$$\frac{1}{(\frac{v_0}{t} + 1)^{\frac{2}{n-1}}} + \frac{1}{(\frac{v_n}{t} + 1)^{\frac{2}{n-1}}} = 1. \quad (5.7)$$

Let $s = \frac{1}{t}, t \neq 0$, and $G(s) = \frac{1}{(sv_0 + 1)^{\frac{2}{n-1}}} + \frac{1}{(sv_n + 1)^{\frac{2}{n-1}}}$, then (5.7) becomes

$$G(s) = 1, s \geq 0. \quad (5.8)$$

Since $v_0 > 0$ and $v_n > 0$, then s_0 is the solution of (5.8) and the value of t_0 is equal to $\frac{1}{s_0}$ where $s_0 > 0$. Thus, $r(x) \geq 0$, for all $x \in [0, 1]$ if $v_i \geq -t_0 = \frac{-1}{s_0}, i \neq 0, i \neq n$, such that s_0 is the unique solution of $G(s) = 1$ with $G(s) = \frac{1}{(v_0s+1)^{\frac{2}{n-1}}} + \frac{1}{(v_ns+1)^{\frac{2}{n-1}}}$.

We proved that there exists $\frac{2^{\frac{n-1}{2}}-1}{M} \leq s_0 \leq \frac{2^{\frac{n-1}{2}}-1}{N}$ for $G(S) = 1$ where $M = \max(v_0, v_n)$ and $N = \min(v_0, v_n)$. Since

$$G'(x) = -\frac{2}{n-1} \left(\frac{v_0}{(sv_0+1)^{\frac{n+1}{n-1}}} + \frac{v_n}{(sv_n+1)^{\frac{n+1}{n-1}}} \right) \leq 0$$

and

$$G''(x) = \frac{2(n+1)}{(n-1)^2} \left(\frac{(v_0)^2}{(sv_0+1)^{\frac{2n}{n-1}}} + \frac{(v_n)^2}{(sv_n+1)^{\frac{2n}{n-1}}} \right) \geq 0,$$

then $G(s)$ is monotone decreasing and convex. Since $\lim_{s \rightarrow \infty} G(s) = 0$, $G(0) = 2$, and by the monotonicity of $G(s)$, then there exists s subject to $G(s) = 1$. Now we need to determine the range of s .

If $v_0 = v_n = \max(v_0, v_n) = M$, then $G(s) \geq \frac{2}{(Ms+1)^{\frac{2}{n-1}}}$. If $v_0 = v_n = \min(v_0, v_n) = N$, then $G(s) \leq \frac{2}{(Ns+1)^{\frac{2}{n-1}}}$. Since $\frac{2}{(Ns+1)^{\frac{2}{n-1}}}$ and $\frac{2}{(Ms+1)^{\frac{2}{n-1}}}$ are also monotone decreasing and convex, then there exists s_1, s_2 such that $\frac{2}{(Ms_1+1)^{\frac{2}{n-1}}} = 1$ and $\frac{2}{(Ns_2+1)^{\frac{2}{n-1}}} = 1$. On solving for s_1 and s_2 , we obtain $s_1 = \frac{2^{\frac{n-1}{2}}-1}{M}$ and $s_2 = \frac{2^{\frac{n-1}{2}}-1}{N}$. Thus, if $G(s) = 1$, then $s_1 \leq s_0 \leq s_2$. Figure 5.1 shows the form of $G(s), s \geq 0$ with the relative location of $s_1 = \frac{2^{\frac{n-1}{2}}-1}{M}, s_2 = \frac{2^{\frac{n-1}{2}}-1}{N}$ and $s = s_0$. □

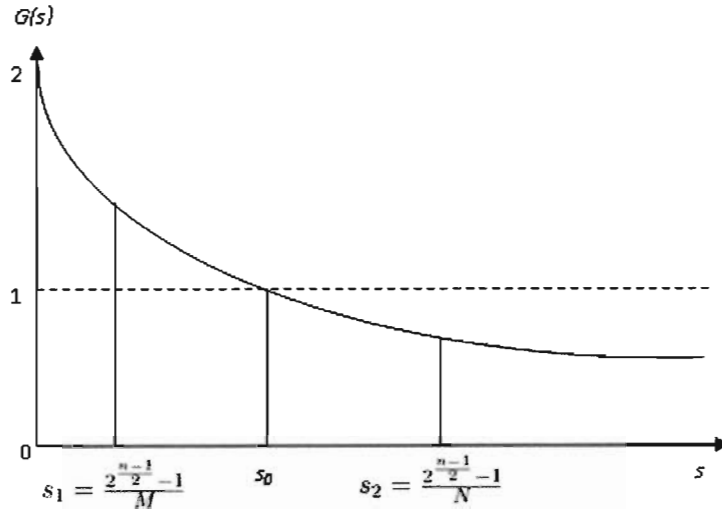


Figure 5.1. Function $G(s)$ with $s \geq 0$ for odd degree- n Said-Ball polynomial curve.

5.1.2 Sufficient Condition for Positivity Preserving Odd Degree- n DP-Ball Curves

Proposition 5.2. Consider the DP-Ball polynomial curve of odd degree- n ($n \geq 3$),

$$r(x) = \sum_{i=0}^n D_i^n(x) d_i, \quad (5.9)$$

where d_i is a DP-Ball control point and $D_i^n(x)$ is DP-Ball of odd degree- n , for all $0 \leq x \leq 1$. If $d_0, d_n > 0, M = \max(d_0, d_n), N = \min(d_0, d_n)$ and $d_i \geq -t_0 = \frac{-1}{s_0}, i \neq 0, i \neq n$, such that s_0 in $\left[\frac{2^{n-1}}{M}, \frac{2^{n-1}}{N}\right]$ is the unique solution of $G(s) = 1$ with $G(s) = \frac{1}{(d_0 s + 1)^{\frac{1}{n-1}}} + \frac{1}{(d_n s + 1)^{\frac{1}{n-1}}}$, then $r(x) \geq 0, \forall x \in [0, 1]$.

Proof. Let all DP-Ball ordinates of DP-Ball polynomial curve of odd degree- n , except of d_0 and d_n , are equal to $-t$ ($t > 0$). From (5.9) we get

$$r(x) = d_0(1-x)^n - t \sum_{i=1}^{n-1} D_i^n(x) + d_n x^n. \quad (5.10)$$

Recall that

$$\sum_{i=0}^n D_i^n(x) = (1-x)^n + \sum_{i=1}^{n-1} D_i^n(x) + x^n = 1, \quad (5.11)$$

that is equivalent to

$$\sum_{i=1}^{n-1} D_i^n(x) = 1 - (1-x)^n - x^n. \quad (5.12)$$

Hence (5.10) becomes

$$r(x) = (d_0 + t)(1-x)^n + (d_n + t)x^n - t. \quad (5.13)$$

Assume that t is fixed. Then, the first and second derivatives of r with respect to x are

$$r'(x) = -n(d_0 + t)(1-x)^{n-1} + n(d_n + t)x^{n-1},$$

and

$$r''(x) = n(n-1) \left((d_0 + t)(1-x)^{n-2} + (d_n + t)x^{n-2} \right).$$

On setting $r'(x) = 0$, this gives

$$\frac{(1-x)^{n-1}}{x^{n-1}} = \frac{(d_n + t)}{(d_0 + t)}, x \neq 0, \text{ or } \frac{1-x}{x} = \left(\frac{(d_n + t)}{(d_0 + t)} \right)^{\frac{1}{n-1}}, x \neq 0.$$

Thus, we obtain

$$x = \frac{(d_0 + t)^{\frac{1}{n-1}}}{(d_0 + t)^{\frac{1}{n-1}} + (d_n + t)^{\frac{1}{n-1}}}.$$

It follows that $d_0 > 0$ and $d_n > 0, 0 < x \leq 1$, implies that $r''(x) > 0$, then the minimum value of r occurs when $x = \frac{(d_0 + t)^{\frac{1}{n-1}}}{(d_0 + t)^{\frac{1}{n-1}} + (d_n + t)^{\frac{1}{n-1}}}$, that is

$$r_{min}(x) = \frac{(d_0 + t)(d_n + t)}{\left((d_0 + t)^{\frac{1}{n-1}} + (d_n + t)^{\frac{1}{n-1}} \right)^{n-1}} - t. \quad (5.14)$$

Observe that if $t = 0, r_{min} > 0$. Now, we describe how to obtain the value of $t_0 > 0$,

to ensure that $r(x)$ preserved the positivity for all $0 \leq x \leq 1$. We rewrite (5.14) to obtain

$$r_{min}(x) = \frac{1}{\left(\frac{1}{(d_0+t)^{\frac{1}{n-1}}} + \frac{1}{(d_n+t)^{\frac{1}{n-1}}}\right)^{n-1}} - t,$$

which equivalent to

$$r_{min}(x) = \frac{t}{\left(\frac{1}{(\frac{d_0}{t}+1)^{\frac{1}{n-1}}} + \frac{1}{(\frac{d_n}{t}+1)^{\frac{1}{n-1}}}\right)^{n-1}} - t. \quad (5.15)$$

The DP-Ball polynomial curve $r(x)$ is positive for all x if $r_{min} > 0$. Thus, the lower bound of $t = t_0$ occurs when $r_{min} = 0$, and this can be achieved by setting the denominator of (5.15) equal to 1. Therefore,

$$\frac{1}{(\frac{d_0}{t}+1)^{\frac{1}{n-1}}} + \frac{1}{(\frac{d_n}{t}+1)^{\frac{1}{n-1}}} = 1. \quad (5.16)$$

Let $s = \frac{1}{t}, t \neq 0$, and $G(s) = \frac{1}{(sd_0+1)^{\frac{1}{n-1}}} + \frac{1}{(sd_n+1)^{\frac{1}{n-1}}}$, then (5.16) becomes

$$G(s) = 1, s \geq 0. \quad (5.17)$$

Since $d_0 > 0$ and $d_n > 0$, then s_0 is the solution of (5.17) and the value of t_0 is equal to $\frac{1}{s_0}$ where $s_0 > 0$. Thus, $r(x) \geq 0$, for all $x \in [0, 1]$ if $d_i \geq -t_0 = \frac{-1}{s_0}, i \neq 0, i \neq n$, such that s_0 is the unique solution of $G(s) = 1$ with $G(s) = \frac{1}{(d_0s+1)^{\frac{1}{n-1}}} + \frac{1}{(d_ns+1)^{\frac{1}{n-1}}}$.

We proved that there exist $\frac{2^{n-1}-1}{M} \leq s_0 \leq \frac{2^{n-1}-1}{N}$ for $G(S) = 1$ where $M = \max(d_0, d_n)$ and $N = \min(d_0, d_n)$. Since

$$G'(x) = -\frac{1}{n-1} \left(\frac{d_0}{(sd_0+1)^{\frac{n}{n-1}}} + \frac{d_n}{(sd_n+1)^{\frac{n}{n-1}}} \right) \leq 0$$

and

$$G''(x) = \frac{n}{(n-1)^2} \left(\frac{(d_0)^2}{(sd_0+1)^{\frac{2n-1}{n-1}}} + \frac{(d_n)^2}{(sd_n+1)^{\frac{2n-1}{n-1}}} \right) \geq 0,$$

then $G(s)$ is monotone decreasing and convex. Since $\lim_{s \rightarrow \infty} G(s) = 0$, $G(0) = 2$, and by the monotonicity of $G(s)$, then there exists s subject to $G(s) = 1$. Now we need to determine the range of s .

If $d_0 = d_n = \max(d_0, d_n) = M$, then $G(s) \geq \frac{2}{(Ms+1)^{\frac{1}{n-1}}}$. If $d_0 = d_n = \min(d_0, d_n) = N$, then $G(s) \leq \frac{2}{(Ns+1)^{\frac{1}{n-1}}}$. Since $\frac{2}{(Ms+1)^{\frac{1}{n-1}}}$ and $\frac{2}{(Ns+1)^{\frac{1}{n-1}}}$ are also monotone decreasing and convex, then there exists s_1, s_2 so that $\frac{2}{(Ms_1+1)^{\frac{1}{n-1}}} = 1$ and $\frac{2}{(Ns_2+1)^{\frac{1}{n-1}}} = 1$. On solving for s_1 and s_2 we obtain $s_1 = \frac{2^{n-1}-1}{M}$ and $s_2 = \frac{2^{n-1}-1}{N}$. Thus, if $G(s) = 1$, then $s_1 \leq s_0 \leq s_2$. Figure.5.2 shows the form of $G(s), s \geq 0$ with the relative location of $s_1 = \frac{2^{n-1}-1}{M}, s_2 = \frac{2^{n-1}-1}{N}$ and $s = s_0$. □

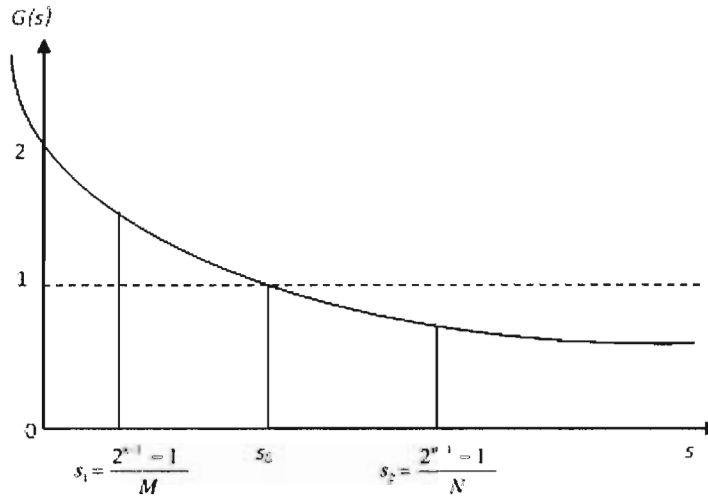


Figure 5.2. Function $G(s)$ with $s \geq 0$ for odd degree- n DP-Ball polynomial curve.

5.1.3 Sufficient Condition for Positivity Preserving Odd Degree- n Wang-Ball Curves

Proposition 5.3. Consider the Wang-Ball curve of odd degree- n ($n \geq 3$)

$$r(x) = \sum_{i=0}^n w_i A_i^n(x), \quad 0 \leq x \leq 1, \quad (5.18)$$

where w_i represents control points of Wang-Ball and $A_i^n(x)$ are Wang-Ball basis functions of odd degree- n . If $w_0, w_n > 0$ and $w_i \geq -t_0, 1 \leq i \leq n-1$, such that $t_0 > 0$ is the unique solution of

$$t^2 - w_0 w_n = 0. \quad (5.19)$$

It follows that $r(x) \geq 0, \forall x \in (0, 1]$. *Proof.* Let $w_0, w_n > 0$ and all Wang-Ball ordinates of Wang-Ball polynomial curve of odd degree- n except of w_0 and w_n , are equal to $-t, (t > 0)$. From (5.18) we get

$$r(x) = w_0(1-x)^2 - t \sum_{i=1}^{n-1} A_i^n(x) + w_n x^2. \quad (5.20)$$

Recall that (2.47)

$$\sum_{i=0}^n A_i^n(x) = (1-x)^2 + \sum_{i=1}^{n-1} A_i^n(x) + x^2 = 1, \quad (5.21)$$

that is equivalent to

$$\sum_{i=1}^{n-1} A_i^n = 1 - (1-x)^2 - x^2. \quad (5.22)$$

On applying (5.22) in (5.20), we obtain

$$r(x) = (w_0 + t)(1-x)^2 + (w_n + t)x^2 - t. \quad (5.23)$$

By taking the first order derivative with respect to x we have

$$r'(x) = -2(w_0 + t)(1 - x) + 2(w_n + t)x. \quad (5.24)$$

The value of r is minimum if $r'(x) > 0$ i.e

$$x = \frac{w_0 + t}{w_0 + 2t + w_n} > 0. \quad (5.25)$$

By substituting equation (5.25) into equation (5.23), this gives the following expression:

$$r_{min}(x) = \frac{(w_0 + t)(w_n + t)}{w_0 + 2t + w_n} - t. \quad (5.26)$$

If $t = 0$, then $r_{min} > 0$. Next, we describe how the value of $t > 0$ is obtained to make sure that $r(x)$ preserved the positivity for all $0 < x \leq 1$. When $r_{min} = 0$, we have the lower bound of t , given as

$$\frac{(w_0 + t)(w_n + t)}{w_0 + 2t + w_n} = t, \quad (5.27)$$

or by rewriting it, we have

$$t^2 - w_0w_n = 0. \quad (5.28)$$

Next, it is shown that there exists a real root $t_0 \in (0, w_0 + w_n)$ of (5.28).

Let $f(t) = t^2 - w_0w_n$. Given that $w_0, w_n, t > 0$, then $f(0) = -w_0w_n < 0$ and $f(w_0 + w_n) = (w_0 + w_n)^2 - w_0w_n > 0$. It follows that there exists $0 < t_0 < (w_0 + w_n)$, such that $f(t_0) = 0$ where t_0 is real root of (5.19). \square

5.2 Sufficient Condition for Positivity Preserving Cubic Ball (Said-Ball, DP-Ball and Wang-Ball Curves)

We derived a sufficient condition for positivity preserving boundary curves for a given positive cubic Ball (Said-Ball, DP-Ball and Wang-Ball) ordinates at vertices of rectangle R , i.e. $b_{00}, b_{30}, b_{03}, b_{33} > 0$. In order to ensure the positivity of boundary curves

$B(u, 0), B(u, 1), B(0, v)$ and $B(1, v)$, we set $b_{10}, b_{20} \geq -t_1, b_{13}, b_{23} \geq -t_2, b_{01}, b_{02} \geq -t_3$ and $b_{31}, b_{32} \geq -t_4$, where $t_1, t_2, t_3, t_4 > 0$ can be obtained from (5.30) for Said-Ball, (5.31) for DP-Ball and (5.34) for Wang-Ball, with $b_0 = b_{00}, b_3 = b_{30}$ along edge $e_1; b_0 = b_{03}, b_3 = b_{33}$ along edge $e_2; b_0 = b_{00}, b_3 = b_{03}$ along edge e_3 ; and $b_0 = b_{30}, b_3 = b_{33}$ along edge e_4 . Since $C_1(u), C_2(u), C_3(v)$ and $C_4(v)$ are the Ball polynomial curve of degree-3, we can use the following Corollary 5.1 for Said-Ball, Corollary 5.2 for DP-Ball and Corollary 5.3 for Wang-Ball to obtain the positivity preserving conditions for each boundary curve.

5.2.1 Sufficient Condition for Positivity Preserving Cubic Said-Ball Curves

If we set $n = 3$ in Proposition 5.1, then we obtain the following corollary.

Corollary 5.1. *Consider the cubic Said-Ball curve,*

$$r(x) = \sum_{i=0}^3 S_i^3(x) v_i, \quad (5.29)$$

where v_i are Said-Ball control points. If v_0, v_3 and $v_i \geq -t_0, 1 \leq i \leq 2$, then t_0 is a unique solution of

$$t^2 - v_0 v_3 = 0. \quad (5.30)$$

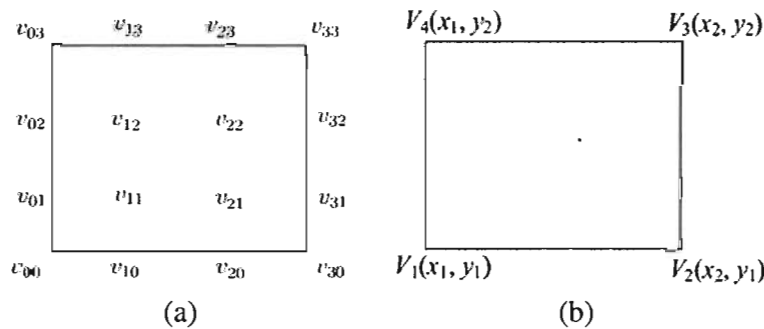


Figure 5.3. (a) Bicubic Said-Ball control points (b) A unit rectangle.

5.2.2 Sufficient Condition for Positivity Preserving Cubic DP-Ball Curves

If we set $n = 3$ in Proposition 5.2, then we obtain the following corollary.

Corollary 5.2. *Consider the cubic DP-Ball curve,*

$$r(x) = \sum_{i=0}^3 D_i^3(x) d_i, \quad (5.31)$$

where d_i are DP-Ball control points. If $d_0, d_3 > 0$ and $d_1, d_2 \geq -t_0$, then t_0 is a unique solution of

$$3t^4 - 4(d_0 + d_3)t^3 + 6d_0d_3t^2 - d_0^2d_3^2 = 0. \quad (5.32)$$

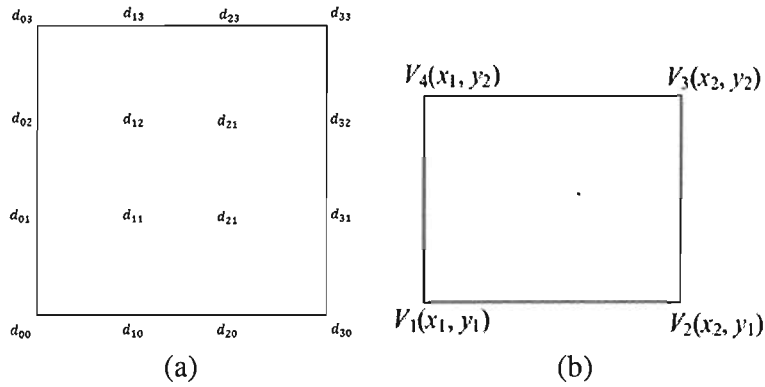


Figure 5.4. (a) Bicubic DP-Ball control points (b) A unit rectangle.

5.2.3 Sufficient Condition for Positivity Preserving Cubic Wang-Ball Curves

If we set $n = 3$ in Proposition 5.3, then we obtain the following corollary.

Corollary 5.3. *Consider the cubic Wang-Ball curve,*

$$r(x) = \sum_{i=0}^3 A_i^3(x) w_i, \quad (5.33)$$

where w_i are Wang-Ball control points. If w_0, w_3 and $w_1, w_2 \geq -t_0$, then t_0 is a unique solution of

$$t^2 - w_0w_3 = 0. \quad (5.34)$$

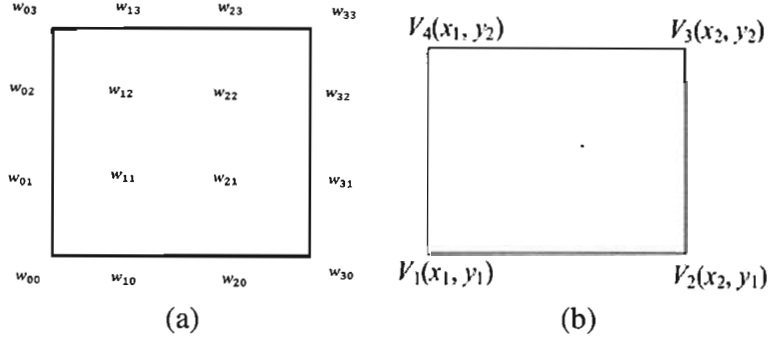


Figure 5.5. (a) Bicubic Wang-Ball control points (b) A unit rectangle.

5.3 Sufficient Condition for Positivity Preserving Quintic Ball (Said-Ball, DP-Ball and Wang-Ball Curves)

Now, we proceed to determine the lower bound on the edges of Ball (Said-Ball, DP-Ball and Wang-Ball) ordinates which ensure the positivity of boundary curves of degree-5 rectangular Ball (Said-Ball, DP-Ball and Wang-Ball) patch S . We derived a sufficient condition for positivity preserving boundary curves for a given positive quintic Ball ordinates at vertices of rectangle R , i.e. $b_{00}, b_{50}, b_{05}, b_{55} > 0$. In order to ensure the positivity of boundary curves $B(u, 0), B(u, 1), B(0, v)$ and $B(1, v)$, we set $b_{i0} \geq -t_1, b_{i5} \geq -t_2, b_{0j} \geq -t_3$ and $b_{5j} \geq -t_4$ for $1 \leq i \leq 4, 1 \leq j \leq 4$, where $t_1, t_2, t_3, t_4 > 0$ can be obtained from (5.36) with $b_0 = b_{00}, b_5 = b_{50}$ along edge e_1 ; $b_0 = b_{05}, b_5 = b_{55}$ along edge e_2 ; $b_0 = b_{00}, b_5 = b_{05}$ along edge e_3 ; and $b_0 = b_{50}, b_3 = b_{55}$ along edge e_4 . Since $C_1(u), C_2(u), C_3(v)$ and $C_4(v)$ are the Ball (Said-Ball, DP-Ball and Wang-Ball) polynomial curve of degree-5, we can use the following Corollary 5.4 for Said-Ball, Corollary 5.5 for DP-Ball and Corollary 5.6 for Wang-Ball to obtain the positivity preserving conditions for each boundary curve.

5.3.1 Sufficient Condition for Positivity Preserving Quintic Said-Ball Curves

If we set $n = 5$ in Proposition 5.1, then we obtain the following corollary.

Corollary 5.4. *Consider the quintic Said-Ball curve,*

$$r(x) = \sum_{i=0}^5 S_i^5(x)v_i, \quad (5.35)$$

where v_i are Said-Ball control points. If v_0, v_5 and $v_i \geq -t_0, 1 \leq i \leq 4$, then t_0 is a unique solution of

$$t^2 + 2t\sqrt{(v_0+t)(v_5+t)} - v_0v_5 = 0. \quad (5.36)$$

5.3.2 Sufficient Condition for Positivity Preserving Quintic DP-Ball Curves

If set put $n = 5$ in Proposition 5.2, then we obtain the following corollary.

Corollary 5.5. *Consider the quintic DP-Ball curve,*

$$r(x) = \sum_{i=0}^5 D_i^5(x)d_i, \quad (5.37)$$

where d_i are DP-Ball control points. If $d_0, d_5 > 0$ and $d_i \geq -t_0, 1 \leq i \leq 4$, then t_0 is a unique solution of

$$\sqrt[4]{d_5+t} + \sqrt[4]{d_0+t} - \sqrt[4]{d_5+t}\sqrt[4]{d_0+t} = 0. \quad (5.38)$$

5.3.3 Sufficient Condition for Positivity Preserving Quintic Wang-Ball Curves

If we set $n = 5$ in Proposition 5.3, then we obtain the following corollary.

Corollary 5.6. *Consider the quintic Wang-Ball curve,*

$$r(x) = \sum_{i=0}^5 A_i^5(x)w_i, \quad (5.39)$$

where w_i are Wang-Ball control points. If $w_0, w_5 > 0$ and $w_i \geq -t_0, 1 \leq i \leq 4$, then t_0 is a unique solution of

$$t^2 - w_0 w_5 = 0. \quad (5.40)$$

5.4 Surface Interpolation Using Positivity Preserving Boundary Curves

By using similar approach of Monterde and Ugail (2006) , the first and second rows (columns) of the coefficients in (4.2) can be obtained by using the boundary control points of Ball (Said-Ball, DP-Ball and Wang-Ball) representation as in (2.23), (2.38), and (2.54) for cubic case as described in Section 4.1.1.2 for Said-Ball, Section 4.1.3.1 for DP-Ball and Section 4.1.4.2 for Wang-Ball; while for quintic case as described in Section 4.1.1.3 for Said-Ball, Section 4.1.3.2 for DP-Ball and Section 4.1.4.3 for Wang-Ball. However, to visualize our proposed method, we have chosen two datasets taken from well known test function as given in Section 4.1.5.

5.4.1 Graphical Examples

In this part, we obtained some graphical examples for positivity preserving by using two test function.

5.4.1.1 Bicubic Patches

Since Corollary 5.1 and Corollary 5.3 yield the same results when $n = 3$, then it is sufficient to apply just one of the corollaries for the cubic case. Figure 5.6, Figure 5.7 and Figure 5.8 show the edges of the cubic Said/Wang-Ball control points in the rectangular domain, the cubic Said/Wang-Ball boundary curves, and the interpolating bicubic Said/Wang-Ball surface, respectively for both functions $f(x,y)$ and $g(x,y)$. Corollary 5.1 was used to generate the results, however, the DP-Ball for the function $g(x,y)$ displayed in Figure 5.9 is generated using Corollary 5.2.

Table 5.1 displays a comparison of the interpolating surfaces between bicubic Bézier, bicubic Said/Wang-Ball and bicubic DP-Ball boundary curves for the test function $g(x,y)$, while Table 5.2 displays a comparison of the interpolating surfaces between bicubic Bézier and bicubic Said/Wang-Ball boundary curves for the test function $f(x,y)$.

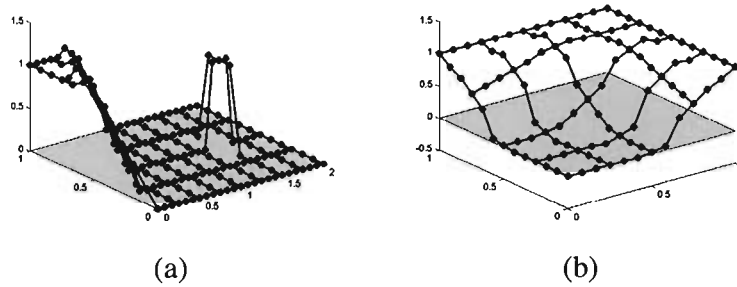


Figure 5.6. Edges Said/Wang-Ball control points for all rectangles (a) Test function $f(x,y)$ (b) Test function $g(x,y)$.

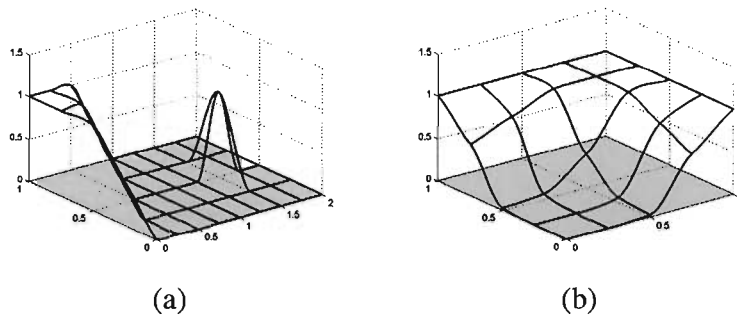


Figure 5.7. Boundary curves Said/Wang-Ball for all rectangles (a) Test function 1, $f(x,y)$ (b) Test function 2, $g(x,y)$.

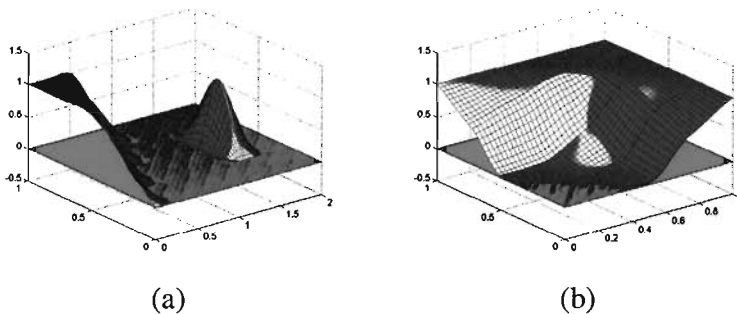


Figure 5.8. Interpolating Said/Wang-Ball surface boundary curves (a) Test function 1, $f(x,y)$ (b) Test function 2, $g(x,y)$.

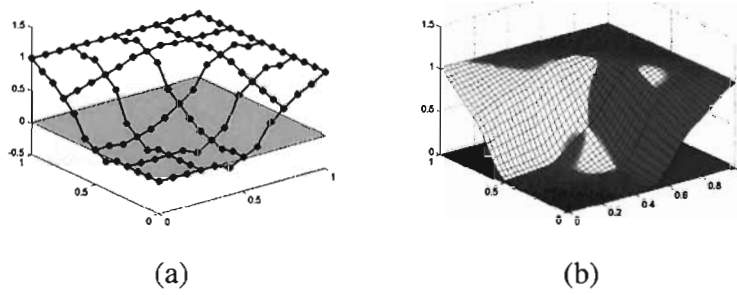


Figure 5.9. Test function $g(x,y)$ (a) Edges DP-Ball control points for all rectangles (b) Interpolating DP-Ball surface boundary curves.

Table 5.1

Comparison of the interpolating surfaces between bicubic Bézier, bicubic Said/Wang-Ball and bicubic DP-Ball boundary curves for the test function $g(x,y)$.

Surface	Number of evaluation points	Number of points below XY -plane and percentage	Minimum value of function
Bézier	1681	47 2.796 %	-0.00047154
Said/Wang-Ball	1681	13 0.77335 %	-0.0001312
DP-Ball	1712	74 4.32243%	-0.00111

As demonstrated in Table 4.1 and Table 5.1, the number of points below the XY -plane for all the surfaces decreased after the positivity preserving by using test function $g(x,y)$. Specifically, the number of points below XY -plane for the bicubic Bézier, bicubic Said/Wang-Ball, and bicubic DP-Ball surfaces had decreased from 291, 231, and 1097 points (see Table 4.1) to 47, 13, and 74 points (Table 5.1), respectively. As in Table 5.1, the bicubic Said/Wang-Ball surface produced the best result because it had the smallest number of points below the XY -plane, followed by the bicubic Bézier surface, and lastly the bicubic DP-Ball surface.

Table 5.2

Comparison of the interpolating surfaces between bicubic Bézier and bicubic Said/Wang-Ball boundary curves for the test function $f(x,y)$.

Surface	Number of evaluation points	Number of points below XY -plane and percentage	Minimum value of function
Bézier	3321	58 1.7465 %	-0.005651
Said/Wang-Ball	3321	47 1.4152 %	-0.0044644

As demonstrated in Table 4.3 and Table 5.2 , the number of points below the XY -plane for all the surfaces decreased after the positivity preserving by using test function $f(x,y)$. Specifically, the number of points below XY -plane for the bicubic Bézier and bicubic Said/Wang-Ball surfaces had decreased from 1134 and 1118 points (see Table 4.3) to 58 and 47 points, (Table 5.2) respectively. As in Table 5.2, the bicubic Said/Wang-Ball surface produced better result compared to bicubic Bézier surface because the former had smaller number of points below the XY -plane, compared to the latter.

5.4.1.2 Biquintic Pathes

Figure 5.10, Figure 5.11 and Figure 5.12 show the edges of the biquintic Said-Ball control points in the rectangular domain, the biquintic Said-Ball boundary curves, and the interpolating biquintic Said-Ball surface, respectively for both functions $f(x,y)$ and $g(x,y)$. Corollary 5.4 was used to generate the results, however, the biquintic DP-Ball for the function $g(x,y)$ displayed in Figure 5.13 is generated using Corollary 5.5. Finally, in Figure 5.14, Figure 5.15 and Figure 5.16, Corollary 5.6 was used to show the edges of the biquintic Wang-Ball control points in the rectangular domain, the biquintic Wang-Ball boundary curves, and the interpolating biquintic Wang-Ball surface, respectively for both functions $f(x,y)$ and $g(x,y)$.

Table 5.3 displays a comparison of the interpolating surfaces between biquintic Bézier, biquintic Said-Ball, biquintic Wang-Ball and biquintic DP-Ball boundary curves for the test function $g(x,y)$, while Table 5.4 displays a comparison of the interpolating surfaces between biquintic Bézier, biquintic Said-Ball and biquintic Wang-Ball boundary curves for the test function $f(x,y)$.

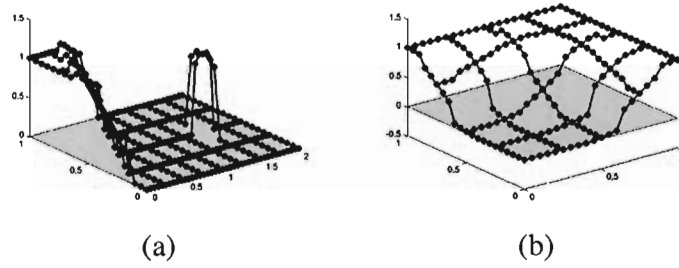


Figure 5.10. Biquintic edges Said-Ball control points for all rectangles (a) Test function $f(x,y)$ (b) Test function $g(x,y)$.

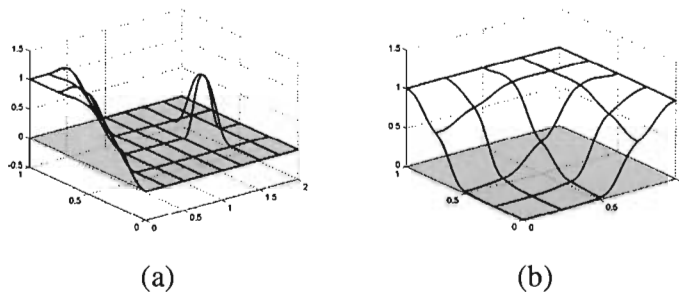


Figure 5.11. Biquintic boundary curves Said-Ball for all rectangles (a) Test function 1, $f(x,y)$ (b) Test function 2, $g(x,y)$.

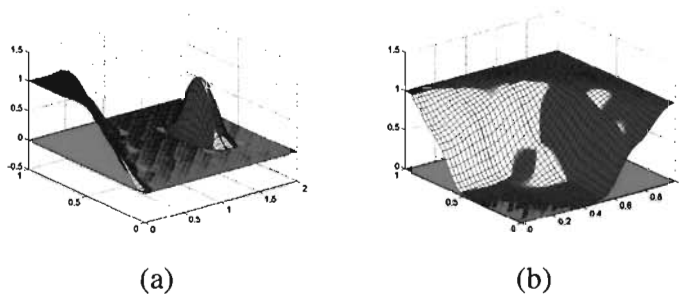


Figure 5.12. Interpolating biquintic Said-Ball surface boundary curves (a) Test function 1, $f(x,y)$ (b) Test function 2, $g(x,y)$.

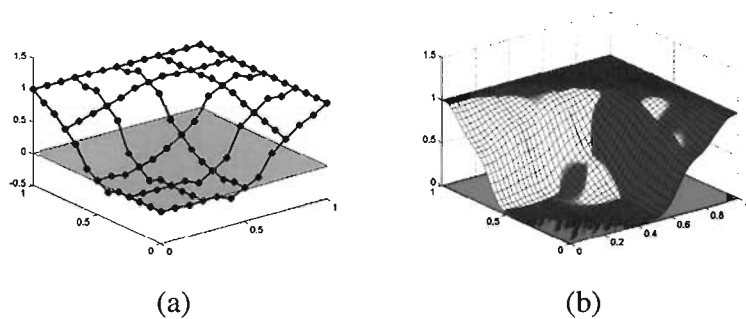


Figure 5.13. Test function $g(x,y)$ (a) Biquintic edges DP-Ball control points for all rectangles (b) Interpolating biquintic DP-Ball surface boundary curves.

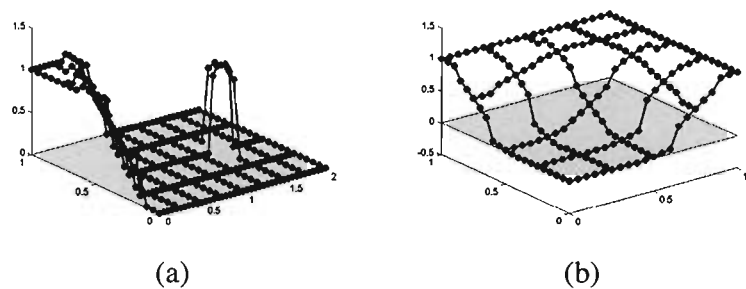


Figure 5.14. Biquintic edges Wang-Ball control points for all rectangles (a) Test function $f(x,y)$ (b) Test function $g(x,y)$.

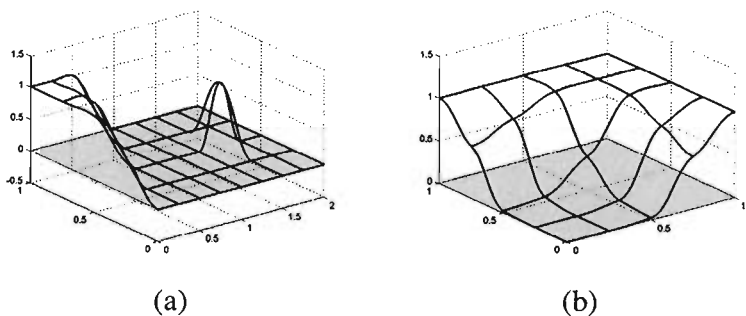


Figure 5.15. Biquintic boundary curves Wang-Ball for all rectangles (a) Test function 1, $f(x,y)$ (b) Test function 2, $g(x,y)$.

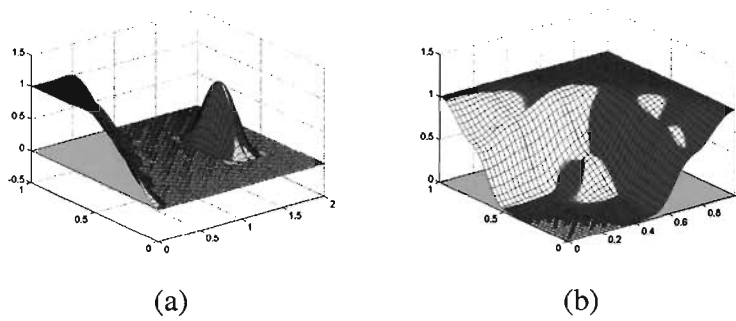


Figure 5.16. Interpolating biquintic Wang-Ball surface boundary curves (a) Test function 1, $f(x,y)$ (b) Test function 2, $g(x,y)$.

Table 5.3

Comparison of the interpolating surfaces between biquintic Bézier, biquintic Said-Ball, biquintic Wang-Ball and biquintic DP-Ball boundary curves for the test function $g(x,y)$.

Surface	Number of evaluation points	Number of points below XY -plane and percentage	Minimum value of function
Bézier	1681	39 2.32 %	-0.0051633
Said-Ball	1681	0 0.0 %	2.3109e-05
Wang-Ball	1681	0 0.0 %	3e-05
DP-Ball	1681	27 1.6062%	-0.0027001

As demonstrated in Table 4.2 and Table 5.3, the number of points below the XY -plane for all the surfaces decreased after the positivity preserving by using test function $g(x,y)$. Specifically, the number of points below XY -plane for the biquintic Bézier, biquintic Said-Ball, biquintic Wang-Ball, and biquintic DP-Ball surfaces had decreased from 291, 246, 151 and 312 points (see Table 4.2) to 39, 0, 0 and 27 points (Table 5.3), respectively. As in Table 5.3, both biquintic Said-Ball and biquintic Wang-Ball surfaces produced the best result, followed by the biquintic DP-Ball surface, and lastly the biquintic Bézier surface.

Table 5.4

Comparison of the interpolating surfaces between biquintic Bézier, biquintic Said-Ball, biquintic Wang-Ball and biquintic DP-Ball boundary curves for the test function $f(x,y)$.

Surface	Number of evaluation points	Number of points below XY-plane and percentage	Minimum value of function
Bézier	3335	124 3.7181 %	-0.022241
Said-Ball	3321	104 3.1316 %	-0.02221
Wang-Ball	3323	77 2.3172 %	-0.014228

As demonstrated in Table 4.4 and Table 5.4 , the number of points below the XY-plane for all the surfaces decreased after the positivity preserving by using test function $f(x,y)$. Specifically, the number of points below XY-plane for the biquintic Bézier, biquintic Said-Ball and biquintic Wang-Ball surfaces had decreased from 1134, 1147 and 1136 points (see Table 4.4) to 124, 104, and 77 points (Table 5.4), respectively. As in Table 5.4, the biquintic Wang-Ball surface produced the best result, followed by the biquintic Said-Ball surface, and lastly the biquintic Bézier surface.

5.5 Image Enlargement Using Cubic Said-Ball, Wang-Ball and DP-Ball Boundary Curves with PDEs

5.5.1 Introduction

In computer graphics design, the process of resizing a digital image is known as image scaling. which involves a trade-off between smoothness, sharpness and efficiency (Kim, Seong & Lee, 2003). With bitmap graphics, when the size of an image is reduced or enlarged, the pixels that form the image become increasingly visible, making the image appear to be smooth if pixels are averaged, or jagged if not.

With vector graphic, the trade-off may be in processing power for re-rendering the image, which may be noticeable as slow re-rendering with still graphics, or slower frame rate and frame skipping in computer animation.

There are a number of techniques one might use to handle the problems of enlarging and reducing an input image especially by using interpolation methods such as nearest neighbor interpolation, bilinear interpolation, bicubic and B-spline interpolation (Han, 2013).

For example, to enlarge an image by a factor 2, the simplest method is to replicate each pixel 4 times and this will lead to more pronounced jagged edges than appeared in the original image.

The similar case applies for reducing an image by an integer divisor of the width by simply keeping every n^{th} pixel, and aliasing of high frequency components in the original will occur.

The more general case of changing the size of an image by an arbitrary amount requires interpolation of the colour informations between pixels.

Resizing an image through upsampling or downsampling is generally common for making smaller imagery fit a bigger screen in fullscreen mode or reducing a higher resolution image to a smaller resolution. For example, in zooming a bitmap image, it is difficult to discover any more information in the image than already exists, and this will effect its quality. Due to some limitation of computer facilities for a faster runtimes, we will focus on image enlargement with our proposed method based on the scaling factor of 2.

5.5.2 Image Scaling Concept

Let the input of an image is given by $m \times n$ pixels; (x,y) and (\acute{x},\acute{y}) are the arbitrary input and output pixels, respectively. If the input pixels are resized by a factor of s_x and s_y , respectively at point $(1,1)$, then the new output of $2m$ by $2n$ pixels will be obtained by the following transformation

$$\begin{bmatrix} \acute{x} \\ \acute{y} \end{bmatrix} = \begin{bmatrix} \frac{ms_x-1}{m-1} & 0 \\ 0 & \frac{ns_y-1}{n-1} \end{bmatrix} \begin{bmatrix} x \\ y \end{bmatrix} + \begin{bmatrix} \frac{m(1-s_x)}{m-1} \\ \frac{n(1-s_y)}{n-1} \end{bmatrix}. \quad (5.41)$$

As an example , we use $m = n = 2$ and scaling factor $s_x = s_y = 2$ as shown in Figure 5.17, where the scaling up 2×2 pixels input image by a factor 2 resulting an output of 4×4 pixels image. Note that, the input pixels with corresponding preserved intensity of output pixels are labeled by circles and the remaining missing information in output pixels are labeled by a square.

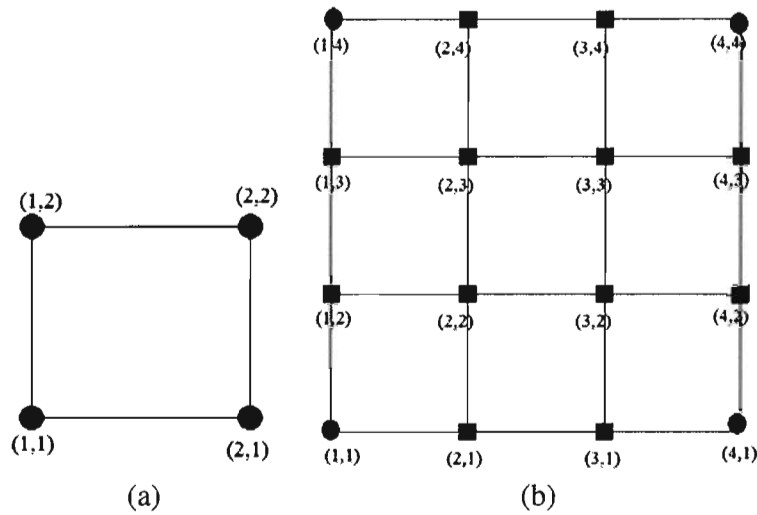


Figure 5.17. (a) 2 by 2 Input pixels (b) 4 by 4 output pixels of by scaling factor 2 of input pixel.

Pixels $(1,1)$, $(4,1)$, $(1,4)$ and $(4,4)$ in the output pixels will preserve the information of the input pixels while the remaining pixels intensity are to be filled.

Transformation of pixels from the input window to the output window can be done using (5.41). In order to find the missing pixels information of the output, these points should be transform to the pixels in the original input pixels by using the inverse transform of (5.41). Thus the points (2,1), (3,1), (1,2), (2,2), (3,2), (4,2), (1,3), (2,3), (3,3), (4,3), (2, 4) and (3,4) of the output window can be represented as $(4/3, 1)$, $(5/3, 1)$, $(1,4/3)$, $(4/3,4/3)$, $(5/3, 4/3)$, $(2,4/3)$, $(1, 5/3)$, $(4/3,5/3)$, $(5/3,5/3)$, $(2, 5/3)$ and $(5/3,2)$ in the input window, respectively, and these points should be interpolated by using a suitable interpolation techniques to obtain the respective intensities of output pixels.

5.5.3 Image Interpolation using Rectangular Patches

Given an $m \times n$ pixels of grayscale input image represented by a $(m - 1) \times (n - 1)$ rectangular patches and being scaled up by a factor of α and β using (5.41), resulting an output image of αm by βn pixels of higher resolution represented by $(\alpha m - 1) \times (\beta n - 1)$ rectangular patches. Let $(x_i, y_j), i = 1, 2, \dots, m, j = 1, 2, \dots, n$ represent the input pixels and z_{ij} (0-255) be its corresponding gray-scale intensity. Our aim is to find the function $z = F(x, y)$ which interpolates the given input pixels (vertices of rectangular patches), that is $F(x_i, y_i) = z_{ij}$.

For the purpose of this application , we consider the use of the polynomial solution of the fourth order PDEs, subject to a given four lines boundary conditions from Said-Ball, DP-Ball and Wang-Ball boundary curves of degree 3 as discussed in Section 4.1.1.2, Section 4.1.3.1 and Section 4.1.4.2, respectively.

We used our rectangulation algorithm to rectangulate the input pixels (x_i, y_i) . In order to construct an interpolation function on each rectangle, beside the intensity values, we also need to estimate the partial derivative at a given input grid by using the method discuss in Section 2.7.

5.5.4 Experimental Result

In this simulation result, we use nine test grayscale images such as Lena (512×512), Rice (640×640), Cameraman (256×256), Nuvola (448×448), Pout (480×480), Tyre (460×460), Monkey Face (512×512), Pepper (600×600) and Thumb Print (250×250) as shown in Figure 5.18. To evaluate the performance of our proposed method, a test image was zoom out to half of its original size by using the simple image interpolation in Matlab (bicubic convolution method), and this image will be scaled up by factor of two to get an original size. We calculate the Peak Signal-to-Noise Ratio (PSNR) for the scaled image based on the original image. The value of PSNR will reflect the quality of image, i.e the larger PSNR means that the higher quality of an image (Han, 2013). We also compare our method with an existing nearest neighbor method, existing bilinear method and an existing bicubic method of Matlab Image Processing toolbox.

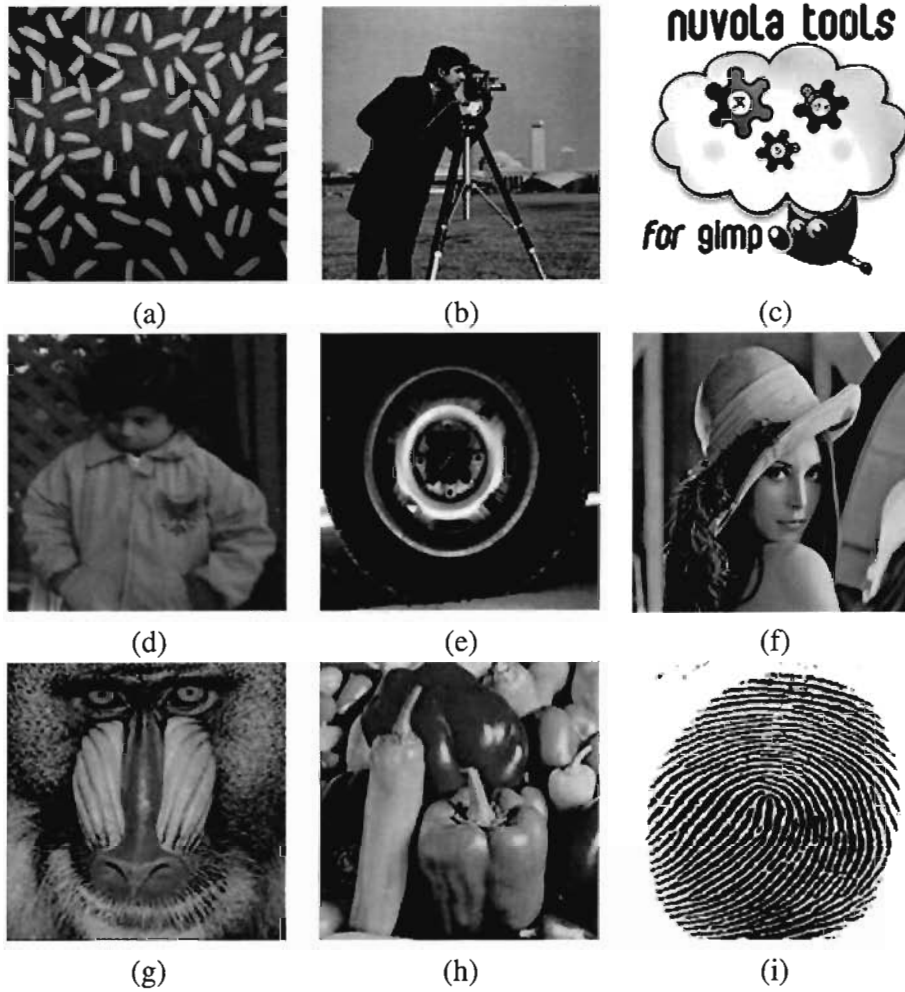
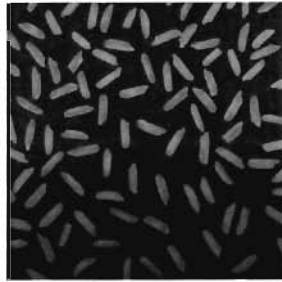
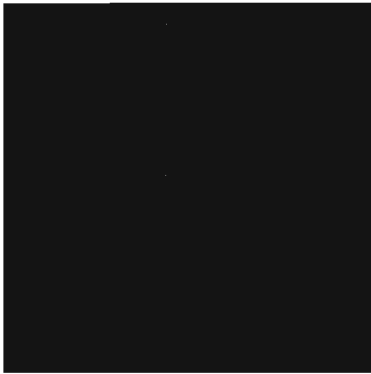


Figure 5.18. (a) Rice (b) Cameraman (c) Nuvola (d) Pout (e) Tyre (f) Lena (g) Monkey Face (h) Pepper (i) Thumb.

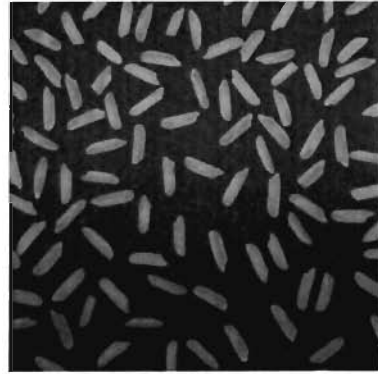
Now, we apply our proposed method to each figure and we compared the PSNR with the image generated by Bézier, Said/Wang-Ball and DP-Ball as follows. Results are shown in Figure 5.19 - Figure 5.27.



(a)



(b)



(c)

Figure 5.19. Result using our proposed method for Rice test image (a) Input image (b) Image without interpolation (c) Image with proposed method.

Table 5.5

Comparison between Said/Wang-Ball and DP-Ball by using PSNR for Rice test image.

Method	PSNR
Proposed	Said/Wang-Ball 39.39
	DP-Ball 39.55
Nearest neighbor	36.80
Bilinear	40.52
Bicubic	43.60

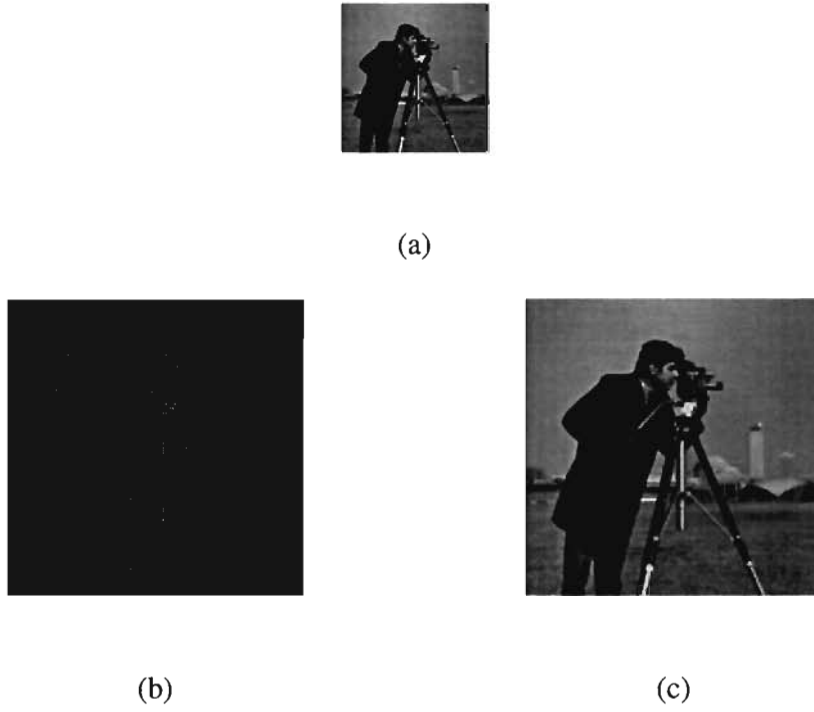


Figure 5.20. Result using our proposed method for Cameraman test image (a) Input image (b) Image without interpolation (c) Image with proposed method.

Table 5.6

Comparison between Said/Wang-Ball and DP-Ball by using PSNR for Cameraman test image.

Method	PSNR	
Proposed	Said/Wang-Ball	40.47
	DP-Ball	40.38
Nearest neighbor	40.38	
Bilinear	39.91	
Bicubic	40.32	



(a)



(b)



(c)

Figure 5.21. Result using our proposed method for Nuvola test image (a) Input image (b) Image without interpolation (c) Image with proposed method.

Table 5.7

Comparison between Said/Wang-Ball and DP-Ball by using PSNR for Nuvola test image.

Method	PSNR
Proposed	Said/Wang-Ball 37.17
	DP-Ball 37.22
Nearest neighbor	36.57
Bilinear	38.11
Bicubic	38.11

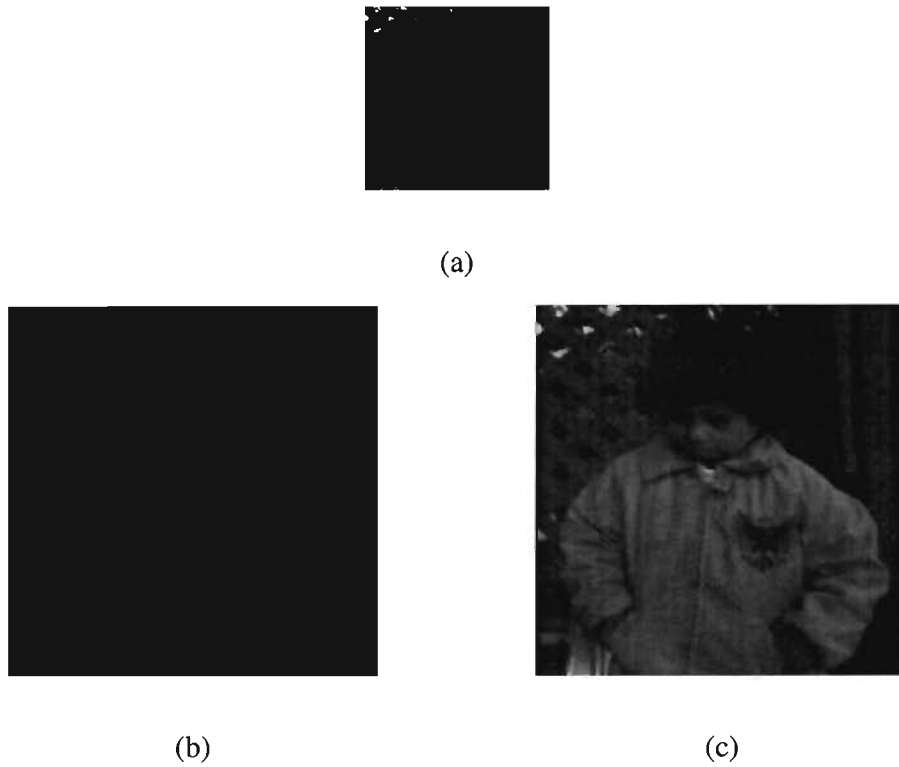


Figure 5.22. Result using our proposed method for Pout test image (a) Input image (b) Image without interpolation (c) Image with proposed method.

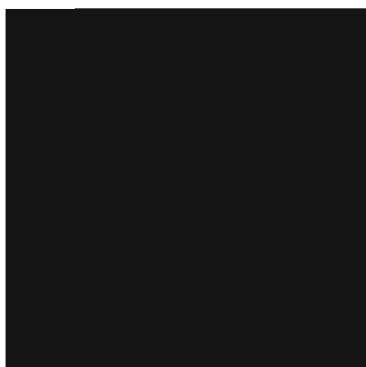
Table 5.8

Comparison between Said/Wang-Ball and DP-Ball by using PSNR for Pout test image.

Method	PSNR
Proposed	Said/Wang-Ball 49.65
	DP-Ball 49.63
Nearest neighbor	46.99
Bilinear	50.48
Bicubic	52.73



(a)



(b)



(c)

Figure 5.23. Result using our proposed method for Tyre test image (a) Input image (b) Image without interpolation (c) Image with proposed method.

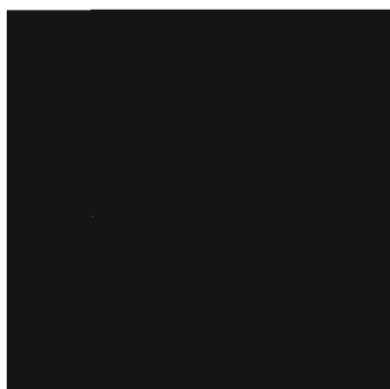
Table 5.9

Comparison between Said/Wang-Ball and DP-Ball by using PSNR for Tyre test image.

Method	PSNR
Proposed	Said/Wang-Ball 40.84
	DP-Ball 41.00
Nearest neighbor	39.33
Bilinear	43.30
Bicubic	46.59



(a)



(b)



(c)

Figure 5.24. Result using our proposed method for Lena test image (a) Input image (b) Image without interpolation (c) Image with proposed method.

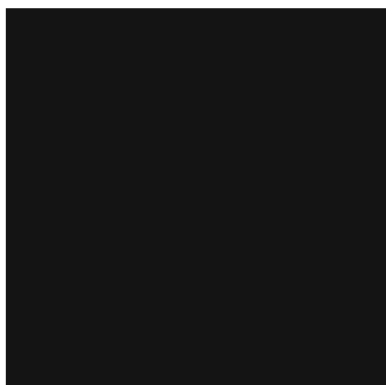
Table 5.10

Comparison between Said/Wang-Ball and DP-Ball by using PSNR for Lena test image.

Method	PSNR
Proposed	Said/Wang-Ball 37.23
	DP-Ball 37.24
Nearest neighbor	36.65
Bilinear	37.08
Bicubic	38.14



(a)



(b)



(c)

Figure 5.25. Result using our proposed method for Monkey test image (a) Input image (b) Image without interpolation (c) Image with proposed method.

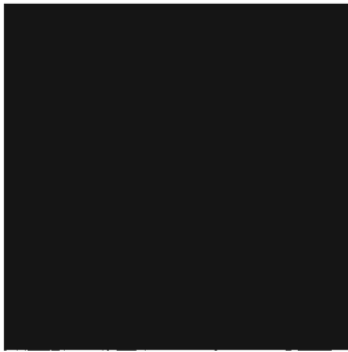
Table 5.11

Comparison between Said/Wang-Ball and DP-Ball by using PSNR for Monkey test image.

Method	PSNR
Proposed	Said/Wang-Ball 37.33
	DP-Ball 37.12
Nearest neighbor	36.89
Bilinear	36.81
Bicubic	40.18



(a)



(b)



(c)

Figure 5.26. Result using our proposed method for Pepper test image (a) Input image (b) Image without interpolation (c) Image with proposed method.

Table 5.12

Comparison between Said/Wang-Ball and DP-Ball by using PSNR for Pepper test image.

Method	PSNR
Proposed	Said/Wang-Ball 39.10
	DP-Ball 39.17
Nearest neighbor	38.25
Bilinear	42.36
Bicubic	45.46

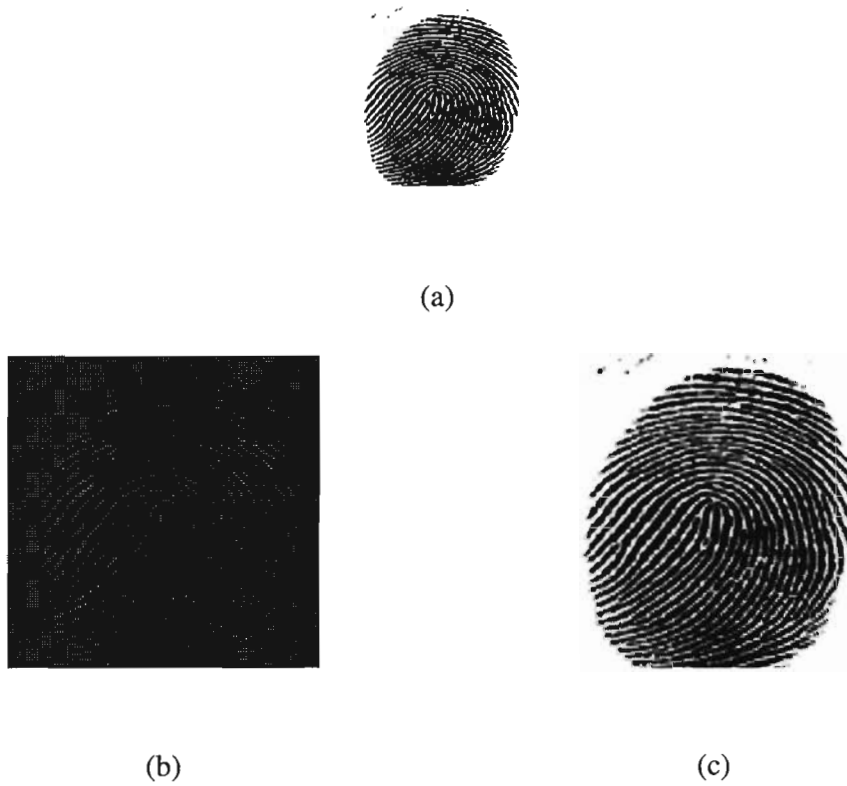


Figure 5.27. Result using our proposed method for Thumb test image (a) Input image (b) Image without interpolation (c) Image with proposed method.

Table 5.13

Comparison between Said/Wang-Ball and DP-Ball by using PSNR for Thumb test image.

Method	PSNR
Proposed	Said/Wang-Ball 36.17
	DP-Ball 36.16
Nearest neighbor	36.38
Bilinear	35.29
Bicubic	36.08

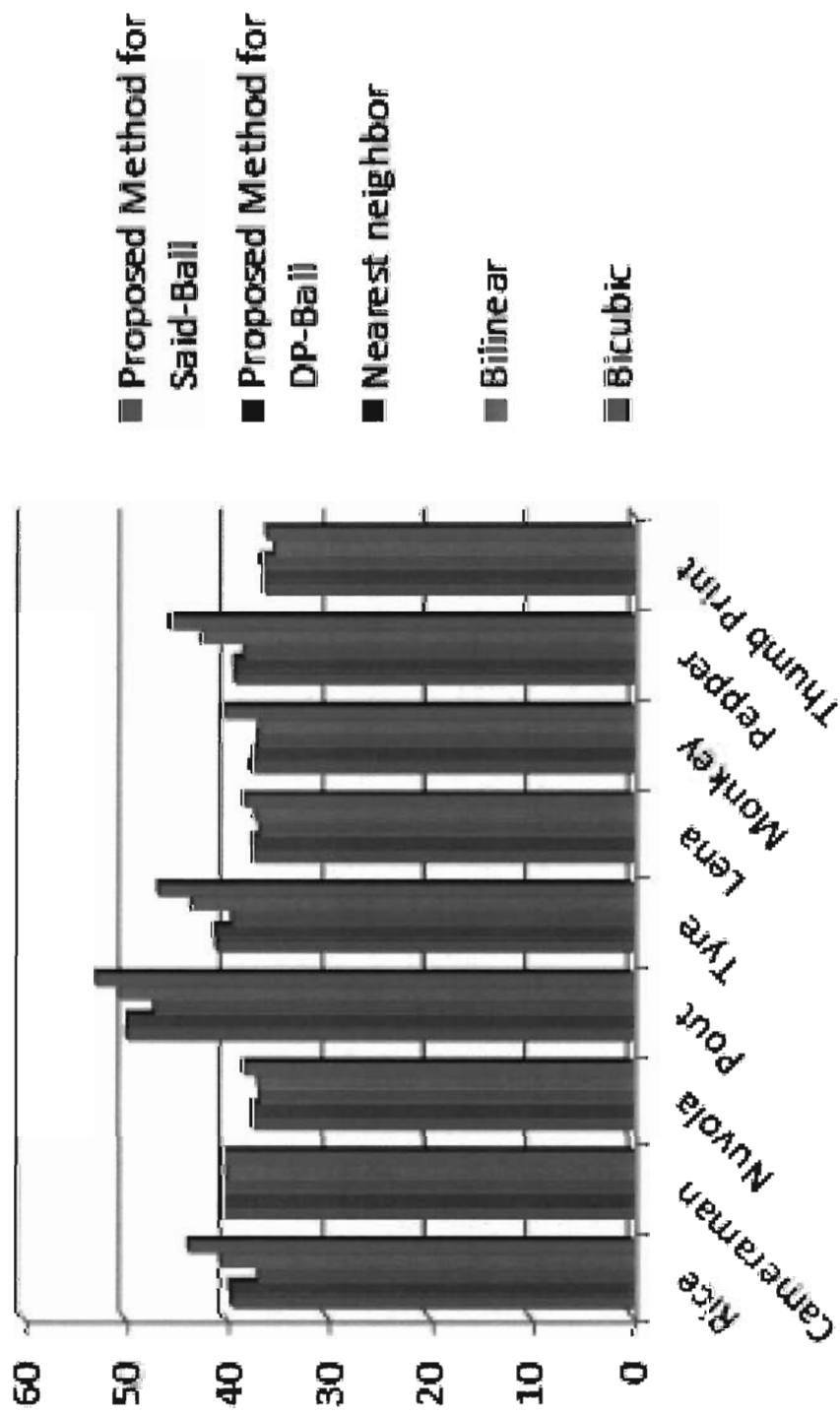


Figure 5.28. Comparison between all image test by PSNR by using the proposed method, nearest neighbor, bilinear and bicubic methods.

The following observations can be obtained from Figure 5.28. For small size images such as Cameraman (256×256) and Thumb (250×250), our proposed method outperformed the bicubic and bilinear methods, but almost comparable to the nearest neighbor method. Furthermore, for large size images such as Rice (640×640), Pout (480×480), Tyre (460×460), Lena (512×512), Monkey (512×512) and Pepper (600×600), the bicubic method gives the best quality of these images because the value of PSNR given by bicubic method is the highest for each example; followed by the bilinear method, then our proposed method and finally the nearest neighbor method. There is an exception for Nuvola (448×448) where the best result came from the bicubic method, followed by our proposed method, then bilinear method, and lastly the nearest neighbor. This is simply because of the estimate of the gradient out pixel. Therefore, there is a need to consider the development of another suitable algorithm for the estimation of the gradient out pixel in the future.

5.5.5 Summary

In this chapter, we have proposed the sufficient conditions for positivity preserving odd degree- n generalized Ball (Said-Ball, DP-Ball and Wang-Ball) boundary curves defined on rectangular grid using a polynomial solution of fourth order linear PDEs in order to improve the positivity preserving of the interpolating surface. We described the sufficient condition on boundary curves for each edges of degree $m \times n$ rectangular Ball patches, where the lower bound of edge generalized Ball ordinates are adjusted independently. Implementations on the well-known test functions using cubic and quintic Ball boundary curves showed that our proposed method are well performed in terms of preserving the positivity of the boundary curves and improved the positivity preserving of overall interpolating surfaces. However, we have proposed to enlarge an image by a factor 2 using the polynomial solution of fourth order linear PDEs.

CHAPTER SIX

CONCLUSION AND FUTURE RESEARCH

6.1 Conclusion

In this thesis, a method for generating Ball surfaces with respect to the boundary information based on a general fourth order PDE is presented. We also presented the generalized Ball (Said-Ball, DP-Ball and Wang-Ball) polynomial solutions for the Laplace and the standard biharmonic equation. The generalized Ball solutions associated with the most general quadratic functional were studied and we took interest in using the monomial matrix form to present a general solution method for generating generalized Ball surfaces based on the Euler-Lagrange equation which arises from the most general quadratic functional.

One of the main challenges associated with computer aided geometric design is to generate a surface with prescribed boundaries. A variety of surface generation methods can be found in existing literature, but these methods depends on the chosen conditions that such a surface must satisfy. One of such conditions that the surface must satisfy, is related to the minimization of the area of the resulting surface. This minimization is in relation with the highly nonlinear area functional and also the Laplace operator (an intrinsic operator which is quite challenging to work with) of the surface defined by its Euler–Lagrange equation. For this reasons, some of the techniques related to the minimization of the area adopt the use of the harmonic functional instead. This is because the Laplace operator is constrained to the parameterisation of the surface and it also presents a less complicated approach for computing good approximations unlike the Laplace–Beltrami operator.

Due to the presence of high nonlinearity of the area functional, it is quite difficult to apply the area functional. With respect to an argument in the theory of minimal

surfaces, the Dirichlet functional is substituted in place of the area functional so that the extremals can be computed easily as the solutions of linear systems.

We have used the monomial matrix approach to present a generalized way of getting approximations to the minimal surfaces, having prescribed boundary curves by the use of a mask. Computing the Dirichlet extremals is another approach for finding these approximations but this comes at a price which is the computational cost. Though the two methods are from the resolution of a system of linear equations of the same size, but when we use the masks, the matrix of the coefficients becomes a sparse matrix, while in the case of the Dirichlet, the matrix of the coefficients is a non-zero matrix.

For generalized Ball surfaces, we have two methods that involve the Laplace operator, that are the minimization of the associated functional which is known as the harmonic functional, and the application of masks for the discretization of the Laplace operator. Another problem associated with the Laplace operator is how to determine the harmonic generalized Ball surfaces. We can show that the harmonic generalized Ball surface is determined solely by the first and last rows (columns) of control points, unlike the biharmonic case, where the generation of a surface is fully determined by all of its boundary control points.

In order to make comparison among the results of the different methods with respect to computational time and surface area for the surface with same boundaries (two opposite boundaries for harmonic and all boundaries for biharmonic), we adopted a natural and quite simple model problem throughout this thesis. We also used a collection of other problems which involves a variety of different boundary configurations to make comparison of the different methods with the existing method in literature for Bézier.

For the Dirichlet approach, we hereby propose a new mask though we have compared between the results from Bézier masks and that of the Dirichlet extremals for different configurations of the boundary conditions. We cannot conclusively say there is a better option, but from the examples conducted and from theoretical arguments, it was noted that when the first fundamental form of the generalized Ball surface at the corners (at these points, this form depends only on the boundary conditions) is close to being isothermal, then we have a better approximation with the Dirichlet extremal in comparison to the results obtained by using the masks. However, if the first fundamental form of the generalized Ball surface at the corners is far from being isothermal, then we have a better approximation when using the masks in comparison to the results obtained by the Dirichlet extremal.

The extremals of the Dirichlet functional are another approach for obtaining (without integrating) an approximation of the surface minimizing area. So, if we want to obtain a better approximation, we can use the extremals of the Dirichlet functionals as the starting point for recursive algorithms that optimize the area functional. As shown in this research work, we can note that the biharmonic operator is not an intrinsic operator. However, the solutions computed can be seen as approximations to the true solutions of the bilaplace–Beltrami operator because of the fact that the Laplace–Beltrami operator reduces to the Laplace operator when the parameterization is isothermal, and the bilaplace–Beltrami operator also reduces to the biharmonic operator.

One vital observation that is worth noting from this thesis is that some of the existing methods in literature for boundary based surface design, such as Bloor–Wilson PDE method, Coons patches, Ugail and Montede method are the peculiar cases of the generalized framework presented in this thesis. We also applied a polynomial solution of fourth order linear PDEs in image enlargement using cubic Ball boundary curves in this research.

This thesis has also proposed the sufficient conditions for positivity preserving odd degree- n generalized Ball boundary curves defined on rectangular grid using a polynomial solution of fourth order linear PDEs in order to improve the positivity preserving of the interpolating surface.

Two new masks are also proposed in relation to harmonic and biharmonic for finding the inner control points, and also an improvement of the Dirichlet method (without going into an iterative method) with better accuracy than the previous existing method for Bézier, but which will now come at a quite high computational cost.

6.2 Future Research

There are areas for future research associated to this work. For instance, the detailed study of how the various coefficients associated with a chosen fourth order PDE affect the shape of the generated surface can be investigated. Also, from our previous findings, we showed that the associated coefficients can be applied to remove the restriction on the (u, v) parameter domain being a square $[0, 1]^2$, and for that reason, surfaces with complicated boundary formulations can be generated easily. Whenever the parametric domain is restricted to the square $[0, 1]^2$, for the PDE used which has a non-intrinsic functional associated with it, we are usually faced with this particular case. For this reason, it would be a great area of interest to investigate the shapes of the surfaces generated by various fourth order PDEs. The aim of this is to develop a surface classification system that would aid in the development of intuitive tools for generating generalized Ball surfaces with respect to boundary information. The generalized algorithm of Said-Ball, DP-Ball and Wang-Ball surfaces could be extended to NB1, NB2, Dejdumrong surfaces and three dimensional Minkowski space in future research, which generate any surfaces based on eighth order PDEs using monomial matrix form.

REFERENCES

- Ahmad, D. & Masud, B. (2014). Variational minimization on string-rearrangement surfaces, illustrated by an analysis of the bilinear interpolation. *Applied Mathematics and Computation*, 233, 72–84.
- Aphirukmatakun, C. & Dejdumrong, N. (2007). An approach to polynomial curve comparison in geometric object database. *International Journal of Computer Science*, 2(4), 240–246.
- Aphirukmatakun, C. & Dejdumrong, N. (2011). Multiple degree elevation and constrained multiple degree reduction for dp curves and surfaces. *Computers & Mathematics with Applications*, 61(8), 2296–2299.
- Arnal, A. & Monterde, J. (2014). Generating harmonic surfaces for interactive design. *Computers & Mathematics with Applications*, 67(10), 1914–1924.
- Arnal, A., Monterde, J. & Ugail, H. (2011). Explicit polynomial solutions of fourth order linear elliptic partial differential equations for boundary based smooth surface generation. *Computer Aided Geometric Design*, 28(6), 382–394.
- Bakhshesh, D. & Davoodi, M. (2014). Approximating of conic sections by dp curves with endpoint interpolation.
- Ball, A. A. (1974). Consurf. part one: introduction of the conic lofting tile. *Computer-Aided Design*, 6(4), 243–249.
- Ball, A. A. (1975). Consurf. part two: description of the algorithms. *Computer-Aided Design*, 7(4), 237–242.
- Ball, A. A. (1977). Consurf. part three: How the program is used. *Computer-Aided Design*, 9(1), 9–12.
- Bloor, M. I. & Wilson, M. J. (1990). Representing pde surfaces in terms of b-splines. *Computer-Aided Design*, 22(6), 324–331.
- Chang, G. (1982). Matrix formulations of bézier technique. *Computer-aided design*, 14(6), 345–350.
- Chen, X. D., Xua, G. & Wanga, Y. (2009). Approximation methods for the plateau-bézier problem. In *Cad/graphics* (pp. 588–591).
- Cosín, C. & Monterde, J. (2002). Bézier surfaces of minimal area. In *Computational science—iccs 2002* (pp. 72–81). Springer.
- Dan, Y. & Xinmeng, C. (2007). Another type of generalized ball curves and surfaces. *Acta Mathematica Scientia*, 27(4), 897–907.
- Dejdumrong, N. (2006). Rational dp-ball curves. In *Computer graphics, imaging and visualisation, 2006 international conference on* (pp. 478–483).
- Dejdumrong, N. (2011). Monomial form is universal. *Journal of Computer and Advanced Technologies*.
- Dejdumrong, N. (2014). *Monomial form approach to the construction and the conversion for curves in cagd*. Taylor & Francis Group, London.
- Delgado, J. & Peña, J. M. (2003a). A linear complexity algorithm for the bernstein basis. In *Geometric modeling and graphics, international conference on* (pp. 162–162).
- Delgado, J. & Peña, J. M. (2003b). A shape preserving representation with an evaluation algorithm of linear complexity. *Computer Aided Geometric Design*, 20(1), 1–10.
- Do Carmo, M. & Perdigo. (1976). *Differential geometry of curves and surfaces* (Vol. 2). Prentice-Hall Englewood Cliffs.

- Du, H. & Qin, H. (2004). A shape design system using volumetric implicit pdes. *Computer-Aided Design*, 36(11), 1101–1116.
- Farin, G. (2002). *Curves and surfaces for computer aided geometric design* [Book]. San Diego: Academic San Diego.
- Farin, G. & Hansford, D. (1999). Discrete coons patches. *Computer Aided Geometric Design*, 16(7), 691–700.
- Faux, I. D. & Pratt, M. J. (1979). *Computational geometry for design and manufacture*. Ellis Horwood Ltd.
- Goodman, T. N. & Said, H. (1991). Properties of generalized ball curves and surfaces. *Computer-Aided Design*, 23(8), 554–560.
- Han, D. (2013). Comparison of commonly used image interpolation methods. In *Proceedings of the 2nd international conference on computer science and electronics engineering*.
- Hu, S., Wang, G. & Sun, J. (1998). A type of triangular ball surface and its properties. *Journal of Computer Science and Technology*, 13(1), 63–72.
- Hu, S., Wang, G. Z. & Jin, T. G. (1996). Properties of two types of generalized ball curves. *Computer-Aided Design*, 28(2), 125–133.
- Itsariyawanich, K. & Dejdumrong, N. (2008). Degree reduction and multiple degree reduction for the dp curves. In *Electrical engineering/electronics, computer, telecommunications and information technology, 2008. ecti-con 2008. 5th international conference on* (Vol. 1, pp. 45–48).
- Jiang, S. R. & Wang, G. J. (2005). Conversion and evaluation for two types of parametric surfaces constructed by ntp bases. *Computers & Mathematics with Applications*, 49(2), 321–329.
- Kahyaolu, K. & Emin. (2014). An approach for minimal surface family passing a curve. *arXiv preprint arXiv 1408.3723*.
- Kim, C. H., Seong, S. M. & Lee, L. S. (2003). Winscale: an image-scaling algorithm using an area pixel model. *Circuits and Systems for Video Technology, IEEE Transactions on*, 13(6), 549–553.
- Li, C. Y., Wang, R. H. & Zhu, C. G. (2013). Designing approximation minimal parametric surfaces with geodesics. *Applied Mathematical Modelling*, 37(9), 6415–6424.
- Monterde, J. (2004). Bézier surfaces of minimal area: The dirichlet approach. *Computer Aided Geometric Design*, 21(2), 117–136.
- Monterde, J. & Ugail, H. (2004). On harmonic and biharmonic bézier surfaces. *Computer Aided Geometric Design*, 21(7), 697–715.
- Monterde, J. & Ugail, H. (2006). A general 4th-order pde method to generate bézier surfaces from the boundary. *Computer Aided Geometric Design*, 23(2), 208–225.
- Phien, H. N. & Dejdumrong, N. (2000). Efficient algorithms for bézier curves. *Computer Aided Geometric Design*, 17(3), 247–250.
- Saaban, A., Man, N. & Karim, S. (2013). Surface interpolation using partial differential equation with positivity preserving cubic bézier curves boundary condition. *Far East Journal of Mathematical Sciences (FJMS)*, 75(2), 257–272.
- Said, H. (1989). A generalized ball curve and its recursive algorithm. *ACM Transactions on Graphics (TOG)*, 8(4), 360–371.
- Sheng, Y., Sourin, A., Castro, G. G. & Ugail, H. (2010). A pde method for patchwise approximation of large polygon meshes. *The Visual Computer*, 26(6-8), 975–

- Tråsdahl, Ø. & Rønquist, E. M. (2011). High order numerical approximation of minimal surfaces. *Journal of Computational Physics*, 230(12), 4795–4810.
- Ugail, H. (2011). *Partial differential equations for geometric design*. Springer.
- Ugail, H., Márquez, M. & Yılmaz, A. (2011). On bézier surfaces in three-dimensional minkowski space. *Computers & Mathematics with Applications*, 62(8), 2899–2912.
- Wang & Cheng. (2001). New algorithms for evaluating parametric surface. *Progress in Natural Science*, 11(2), 142–148.
- Wang & Guo. (2012). Extending and correcting some research results on minimal and harmonic surfaces. *Computer Aided Geometric Design*, 29(1), 41–50.
- Wang, G. (1987). Ball curve of high degree and its geometric properties. *Applied Mathematics: A journal of Chinese universities*, 2(1), 126–140.
- Xua, G. & Wang, G. Z. (2010). Quintic parametric polynomial minimal surfaces and their properties. *Differential Geometry and its Applications*, 28(6), 697–704.
- Yang, H. & Wang, G. (2015). Optimized design of bézier surface through bézier geodesic quadrilateral. *Journal of Computational and Applied Mathematics*, 273, 264–273.
- Zhang, J. & You, L. (2004). Fast surface modelling using a 6th order pde. In *Computer graphics forum* (Vol. 23, pp. 311–320).
- Zhanga, J., Caia, P. & Wanga, G. (2011). A new approach to design rational harmonic surface over rectangular or triangular domain. *Journal of Information & Computational Science*, 8(1), 71–83.